Electronic Supplementary Material (ESI) for RSC Advances.

Syntheses, structural, photophysical and theoretical studies of heteroleptic cycloplatinated guanidinate(1−) complexes bearing acetylacetonate and picolinate ancillary ligands

Vasudha Thakur,[a] Jisha Mary Thomas,[b] Mohammad Adnan,[c] Chinnappan Sivasankar,[b] G. Vijaya Prakash,[c] and Natesan Thirupathi*[a]

[a]*Department of Chemistry, University of Delhi, Delhi 110 007, India. Email: tnat@chemistry.du.ac.in, thirupathi_n@yahoo.com*

[b]*Catalysis and Energy Laboratory, Department of Chemistry, Pondicherry University, Puducherry 605 014, India. E-mail: siva.che@pondiuni.edu.in*

[c] *Nanophotonics Laboratory, Department of Physics, Indian Institute of Technology, Delhi, New Delhi-110016, India. Email: prakash@physics.iitd.ac.in*

General considerations K_2PtCl_4 (Alfa Aesar), $Ag(OC(O)CF_3)$ (Spectrochem) and NaOAc (Sigma Aldrich) were purchased from commercial vendors and used as received. The IR spectral data were obtained through ATR method from powdered samples on an IRAffinity−1 Shimadzu FTIR spectrometer in the frequency range 400–4000 cm^{-1}. Elemental analyses were performed on an Elementar Analysensysteme GmbH VarioEL V3.00 and VarioEL Cube. Time of flight mass (TOF−MS) spectra were recorded on Agilent Technologies 6530, Accurate-Mass Q-TOF LC/MS instrument using electrospray positive ion mode. ^{1}H, ^{13}C and ^{19}F NMR spectra were recorded on a JEOL ECX 400 NMR spectrometer operating at 400, 100.5, and 376.5 MHz (with CF_3COOH as an external standard), respectively. ^{195}Pt NMR spectra of **10**–**13** were recorded on a Bruker AV-400 NMR spectrometer operating at 85.8 MHz (with K_2PtCl_4 as an external standard).^{195}Pt NMR spectra of **7**–**9** and **14**–**19** were recorded on a JEOL ECX 400 NMR spectrometer operating at 85.8 MHz (with K_2PtCl_4 as an external standard). The chemical shifts are reported in ppm relative to tetramethylsilane or residual solvent signal. Melting points were recorded on a Buchi melting point apparatus (Model: M−560) and the reported values are uncorrected.

Optical measurements

The microscopic optical images (Bright field), PL images and crystalline state visible emission spectra were recorded using a modified confocal high-resolution microscope (Olympus BX-51). The modified microscope is equipped with a fiber coupled 400nm (±5nm) diode laser and -xenon lamp as sources. The emission spectra and images were collected, respectively by a fiber optic spectrometer (Ocean Optics, Maya 2000Pro) and a camera (Olympus, DP26) through a 425 nm long-pass filter in specular reflection mode.[1]

Syntheses of some useful compounds

Symmetrical *N*,*N*′,*N*″-triarylguanidines, [ArN=C(NHAr)$_2$] (Ar = 2-(MeO)C$_6$H$_4$, 2-MeC$_6$H$_4$, 4-MeC$_6$H$_4$, 2,4-Me$_2$C$_6$H$_3$,[2] 2,5-Me$_2$C$_6$H$_3$[3], 2-FC$_6$H$_4$[4] and 2-ClC$_6$H$_4$[5]), *cis*-[PtCl$_2$(S(O)Me$_2$)$_2$], *cis*-[Pt(TFA)$_2$(S(O)Me$_2$)$_2$][6] and **1**–**5**[3,5,6] were prepared following the literature procedures.

[ArN=C(N(H)Ar)$_2$] (Ar = 2-BrC$_6$H$_4$) *N*,*N*′-Bis(2-bromophenyl)thiourea (386 mg, 1.00 mmol), 2-bromoaniline (190 mg, 1.10 mmol), KOH (675 mg as 70% aq. solution) and nitrobenzene (100 mg) were charged into a 25 mL round bottom (RB) flask. The contents in the RB flask were gradually heated up to 110 °C and maintained at the same temperature, while being stirred for 8 h. The reaction mixture was cooled to RT and diluted with water (10 mL). The organic portion was extracted with CH_2Cl_2 (3 × 5 mL) and the extract dried over anhydrous Na_2SO_4 for an hour and filtered. The volatiles from the extract were removed under vacuum to afford a dirty white solid. Subsequently, the solid was purified by column chromatography using 5% ethyl acetate:*n*-hexane (1/5, v/v) mixture as eluent to afford the guanidine as white flaky solid. Yield = 85% (445.3 mg, 0.849 mmol). Mp: 131.4 °C. Anal. Calcd. for $C_{19}H_{14}N_3Br_3$ (M_w = 524.05): C, 43.55; H, 2.69; N, 8.02. Found: C, 43.35; H, 2.54; N, 7.80. ATR–IR (cm^{-1}): ν(NH) 3368 (br, w); ν(C=N) 1632 (m). ESI Mass (HRMS) m/z [ion] Calcd.: 523.8796 [M+H]$^+$. Found 523.8832. ^{1}H NMR ($CDCl_3$, 400 MHz): δ_H 6.93 (br, 3 H, Ar*H* (1 H), N*H* (2 H)), 7.30 (t, J_{HH} = 7.8 Hz, 6 H, Ar*H*), 7.55 (d, J_{HH} = 7.6 Hz, 5 H, Ar*H*). ^{13}C{^{1}H} NMR ($CDCl_3$, 100.5 MHz): δ_C 122.9, 124.0, 125.4, 126.7, 128.6, 129.7, 133.0, 144.1.

[ArN=C(N(H)Ar)$_2$] (Ar = 4-FC$_6$H$_4$) *N*,*N*′-Bis(4-fluorophenyl)thiourea (500 mg, 1.89 mmol), 4-fluoroaniline (210 mg, 1.89mmol), KOH (260 mg as 35% aq. solution) and nitrobenzene (100 mg) were charged into a 25 mL RB flask. The contents in the RB flask were gradually heated up to 110 °C and maintained at the same temperature, while being stirred for 8 h. The reaction mixture was cooled to RT and diluted with water (10 mL). The organic portion was extracted with CH_2Cl_2 (3 × 5 mL) and the extract dried over anhydrous Na_2SO_4 for an hour and filtered. The volatiles from the extract were removed under vacuum to afford a dirty white solid. Subsequently, the solid was purified by column chromatography using 10% ethyl acetate:*n*-hexane (1/10, v/v) mixture as eluent to afford the guanidine as white solid. Yield = 71% (458.5 mg, 1.343 mmol). Mp: 105.2 °C. ATR–IR (cm^{-1}): ν(NH) 3398 (w); ν(C=N) 1631 (s); 826 (s). ESI Mass (HRMS) m/z [ion] Calcd.: 341.1140 $[M+H]^+$. Found: 341.1159. ^{1}H NMR ($CDCl_3$, 400 MHz): δ_H 5.72 (br, 2 H, N*H*), 6.98–7.02 (m, 6 H, Ar*H*), 7.15 (br, 6 H, Ar*H*). $^{13}C\{^1H\}$ NMR ($CDCl_3$, 100.5 MHz): δ_C 116.0, 116.2, 122.9, 125.7, 129.5, 139.8, 145.8, 146.1, 158.0, 160.3. $^{19}F\{^1H\}$ NMR ($CDCl_3$, 376.31 MHz): δ_F –116.3 and –120.8.

X-Ray crystallography Details of data collection, structure solution and refinement for structurally characterized compounds are presented in Tables S1 and S2. X-ray crystallographic diffraction data for **11** were collected on a Brukeraxs kappa apex2 Diffractometer with a CCD area detector (MoKα, 0.71073 Å, graphite monochromator).[7] Frames were collected at 293 K by ω, φ, and 2θ rotation at 10 s per frame with *APEX2*.[8] The measured intensities were reduced to F^2 with *SAINT*/*XPREP* and corrected for absorption with *SADABS*.[9] X-ray crystallographic diffraction data for **12–19** were collected at 298 K on an Oxford Xcalibur, Eos diffractometer (4-circle kappa goniometer, Eos CCD

detector, omega scans, graphite monochromator, and a single wavelength Enhance X-ray source with MoKα radiation).[10] Pre-experiment, data collection, data reduction, and absorption corrections were performed with the CrysAlisPro software suite.[11] The structures were solved and refined using the SHELX-2017 program package and SHELXL-2017/1 (within the WinGX program package).[12] Non-hydrogen atoms were refined anisotropically. C−H/N−H hydrogen atoms were placed in geometrically calculated positions by using a riding model. The molecular structures were created with Olex2 program.[13]

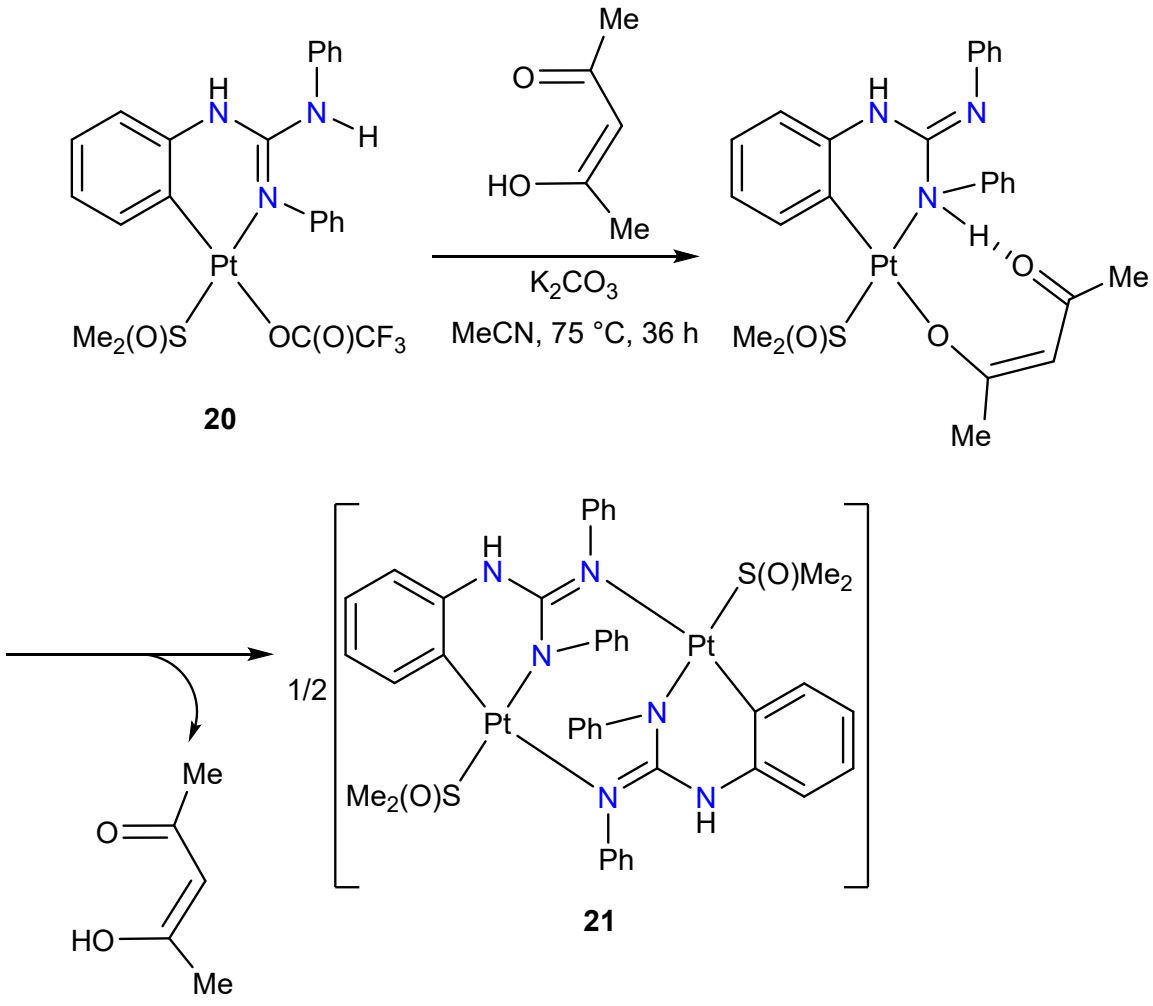

Scheme S1. Reaction of **20** with acacH and K_2CO_3 under the optimized conditions.

Table S1 Crystallographic data for **11**, **12**, **13**·0.5 toluene, **14** and **15**.

	11	**12**	**13**·0.5 toluene	**14**	**15**
Formula	$C_{27}H_{29}N_3O_2Pt$	$C_{27}H_{29}N_3O_2Pt$	$C_{63.25}H_{74}N_6O_4Pt_2$	$C_{30}H_{35}N_3O_2Pt$	$C_{24}H_{20}N_3O_2F_3Pt$
Fw	622.62	622.62	1368.43	664.70	634.52
Temperature (K)	296(2) K	298(2)	293(2)	298(2)	293(2)
Wavelength (Å)	0.71073	0.71073	0.71073	0.71073	0.71073
Crystal system	Triclinic	Triclinic	Triclinic	Triclinic	Orthorhombic
Space group	*P-1*	*P-1*	*P-1*	*P-1*	$Pca2_1$
a (Å)	10.5977(5)	11.0129(7)	12.4667(5)	10.8336(5)	23.5630(5)
b (Å)	10.9118(5)	11.7585(8)	13.3851(7)	10.9407(6)	5.29830(10)
c (Å)	11.3038(5)	20.8975(11)	18.9089(6)	12.9074(5)	18.4229(3)
α (deg)	70.094(2)	105.026(5)	93.304(3)	75.575(4)	90
β (deg)	79.697(2)	96.671(5)	98.761(3)	88.599(4)	90
γ (deg)	80.099(2)	95.534(5)	104.327(4)	70.372(4)	90
Volume (Å^3)	1200.51(10)	2573.2(3)	3006.5(2)	1392.61(12)	2299.99(8)
Z	2	4	2	2	4
ρ_{calcd} (Mg/m^3)	1.722	1.607	1.516	1.585	1.832
μ(Mo Kα) (mm^{-1})	5.873	5.480	4.698	5.068	6.151
F(000)	612	1224	1367	660	1224
θ range (deg)	2.969 – 26.370°	3.312–26.372	3.003–26.372	3.312–26.371	3.459–26.369
No. of reflns collected	20918	35935	40424	19670	29520
No. of reflns used	4900	10493	12285	5685	4706
Parameters	414	595	694	325	345
R_1 [I>2σ(I)][a]	0.0126	0.0761	0.0672	0.0486	0.0360
wR_2 (all reflns)[b]	0.0316	0.1056	0.1412	0.1093	0.0822
GooF on F^2 [c]	1.030	0.980	0.970	1.049	1.092
Largest diff. peak and hole, (e·Å^{-3})	0.434/–0.492	0.985/–1.010	0.772/–0.708	1.683/–0.689	0.90/–0.81

[a] $R_1 = \Sigma||F_o| - |F_c||/\Sigma|F_o|$; [b] $wR_2 = \{\Sigma[w(F_o^2 - F_c^2)^2]/\Sigma[w(F_o^2)^2]\}^{1/2}$; [c] $S = \{\Sigma[w(F_o^2 - F_c^2)^2]/(n-p)\}^{1/2}$

Table S2 Crystallographic data for **16**, **17**, **18** and **19**.

	16	**17**	**18**	**19**
Formula	$C_{24}H_{20}Cl_3N_3O_2Pt$	$C_{24}H_{20}Br_3N_3O_2Pt$	$C_{24}H_{20}F_3N_3O_2Pt$	$C_{28}H_{26}N_4O_5Pt$
Fw	683.87	817.25	634.52	693.62
Temperature (K)	298(2)	293(2)	298(2)	298(2)
Wavelength (Å)	0.71073	0.71073	0.71073	0.71073
Crystal system	Monoclinic	Monoclinic	Monoclinic	Monoclinic
Space group	$P2_1/n$	$P2_1/n$	$P2_1/c$	$P2_1/n$
a (Å)	9.6602(3)	9.8997(3)	10.2195(4)	9.9894(3)
b (Å)	13.4897(4)	13.5956(4)	10.2608(5)	22.7931(7)
c (Å)	18.9814(6)	18.9893(5)	21.3421(8)	11.6752(3)
α (deg)	90	90	90	90
β (deg)	99.169(3)	99.627(2)	90.459(3)	93.968(3)
γ (deg)	90	90	90	90
Volume (Å^3)	2441.92(13)	2519.82(13)	2237.87(16)	2651.95(13)
Z	4	4	4	4
ρ_{calcd} (Mg/m^3)	1.860	2.154	1.883	1.737
μ(Mo Kα) (mm^{-1})	6.101	10.352	6.322	5.336
F(000)	1320	1536	1224	1360
θ range (deg)	3.595–26.372	3.569–26.372	3.391–26.372	3.306–26.367
No. of reflns collected	33882	34866	29916	36627
No. of reflns used	4974	5136	4562	5400
Parameters	298	264	346	343
R_1 [I>2σ(I)][a]	0.0460	0.0690	0.0387	0.0401
wR_2 (all reflns)[b]	0.1141	0.2107	0.0899	0.0730
GooF on F^2 [c]	1.049	0.932	1.095	1.194
Largest diff. peak and hole, (e·Å^{-3})	2.406/–1.348	2.031/–0.895	1.619/–1.545	0.836/–0.764

[a] $R_1 = \Sigma\left|\,|F_o| - |F_c|\,\right| / \Sigma|F_o|$; [b] $wR_2 = \{\Sigma[w(F_o^2 - F_c^2)^2] / \Sigma[w(F_o^2)^2]\}^{1/2}$; [c] $S = \{\Sigma[w(F_o^2 - F_c^2)^2] / (n-p)\}^{1/2}$

Table S3 Selected bond distances (Å) of **11**, and **13**·0.5 toluene

	11	**12**§	**13**·0.5 toluene §
Pt(1)-C(15)	1.9853(19)	1.973(11)/1.973(11)	1.992(8)/1.998(9)
Pt(1)-N(1)	2.0090(15)	2.012(8)/2.015(8)	1.996(8)/1.995(6)
Pt(1)-O(1)	2.0131(14)	2.015(6)/1.997(7)	2.015(7)/2.019(5)
Pt(1)-O(2)	2.0933(14)	2.077(8)/2.071(7)	2.086(6)/2.089(6)
N(1)-C(1)	1.308(2)	1.312(12)/1.303(12)	1.302(12)/1.304(9)
N(3)-C(1)	1.344(2)	1.351(13)/1.357(13)	1.340(10)/1.360(9)
N(2)-C(1)	1.370(2)	1.391(12)/1.380(12)	1.367(12)/1.369(9)

§Two molecules per asymmetric unit were found in the crystal lattice.

Table S4 Selected bond distances (Å) of **14–18**

	14	**15**	**16**	**17**	**18**
Pt(1)-C(15)	1.998(7)	1.986(10)	1.975(7)	2.010(8)	1.984(6)
Pt(1)-N(1)	2.001(5)	2.005(8)	2.005(5)	2.008(11)	2.012(5)
Pt(1)-O(1)	2.004(4)	2.007(8)	2.016(5)	2.027(9)	2.016(4)
Pt(1)-O(2)	2.098(4)	2.074(8)	2.083(5)	2.091(10)	2.075(4)
N(1)-C(1)	1.278(8)	1.310(12)	1.289(8)	1.346(17)	1.303(7)
N(3)-C(1)	1.373(8)	1.332(12)	1.356(9)	1.300(19)	1.339(8)
N(2)-C(1)	1.362(8)	1.357(14)	1.368(9)	1.396(19)	1.355(7)

Table S5 Selected bond distances (Å) of **19**.

Pt(1)-C(15)	1.993(5)
Pt(1)-N(1)	2.007(4)
Pt(1)-N(4)	2.009(4)
Pt(1)-O(4)	2.121(4)
N(1)-C(1)	1.315(6)
N(3)-C(1)	1.362(6)
N(2)-C(1)	1.362(6)

Table S6 Bond angles (deg) of **11**−**13**

	11	**12**[§]	**13**·0.5 toluene[§]
C(15)-Pt(1)-N(1)	91.80(7)	92.9(4)/91.4(4)	92.1(4)/92.3(3)
C(15)-Pt(1)-O(1)	89.48(7)	88.3(4)/88.9(4)	90.3(3)/89.9(3)
N(1)-Pt(1)-O(1)	174.43(6)	178.2(4)/178.3(4)	177.5(3)/177.8(3)
C(15)-Pt(1)-O(2)	178.06(6)	179.8(4)/178.2(4)	177.0(3)/179.5(3)
N(1)-Pt(1)-O(2)	88.51(6)	87.3(4)/88.8(3)	87.9(3)/87.8(3)
O(1)-Pt(1)-O(2)	90.39(6)	91.6(3)/90.8(3)	89.7(3)/90.0(2)
N(1)-C(1)-N(3)	122.62(17)	124.0(11)/121.9(11)	122.1(10)/122.0(8)
N(1)-C(1)-N(2)	122.77(17)	119.6(11)/122.2(11)	122.9(9)/122.9(8)
N(3)-C(1)-N(2)	114.60(18)	116.4(11)/115.8(11)	115.0(10)/115.1(8)

[§]Two molecules per asymmetric unit were found in the crystal lattice.

Table S7 Bond angles (deg) of **14–18**

	14	**15**	**16**	**17**	**18**
C(15)-Pt(1)-N(1)	88.5(2)	92.0(3)	91.4(2)	92.5(4)	91.9(2)
C(15)-Pt(1)-O(1)	90.4(2)	88.5(4)	90.8(3)	89.2(4)	89.6(2)
N(1)-Pt(1)-O(1)	176.2(2)	179.2(3)	177.8(2)	178.3(4)	178.40(19)
C(15)-Pt(1)-O(2)	177.1(2)	179.1(4)	179.5(2)	178.2(4)	177.26(18)
N(1)-Pt(1)-O(2)	90.5(2)	88.9(3)	88.3(2)	87.9(4)	89.20(17)
O(1)-Pt(1)-O(2)	90.39(19)	90.6(4)	89.5(2)	90.5(4)	89.24(17)
N(1)-C(1)-N(3)	121.3(6)	122.3(9)	122.9(6)	123.5(15)	123.4(5)
N(1)-C(1)-N(2)	124.6(6)	121.9(8)	121.0(7)	118.6(16)	120.9(6)
N(3)-C(1)-N(2)	114.1(6)	115.8(9)	116.2(6)	117.9(13)	115.6(5)

Table S8 Bond Angles (deg) of **19**.

C(15)-Pt(1)-N(1)	88.23(19)
C(15)-Pt(1)-N(4)	99.1(2)
N(1)-Pt(1)-O(4)	93.07 (15)
N(4)-Pt(1)-O(4)	80.12(17)
C(15)-Pt(1)-O(4)	174.70(17)
N(1)-Pt(1)-N(4)	170.90(16)
N(1)-C(1)-N(3)	121.4(5)
N(1)-C(1)-N(2)	121.7(4)
N(3)-C(1)-N(2)	116.8(5)

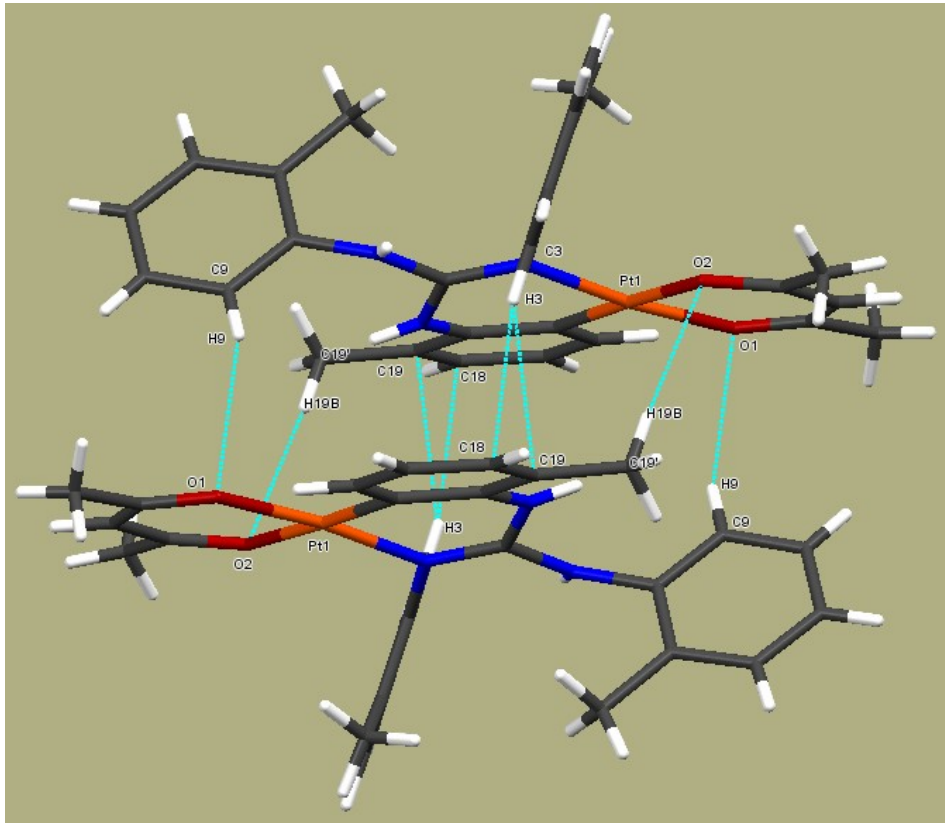

Fig. S1 Crystal packing diagram of **11**, illustrating intermolecular interactions. The intermolecular distances (Å) and angles (deg.) are: (i) C9····O1 = 3.247, H9····O1 = 2.545 and C9–H9–O1 = 136.63. (ii) C19′····O2 = 3.553, O2····H19B = 2.611 and C19′–H19B–O2 = 174.27. (iii) C3····C18 = 3.713, H3····C18 = 2.814, C3–H3–C18 = 160.88. (iv) C3····C19 = 3.616, H3····C19 = 2.751, C3–H3–C19 = 153.71. In **11**, the reference molecule and inversion related adjacent molecule are linked by C–H···O and C–H···π interactions.

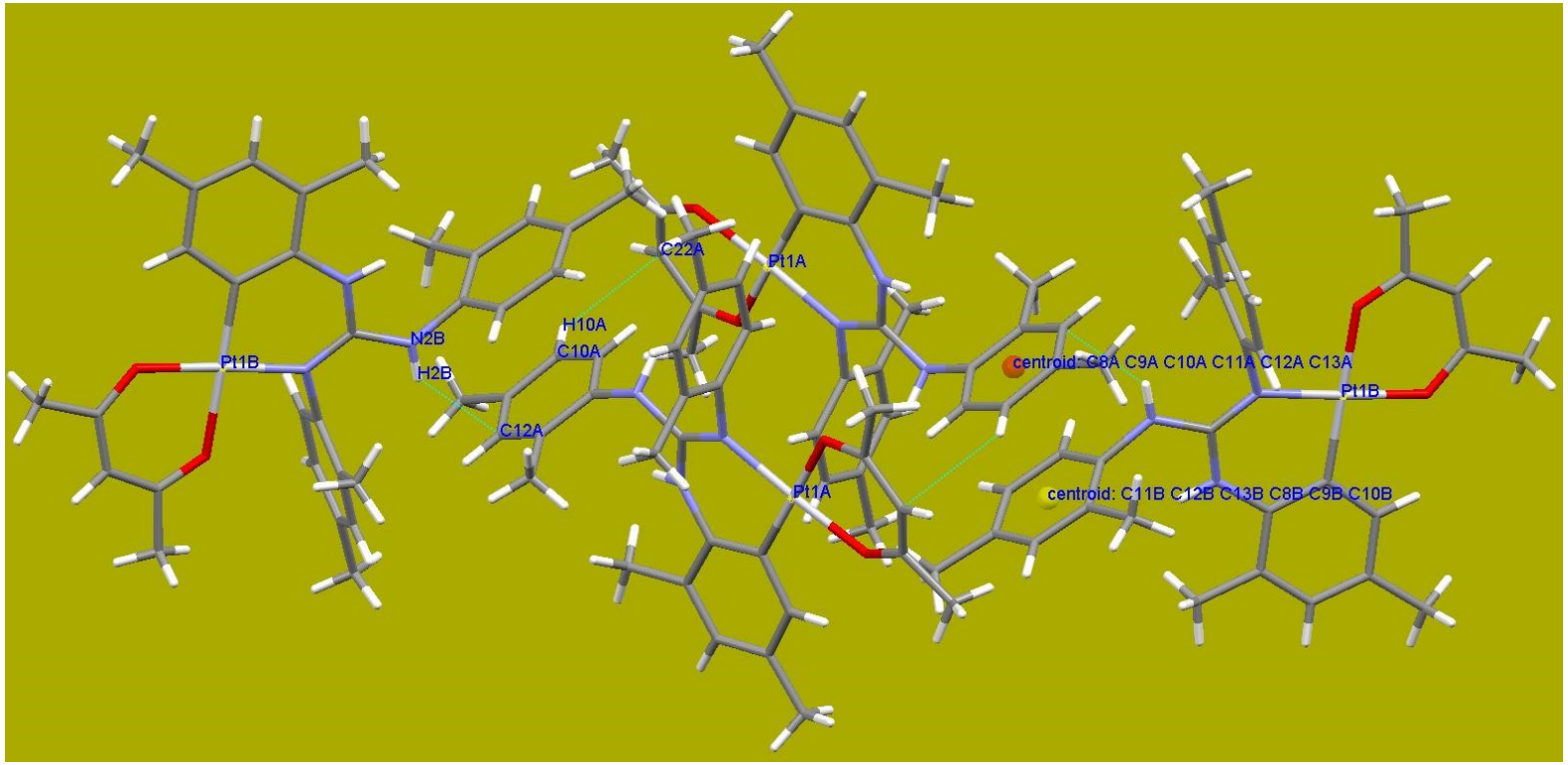

Fig. S2 Crystal packing diagram of **13**·0.5 toluene, illustrating intermolecular interactions. Toluene is omitted for clarity. The intermolecular distances (Å) and angles (deg.) are: (i) C12A····N2B = 3.414, H2B····C12A = 2.691 and C12A–H2B–N2B = 142.68. (ii) C10A····C22A = 3.650, C22A····H10A = 2.897 and C710A–H10A–C22A = 138.84. In **13**·0.5 toluene, there are two molecules in an asymmetric unit (Z' = 2). These two molecules are linked by N–H···π and π···π interactions.

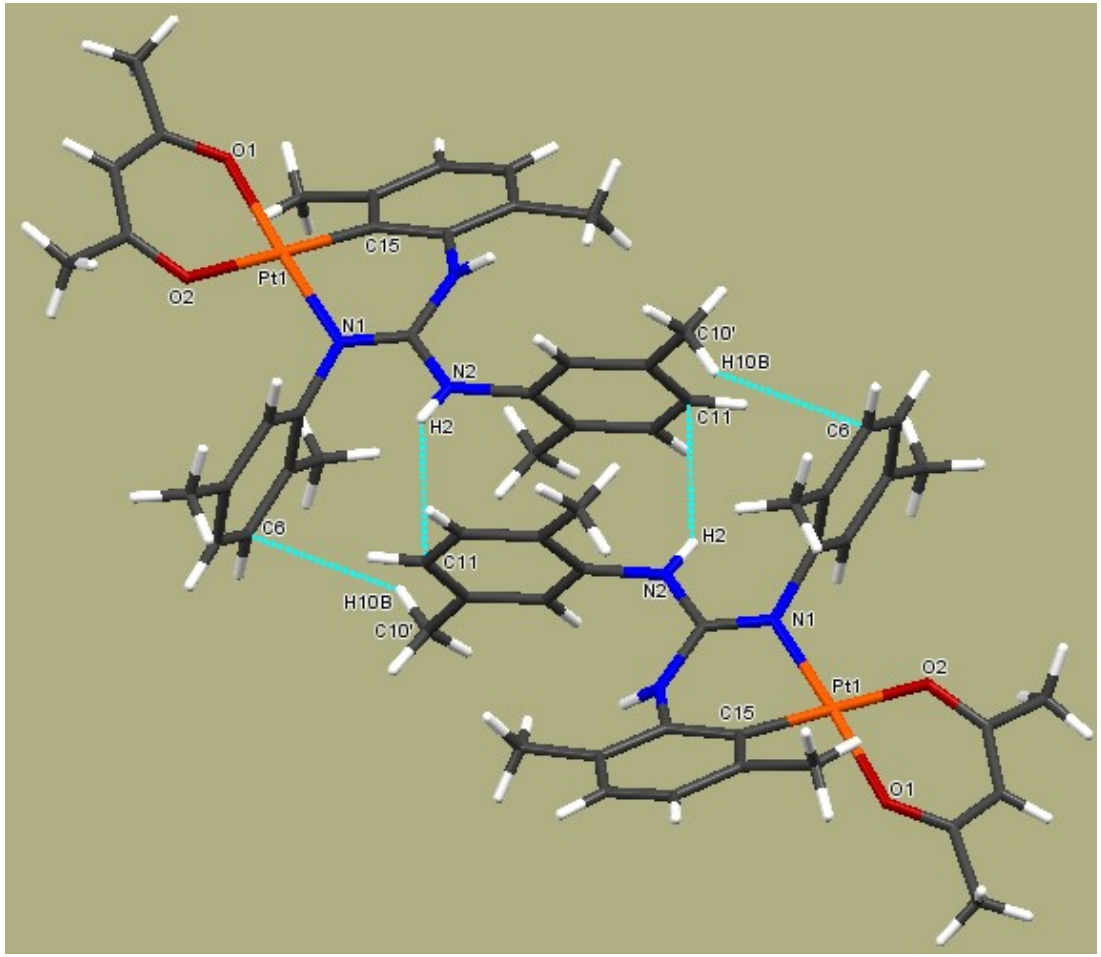

Fig. S3 Crystal packing diagram of **14**, illustrating intermolecular interactions. The intermolecular distances (Å) and angles (deg.) are: (i) C6····C10′ = 3.710, H10B····C6 = 2.893 and C6–H10B–C10′ = 143.64. (ii) N2····C11 = 3.563, C11····H2 = 2.837 and N2–H2–C11 = 143.34. In **14**, the reference and inversion related adjacent molecules are linked by one pair of N–H···π and one pair of C–H···π interactions to form a dimer.

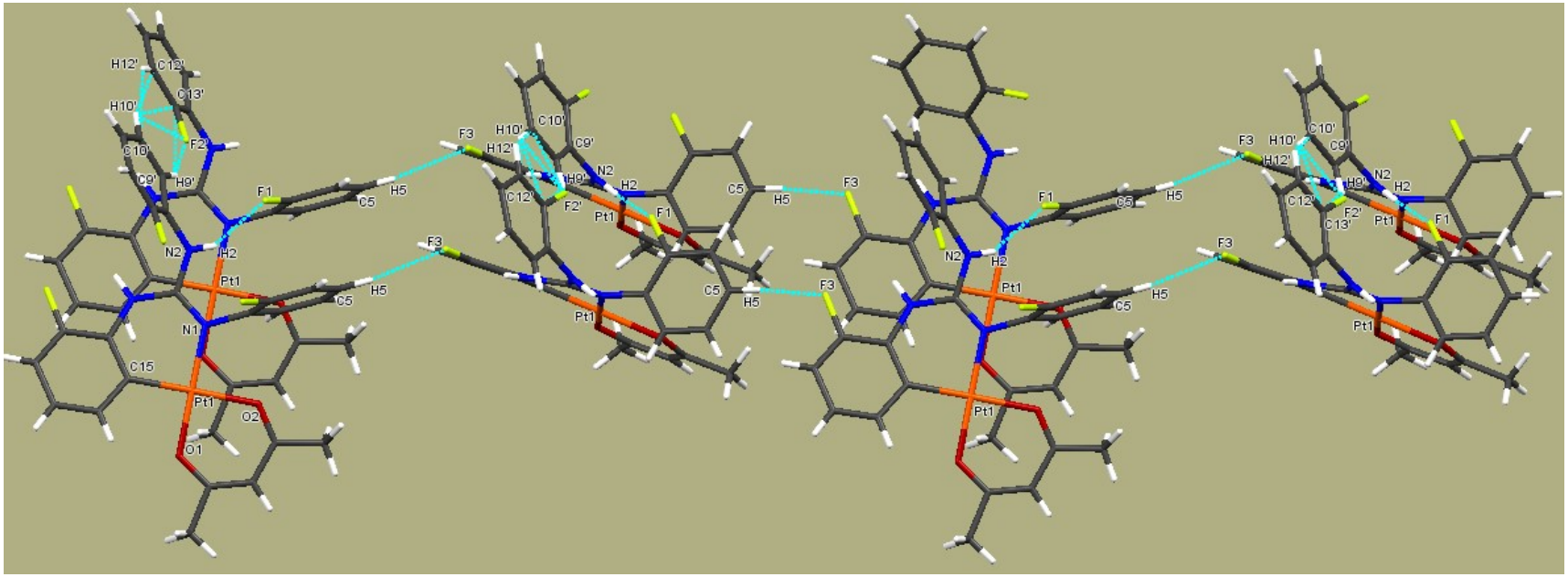

Fig. S4 Crystal packing diagram of **15**, illustrating intermolecular interactions. The intermolecular distances (Å) and angles (deg.) are: (i) C5····F3 = 3.371, H5····F3 = 2.454 and C5–H5–F3 = 168.59. (ii) C24····F2 = 3.092, F2····H24B = 2.338 and F2–C24B–C24 = 134.72. (iii) N2····F1 = 3.086, F1····H2 = 2.304 and N2–H2–F1 = 151.52. (iv) C9····C14= 3.545, C14····H9 = 2.854 and C9–H9–C14 = 131.94. (v) C9····C19 = 3.471, C19····H9 = 2.652 and C9–H9–C19 = 147.26. The rotational disorder of one of the aryl rings in **15** precluded our discussion about the intermolecular interactions in the crystal lattice.

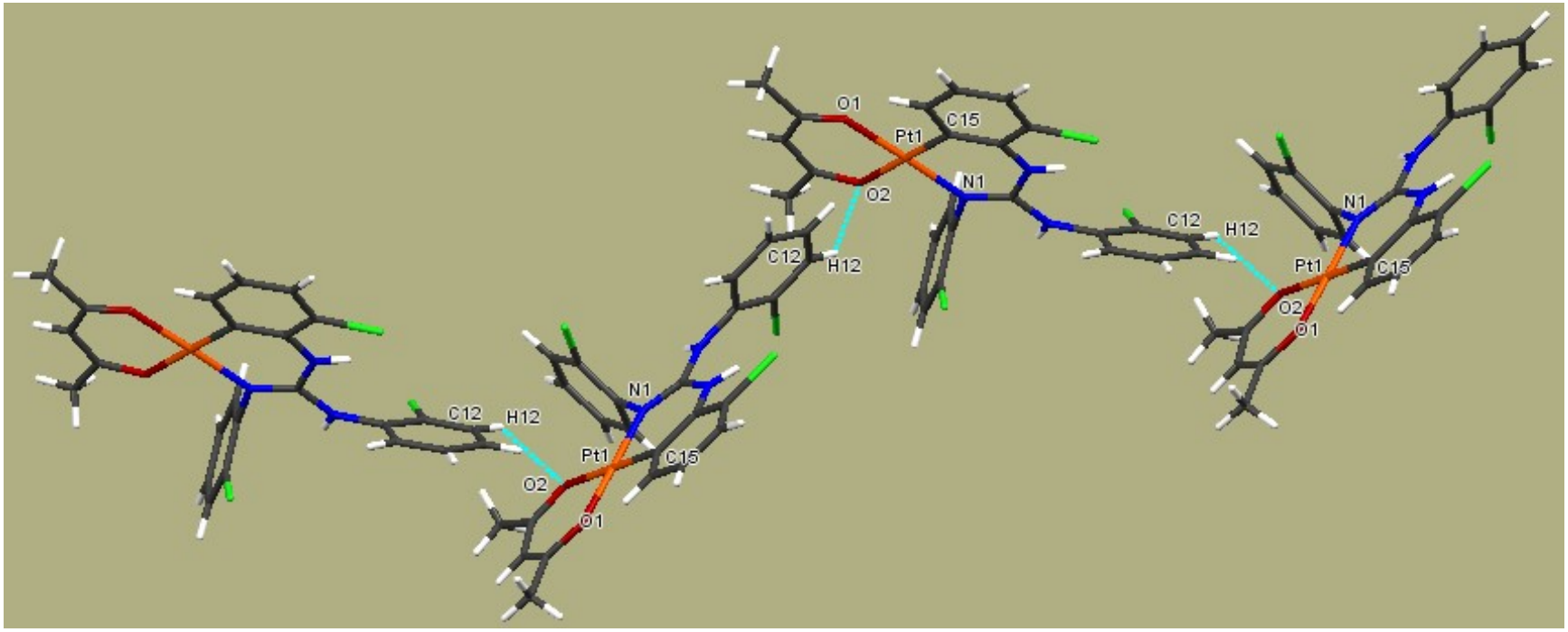

Fig. S5 Crystal packing diagram of **16**, illustrating intermolecular interactions. The intermolecular distances (Å) and angles (deg.) are: (i) C12···O2 = 3.490, H12···O2 = 2.718 and C12–H12–O2 = 140.98. In the crystal lattice of **16**, the reference molecule is linked to the neighboring molecules only via intermolecular C–H···O hydrogen bond leading to the formation of a one-dimensional chain.

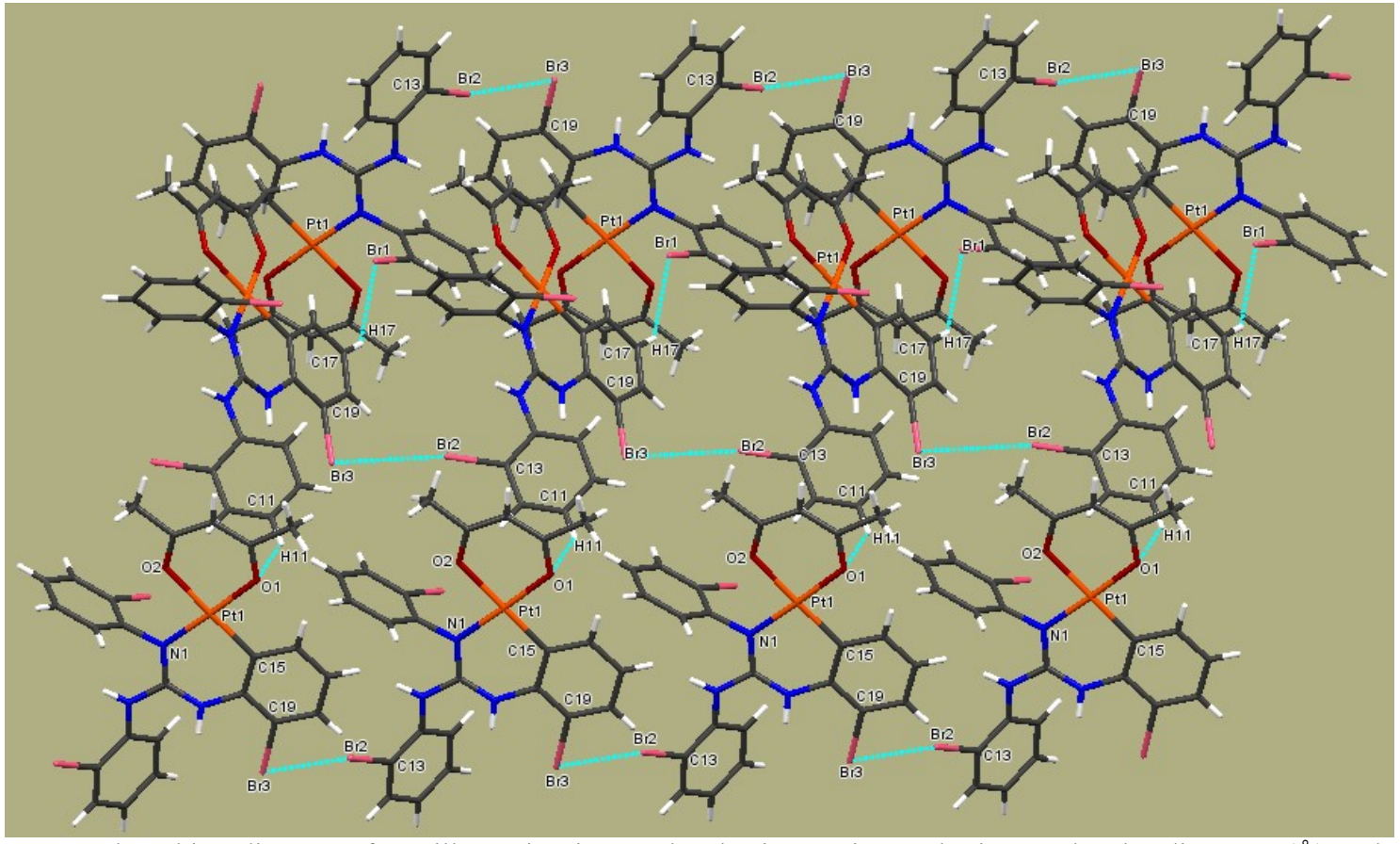

Fig. S6 Crystal packing diagram of **17**, illustrating intermolecular interactions. The intermolecular distances (Å) and angles (deg.) are: (i) Br2···Br3 = 3.634, C13–Br2–Br3 = 168.15, C19–Br3–Br2 = 94.52. (ii) O1···C11 = 3.311, O1···H11 = 2.700 and C11–H11–O1 = 124.02. (iii) Br1···C17 = 3.676, Br1···H17 = 2.962 and Br1–H17–C17 = 134.68. In **17**, the reference molecule is linked to two adjacent identical molecules via type II halogen bond[14] to form a one-dimensional chain and this chain is linked to two adjacent chains related by screw axis and glide plane via C–H···Br and C–H···O hydrogen bonds respectively and thus forms a two-dimensional layer structure. Halogen bonding in weakly luminescent platinacycle, [Pt(ND-$\kappa C,\kappa N$)(Cl)(PPh_3)] derived from 2-(2-benzothienyl)pyridine and $IC_6F_5/I_2C_6F_4$ were shown to amplify photophysical performance of the resulting adducts formed from the aforementioned pair.[15]

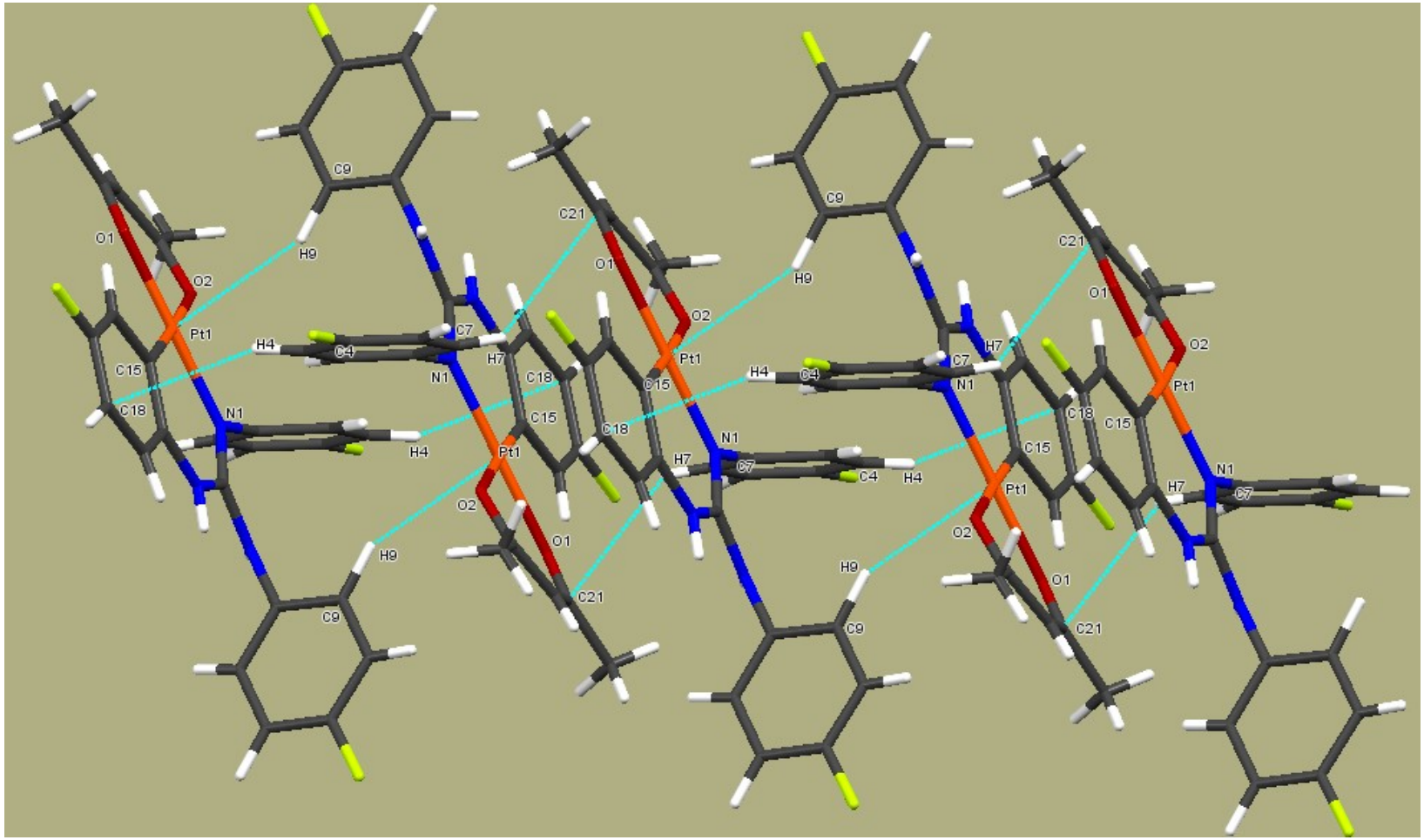

Fig. S7 Crystal packing diagram of **18**, illustrating intermolecular interactions. The intermolecular distances (Å) and angles (deg.) are: (i) Pt1····C9 = 3.863, Pt1····H9 = 2.876, Pt1–H9–C9 = 152.47. (ii) C7····C21 = 3.551, C21····H7 = 2.896 and C7–H7–C21 = 135.72. (iii) C4····C18 = 3.740, C18····H4 = 2.895 and C18–H4–C4 = 156.81. In **18**, the F atom in 4th position of the N(H)Ar unit simultaneously acts as a bifurcated acceptor, one involving type II halogen bond with the inversion related adjacent molecule and the other involving N–H···F hydrogen bond with the adjacent molecule related by screw axis. The reference molecule and inversion related adjacent molecule are linked by a pair of C–H···Pt interactions.

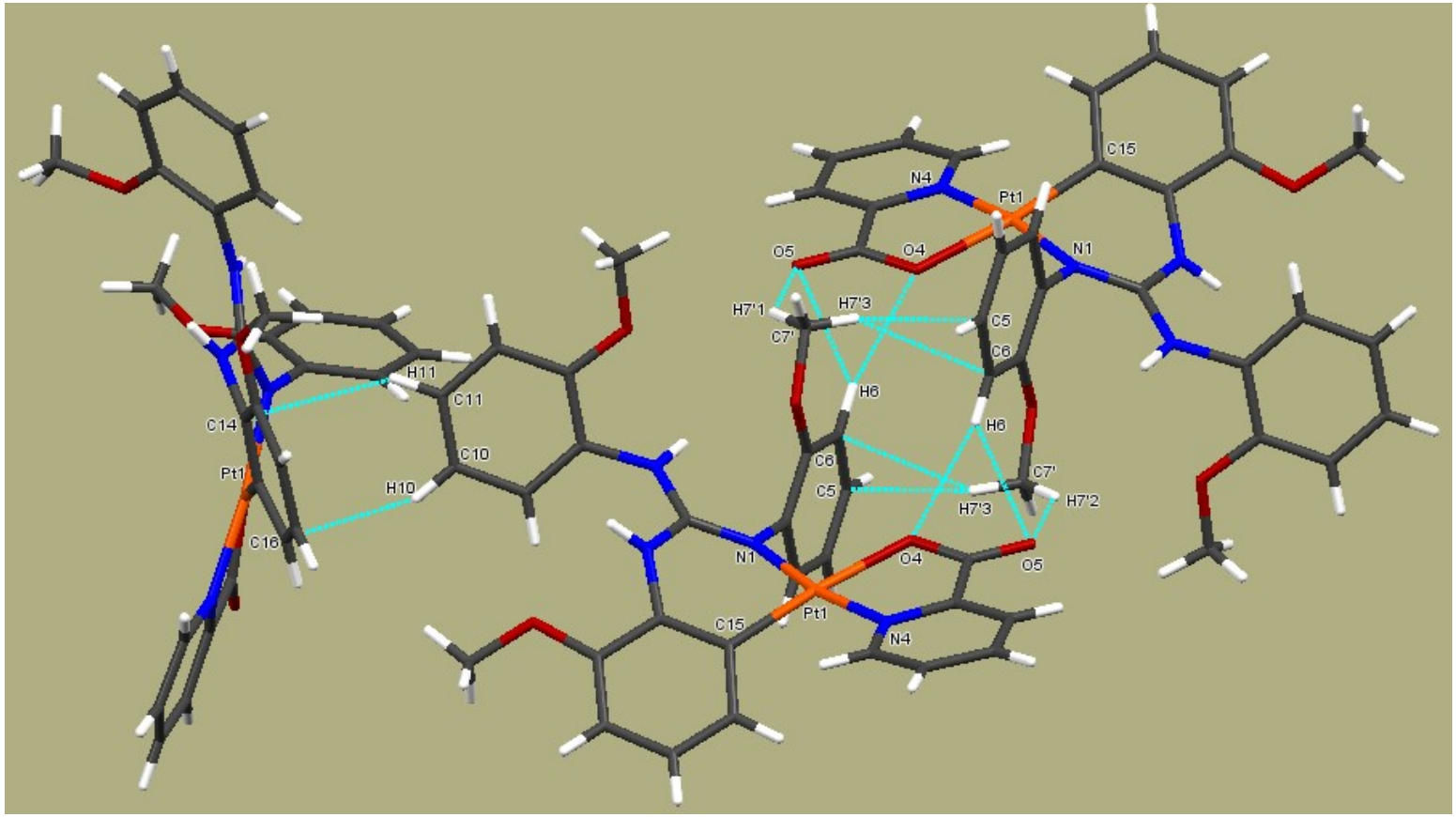

Fig. S8 Crystal packing diagram of **19**, illustrating intermolecular interactions. The intermolecular distances (Å) and angles (deg.) are: (i) C11····H11 = 0.931, H11····C14 = 2.858 and C14–H11–C11 = 145.70. (ii) C10····H10 = 0.929, H10····C16 = 2.712 and C16–H10–C10 = 143.17. (iii) C7′····H7′1 = 0.960 Å, H7′1····O5 = 2.700 and O5–H7′1–C7′ = 132.44. (iv) C6····H6 = 0.930, H6····O5 = 2.705 and O5–H6–C6 = 139.47. (v) C6····H6 = 0.930, H6····O4 = 2.611 and O4–H6–C6 = 167.19. (vi) C7′····H7′3 = 0.960, H7′3····C5 = 2.882 and C5–H7′3–C7′ = 126.67°. (vii) C7′····H7′3 = 0.960, H7′3····C6 = 2.805 and C6–H7′3–C7′ = 134.94. In **19**, the reference molecule is linked to the adjacent molecule related by an inversion symmetry through a pair of bifurcated C–H···O, normal C–H···O hydrogen bonds and a pair of C–H···π interactions on one side and through a pair of C–H···π interactions with the glide related adjacent molecule on the other side.

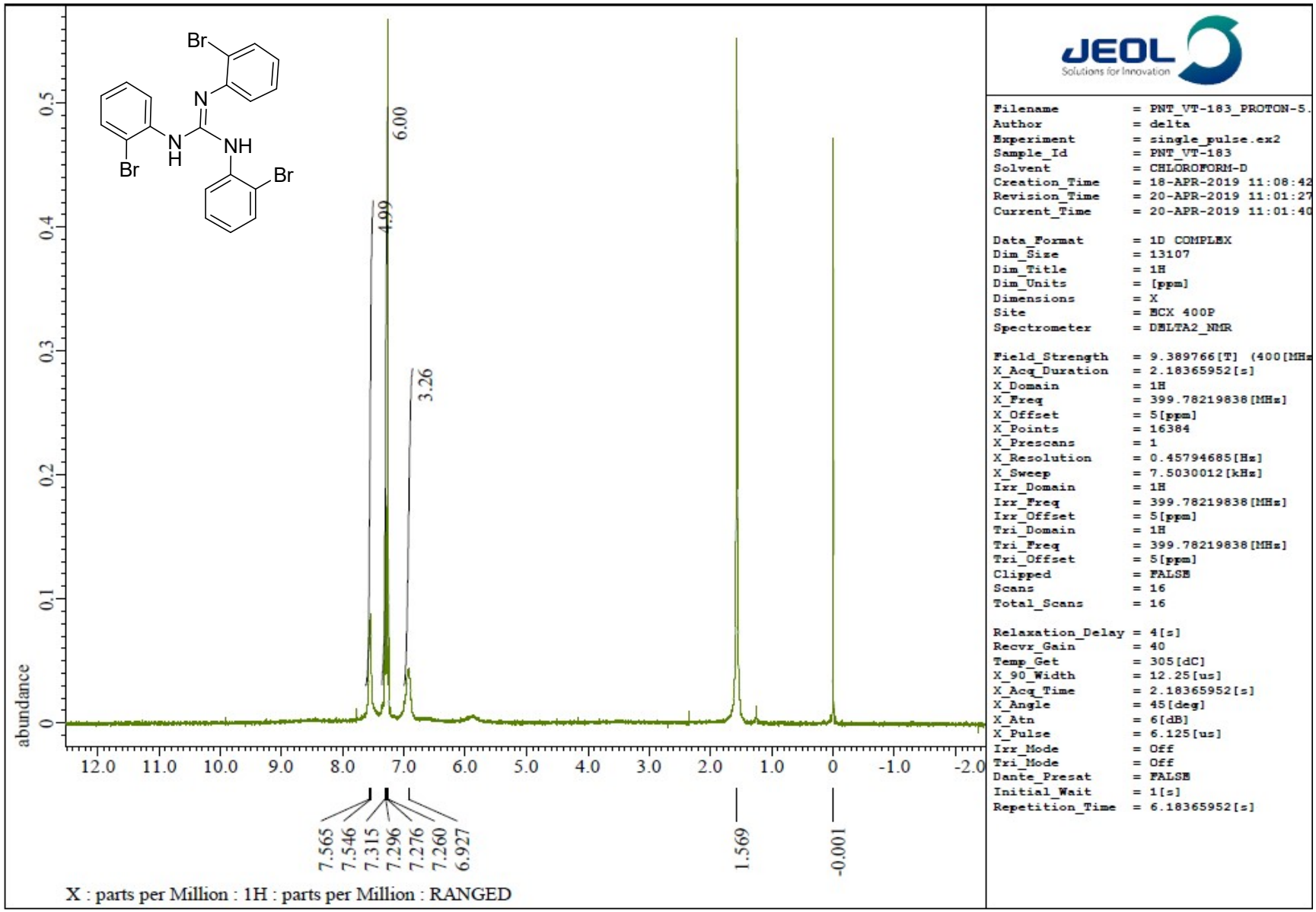

Fig. S9 ^{1}H NMR ($CDCl_3$, 400 MHz) spectrum of [ArN=C(N(H)Ar)$_2$] (Ar = 2-BrC_6H_4).

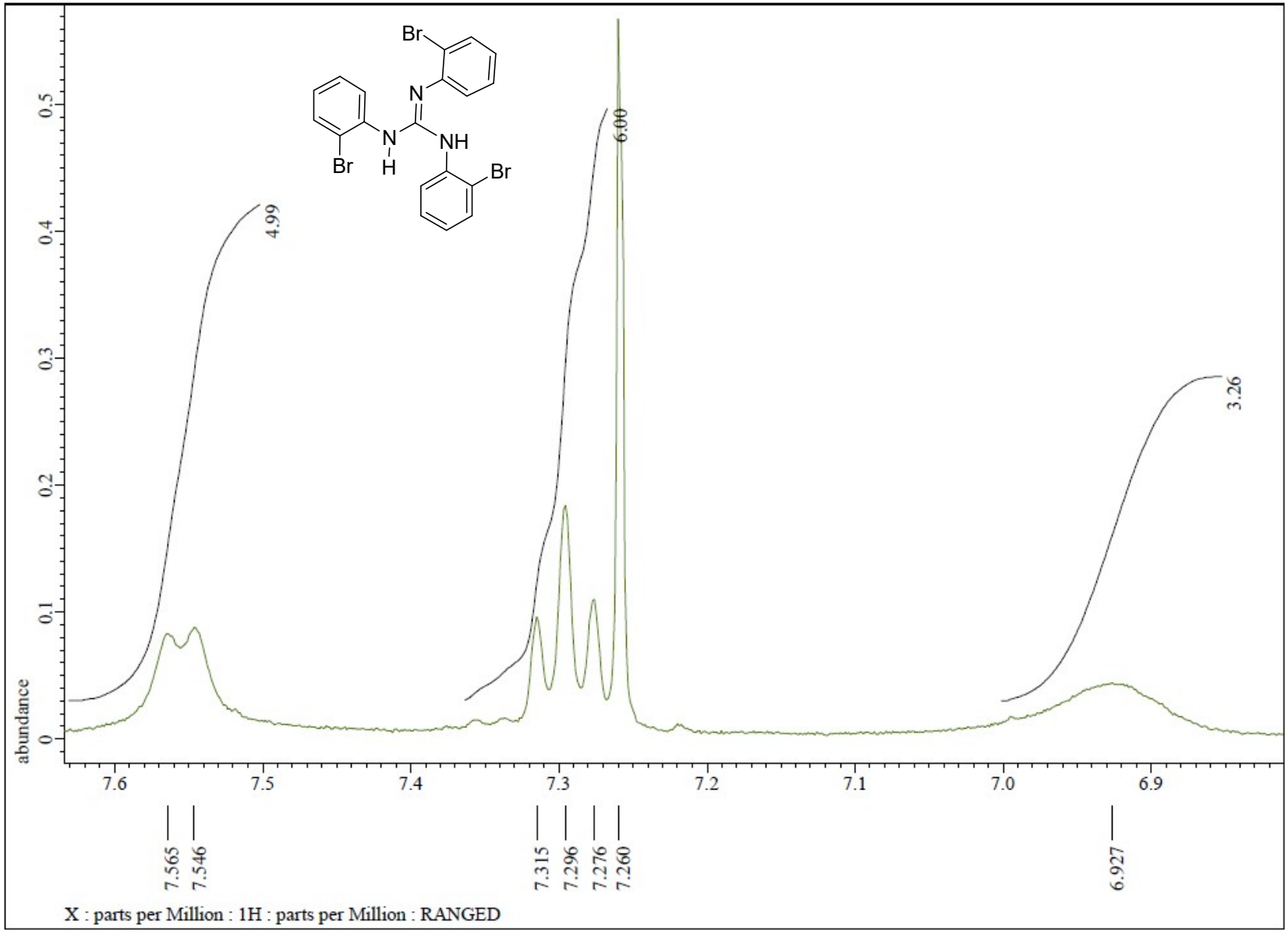

Fig. S10 ^{1}H NMR ($CDCl_3$, 400 MHz) spectrum of [ArN=C(N(H)Ar)$_2$] (Ar = 2-BrC_6H_4) in the indicated region.

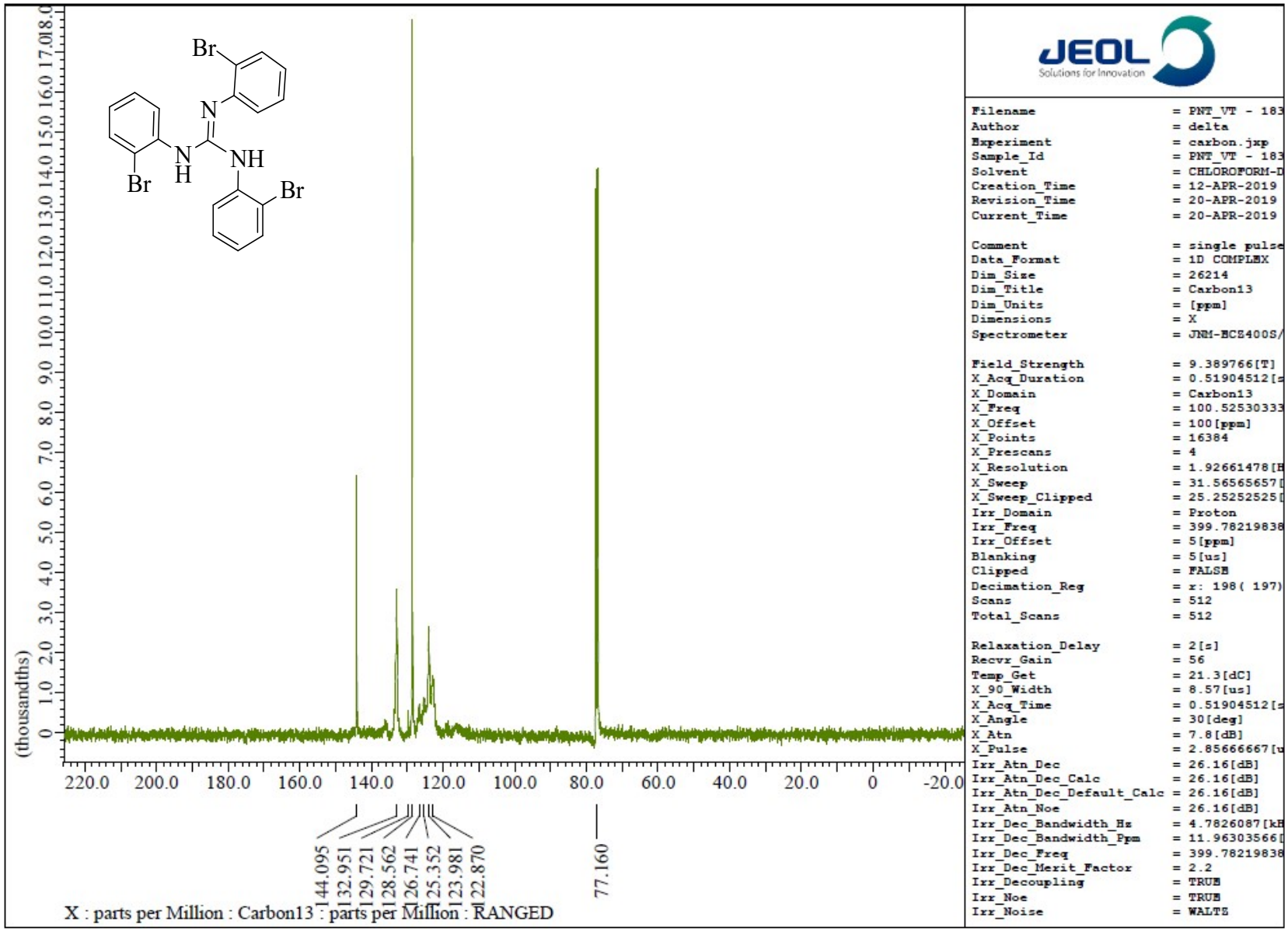

Fig. S11 $^{13}C\{^{1}H\}$NMR ($CDCl_3$, 100.5 MHz) spectrum of $[ArN{=}C(N(H)Ar)_2]$ (Ar = 2-BrC_6H_4).

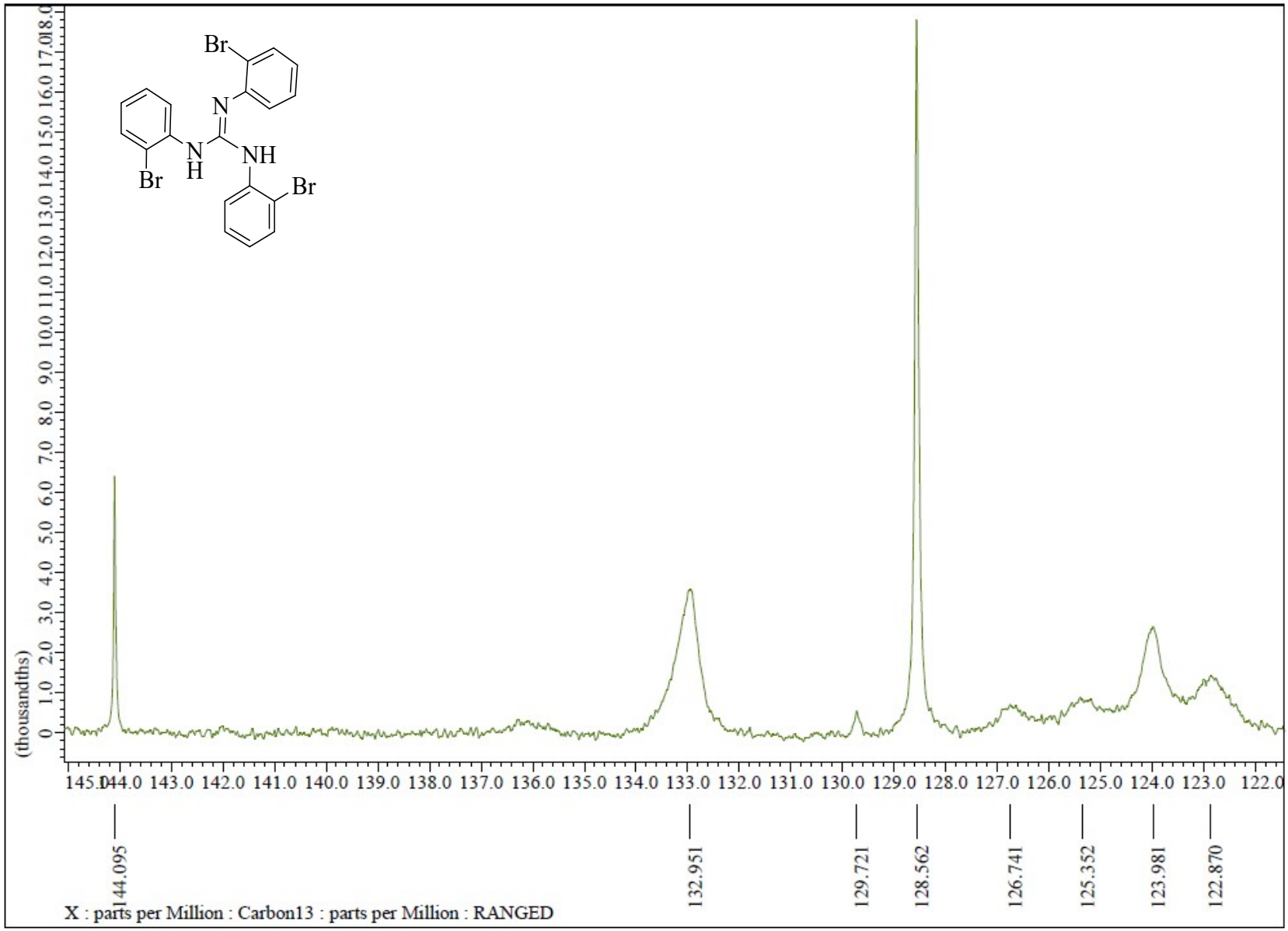

Fig. S12 $^{13}C\{^{1}H\}$ NMR ($CDCl_3$, 100.5 MHz) spectrum of $[ArN{=}C(N(H)Ar)_2]$ (Ar = 2-BrC_6H_4) in the indicated region.

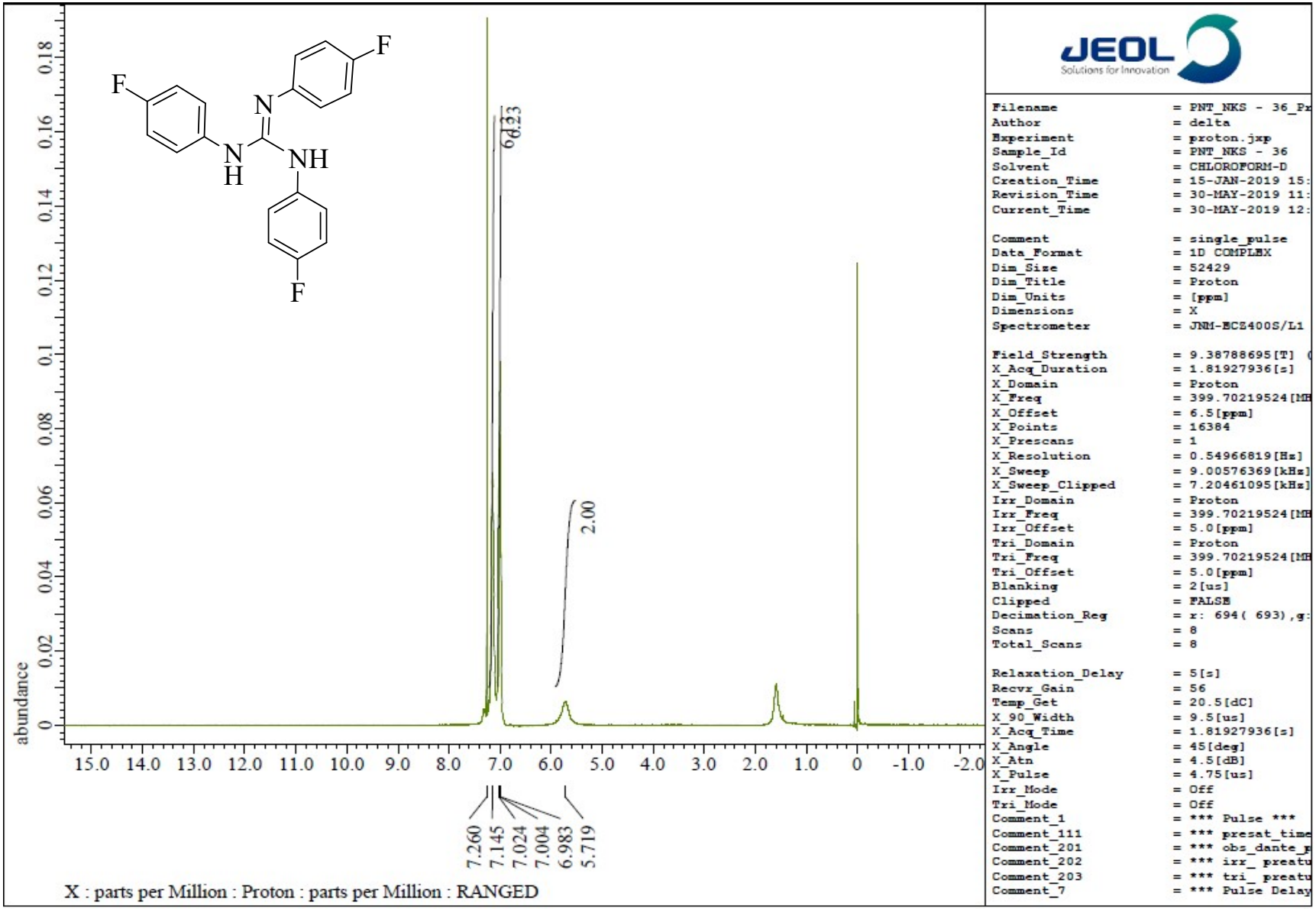

Fig. S13 ^{1}H NMR ($CDCl_3$, 400 MHz) spectrum of [ArN=C(N(H)Ar)$_2$] (Ar = 4-FC_6H_4).

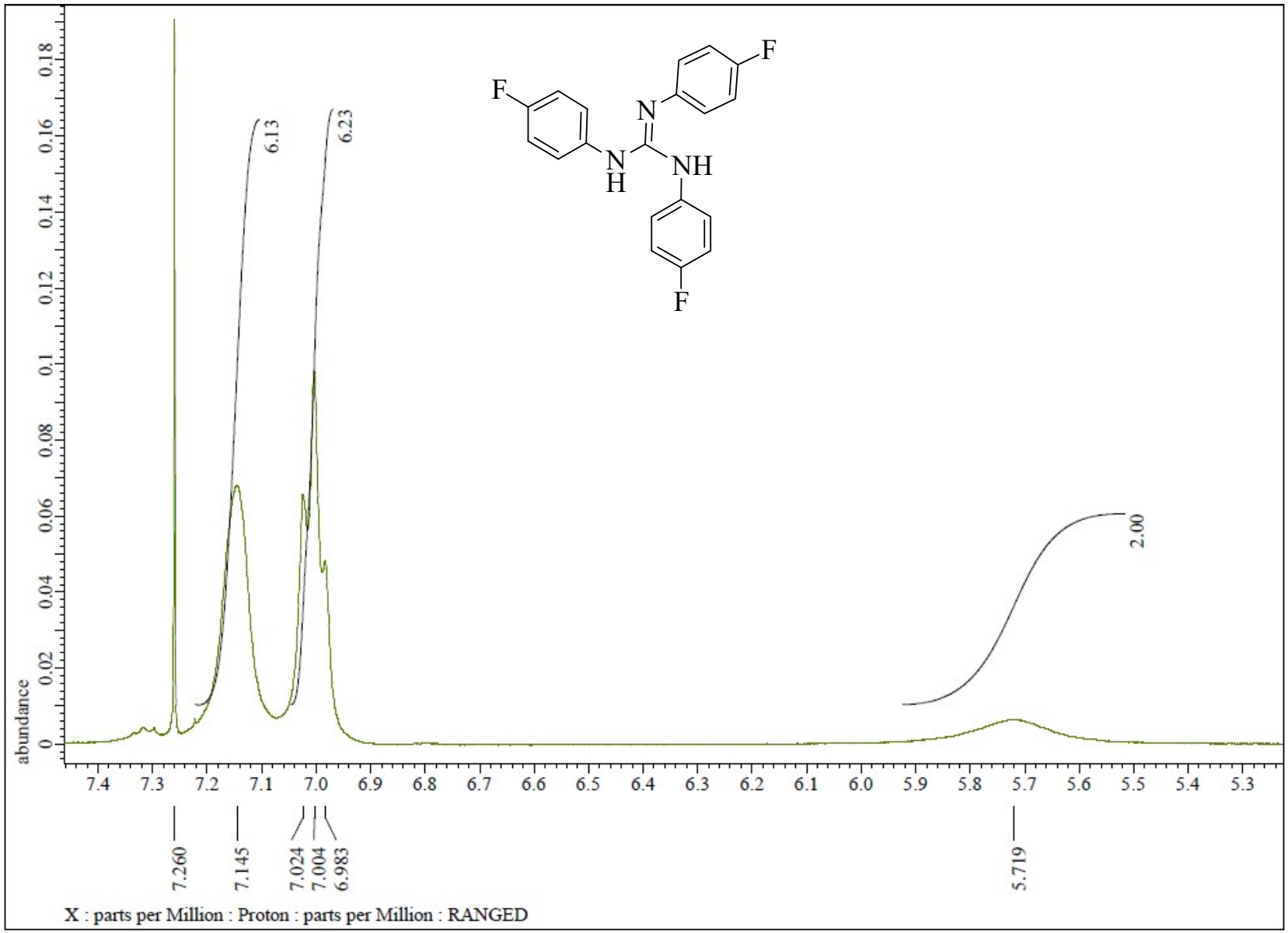

Fig. S14 ^{1}H NMR ($CDCl_3$, 400 MHz) spectrum of [ArN=C(N(H)Ar)$_2$] (Ar = 4-FC_6H_4) in the indicated region.

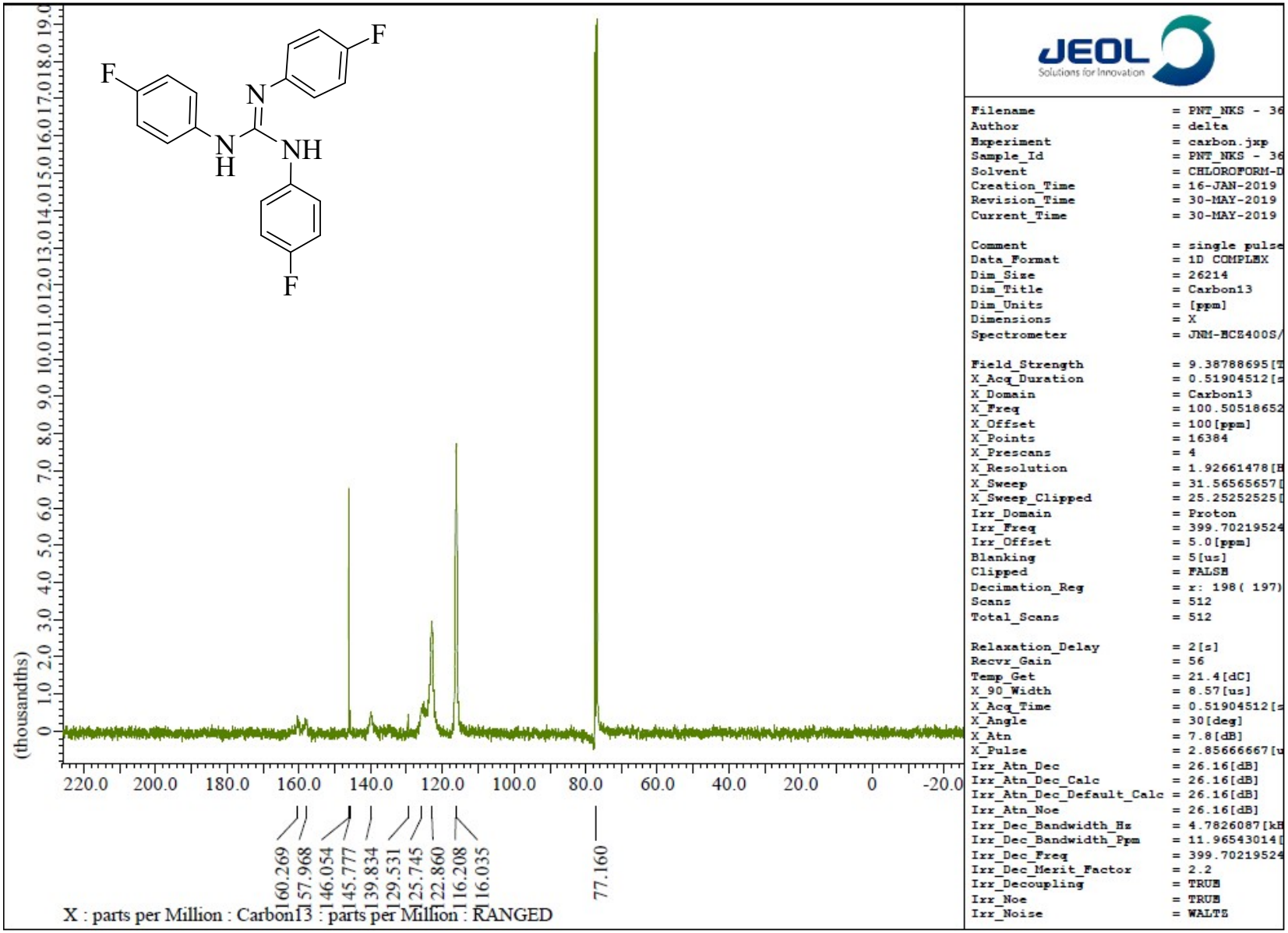

Fig. S15 $^{13}C\{^{1}H\}$ NMR ($CDCl_3$, 100.5 MHz) spectrum of $[ArN{=}C(N(H)Ar)_2]$ (Ar = 4-FC_6H_4).

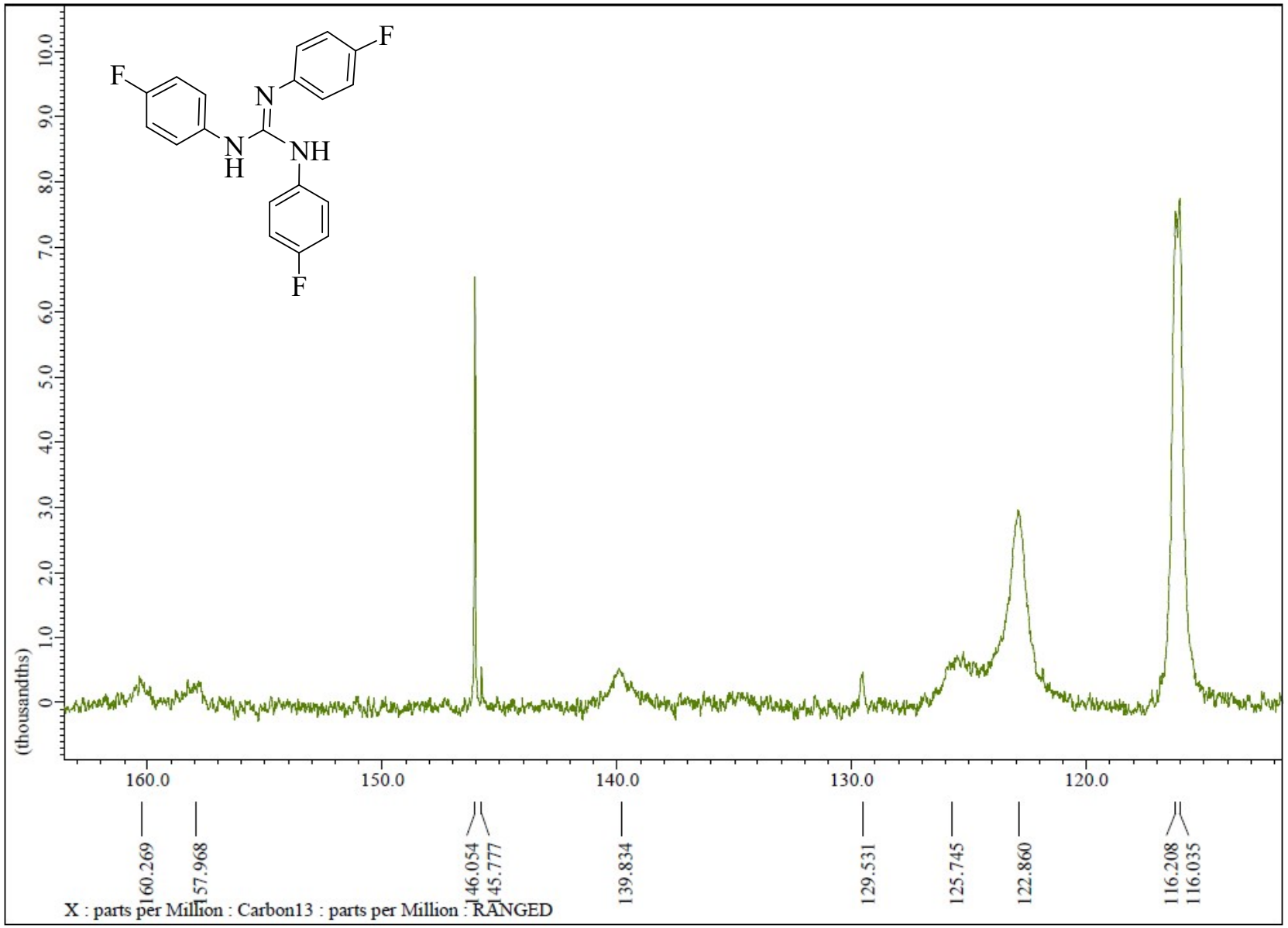

Fig. S16 $^{13}C\{^{1}H\}$ NMR ($CDCl_3$, 100.5 MHz) spectrum of $[ArN{=}C(N(H)Ar)_2]$ (Ar = 4-FC_6H_4) in the indicated region.

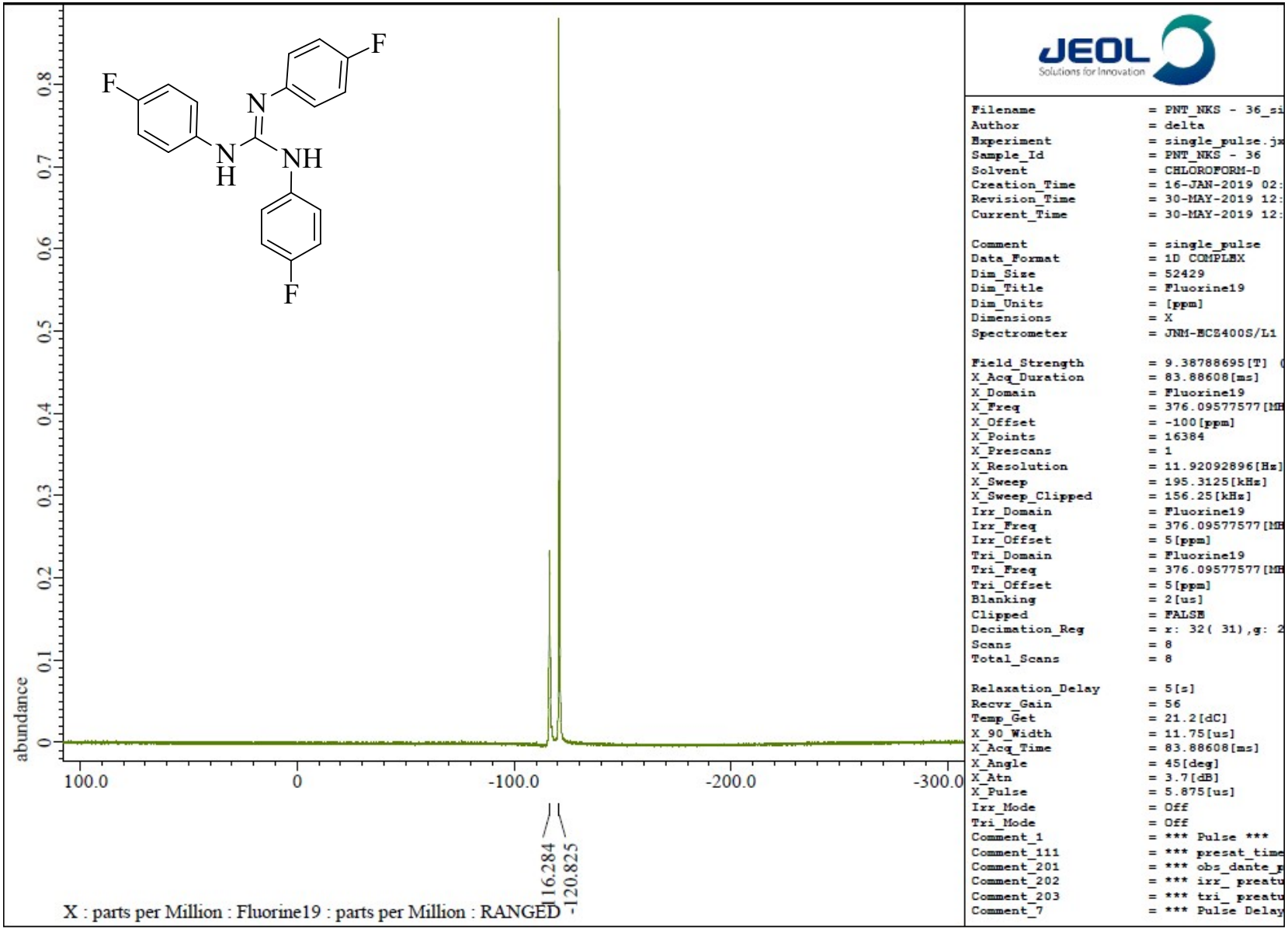

Fig. S17 $^{19}F\{^{1}H\}$ NMR ($CDCl_3$, 376.31 MHz) spectrum of $[ArN{=}C(N(H)Ar)_2]$ (Ar = 4-FC_6H_4).

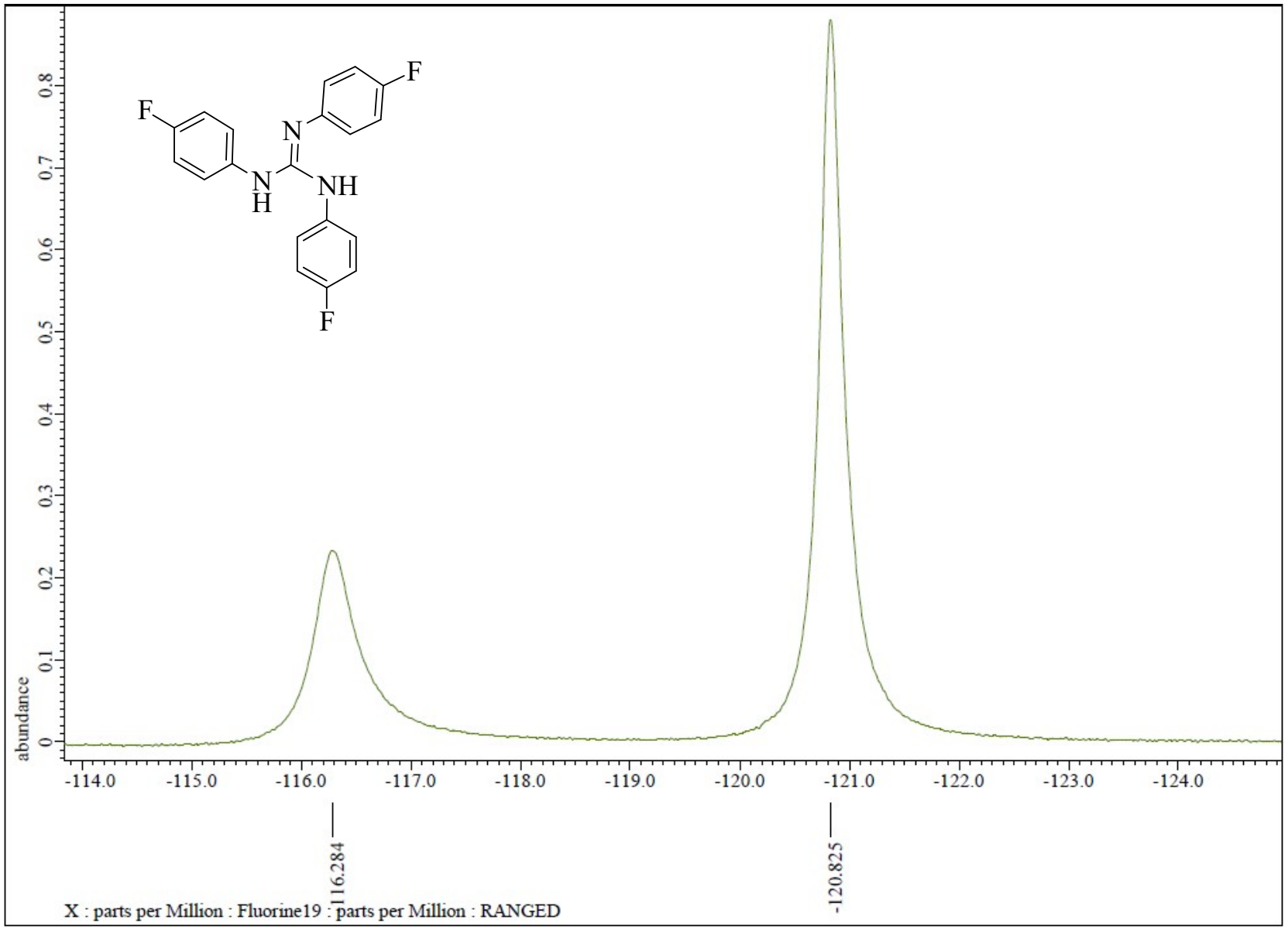

Fig. S18 $^{19}F\{^{1}H\}$ NMR ($CDCl_3$, 376.31 MHz) spectrum of [ArN=C(N(H)Ar)$_2$] (Ar = 4-FC_6H_4).

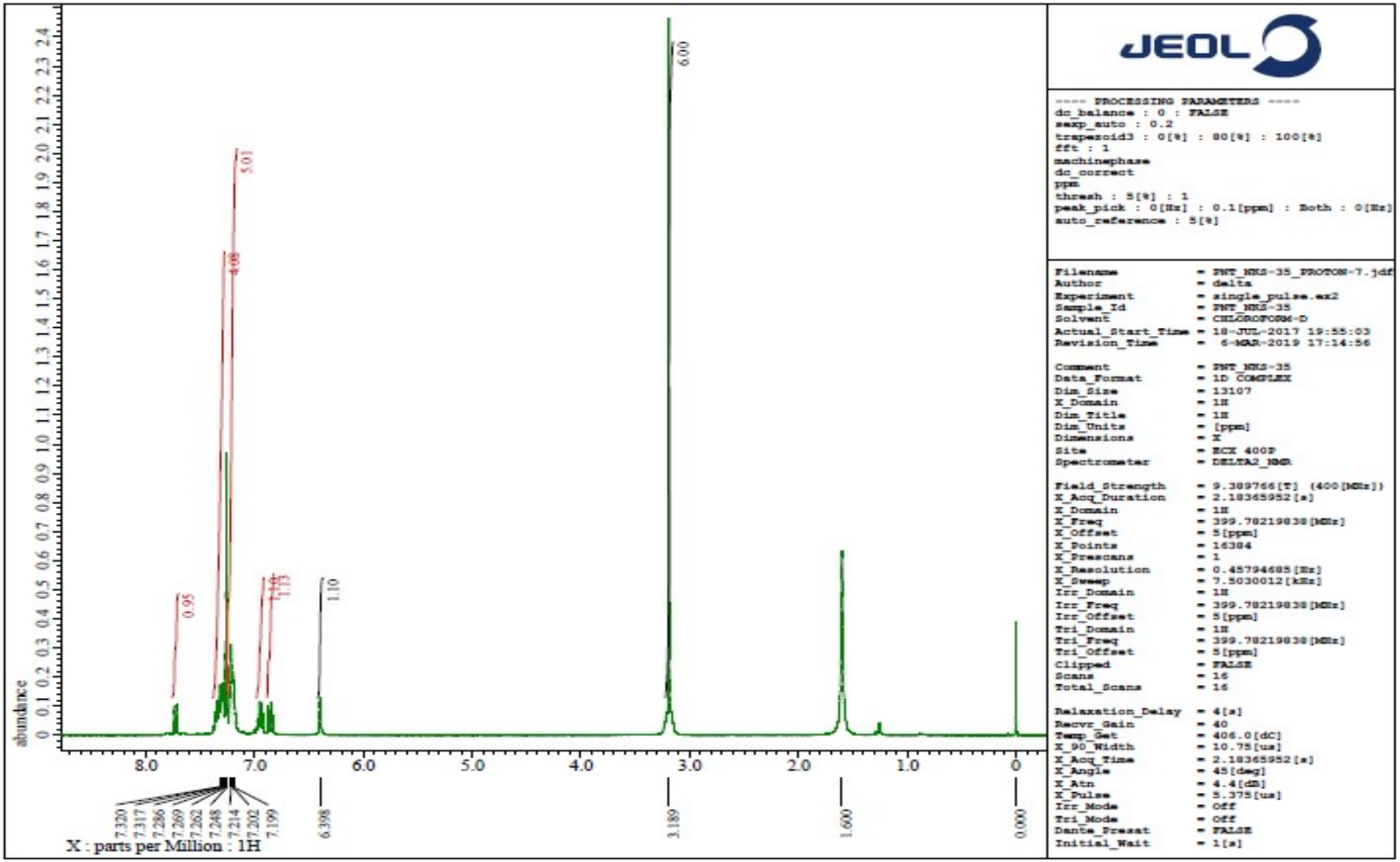

Fig. S19 ^{1}H NMR ($CDCl_3$, 400MHz) spectrum of complex **6**.

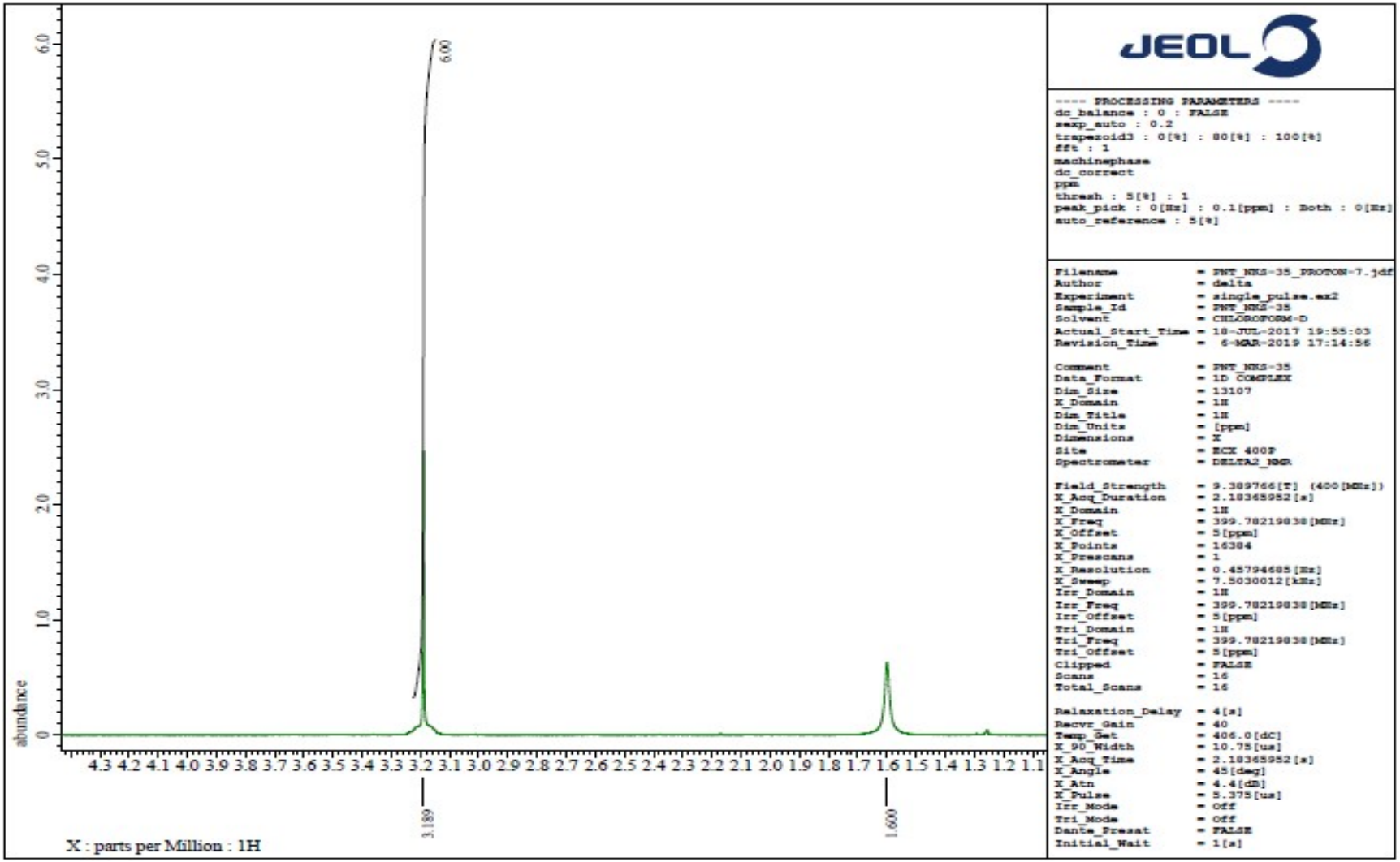

Fig. S20 ^{1}H NMR ($CDCl_3$, 400MHz) spectrum of complex **6** in the indicated region.

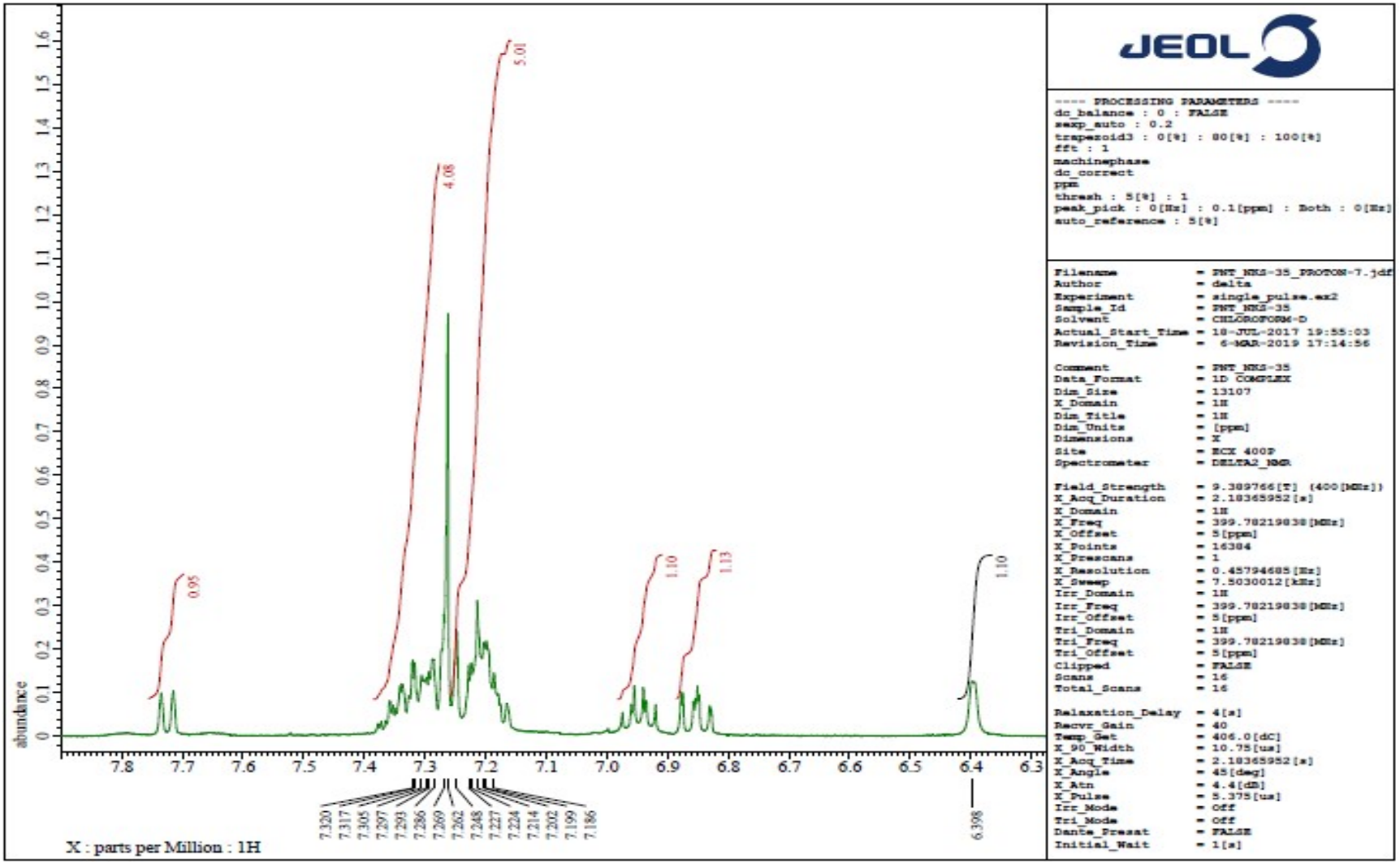

Fig. S21 ^{1}H NMR ($CDCl_3$, 400MHz) spectrum of complex **6** in the indicated region.

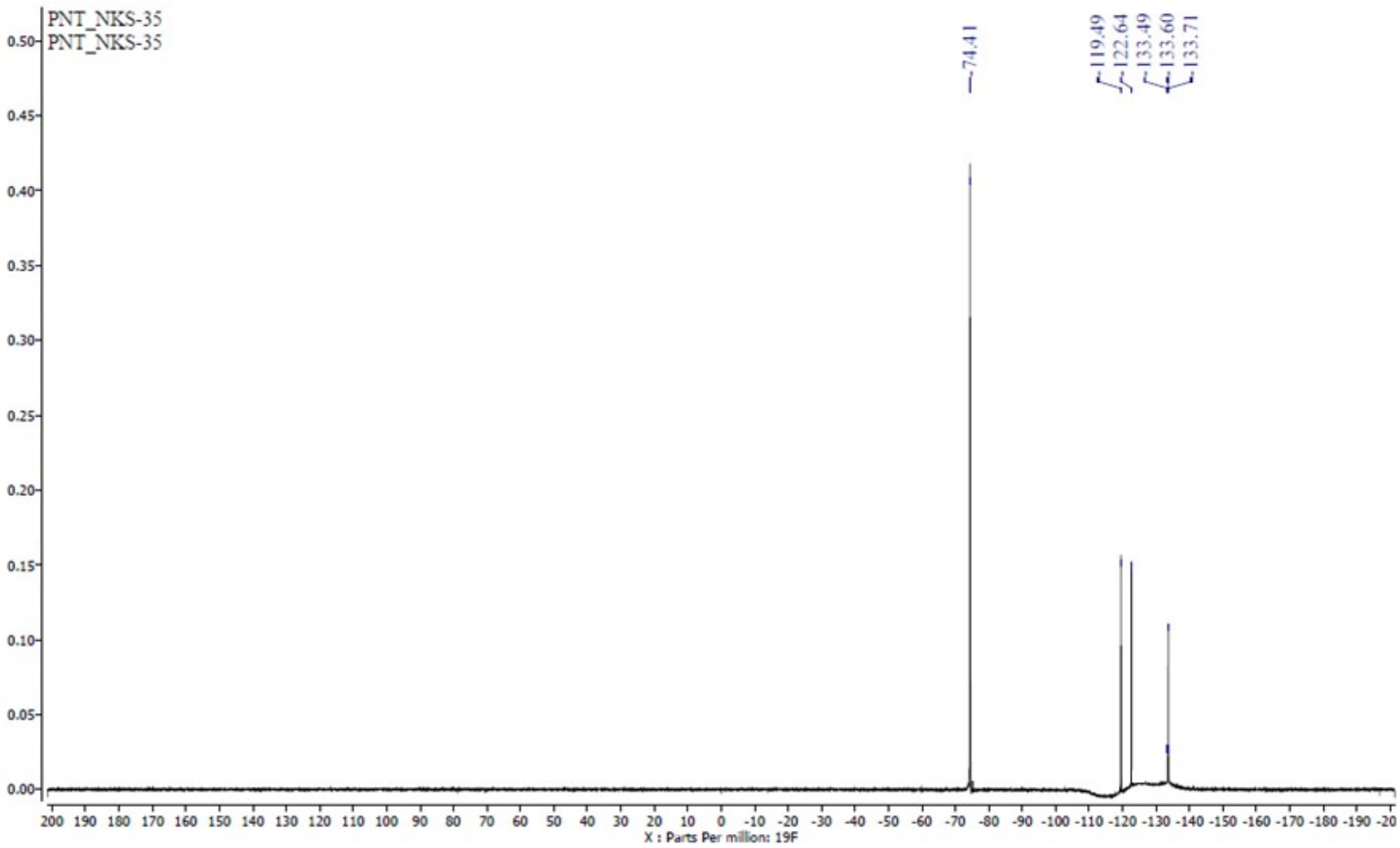

Fig. S22 $^{19}F\{^{1}H\}$ NMR ($CDCl_3$, 376.31MHz) spectrum of complex **6**.

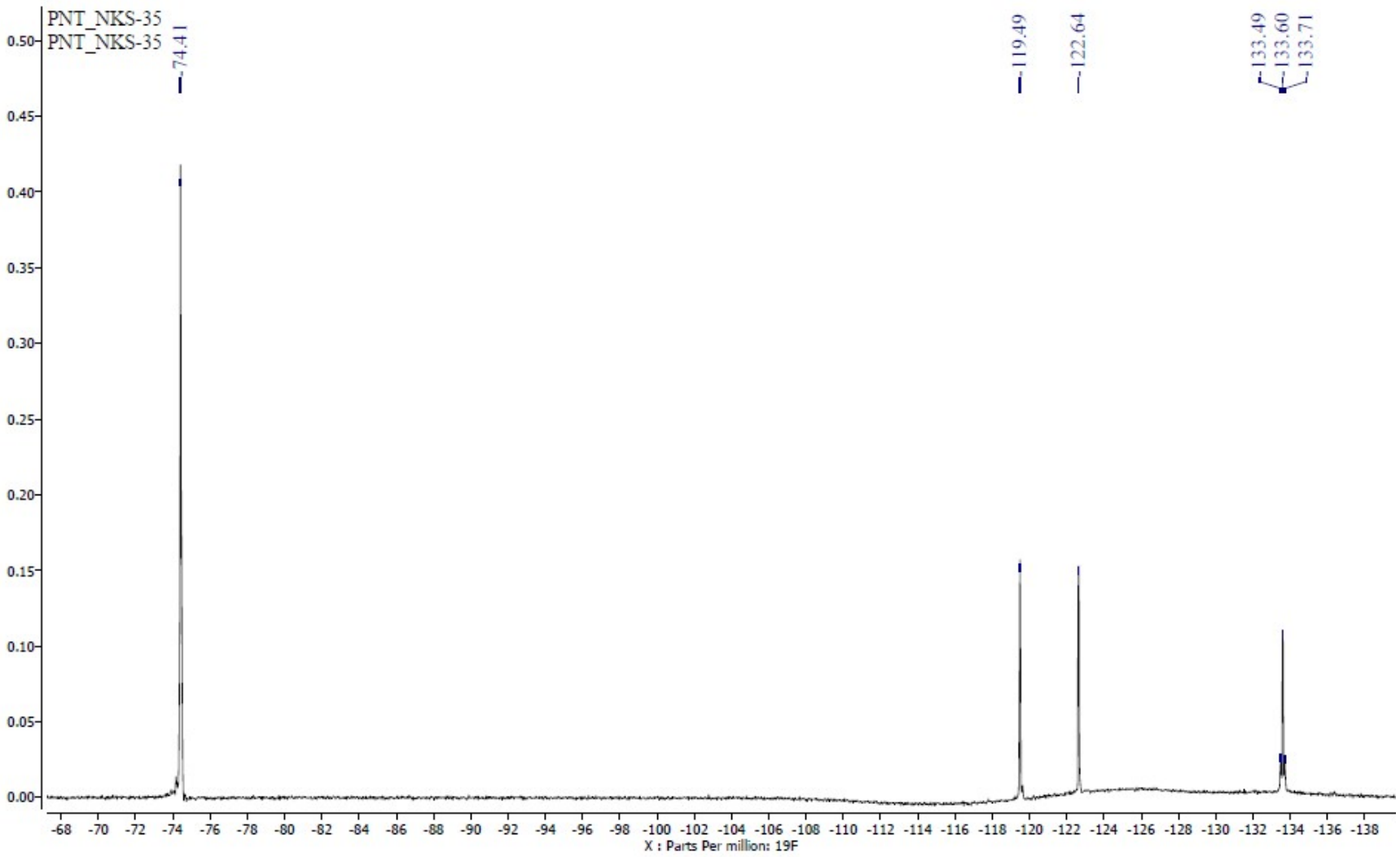

Fig. S23 $^{19}F\{^{1}H\}$ NMR ($CDCl_3$, 376.31MHz) spectrum of complex **6** in the indicated region.

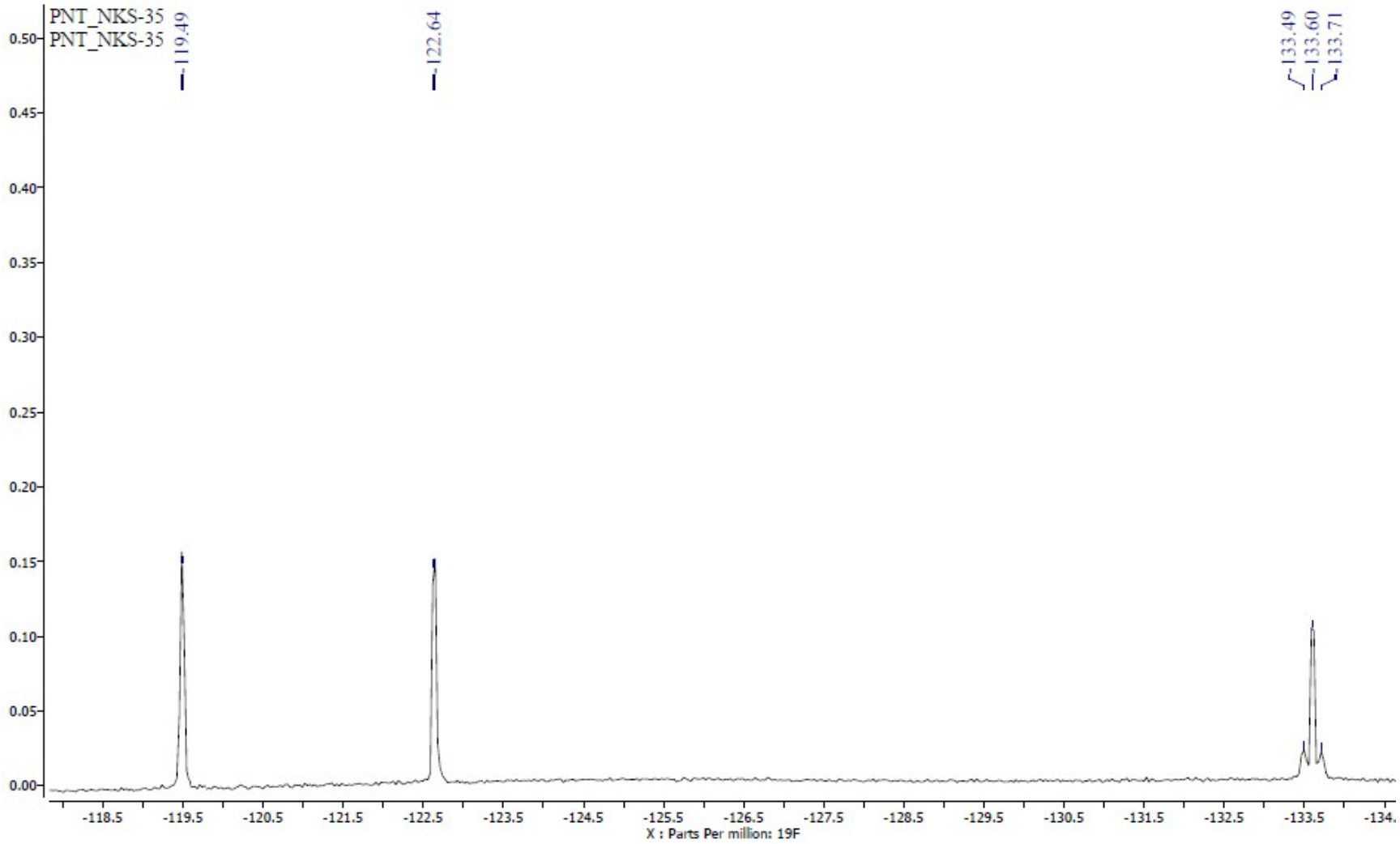

Fig. S24 $^{19}F\{^{1}H\}$ NMR ($CDCl_3$, 376.31MHz) spectrum of complex **6** in the indicated region.

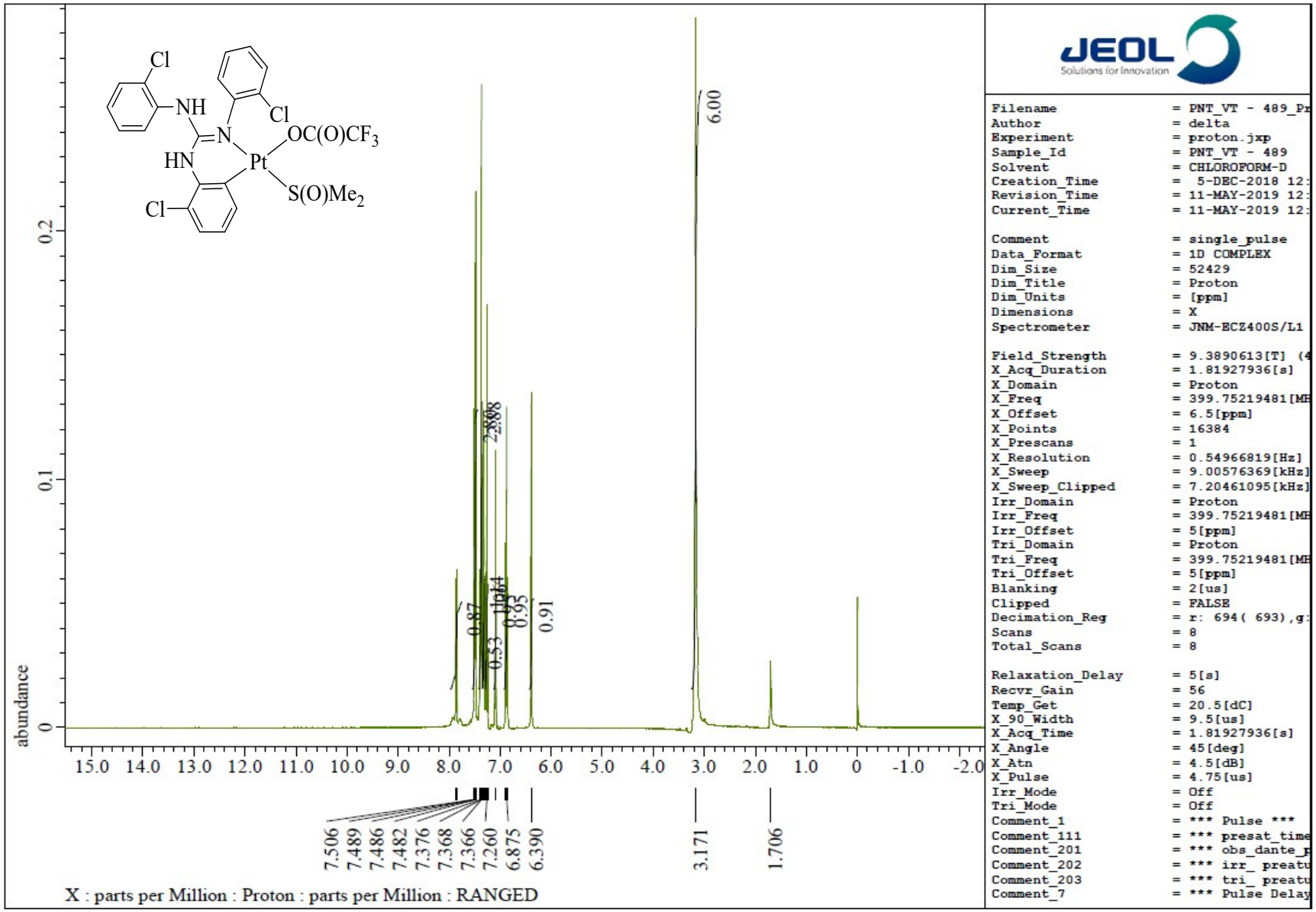

Fig. S25 ^{1}H NMR ($CDCl_3$, 400 MHz) spectrum of **7**.

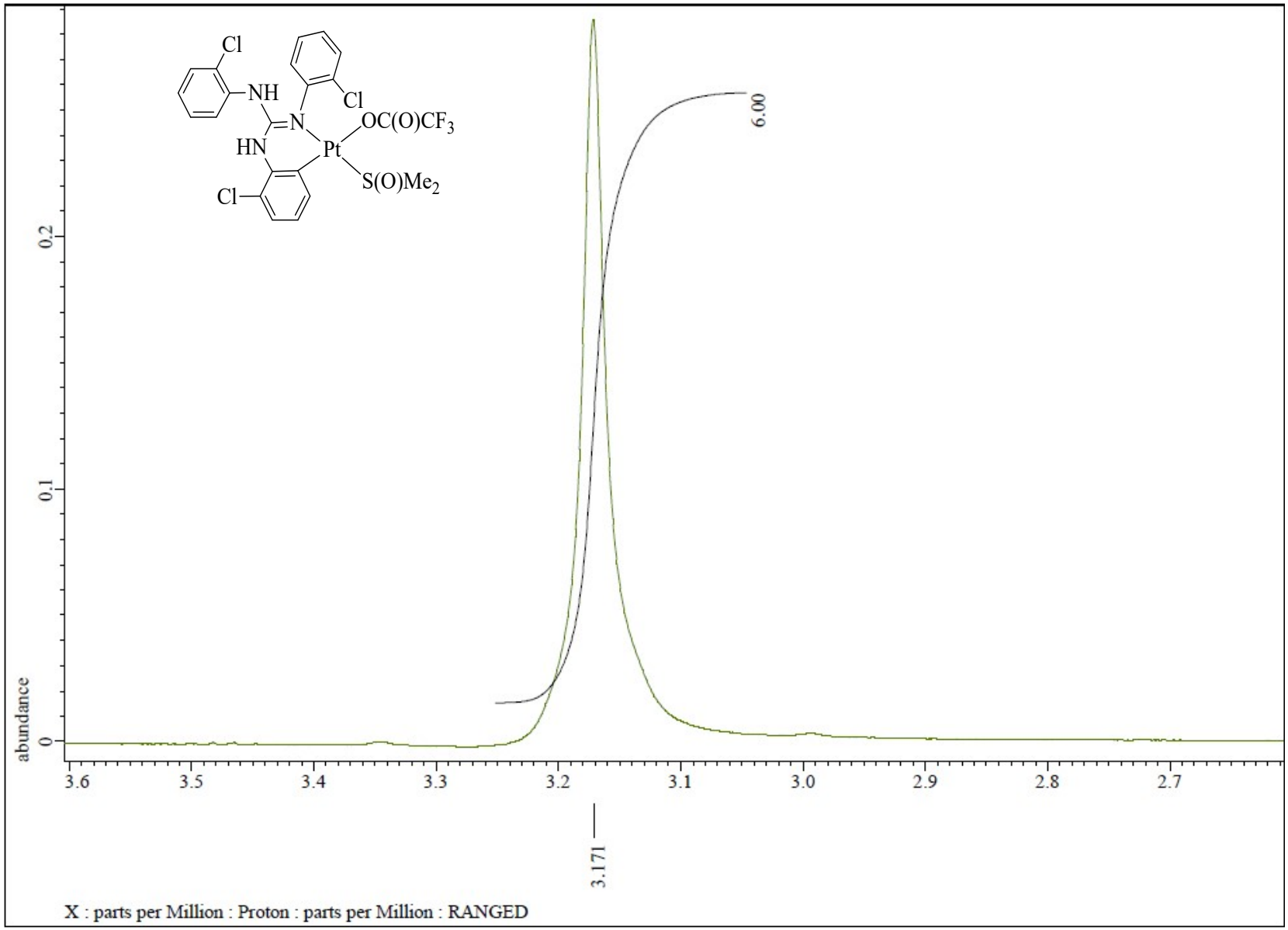

Fig. S26 ^{1}H NMR ($CDCl_3$, 400 MHz) spectrum of **7** in the indicated region.

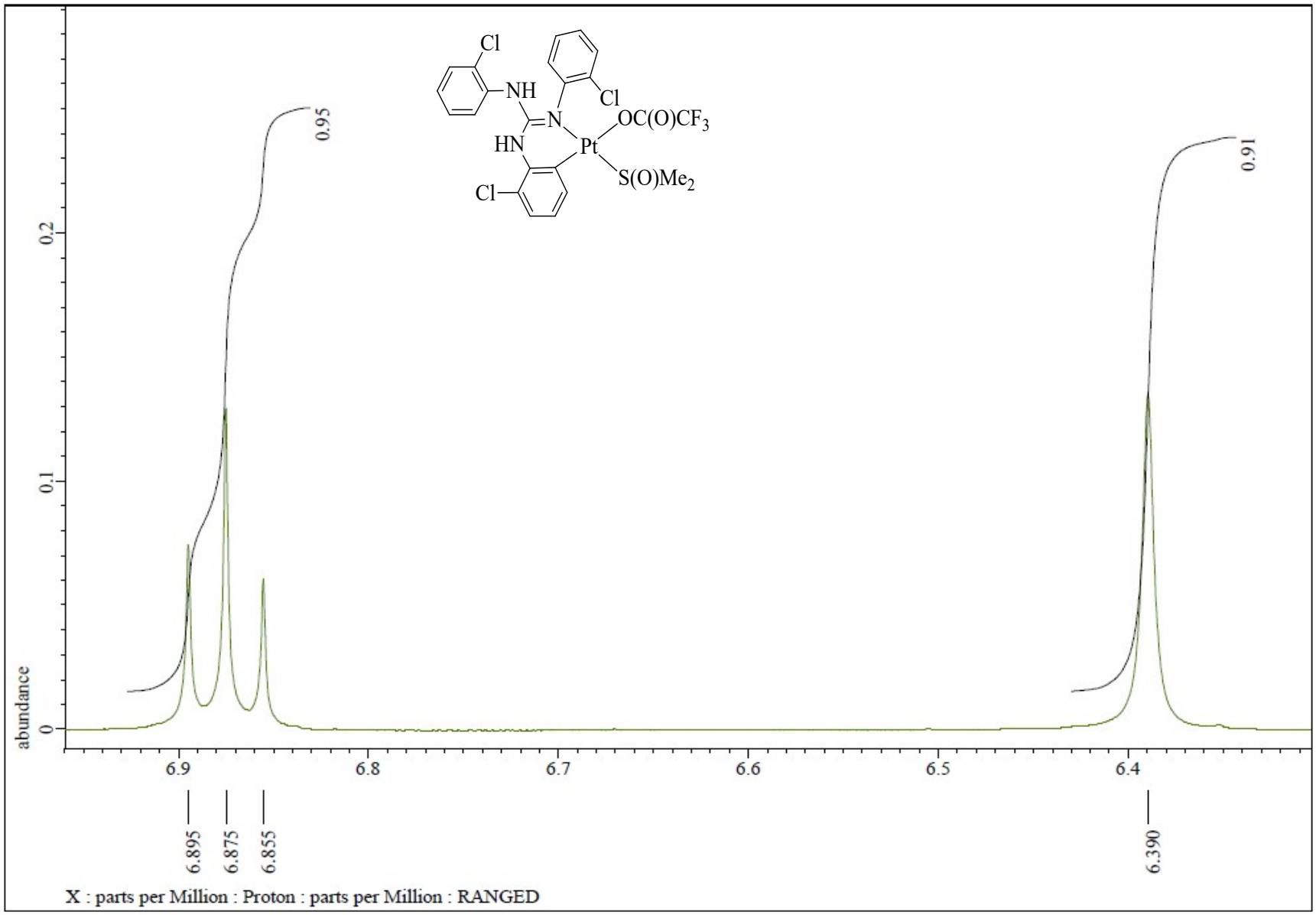

Fig. S27 ^{1}H NMR ($CDCl_3$, 400 MHz) spectrum of **7** in the indicated region.

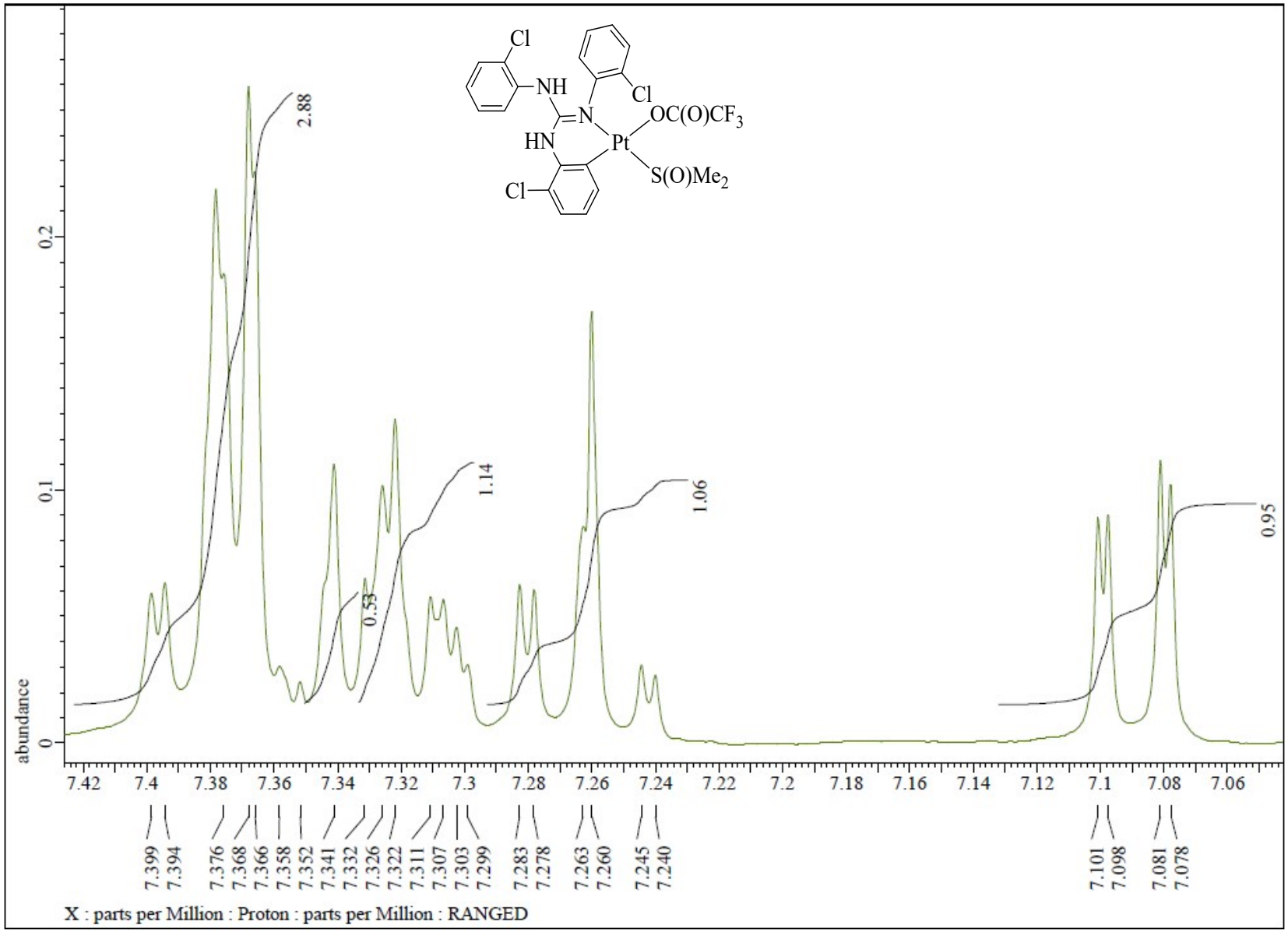

Fig. S28 ^{1}H NMR ($CDCl_3$, 400 MHz) spectrum of **7** in the indicated region.

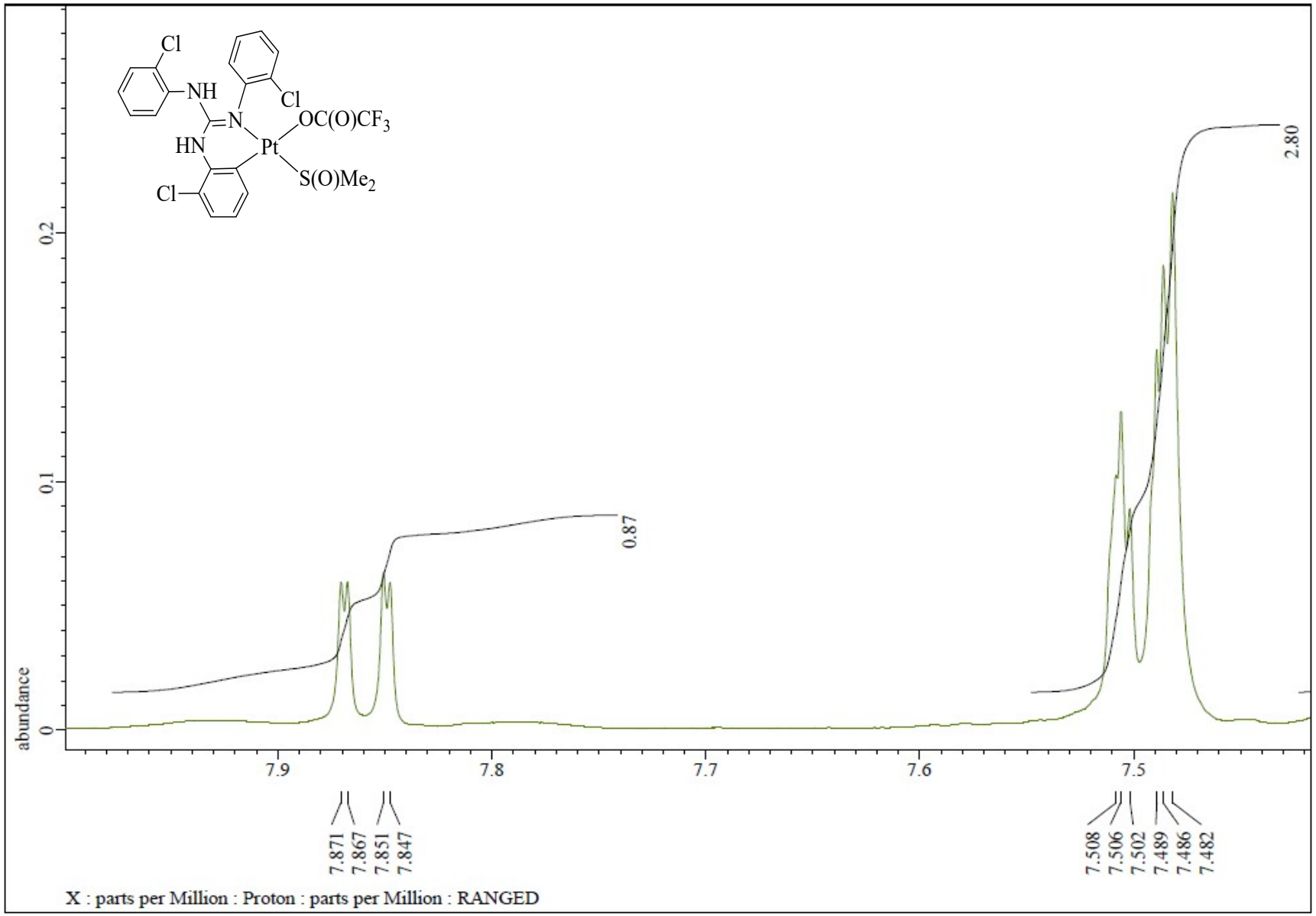

Fig. S29 ^{1}H NMR ($CDCl_3$, 400 MHz) spectrum of **7** in the indicated region.

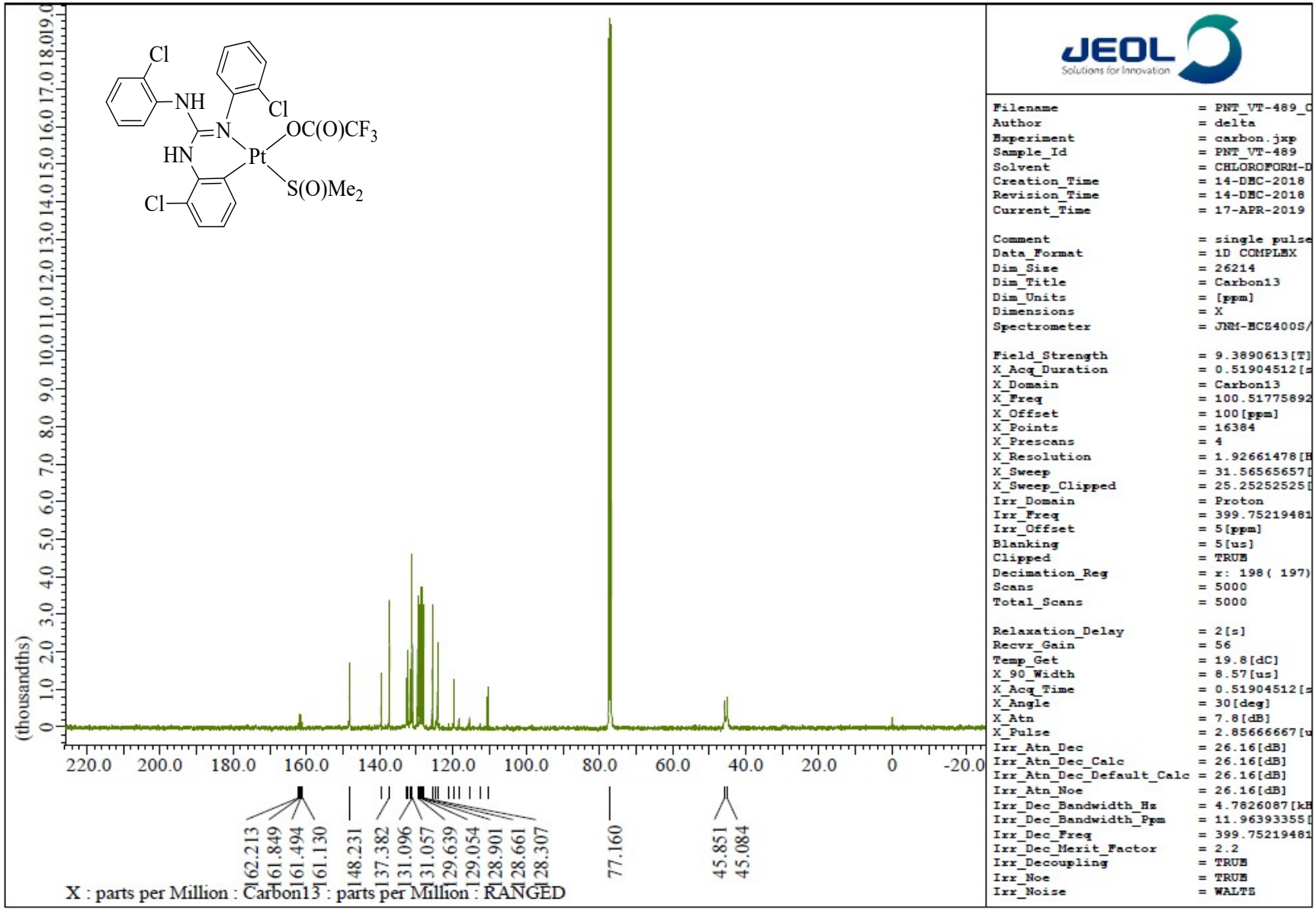

Fig. S30 $^{13}C\{^{1}H\}$ NMR ($CDCl_3$, 100.5 MHz) spectrum of **7**.

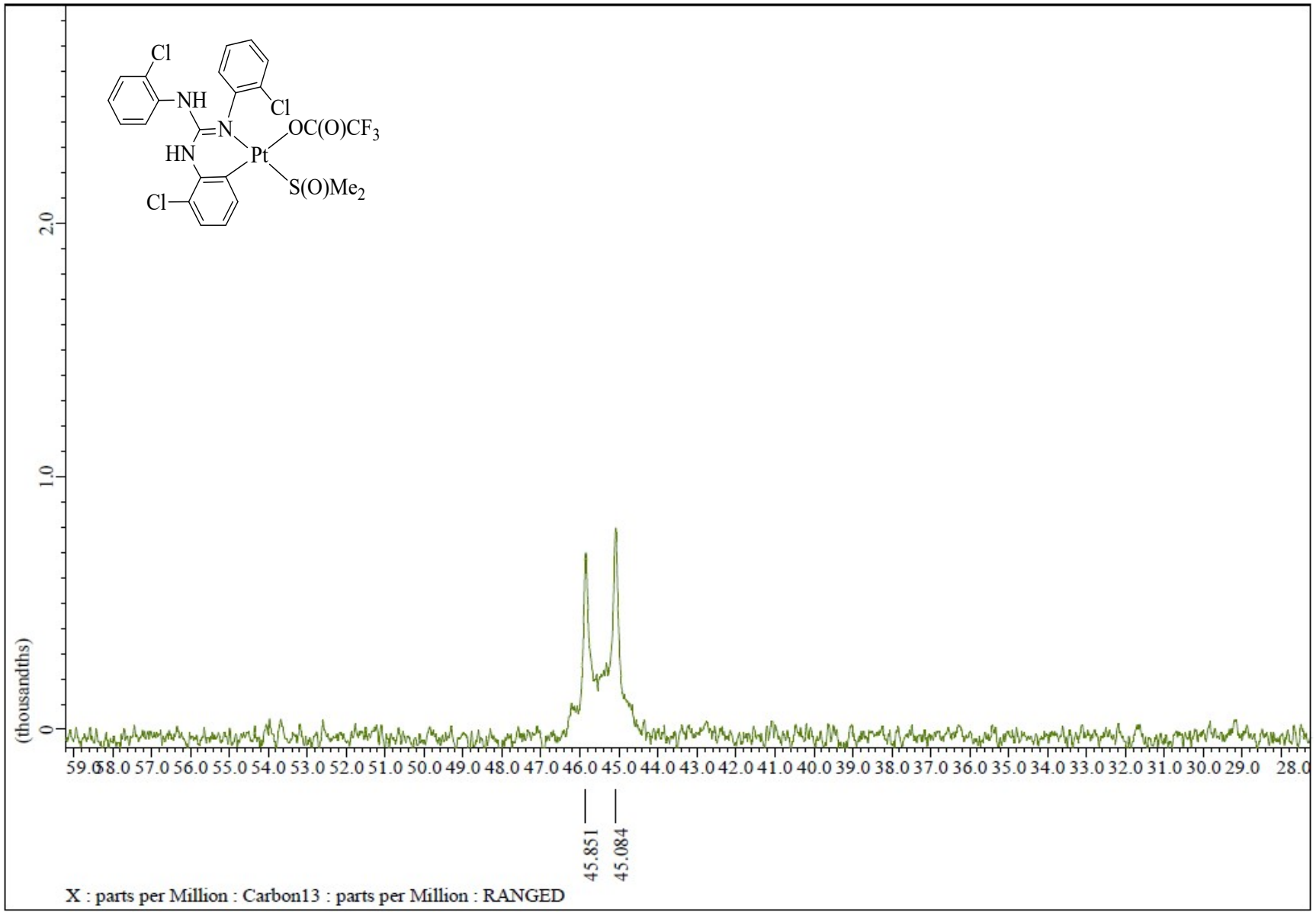

Fig. S31 $^{13}C\{^{1}H\}$ NMR ($CDCl_3$, 100.5 MHz) spectrum of **7** in the indicated region.

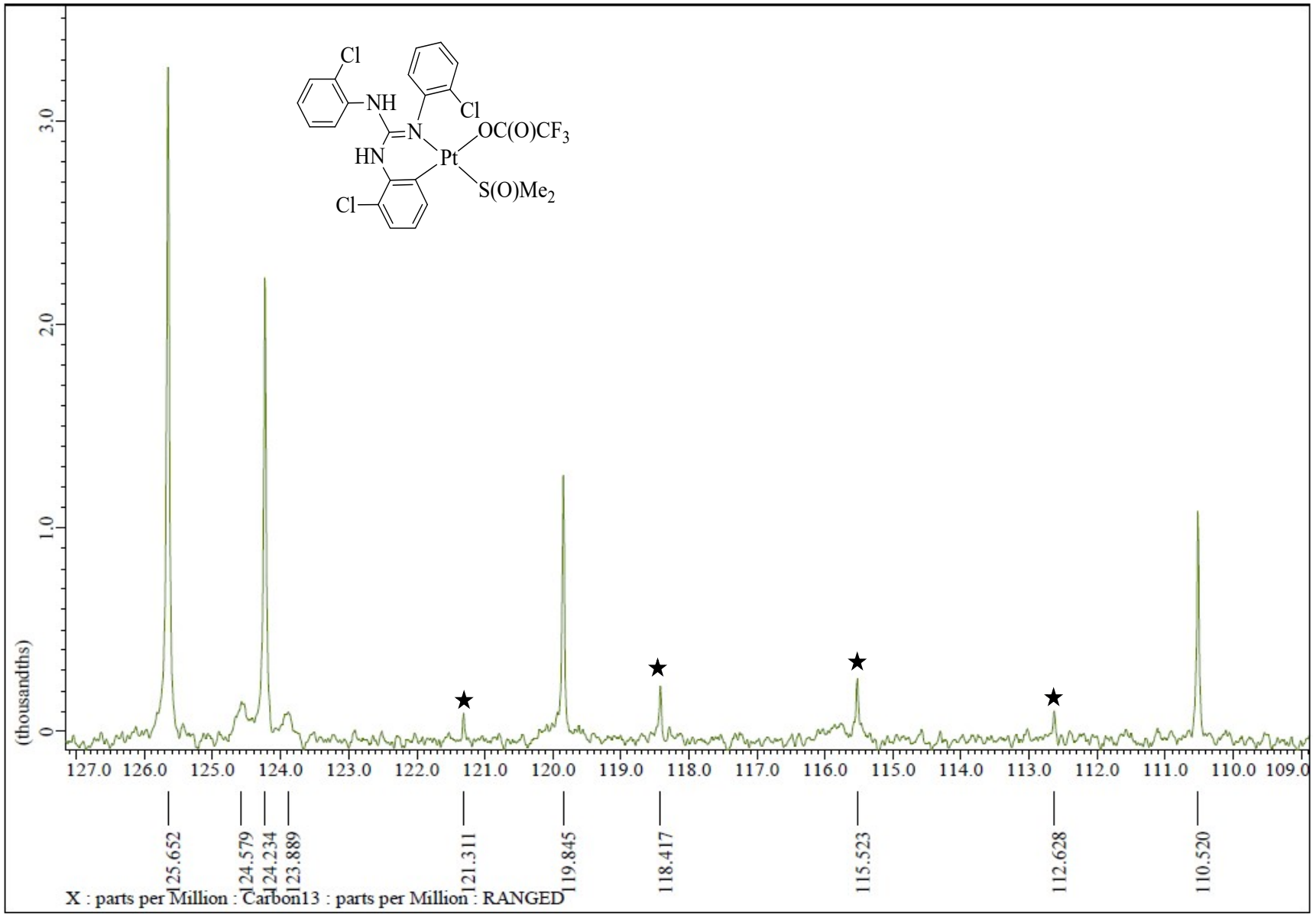

Fig. S32 $^{13}C\{^{1}H\}$ NMR ($CDCl_3$, 100.5 MHz) spectrum of **7** in the indicated region.

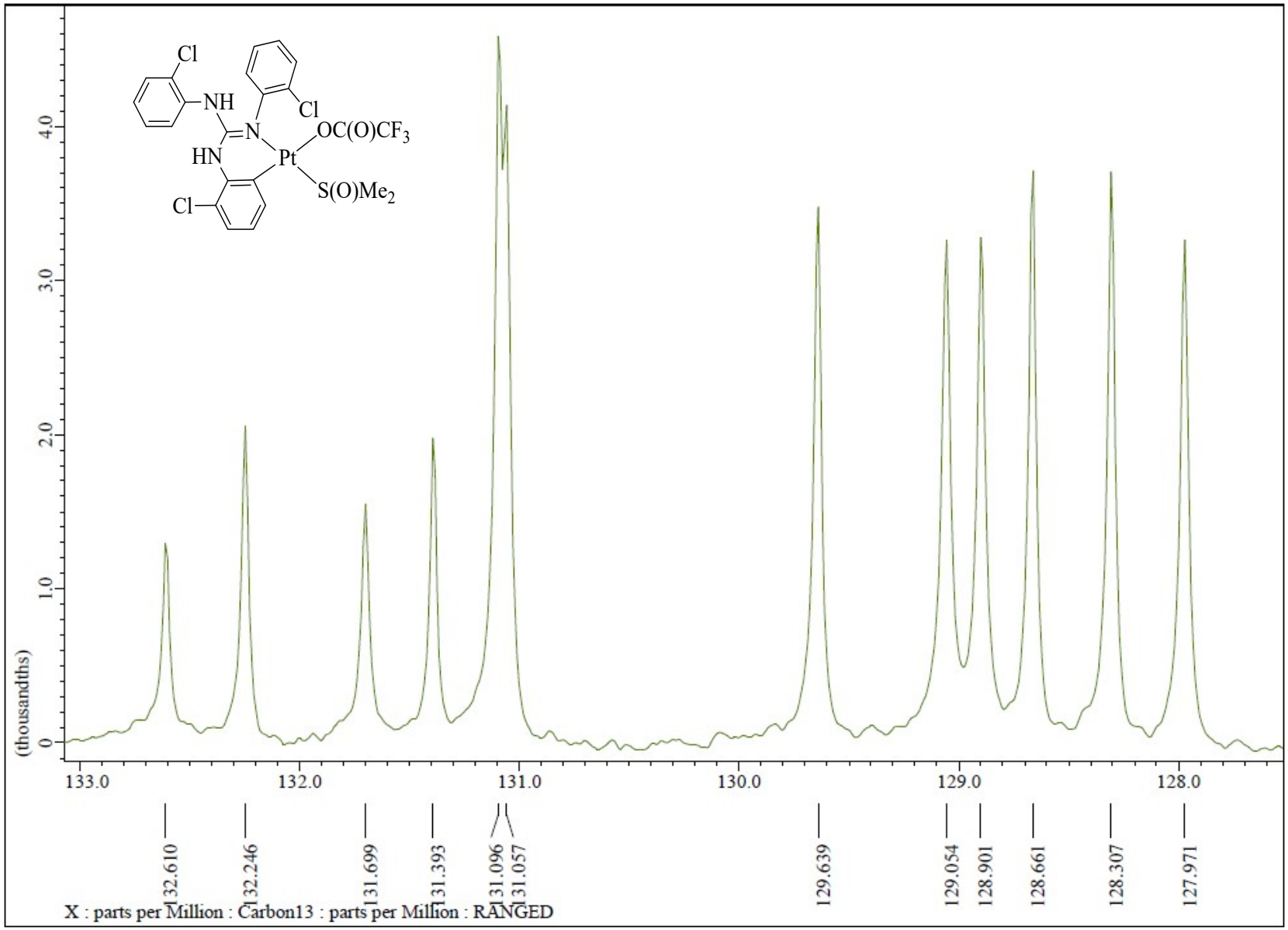

Fig. S33 $^{13}C\{^{1}H\}$ NMR ($CDCl_3$, 100.5 MHz) spectrum of **7** in the indicated region.

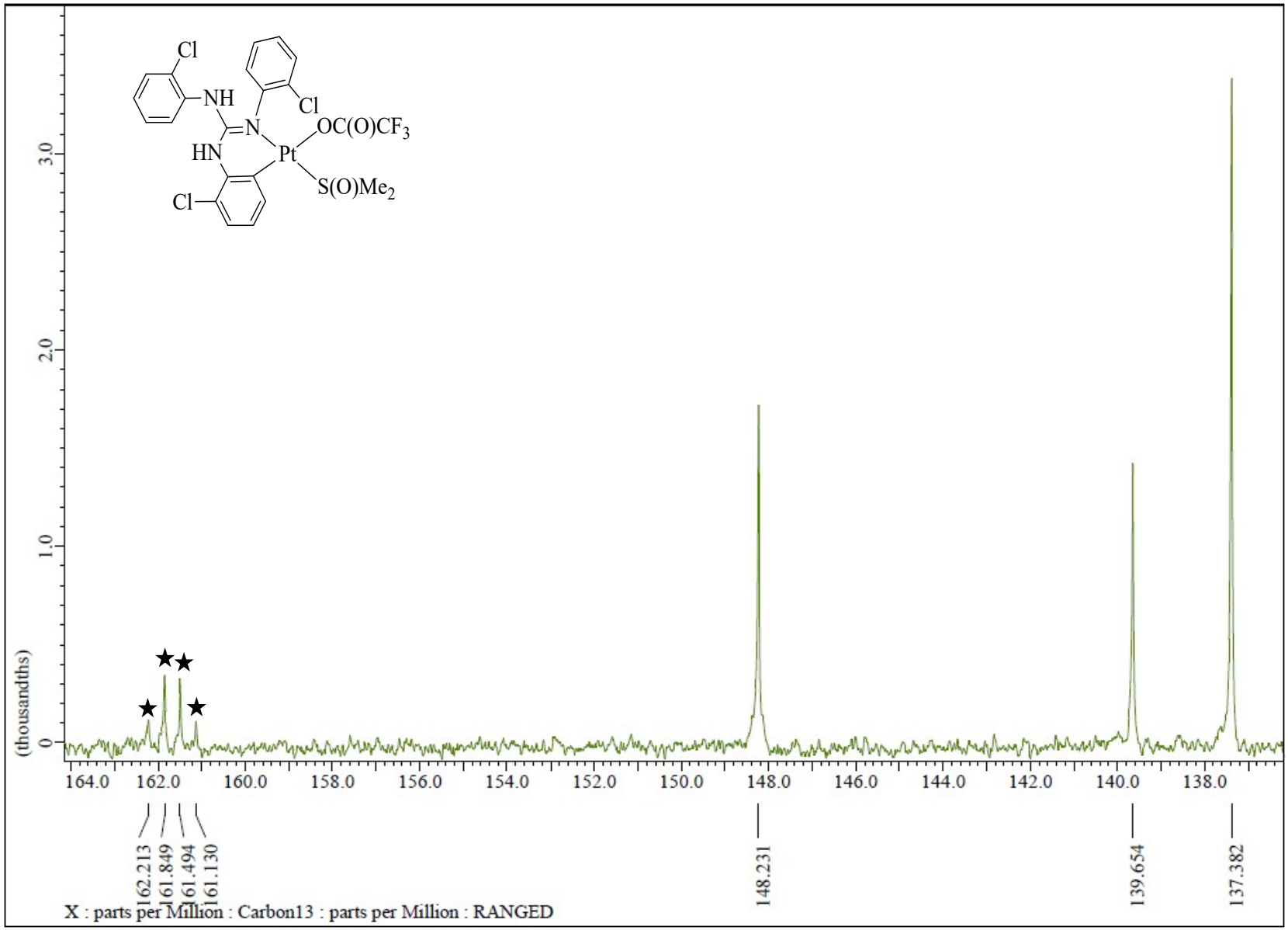

Fig. S34 $^{13}C\{^{1}H\}$ NMR ($CDCl_3$, 100.5 MHz) spectrum of **7** in the indicated region.

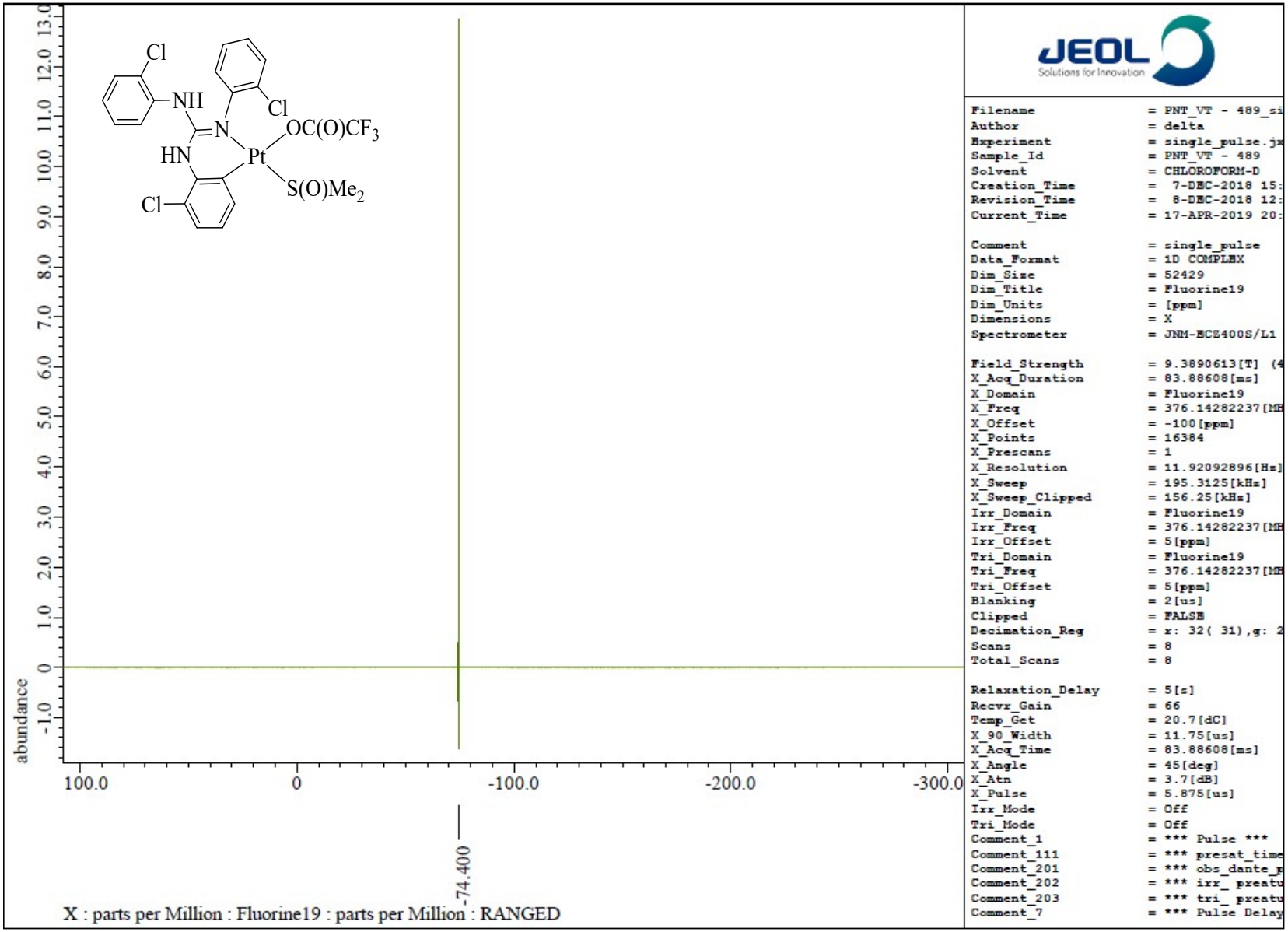

Fig. S35 $^{19}F\{^{1}H\}$ NMR ($CDCl_3$, 376.31 MHz) spectrum of **7**.

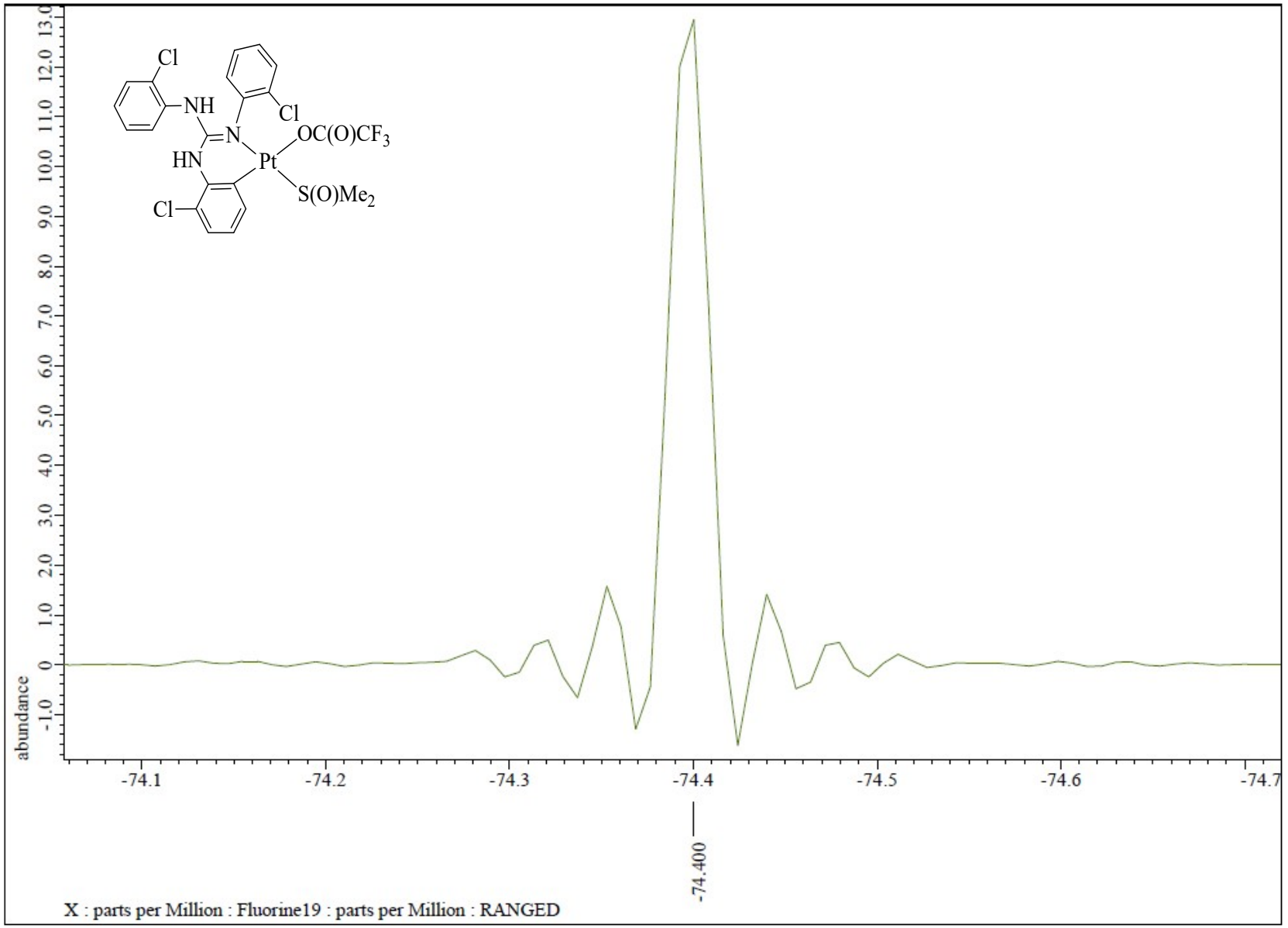

Fig. S36 $^{19}F\{^{1}H\}$ NMR ($CDCl_3$, 376.31 MHz) spectrum of **7** in the indicated region.

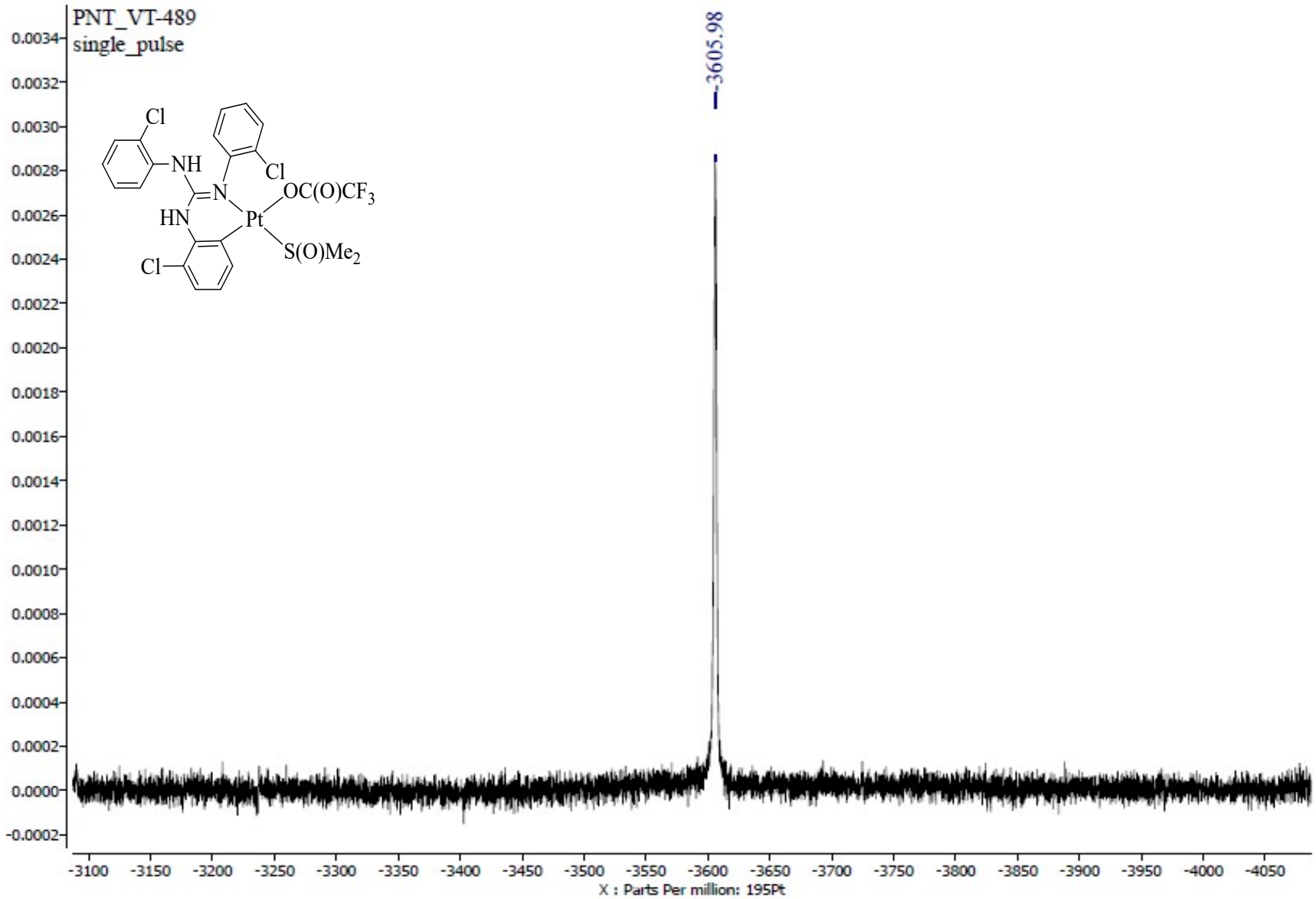

Fig. S37 $^{195}Pt\{^{1}H\}$ NMR ($CDCl_3$, 85.8 MHz) spectrum of **7**.

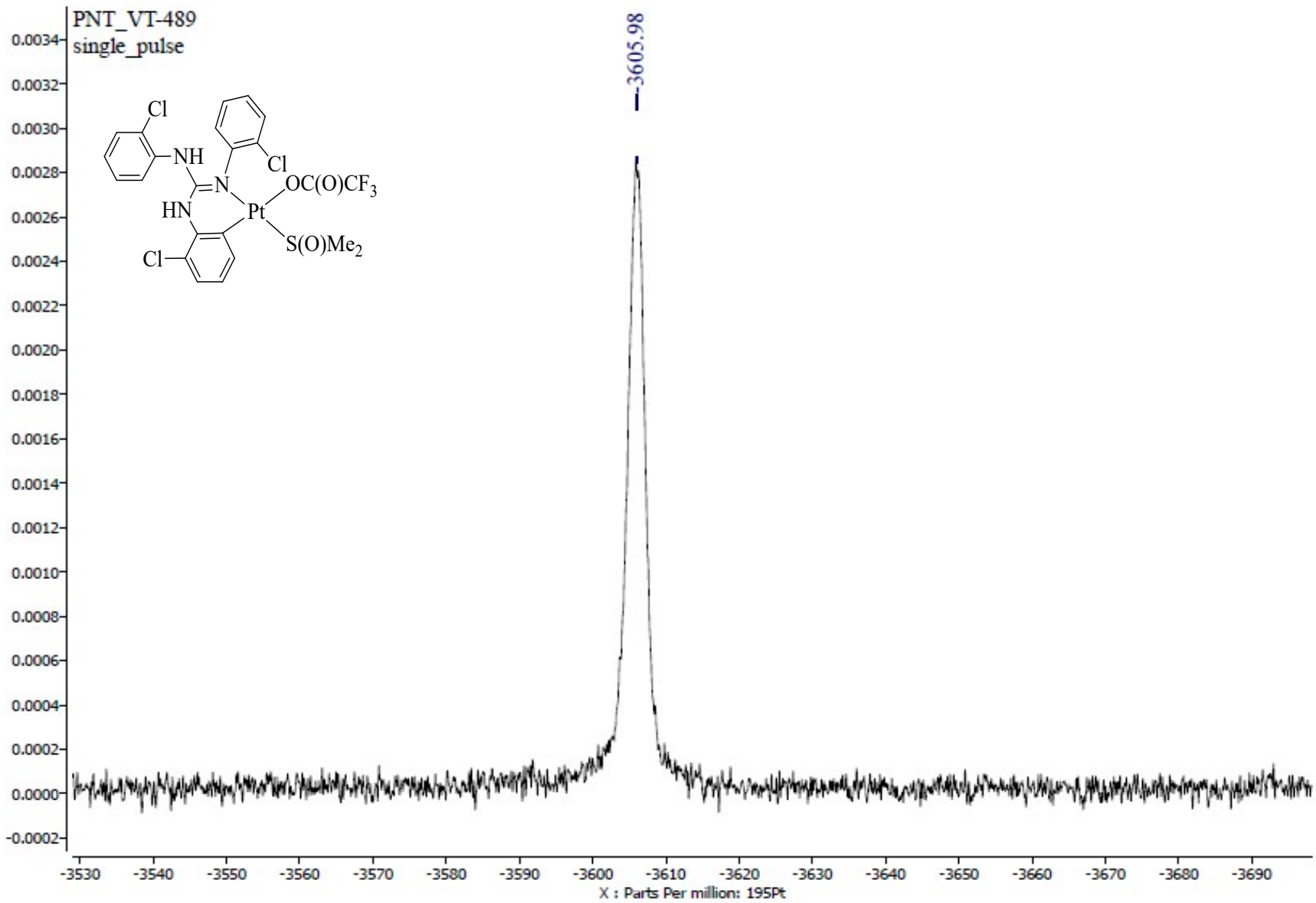

Fig. S38 $^{195}Pt\{^{1}H\}$ NMR ($CDCl_3$, 85.8 MHz) spectrum of **27**.

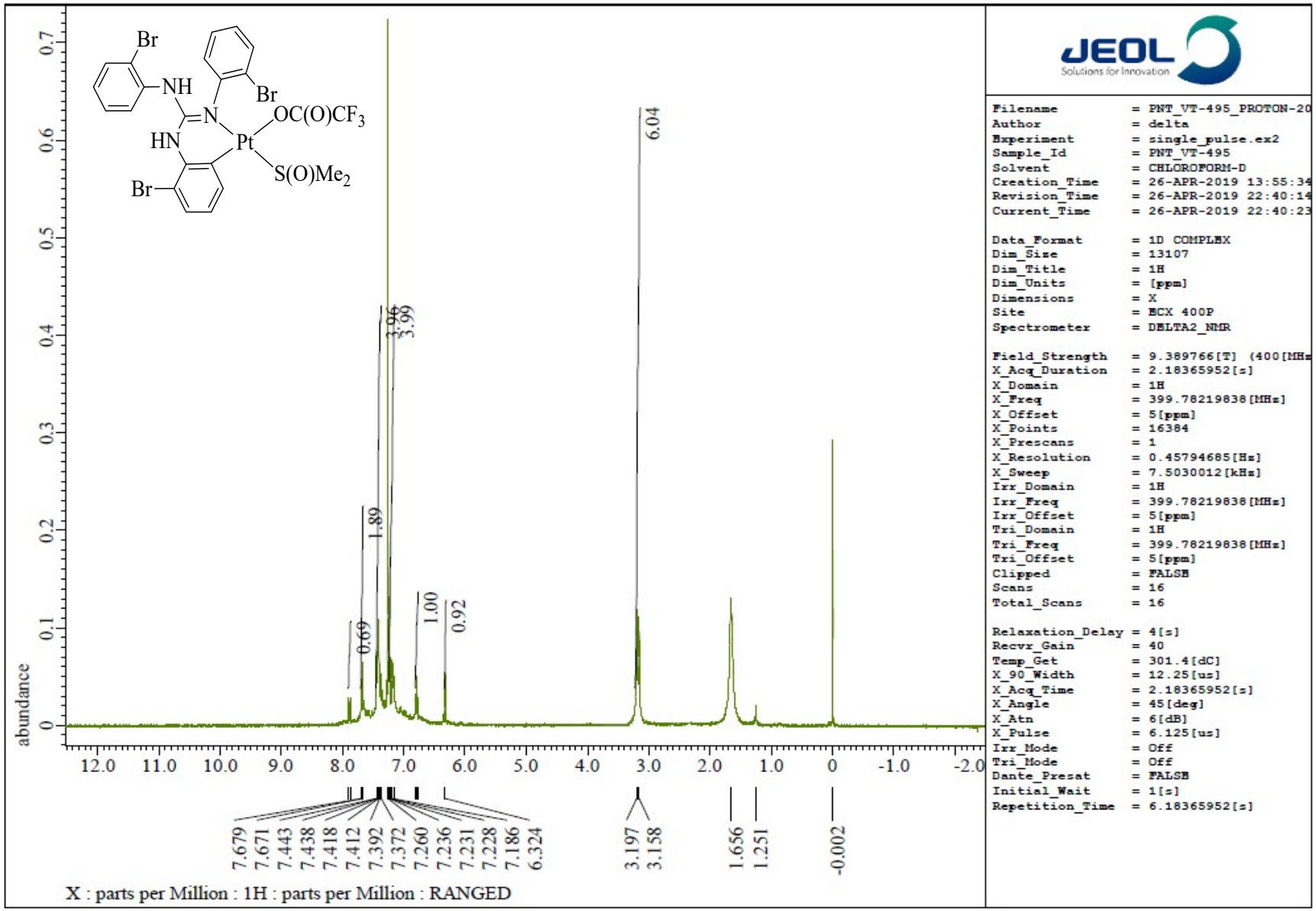

Fig. S39 ^{1}H NMR ($CDCl_3$, 400 MHz) spectrum of **8**.

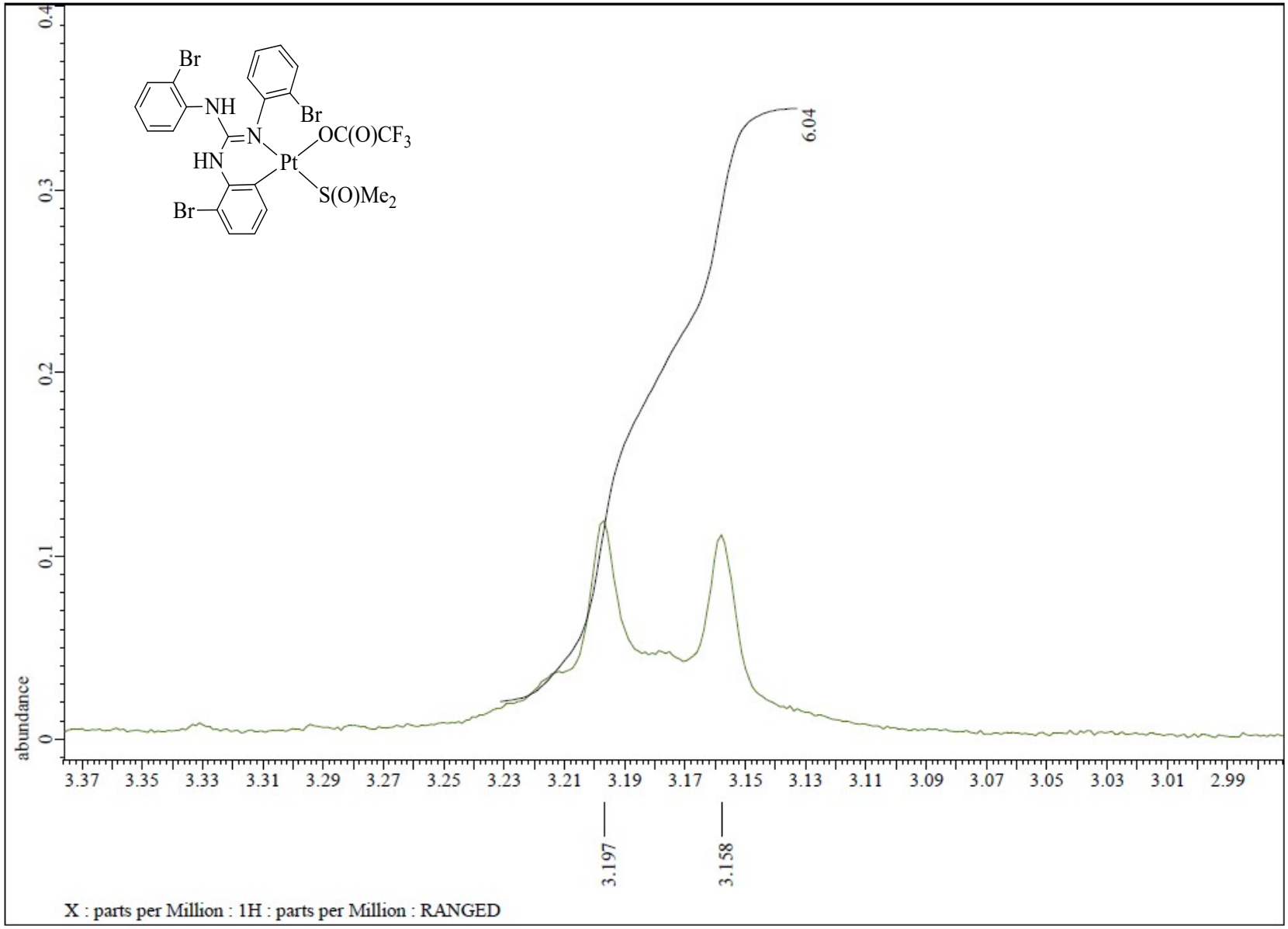

Fig. S40 ^{1}H NMR ($CDCl_3$, 400 MHz) spectrum of **8** in the indicated region.

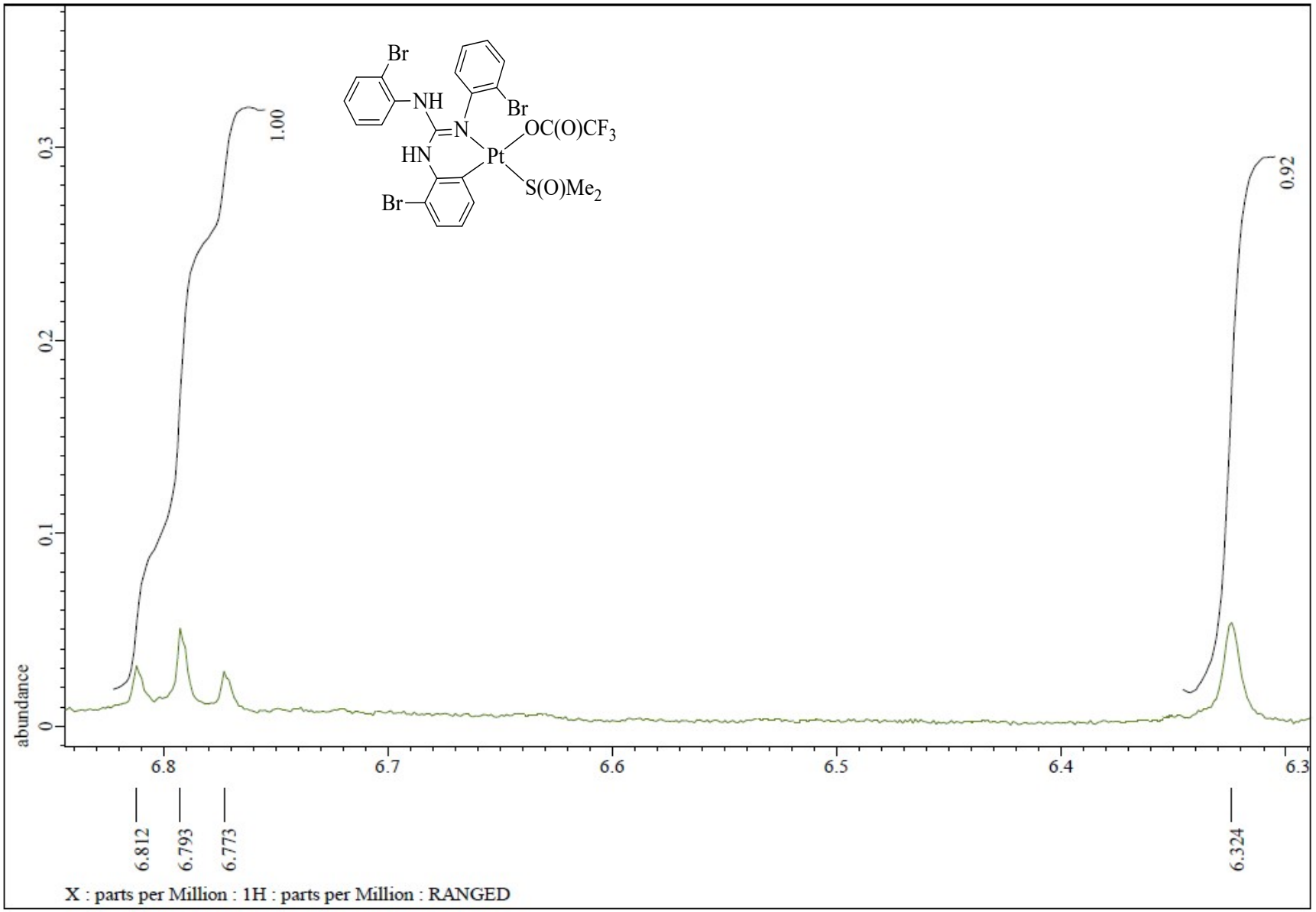

Fig. S41 ^{1}H NMR ($CDCl_3$, 400 MHz) spectrum of **8** in the indicated region.

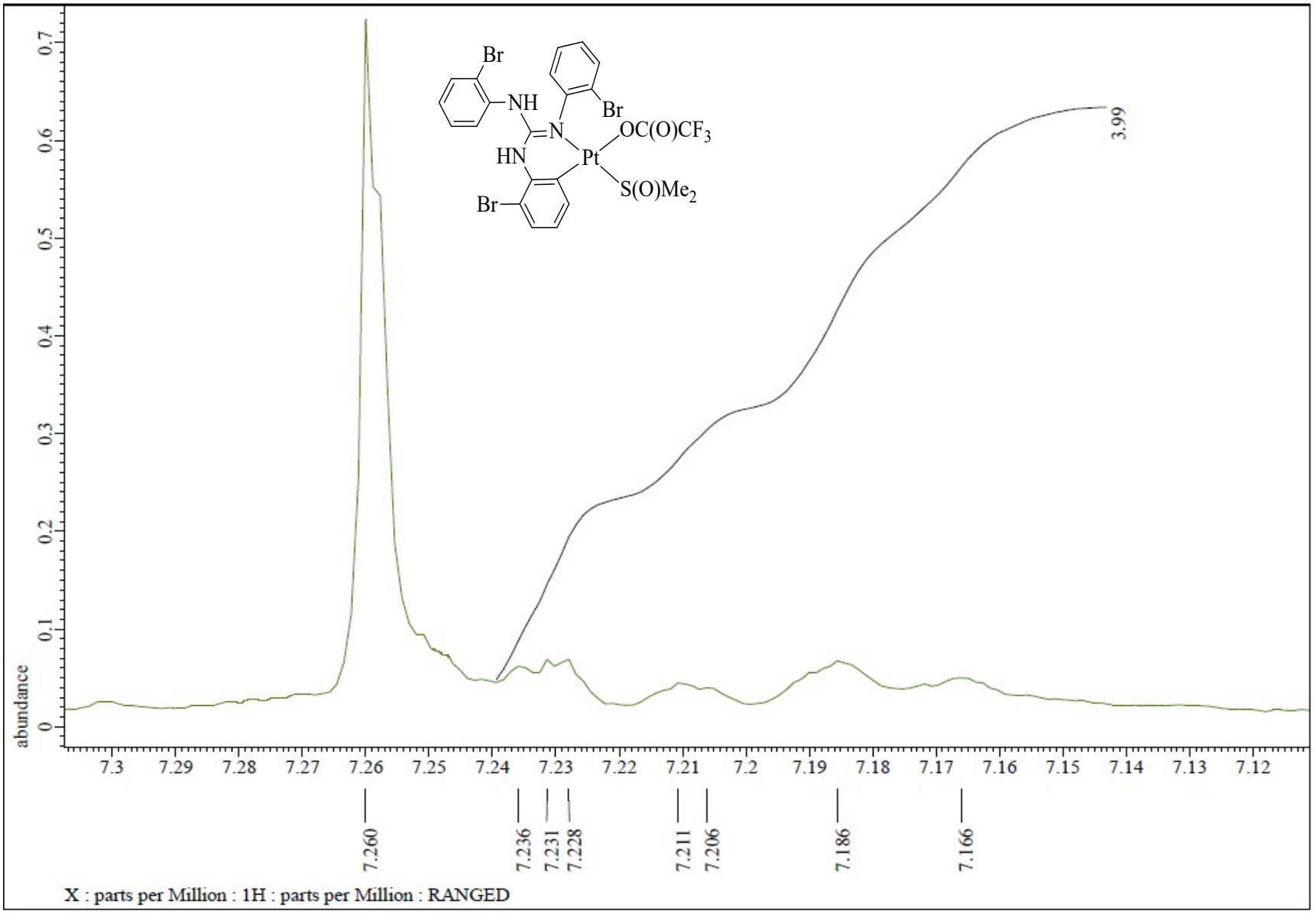

Fig. S42 ^{1}H NMR ($CDCl_3$, 400 MHz) spectrum of **8** in the indicated region.

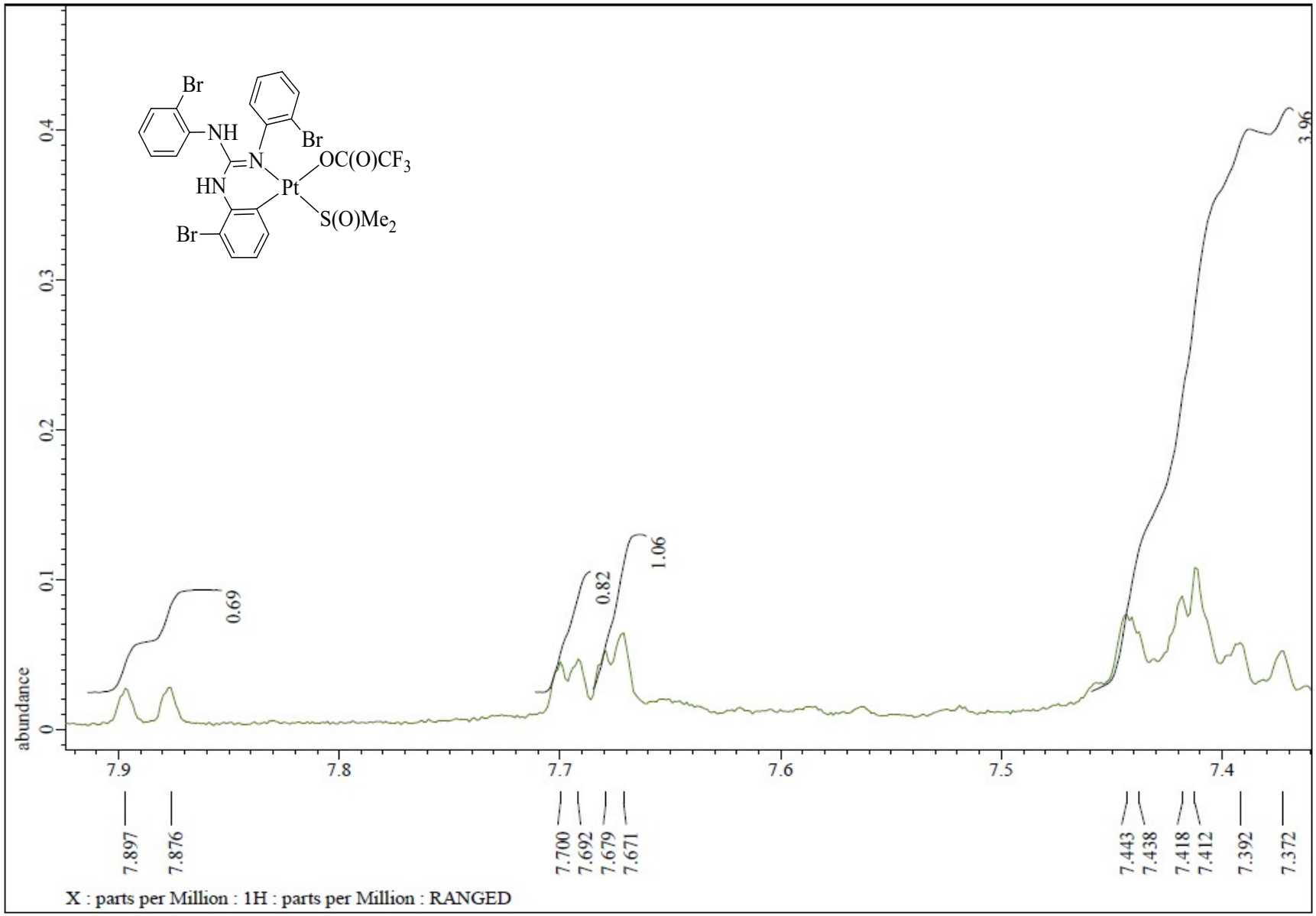

Fig. S43 ^{1}H NMR ($CDCl_3$, 400 MHz) spectrum of **8** in the indicated region.

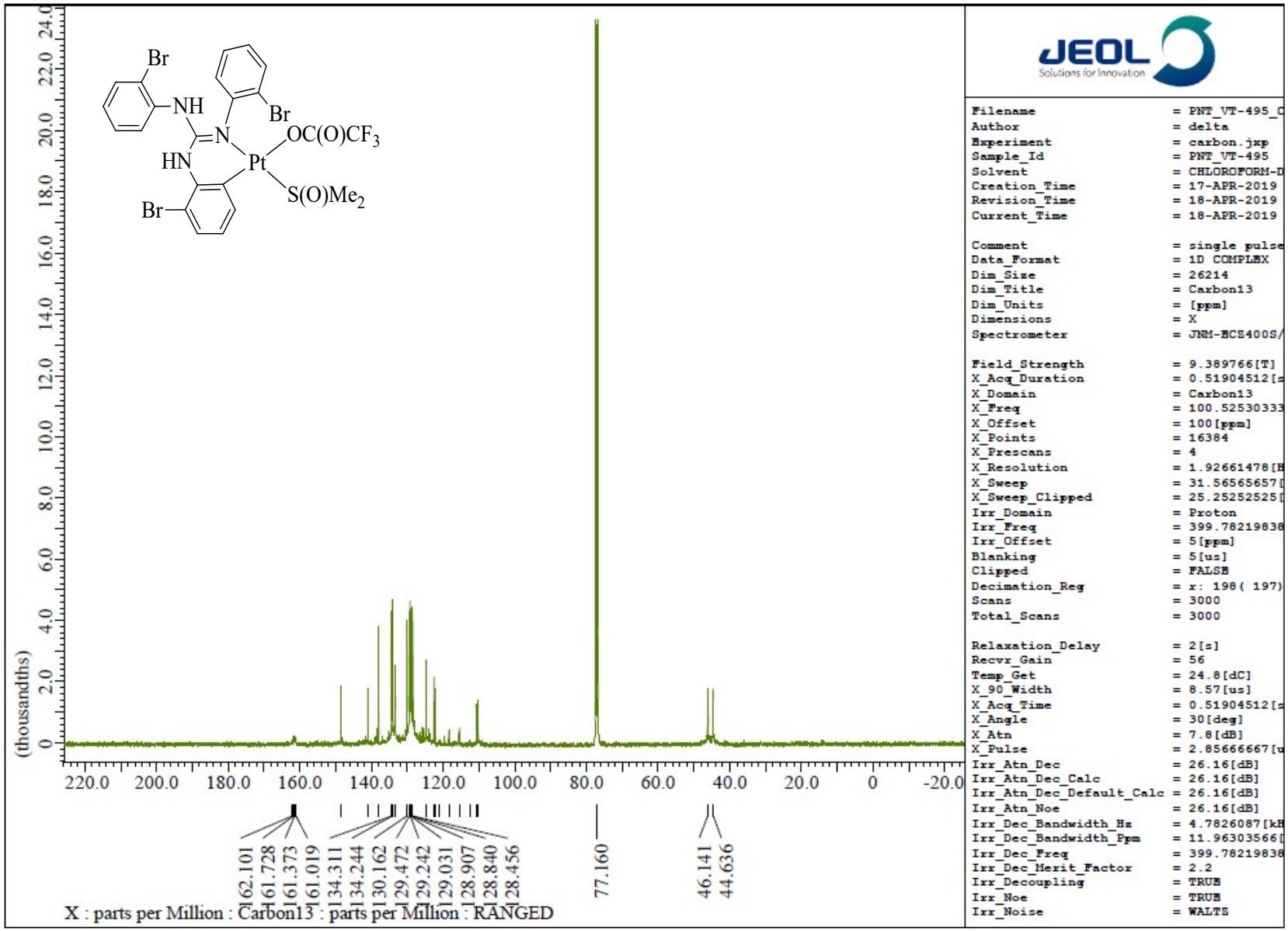

Fig. S44 ^{13}C NMR ($CDCl_3$, 100.5 MHz) spectrum of **8**.

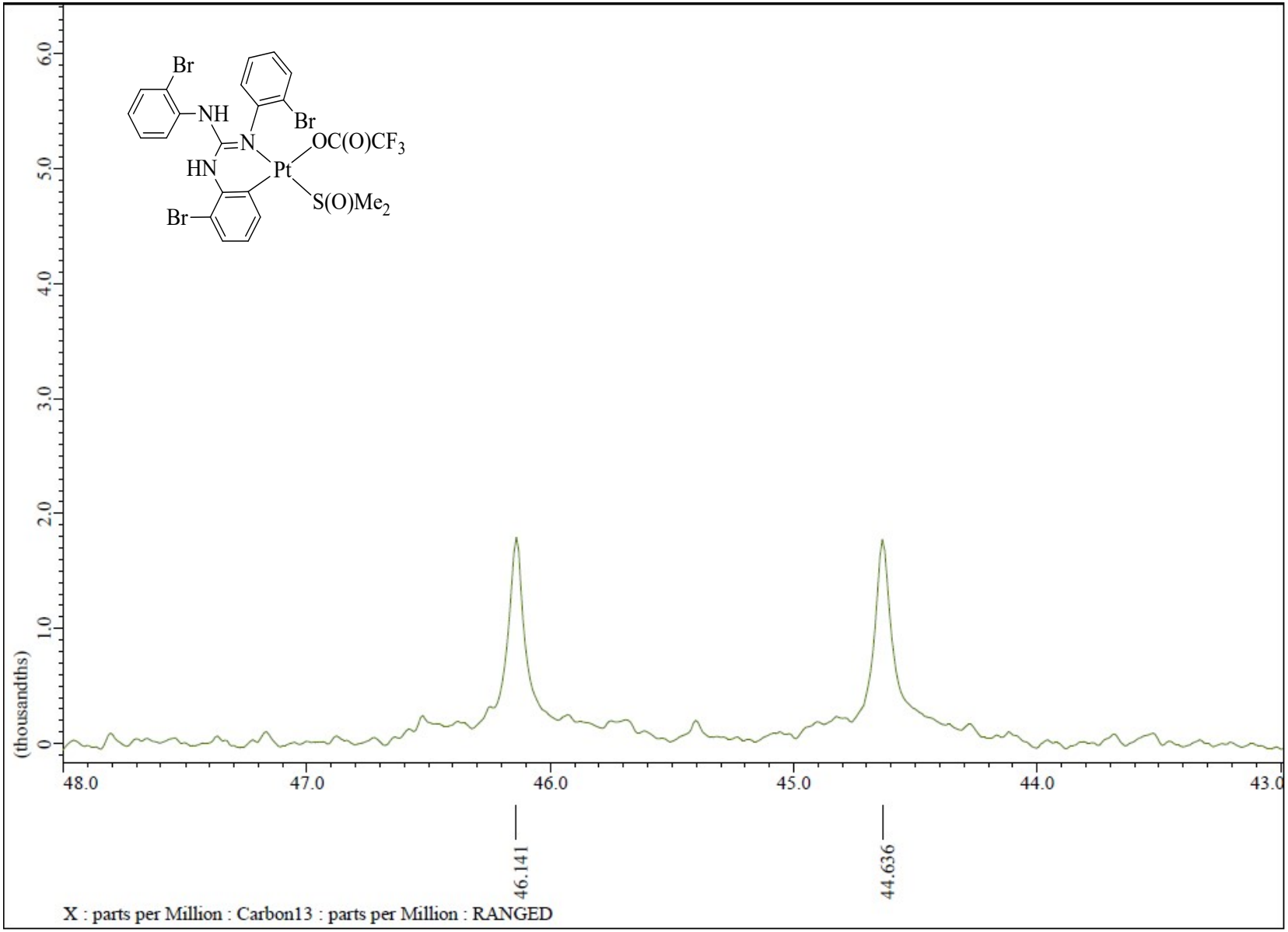

Fig. S45 ^{13}C NMR ($CDCl_3$, 100.5 MHz) spectrum of **8** in the indicated region.

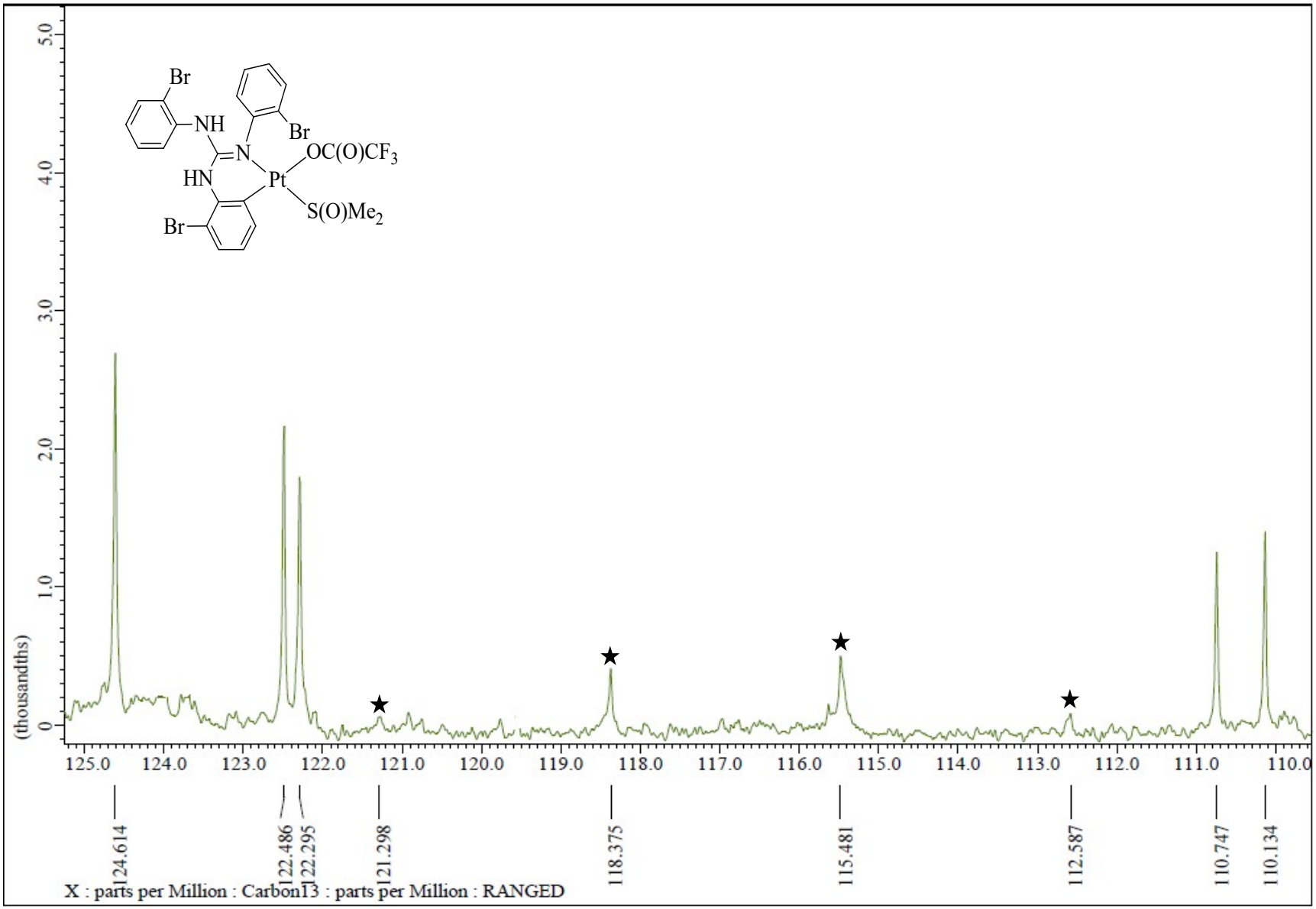

Fig. S46 ^{13}C NMR ($CDCl_3$, 100.5 MHz) spectrum of **8** in the indicated region.

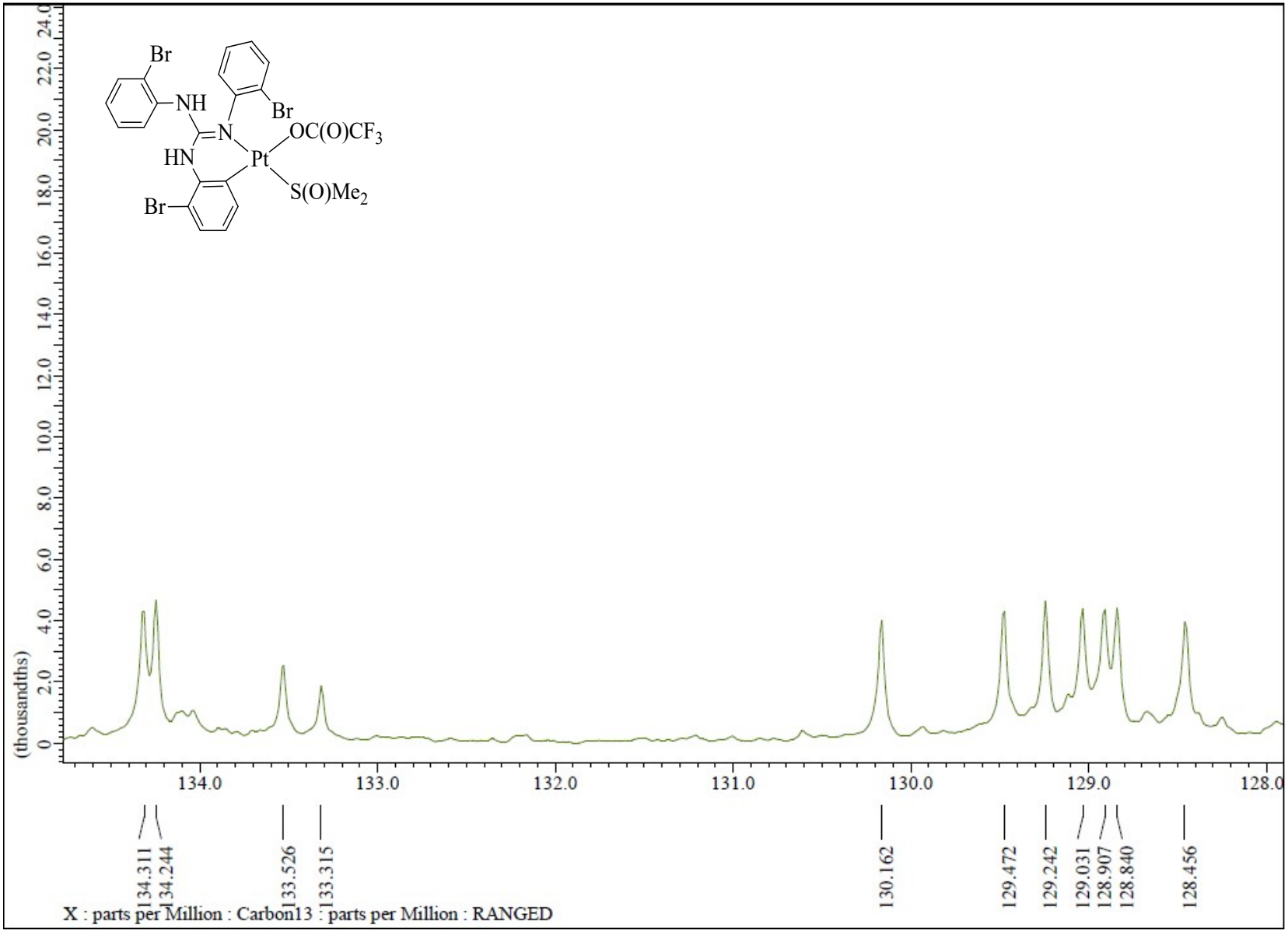

Fig. S47 ^{13}C NMR ($CDCl_3$, 100.5 MHz) spectrum of **8** in the indicated region.

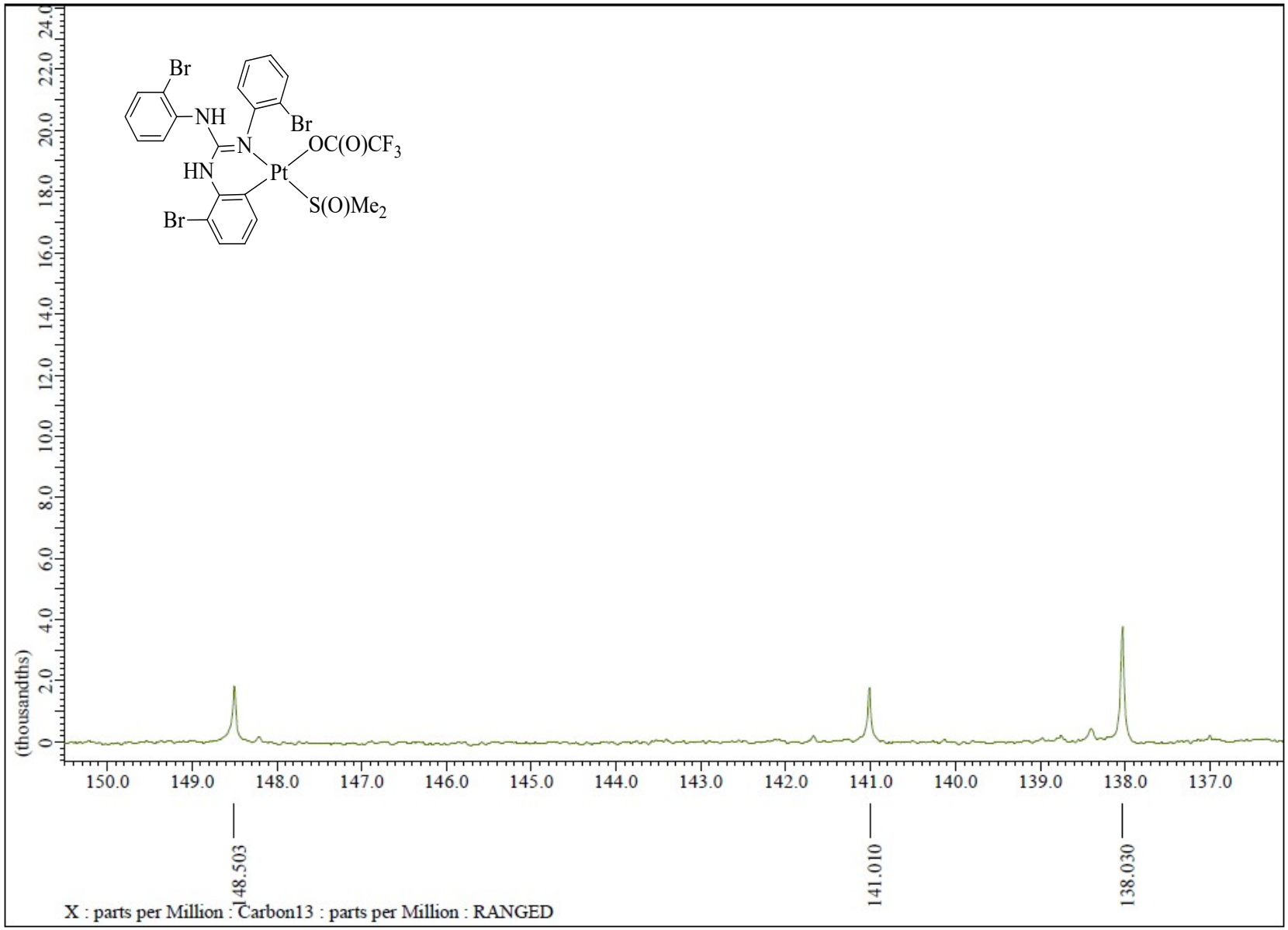

Fig. S48 ^{13}C NMR ($CDCl_3$, 100.5 MHz) spectrum of **8** in the indicated region.

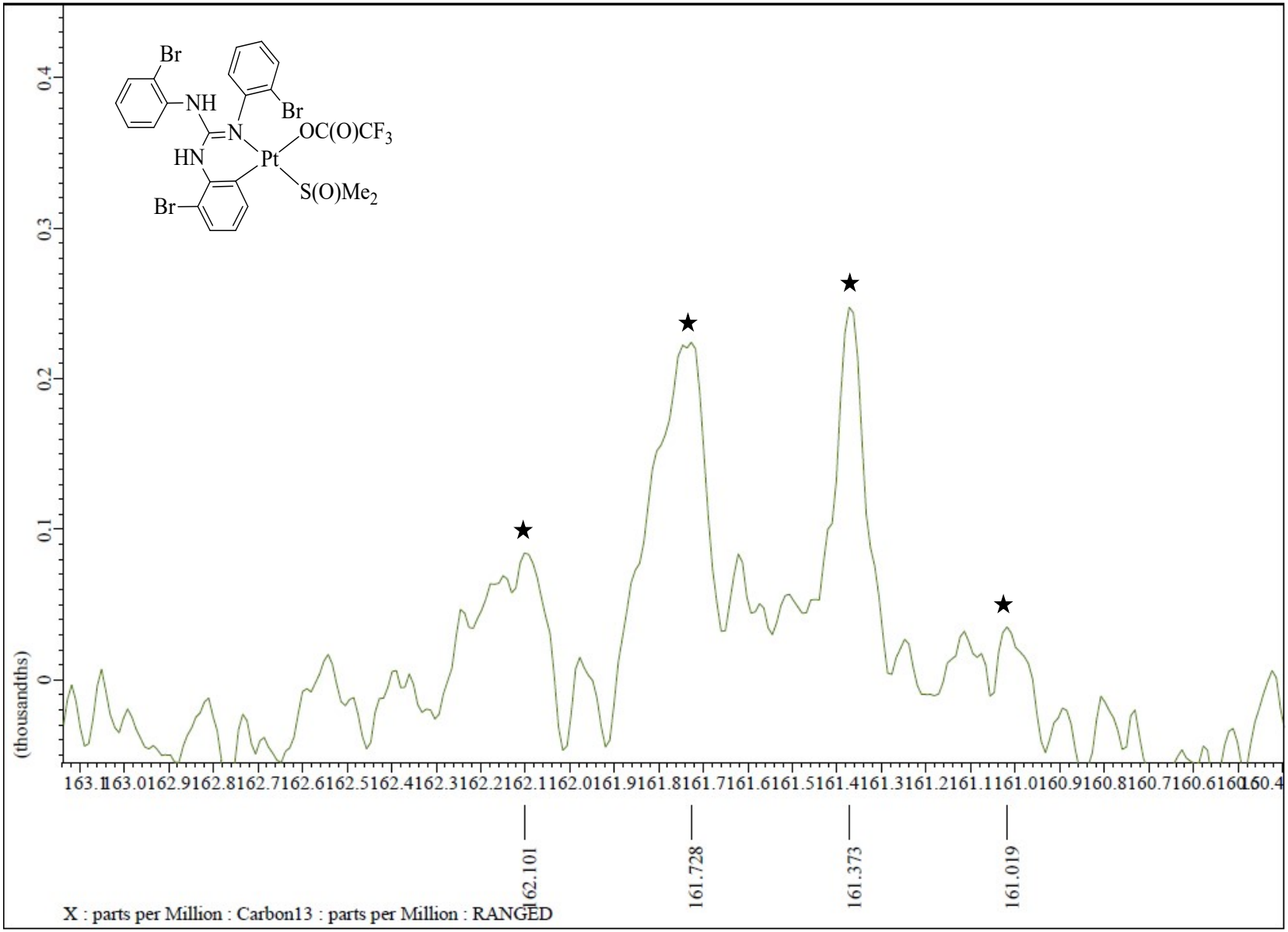

Fig. S49 ^{13}C NMR ($CDCl_3$, 100.5 MHz) spectrum of **8** in the indicated region.

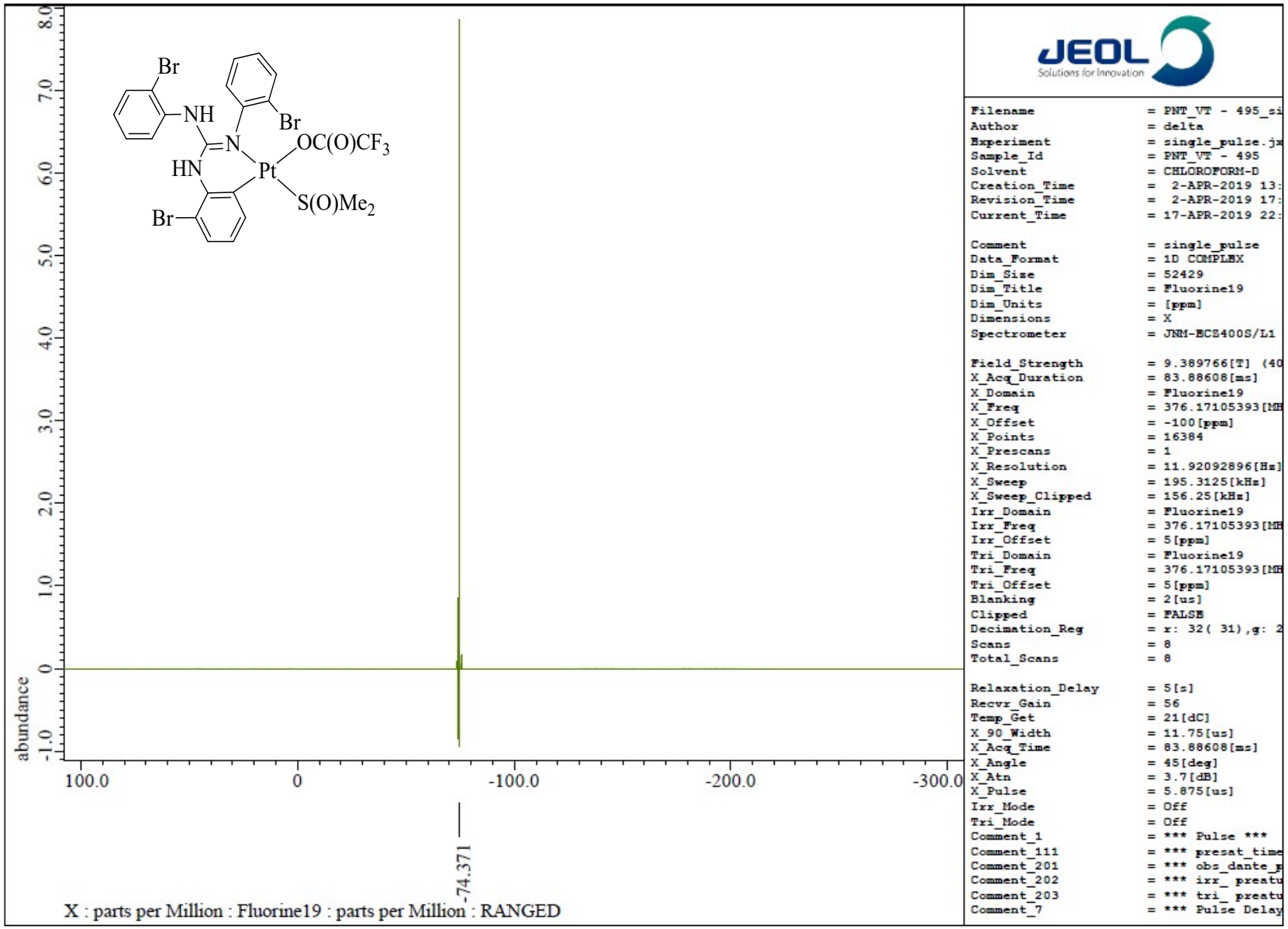

Fig. S50 $^{19}F\{^{1}H\}$ NMR ($CDCl_3$, 376.31 MHz) spectrum of **8**.

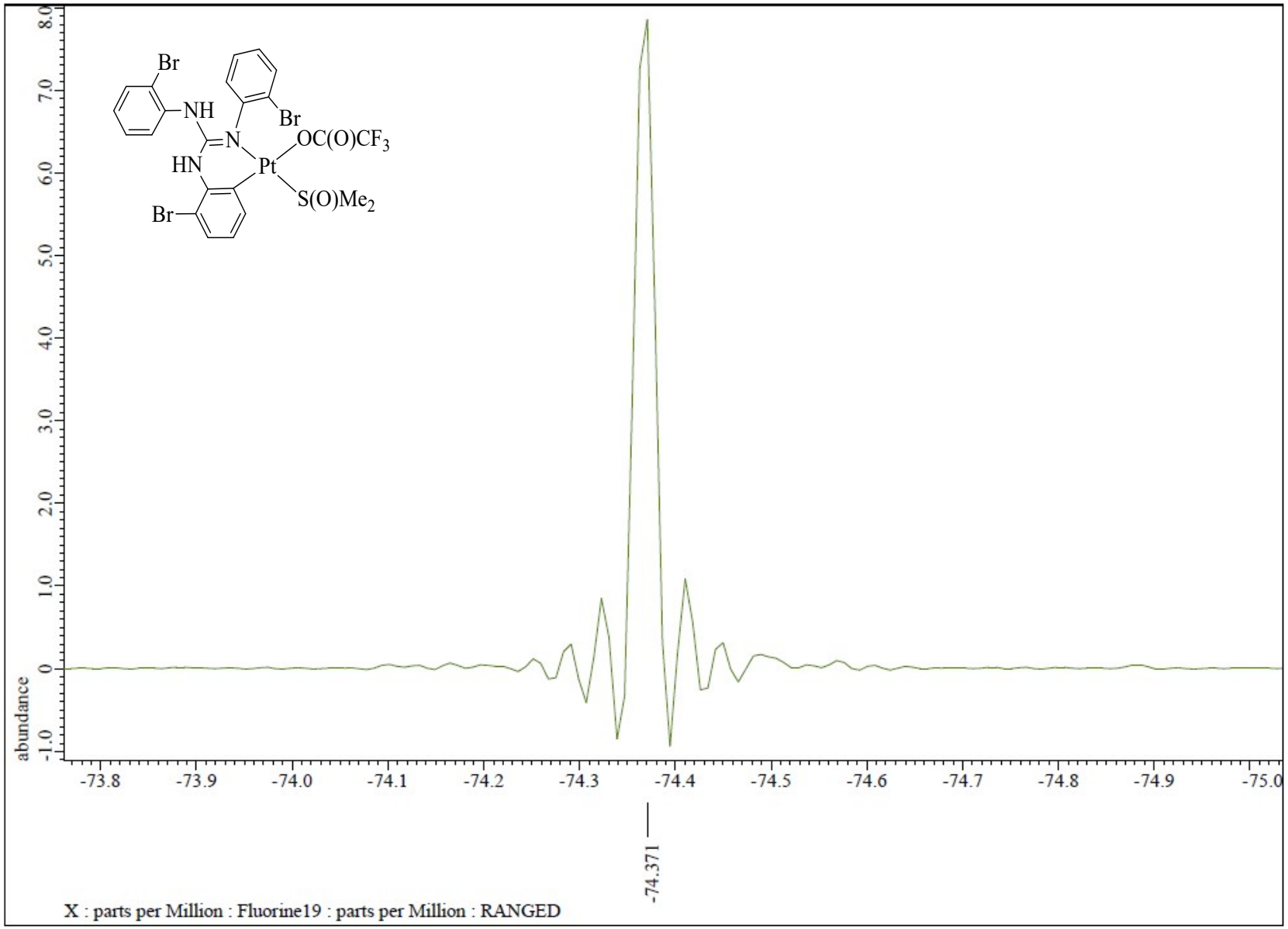

Fig. S51 $^{19}F\{^{1}H\}$ NMR ($CDCl_3$, 376.31 MHz) spectrum of **8** in the indicated region.

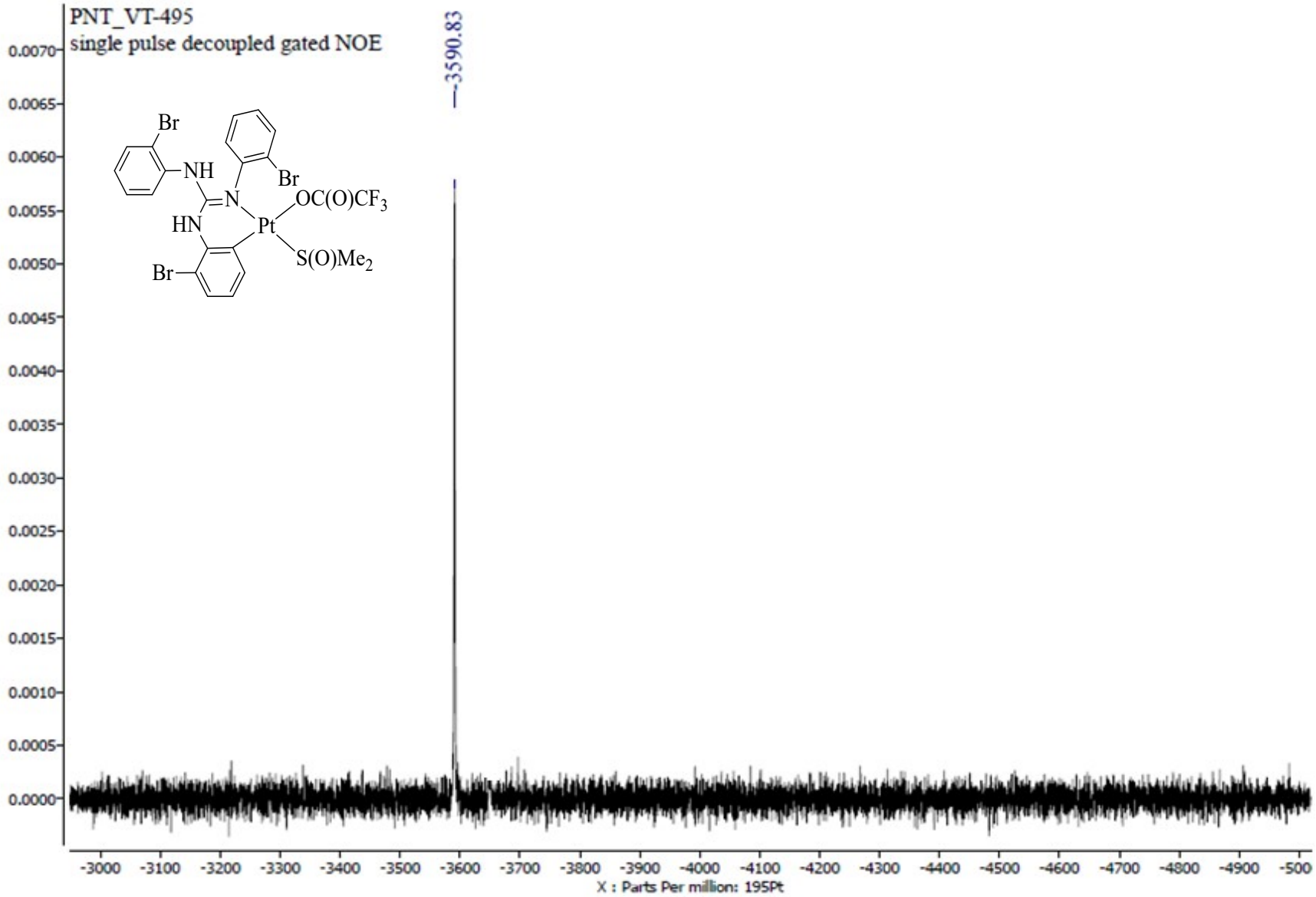

Fig. S52 $^{195}Pt\{^{1}H\}$ NMR ($CDCl_3$, 85.8 MHz) spectrum of **8**.

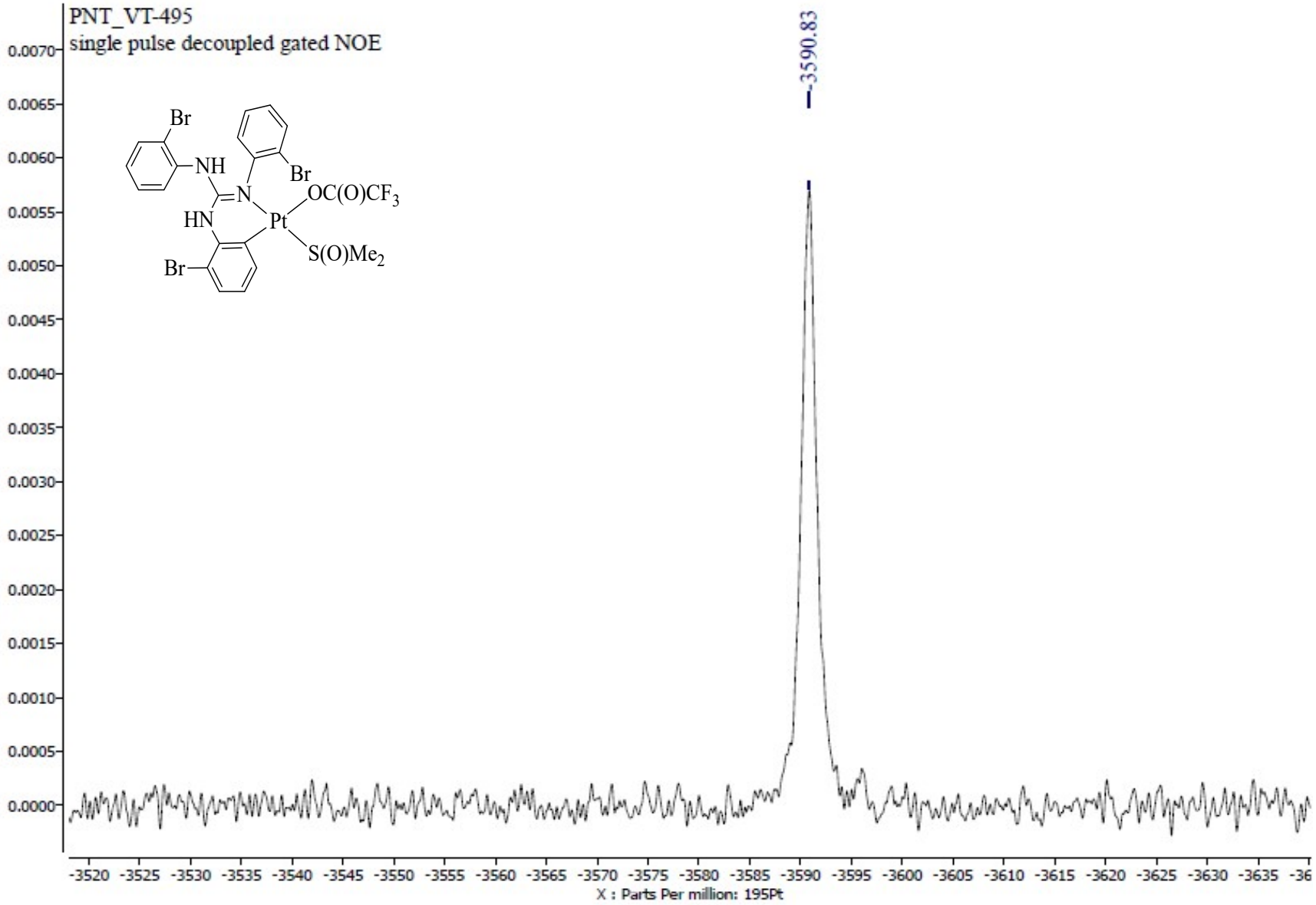

Fig. S53 $^{195}Pt\{^{1}H\}$ NMR ($CDCl_3$, 85.8 MHz) spectrum of **8** in the indicated region.

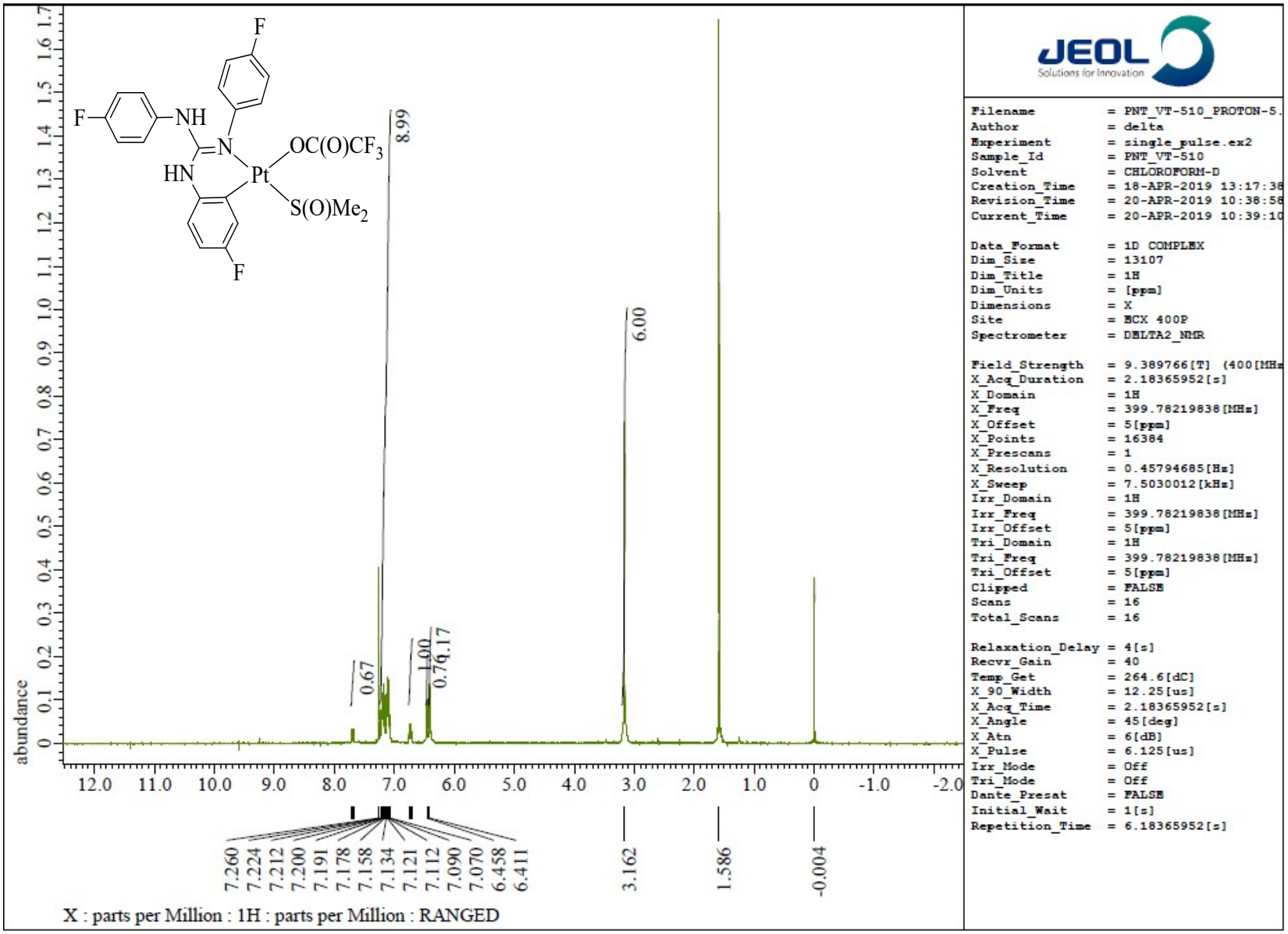

Fig. S54 ^{1}H NMR ($CDCl_3$, 400 MHz) spectrum of **9**.

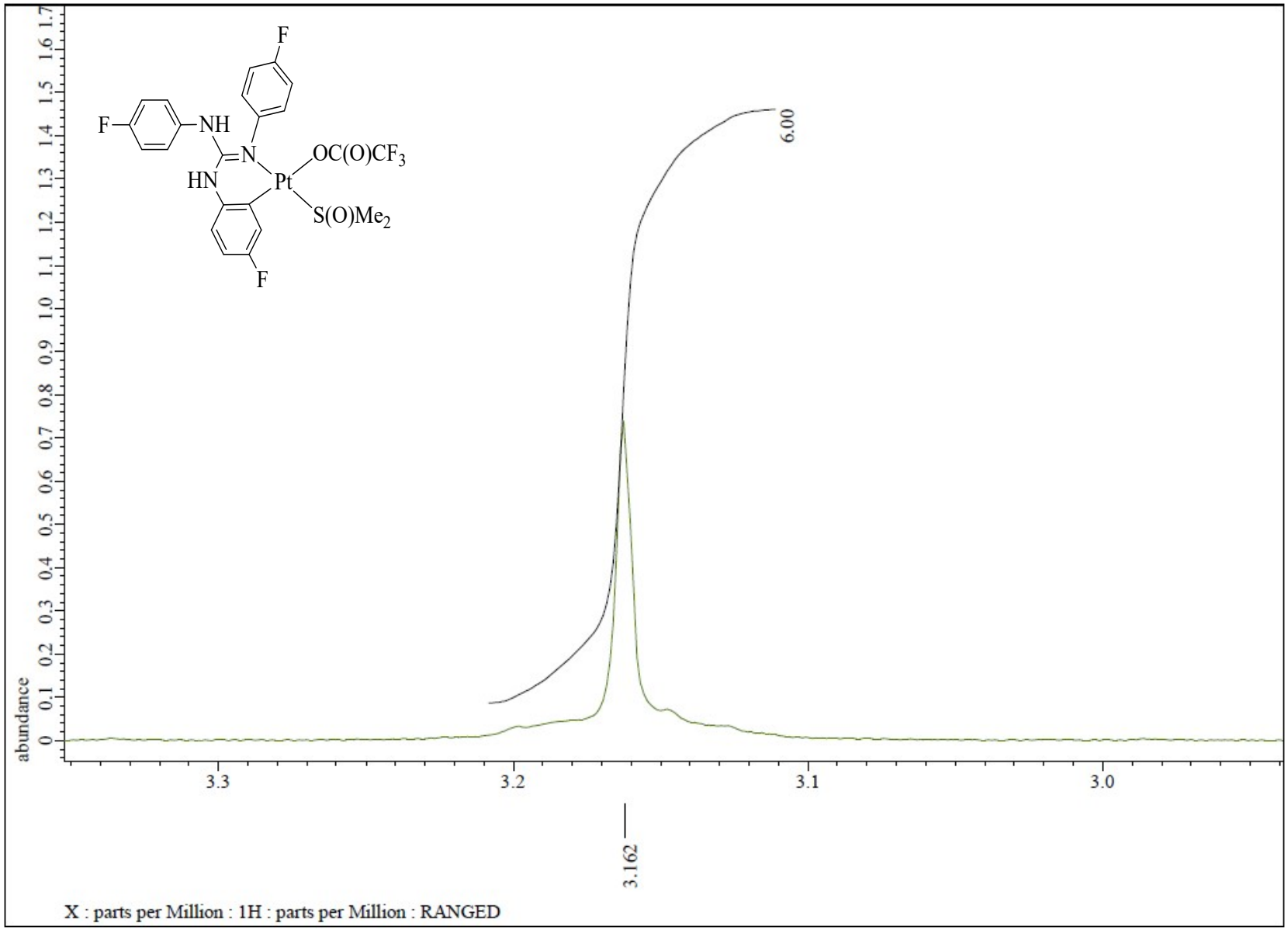

Fig. S55 ^{1}H NMR ($CDCl_3$, 400 MHz) spectrum of **9** in the indicated region.

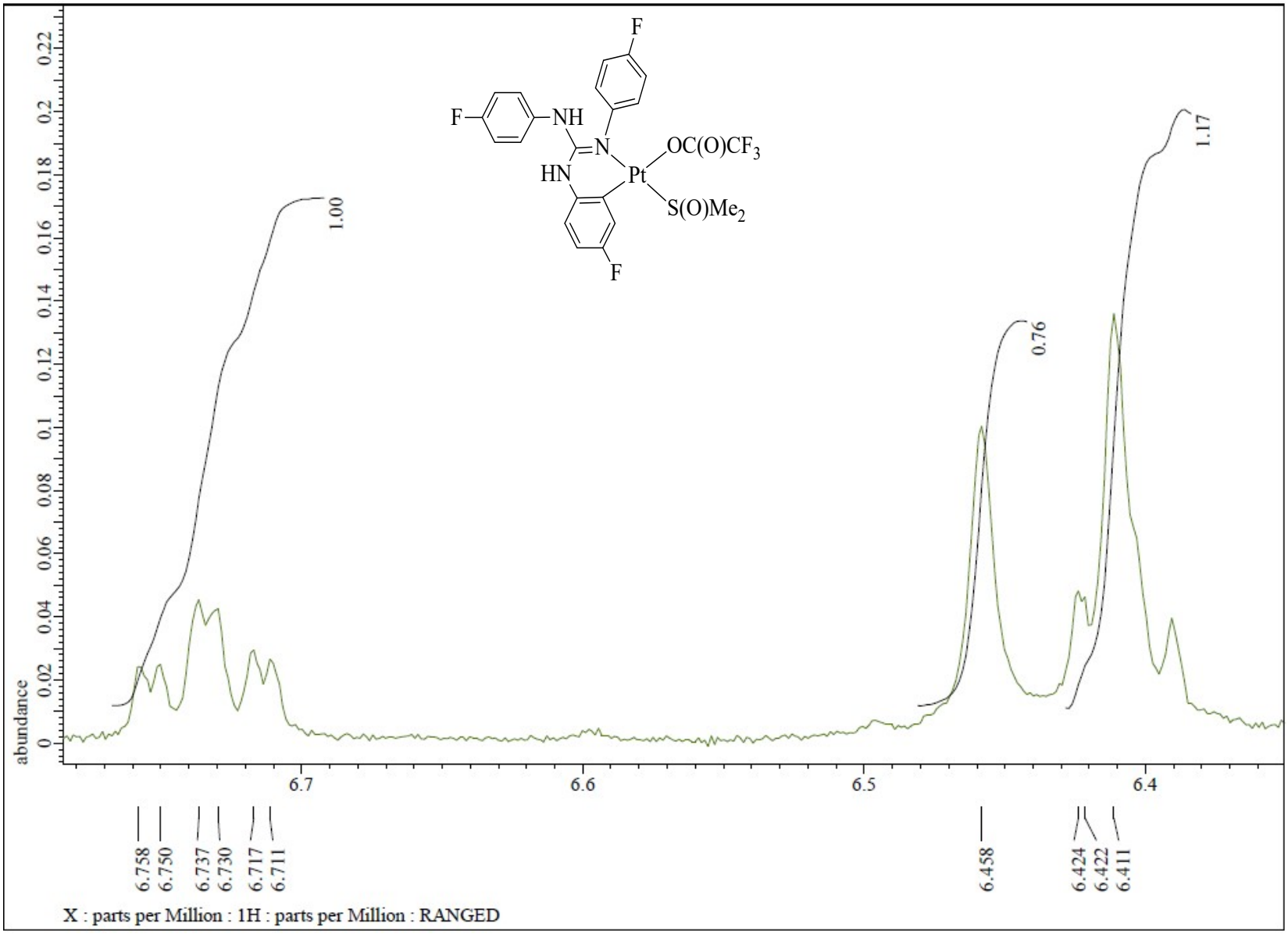

Fig. S56 ^{1}H NMR ($CDCl_3$, 400 MHz) spectrum of **9** in the indicated region.

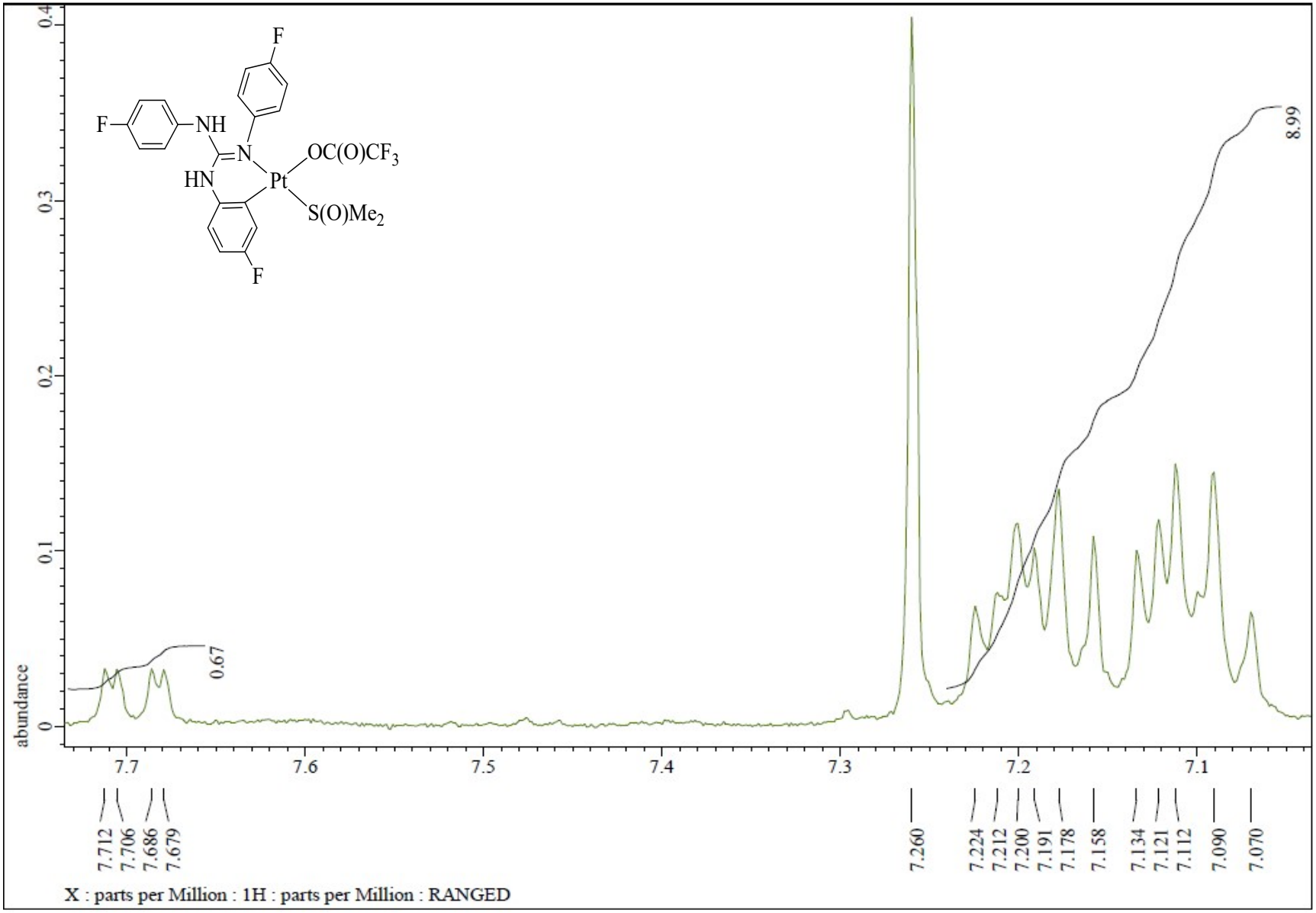

Fig. S57 ^{1}H NMR ($CDCl_3$, 400 MHz) spectrum of **9** in the indicated region.

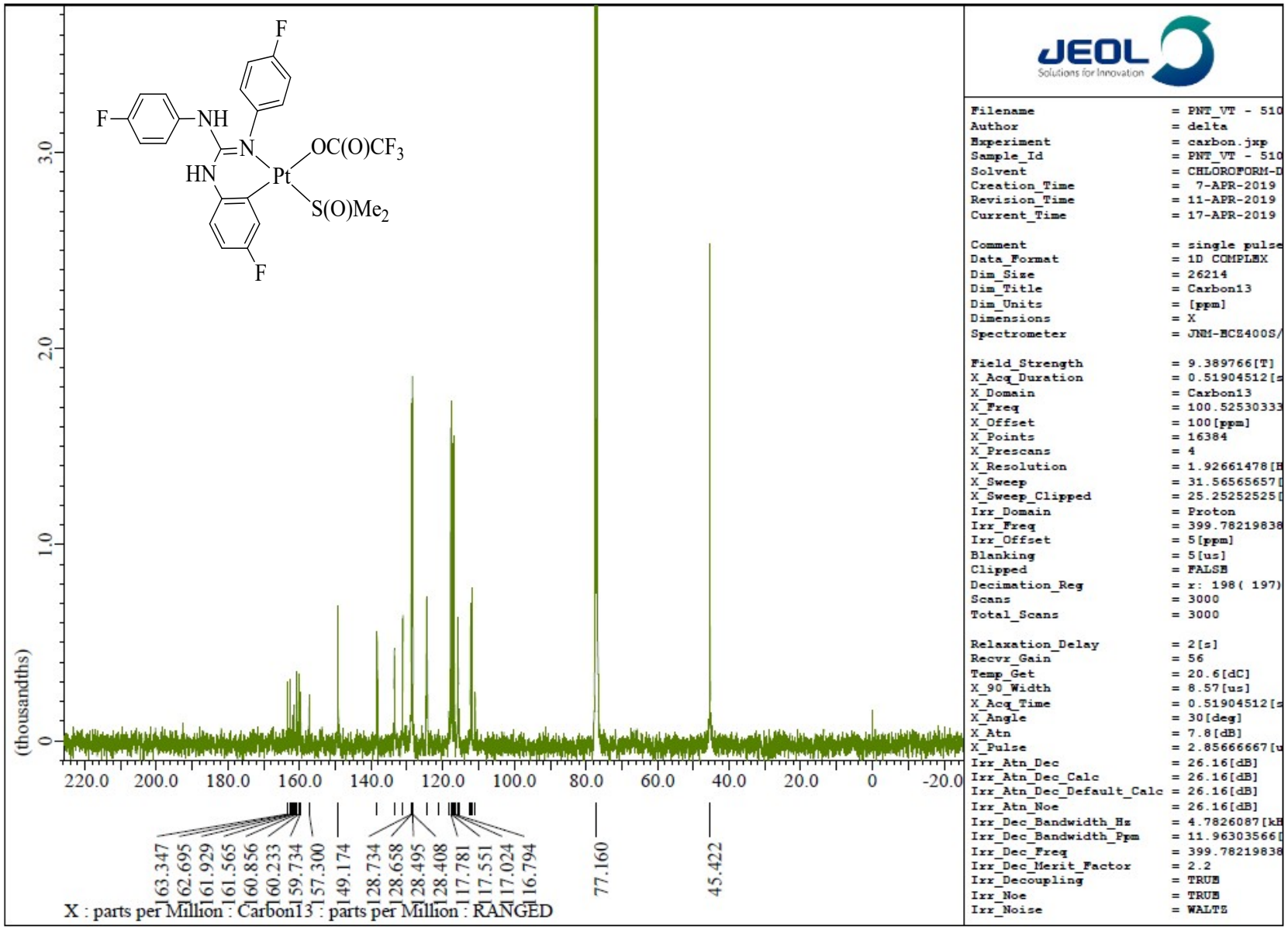

Fig. S58 $^{13}C\{^{1}H\}$ NMR ($CDCl_3$, 100.5 MHz) spectrum of **9**.

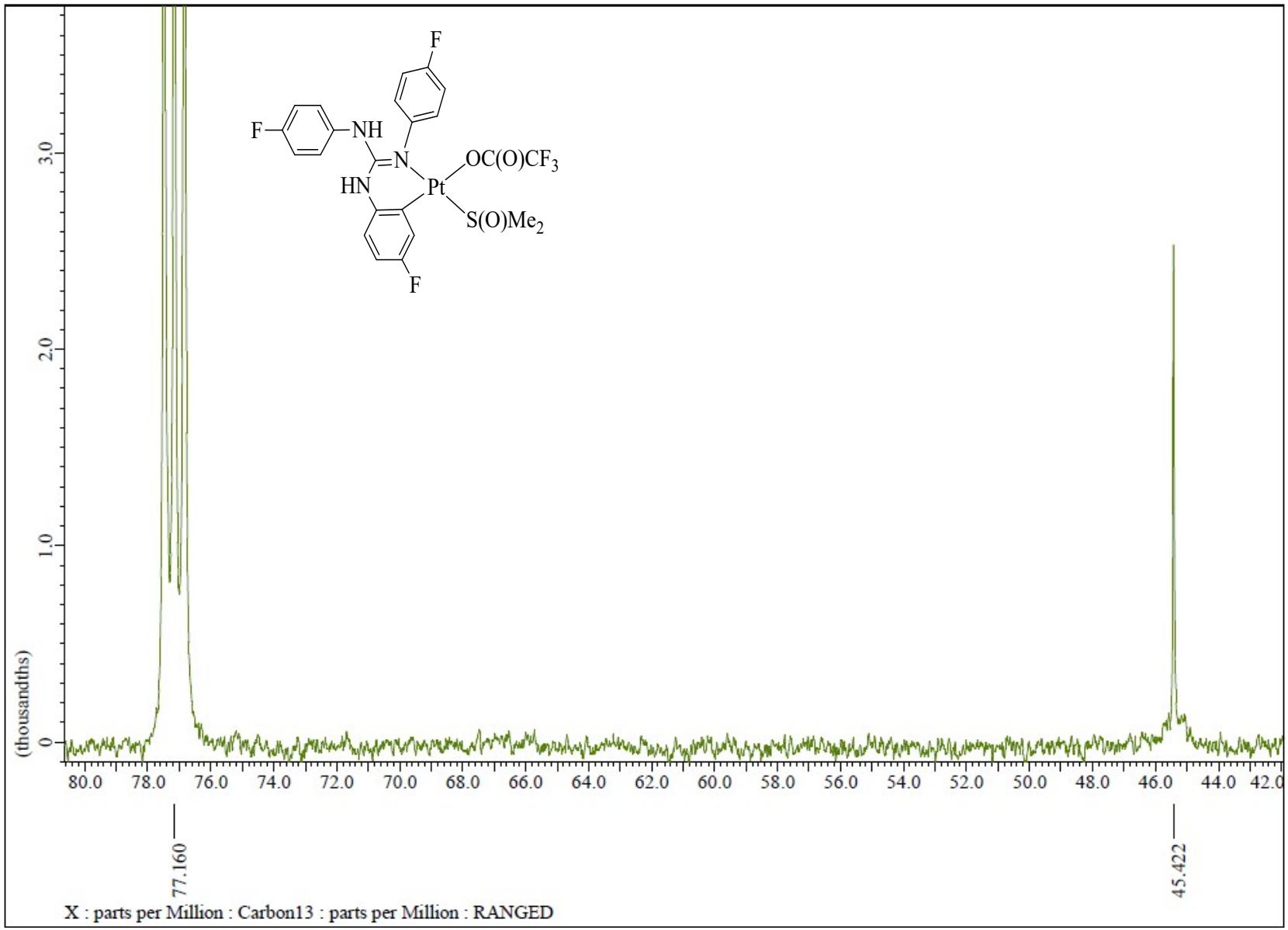

Fig. S59 $^{13}C\{^{1}H\}$ NMR ($CDCl_3$, 100.5 MHz) spectrum of **9** in the indicated region.

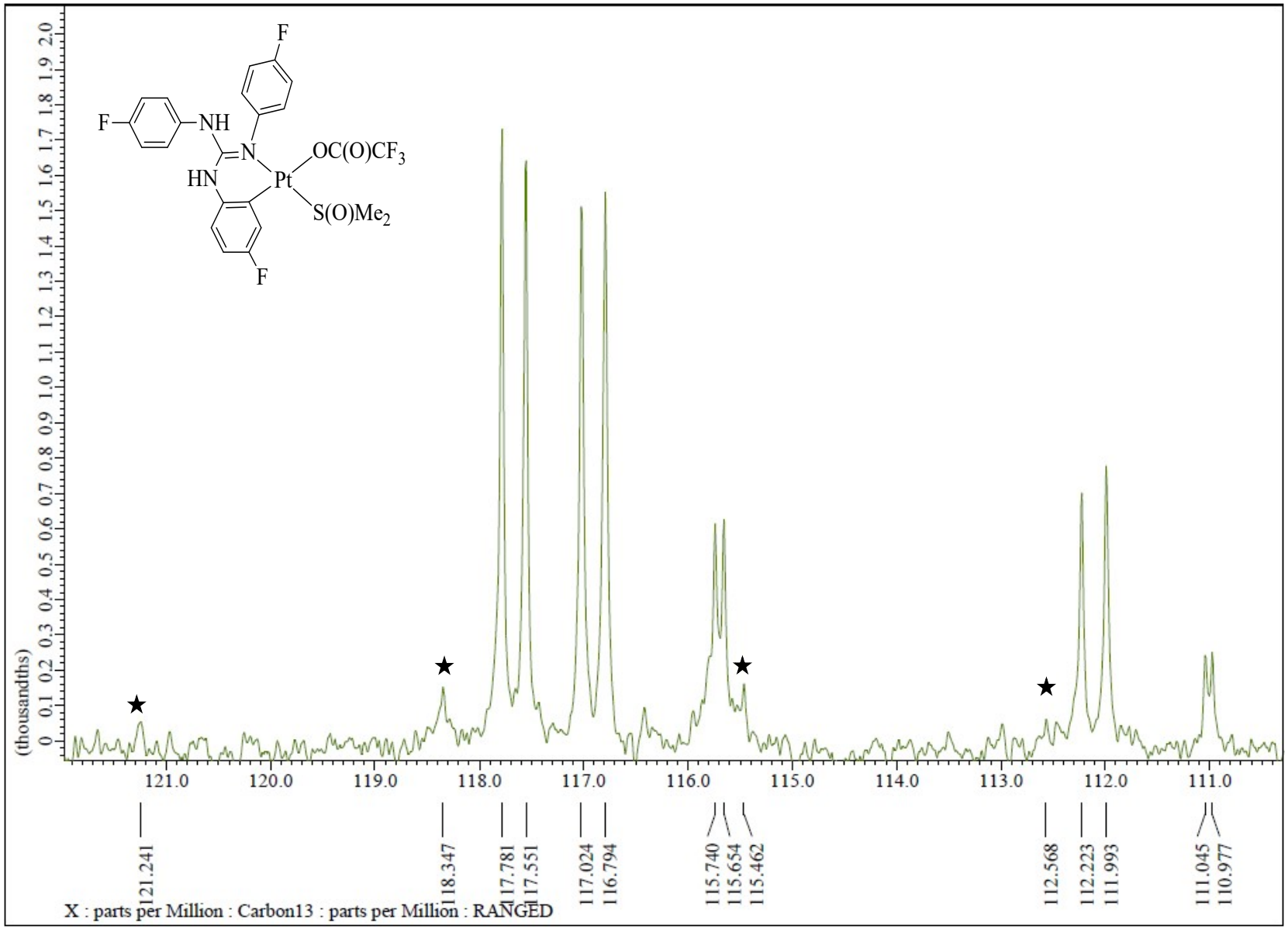

Fig. S60 $^{13}C\{^{1}H\}$ NMR ($CDCl_3$, 100.5 MHz) spectrum of **9** in the indicated region.

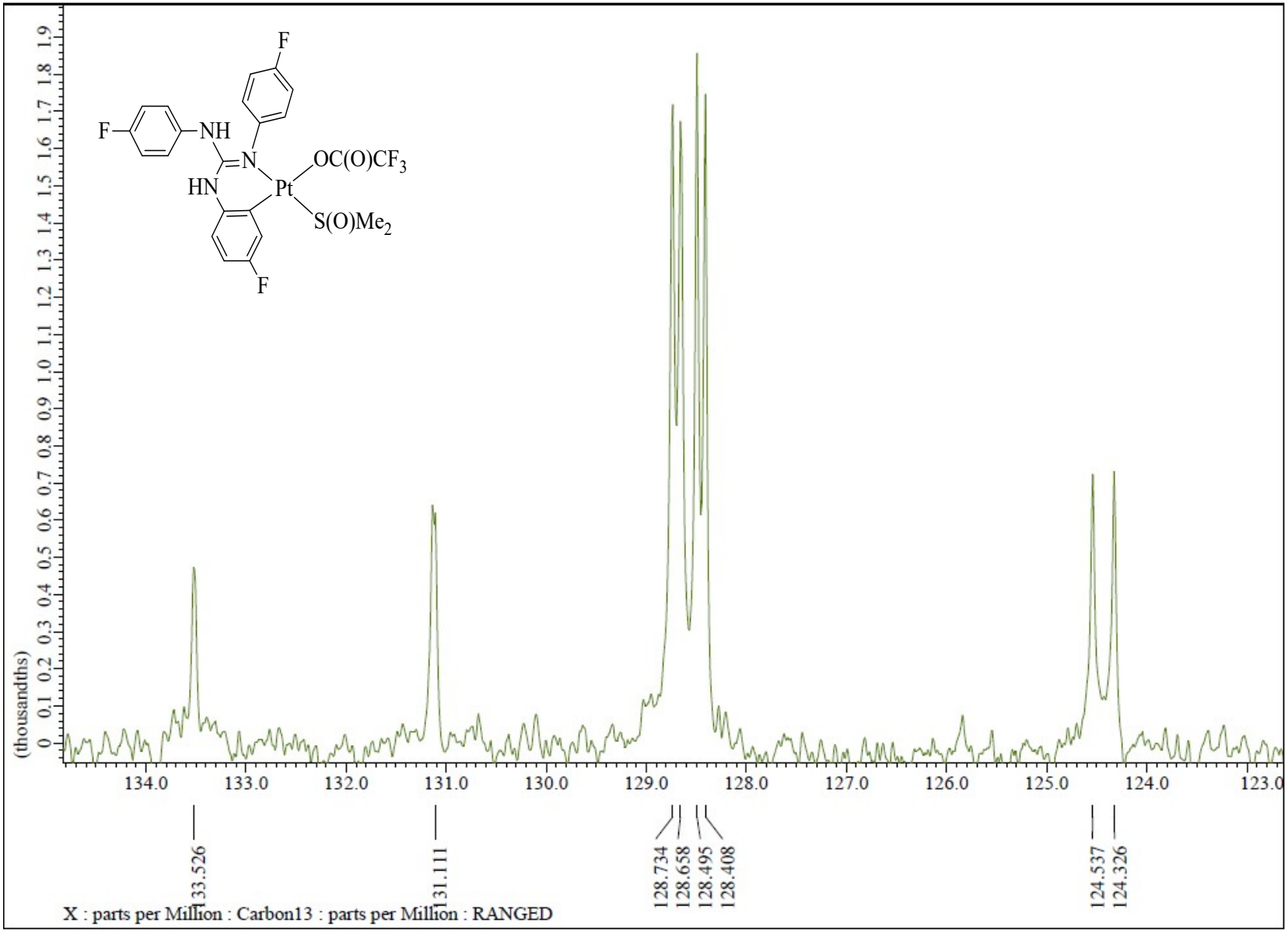

Fig. S61 $^{13}C\{^{1}H\}$ NMR ($CDCl_3$, 100.5 MHz) spectrum of **9** in the indicated region.

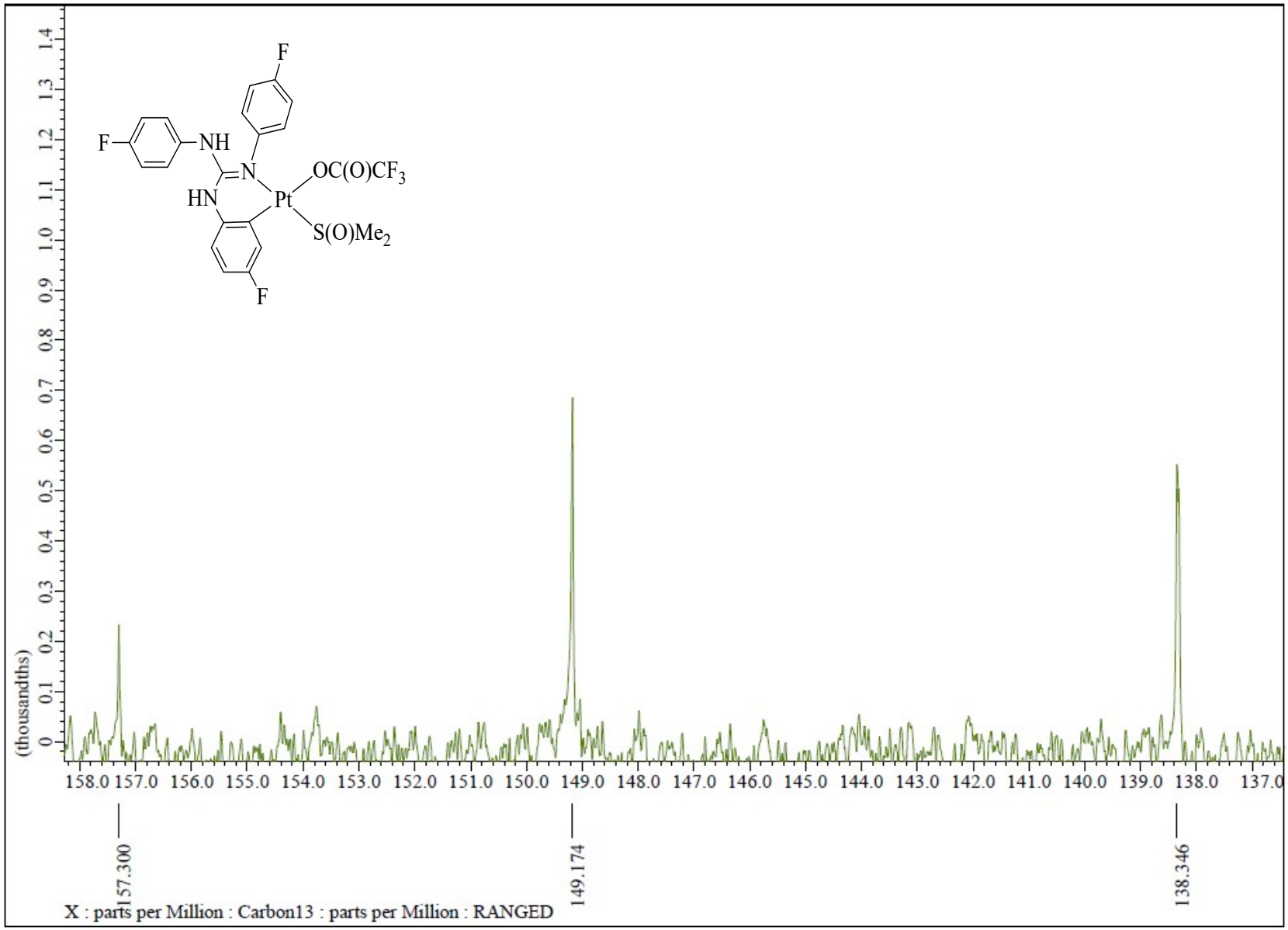

Fig. S62 $^{13}C\{^{1}H\}$ NMR ($CDCl_3$, 100.5 MHz) spectrum of **9** in the indicated region.

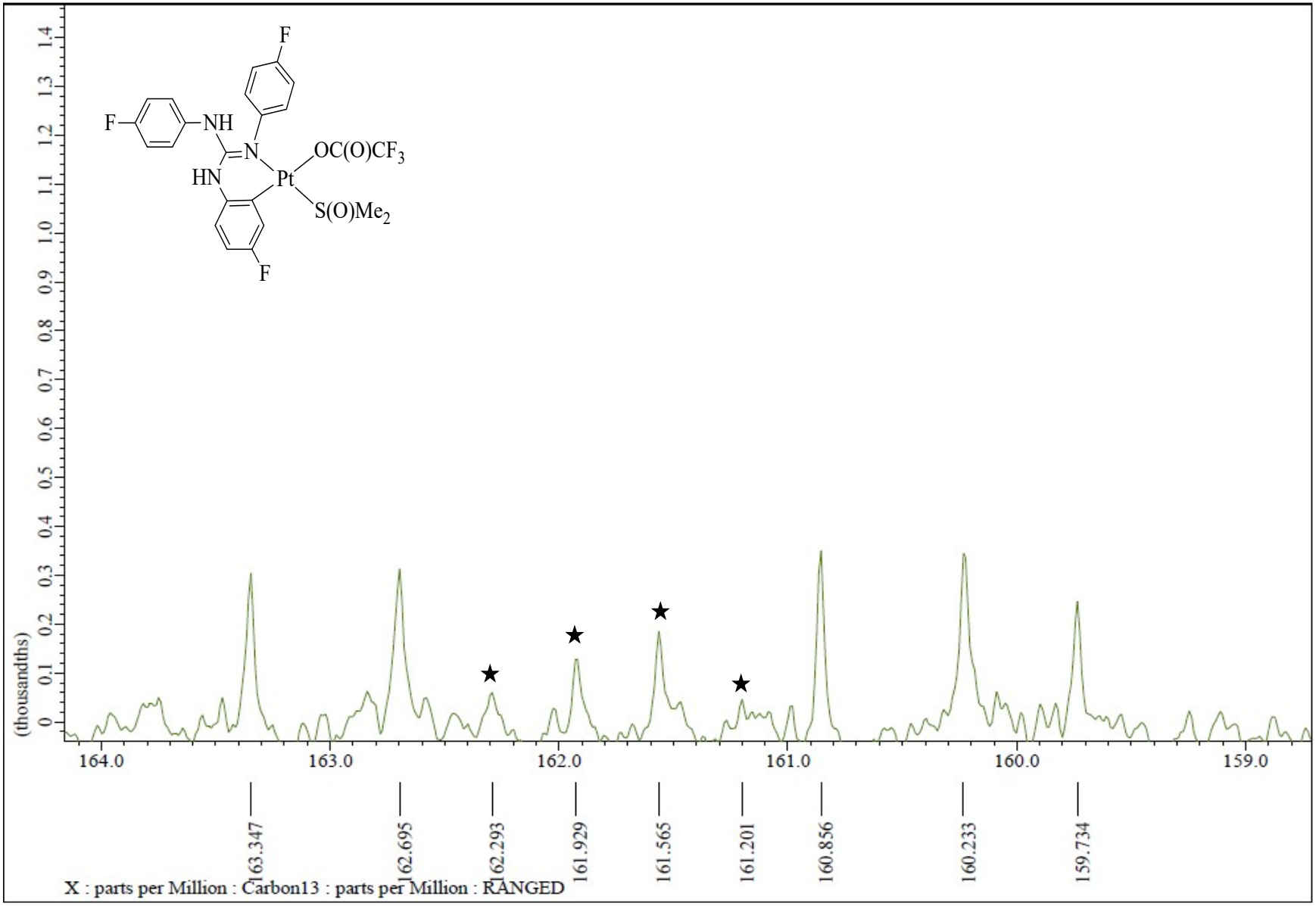

Fig. S63 $^{13}C\{^{1}H\}$ NMR ($CDCl_3$, 100.5 MHz) spectrum of **9** in the indicated region.

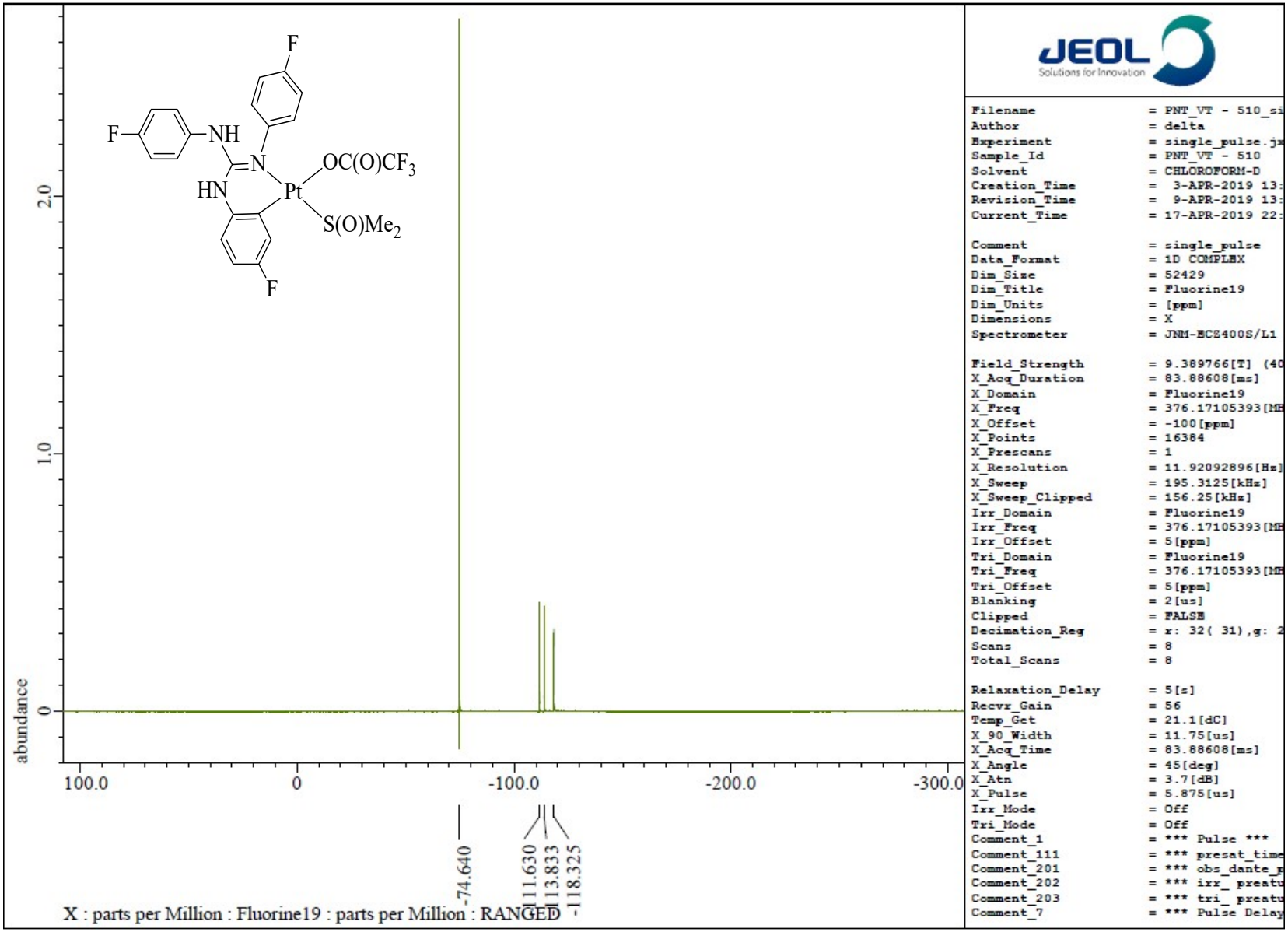

Fig. S64 $^{19}F\{^{1}H\}$ NMR ($CDCl_3$, 376.31 MHz) spectrum of **9**.

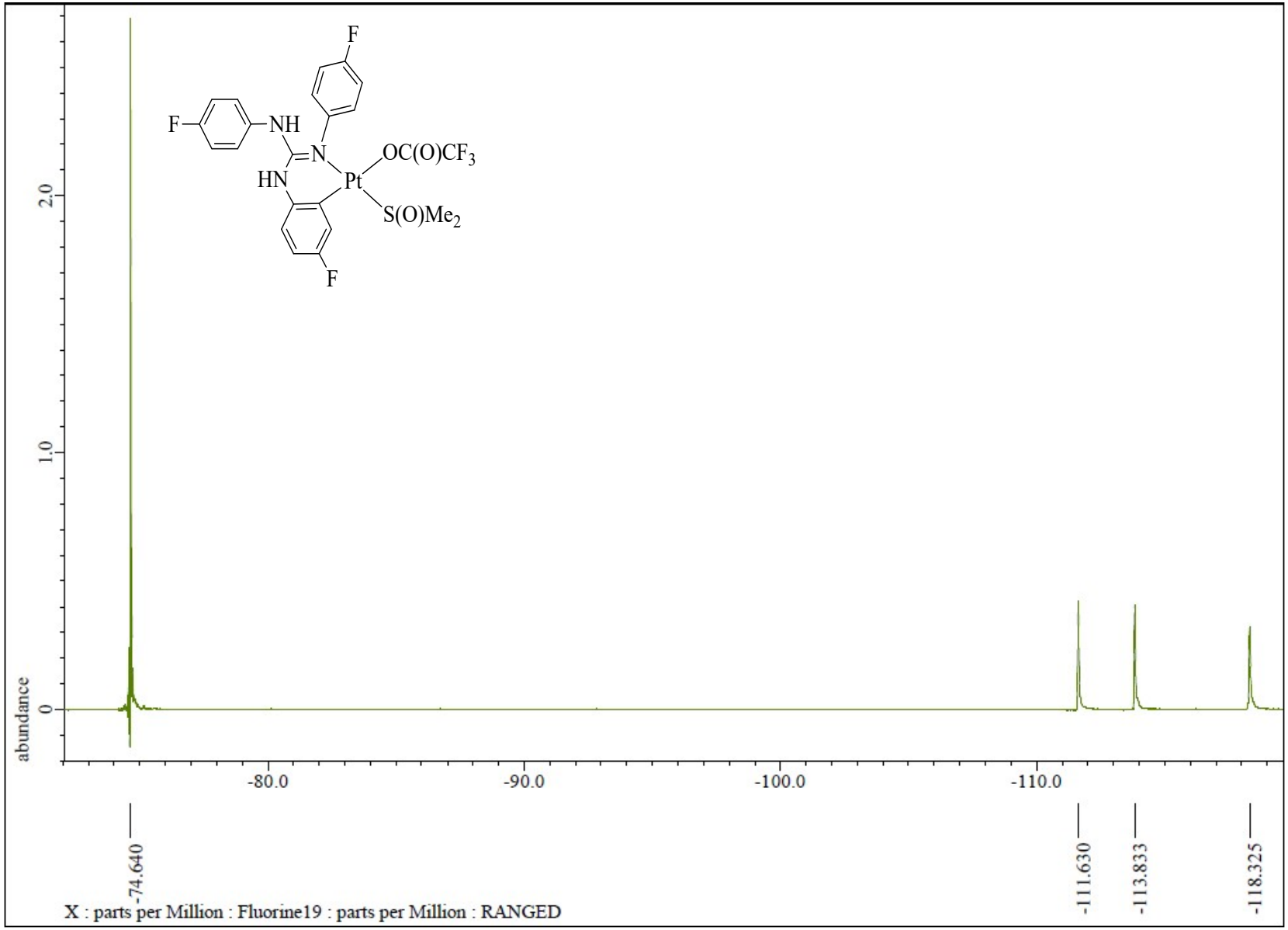

Fig. S65 $^{19}F\{^{1}H\}$ NMR ($CDCl_3$, 376.31 MHz) spectrum of **9** in the indicated region.

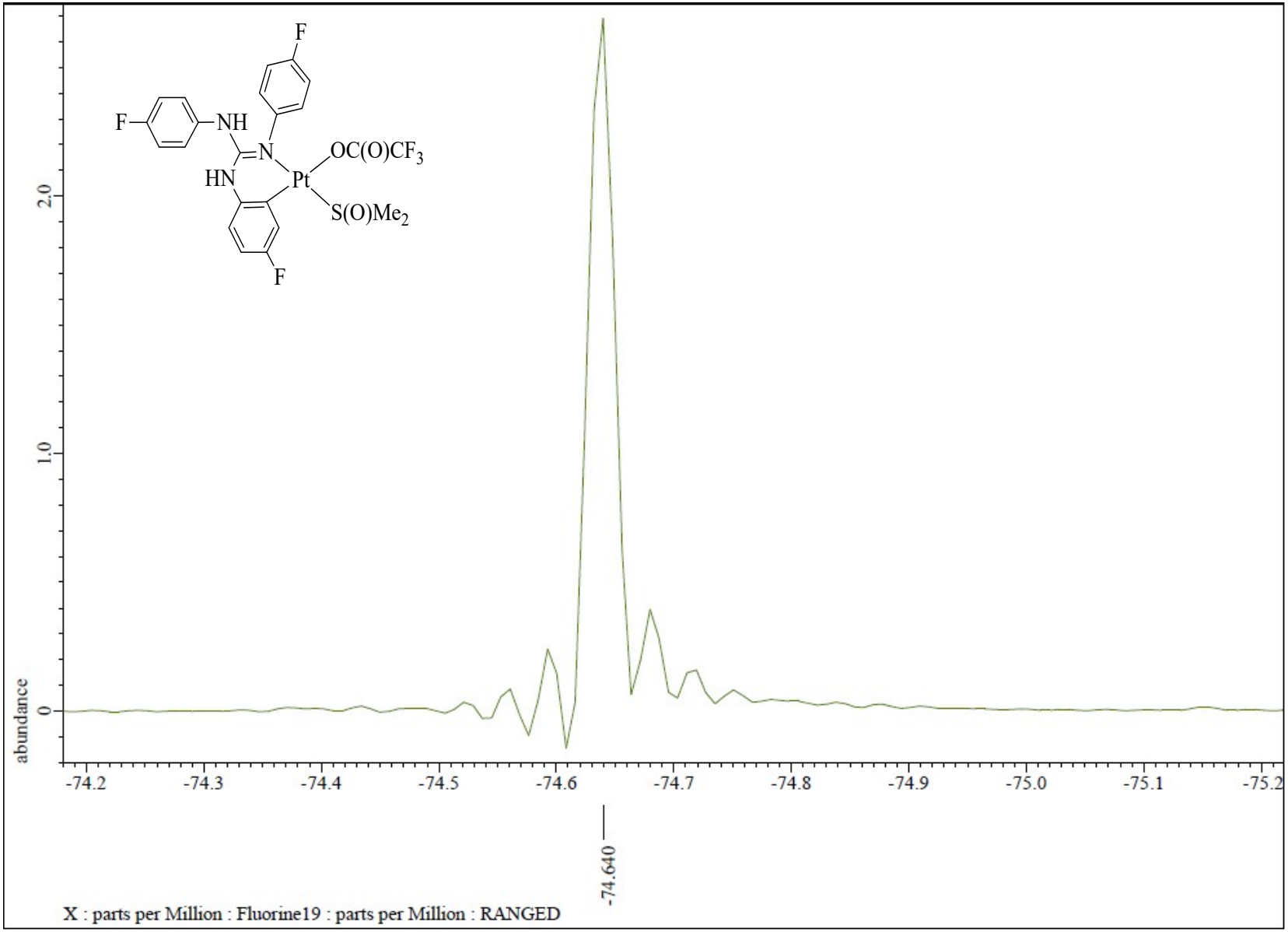

Fig. S66 $^{19}F\{^{1}H\}$ NMR ($CDCl_3$, 376.31 MHz) spectrum of **9** in the indicated region.

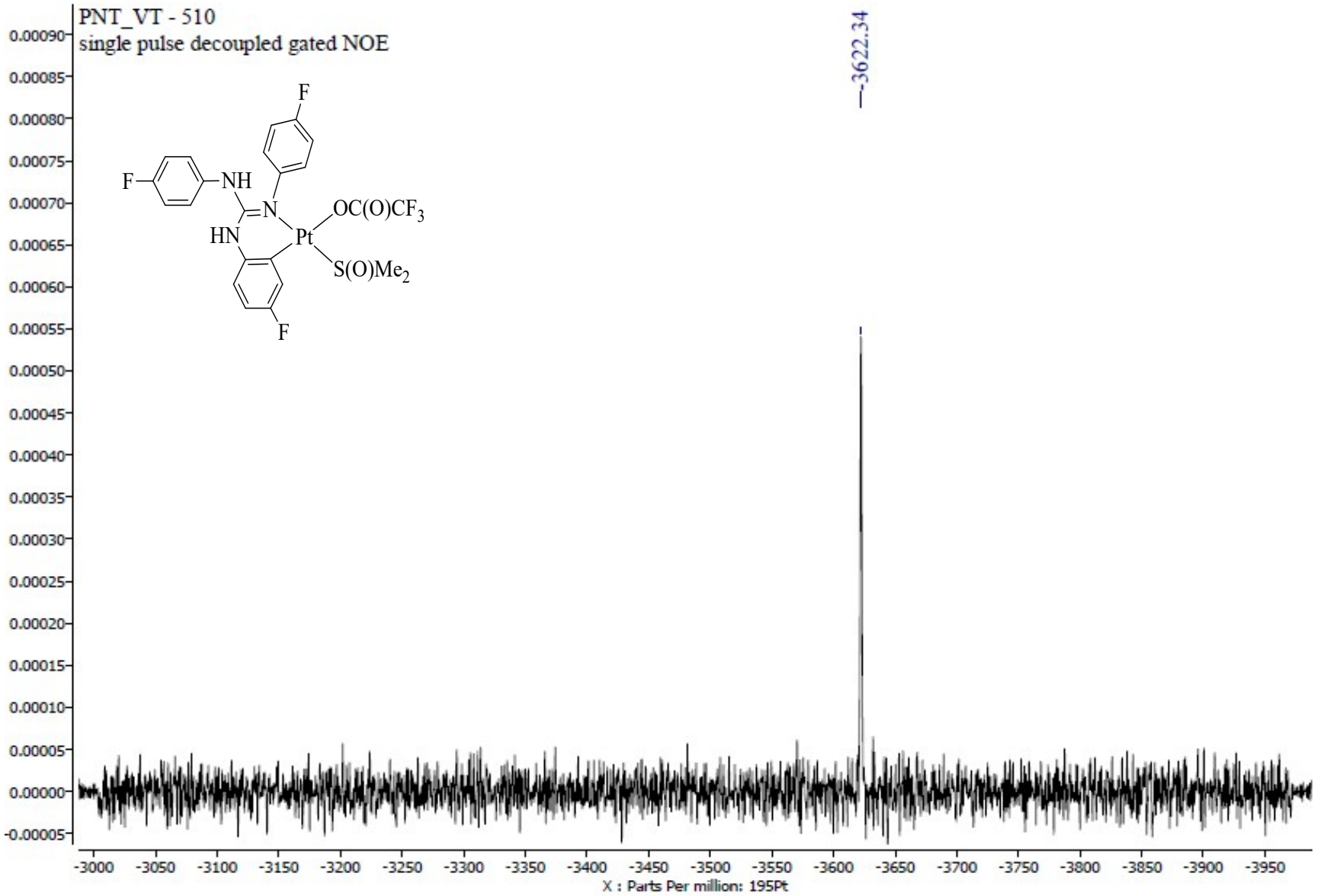

Fig. S67 $^{195}Pt\{^{1}H\}$ NMR ($CDCl_3$, 85.8 MHz) spectrum of **9**.

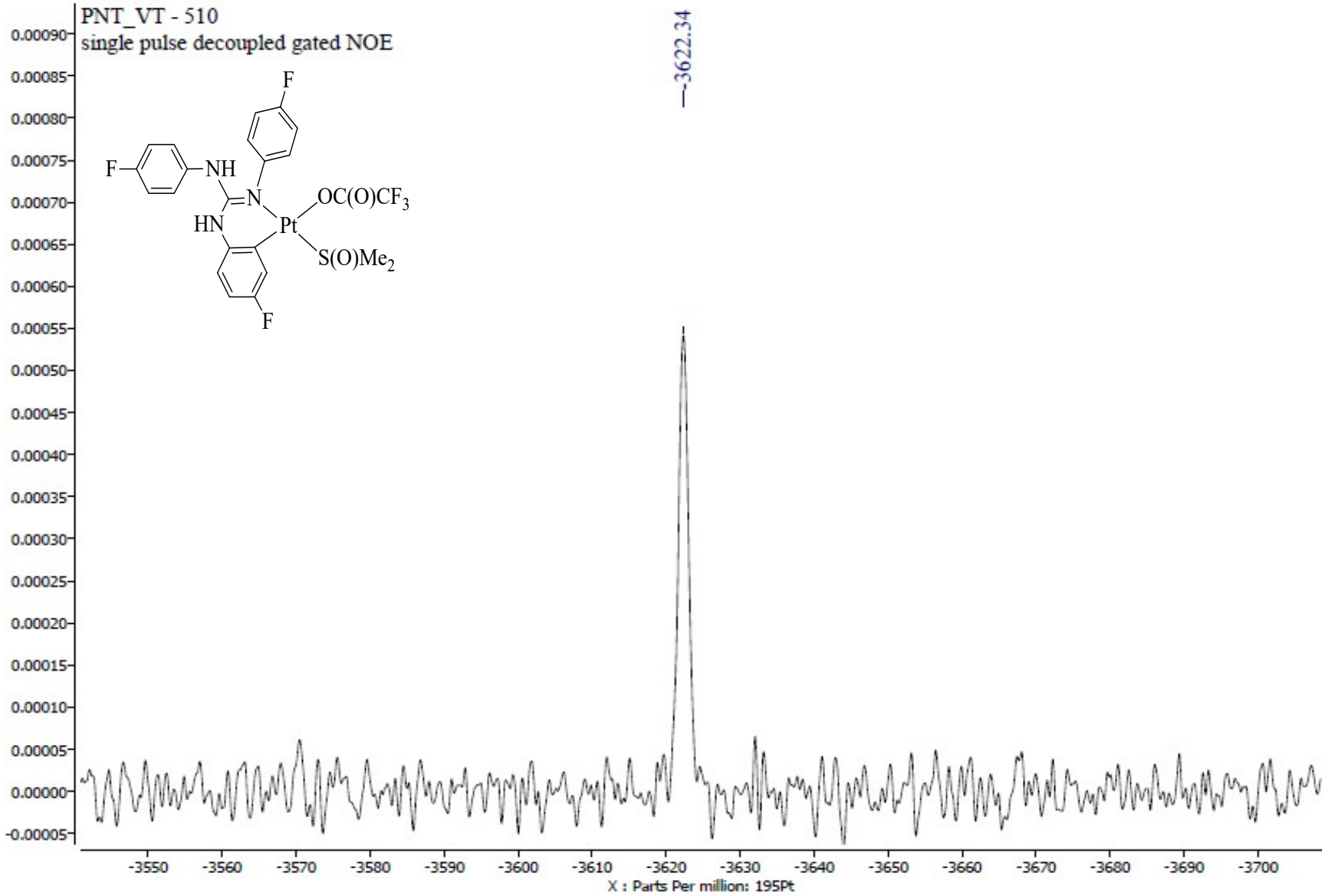

Fig. S68 $^{195}Pt\{^{1}H\}$ NMR ($CDCl_3$, 85.8 MHz) spectrum of **9** in the indicated region.

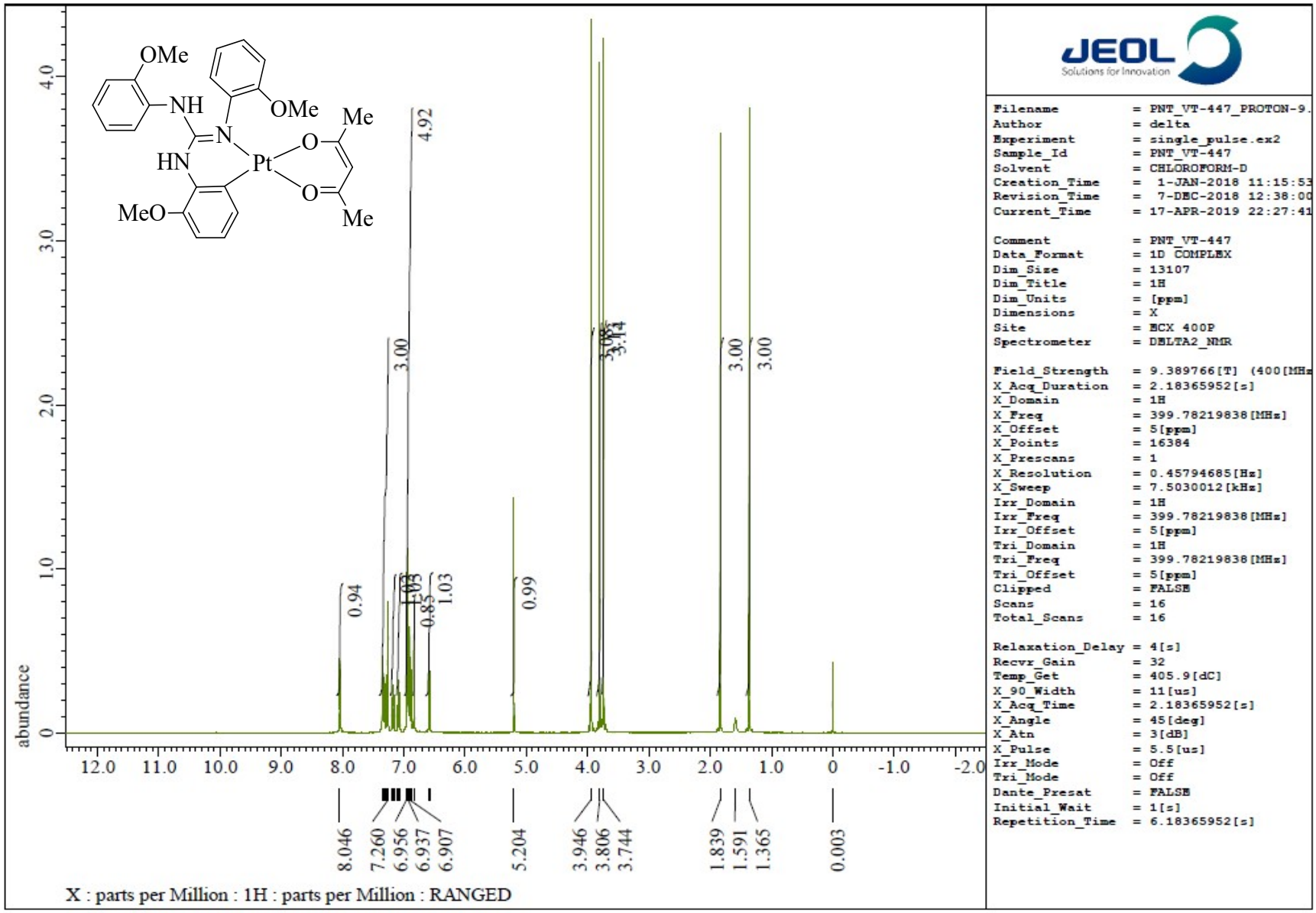

Fig. S69 ^{1}H NMR ($CDCl_3$, 400 MHz) spectrum of **10**.

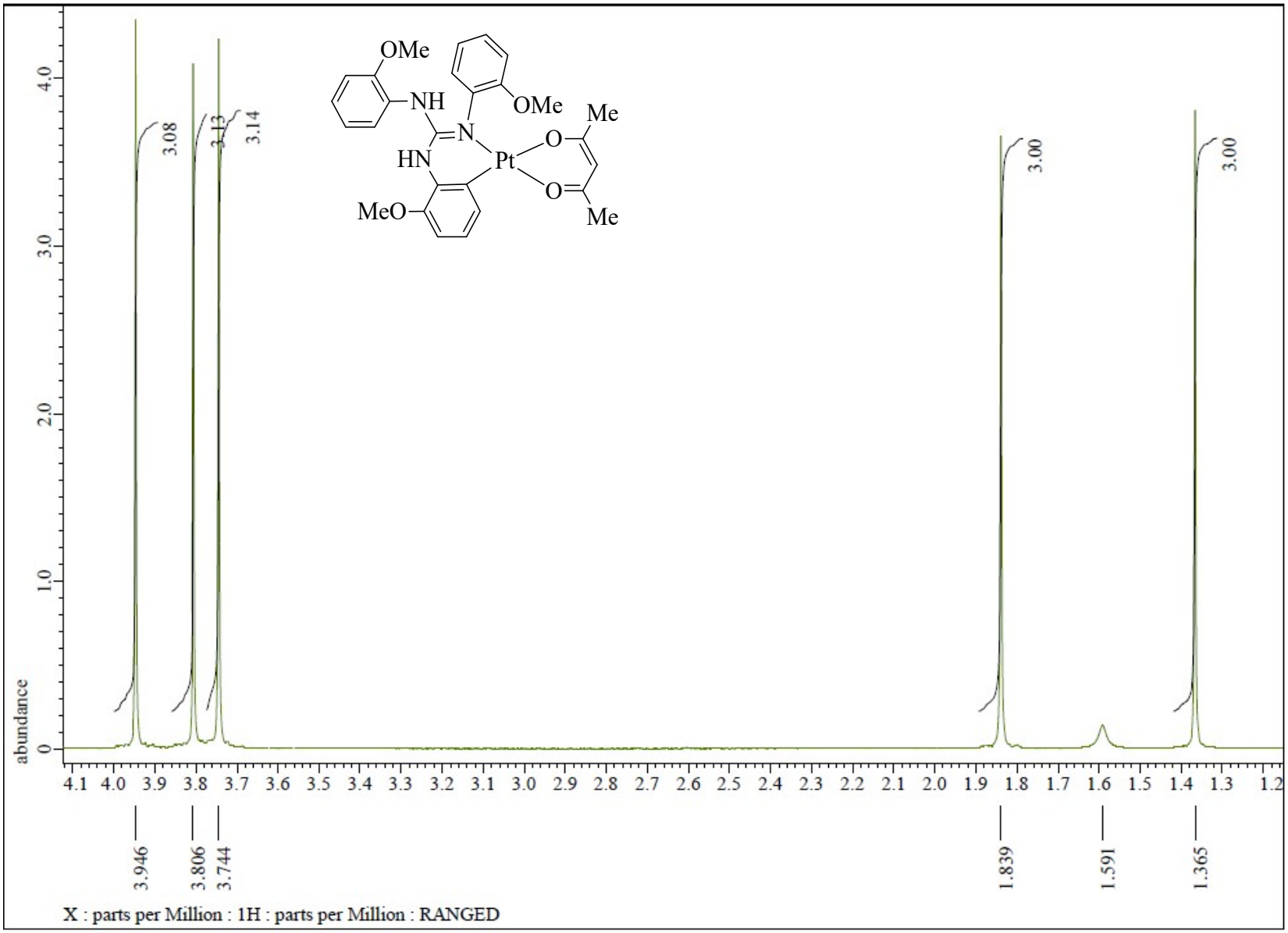

Fig. S70 ^{1}H NMR ($CDCl_3$, 400 MHz) spectrum of **10** in the indicated region.

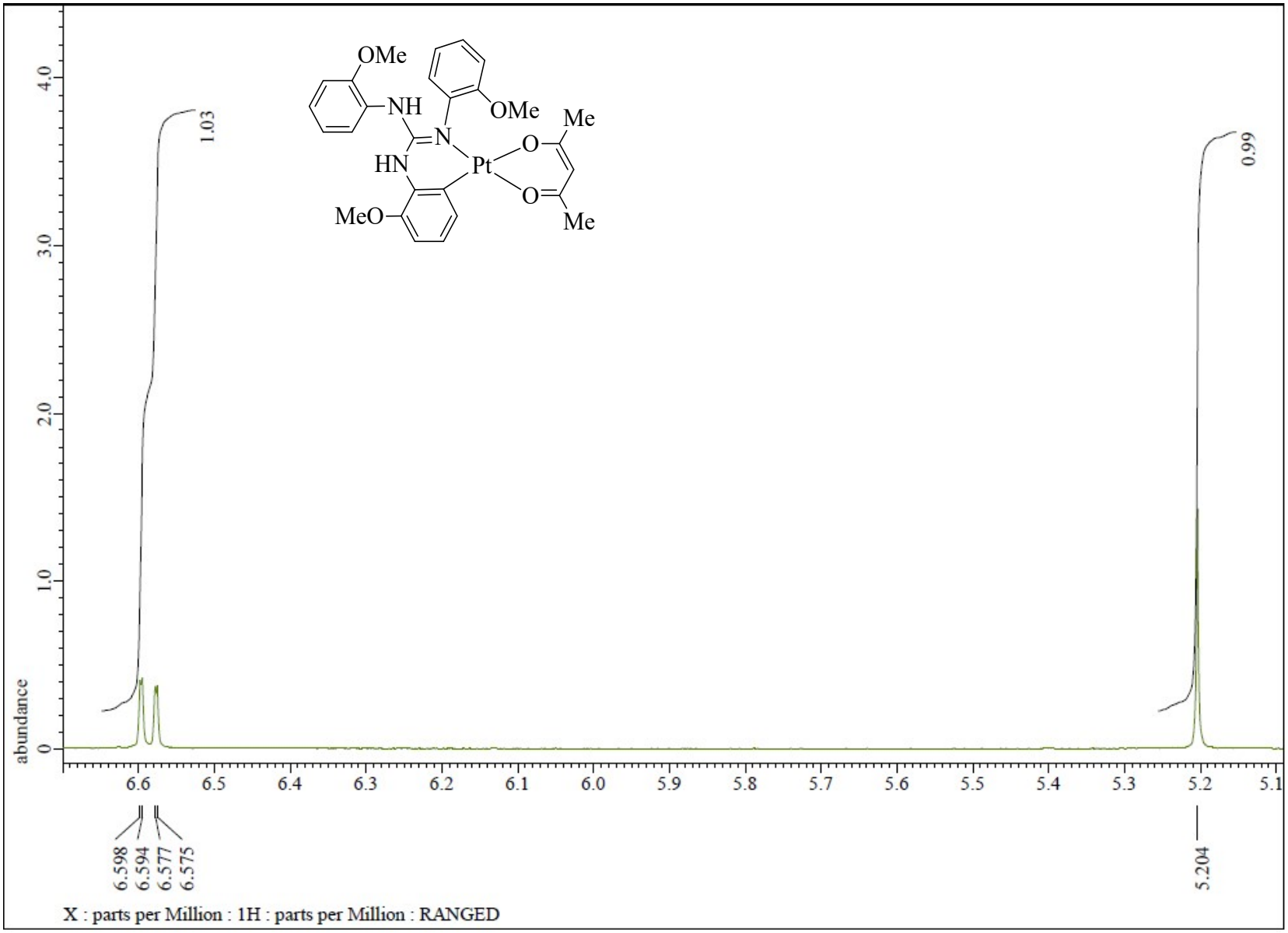

Fig. S71 ^{1}H NMR ($CDCl_3$, 400 MHz) spectrum of **10** in the indicated region.

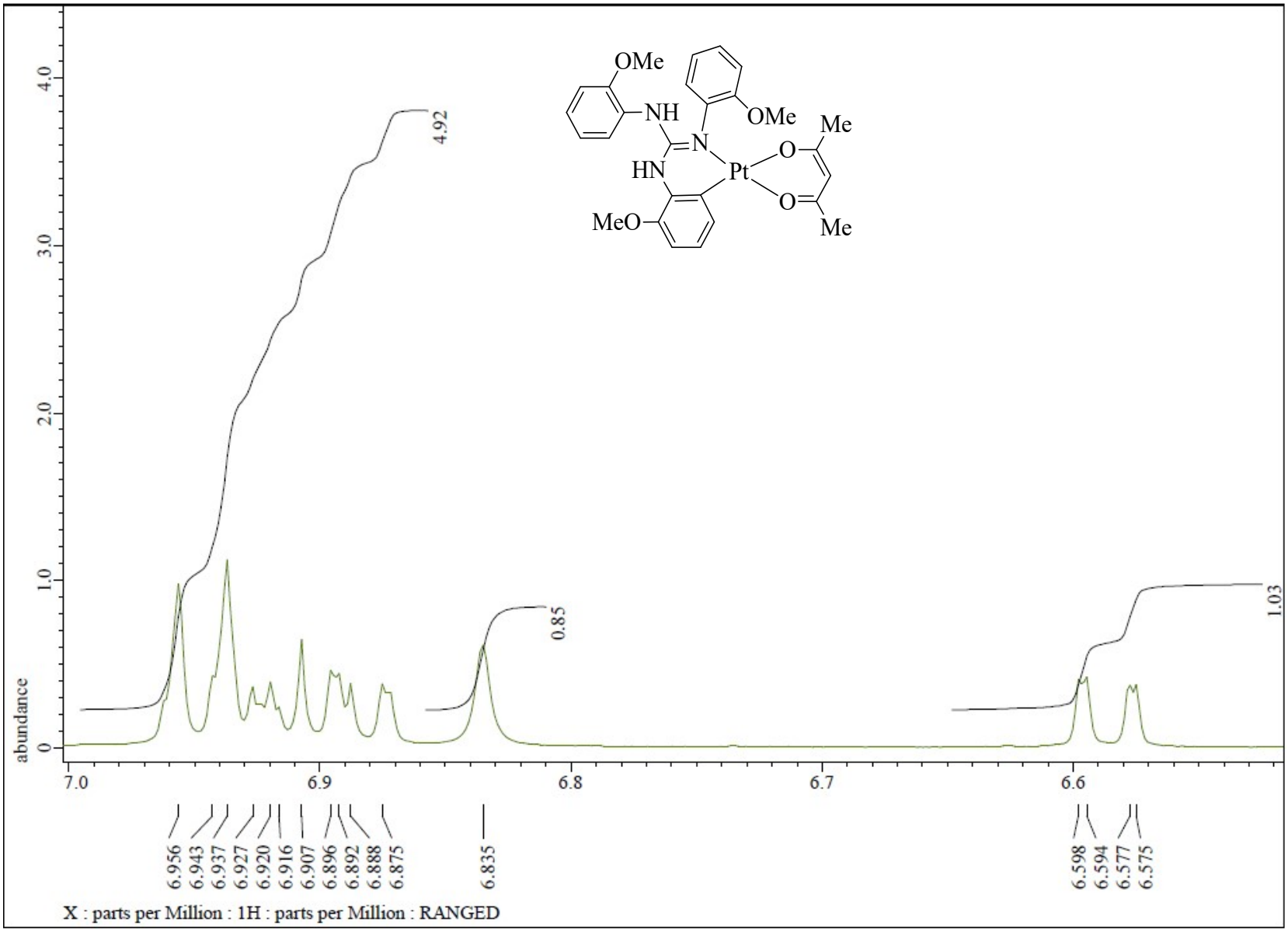

Fig. S72 ^{1}H NMR ($CDCl_3$, 400 MHz) spectrum of **10** in the indicated region.

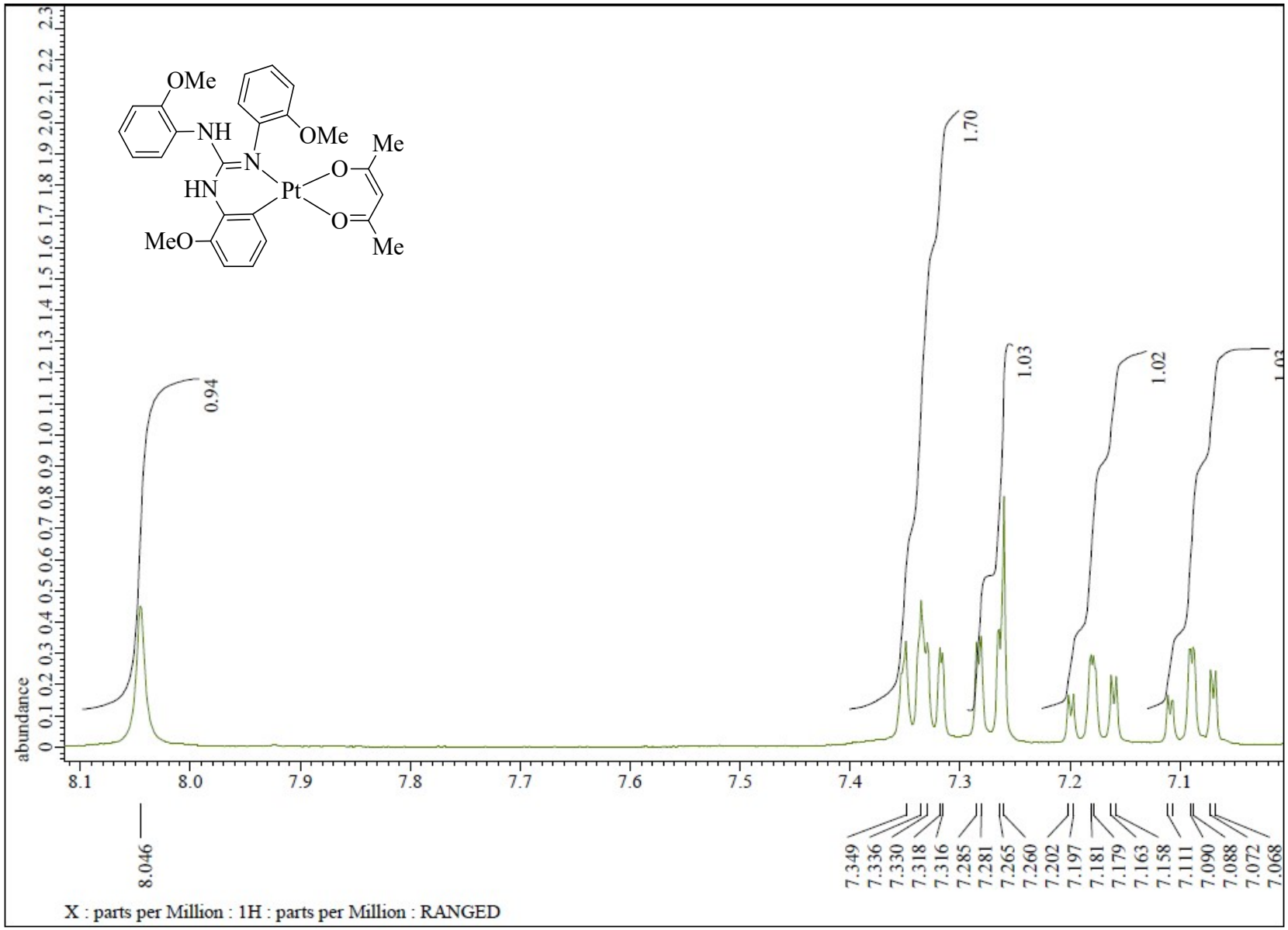

Fig. S73 ^{1}H NMR ($CDCl_3$, 400 MHz) spectrum of **10** in the indicated region.

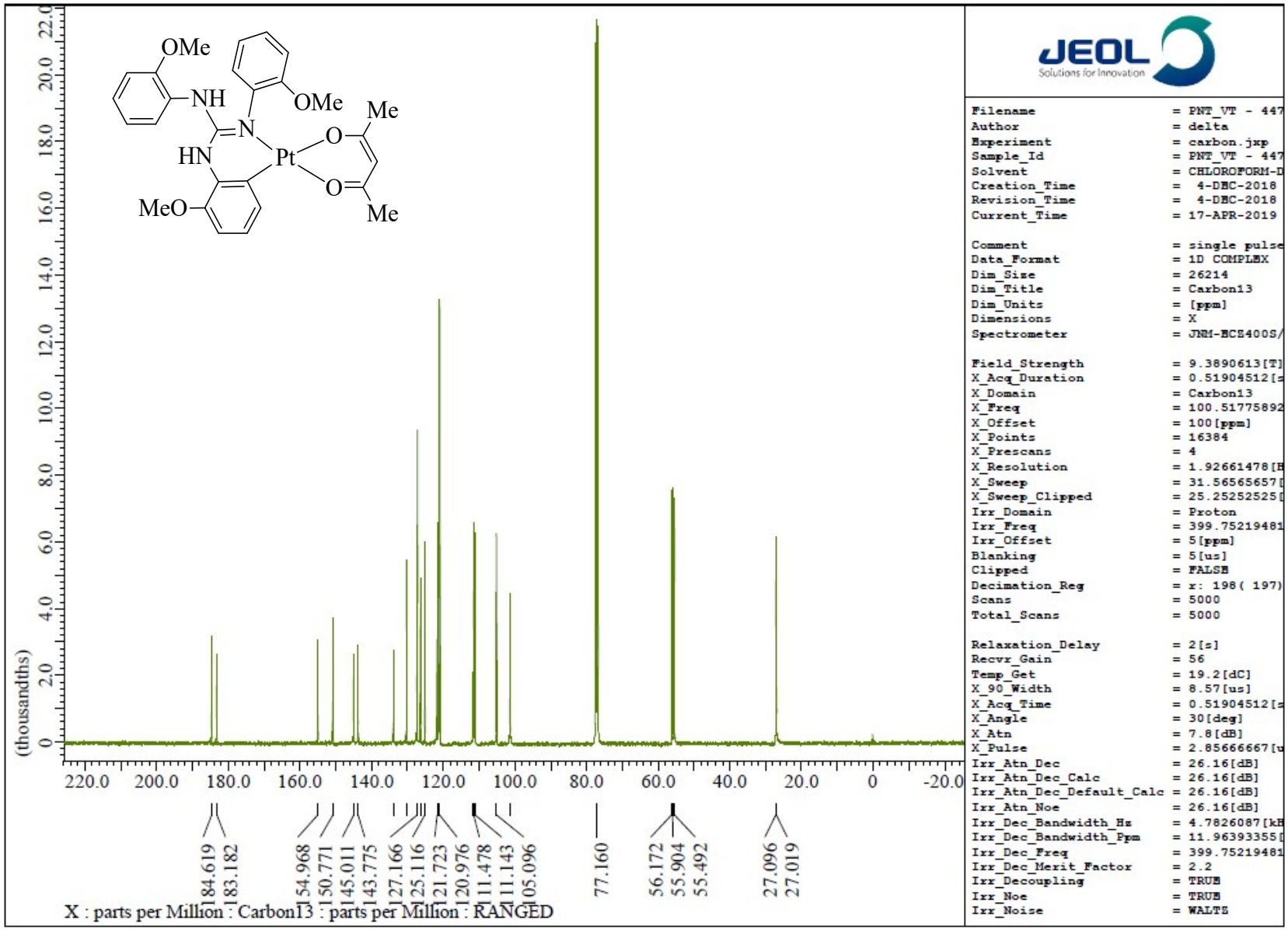

Fig. S74 ^{13}C NMR ($CDCl_3$, 100.5 MHz) spectrum of **10**.

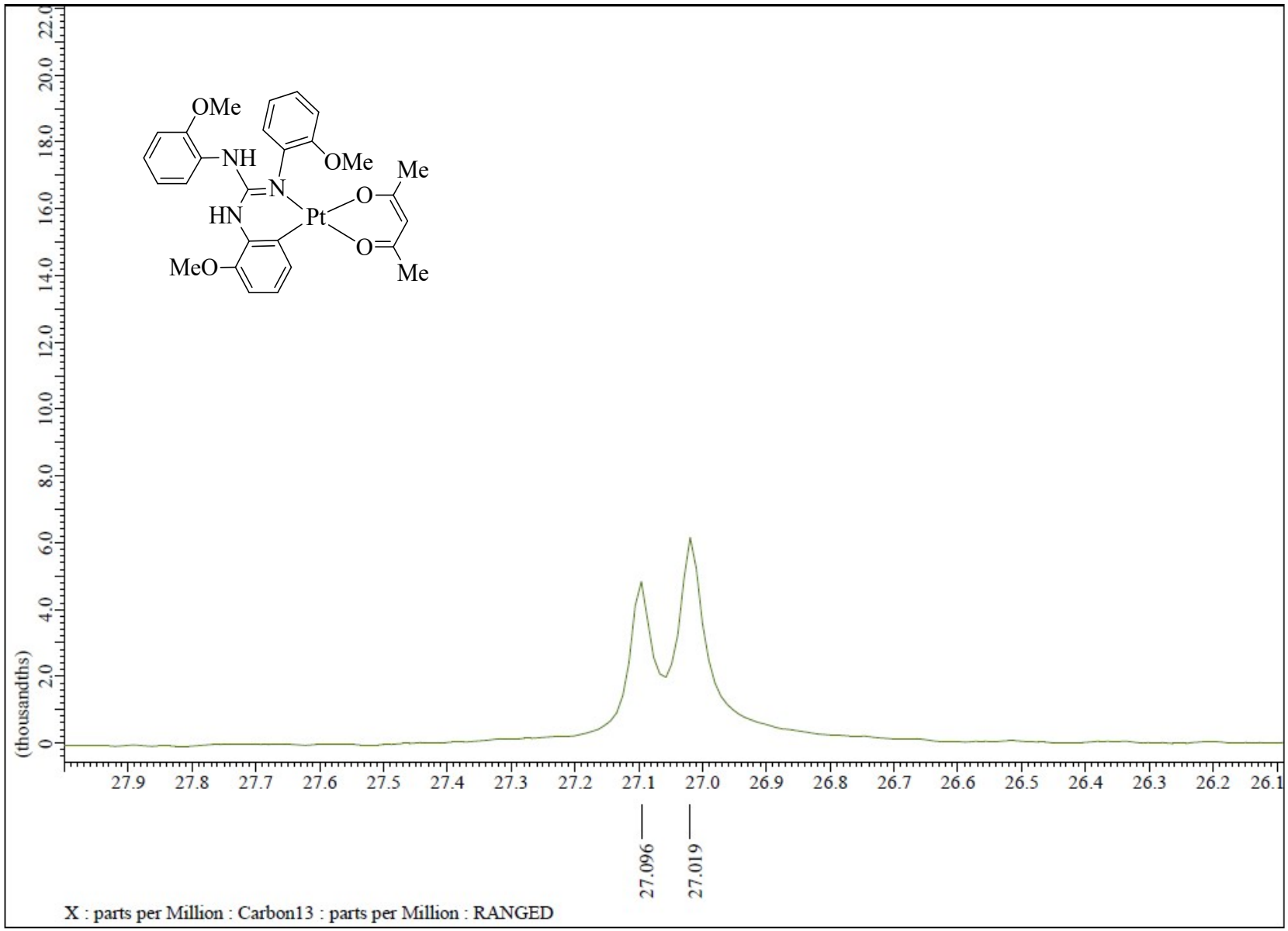

Fig. S75 ^{13}C NMR ($CDCl_3$, 100.5 MHz) spectrum of **10** in the indicated region.

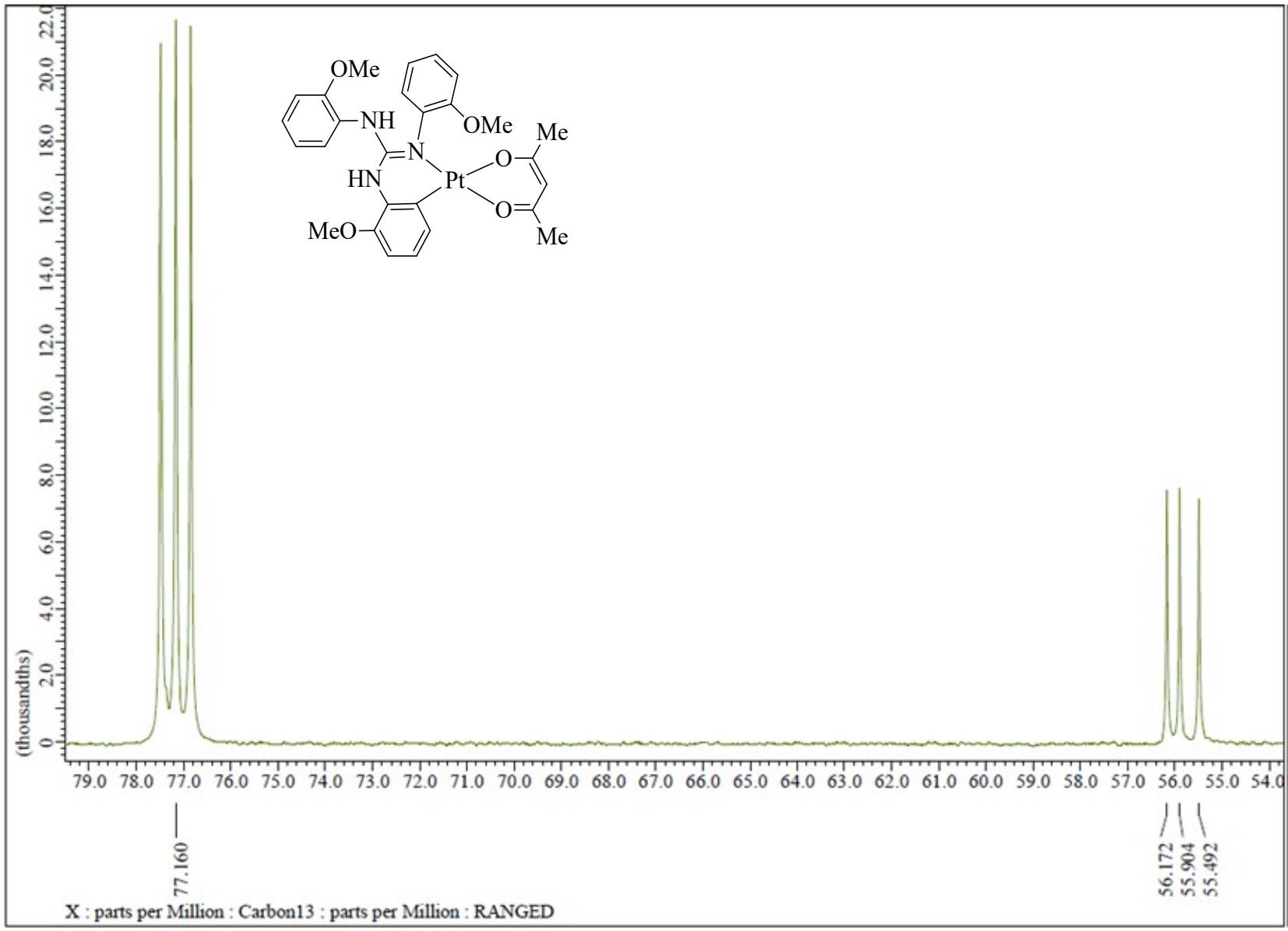

Fig. S76 ^{13}C NMR ($CDCl_3$, 100.5 MHz) spectrum of **10** in the indicated region.

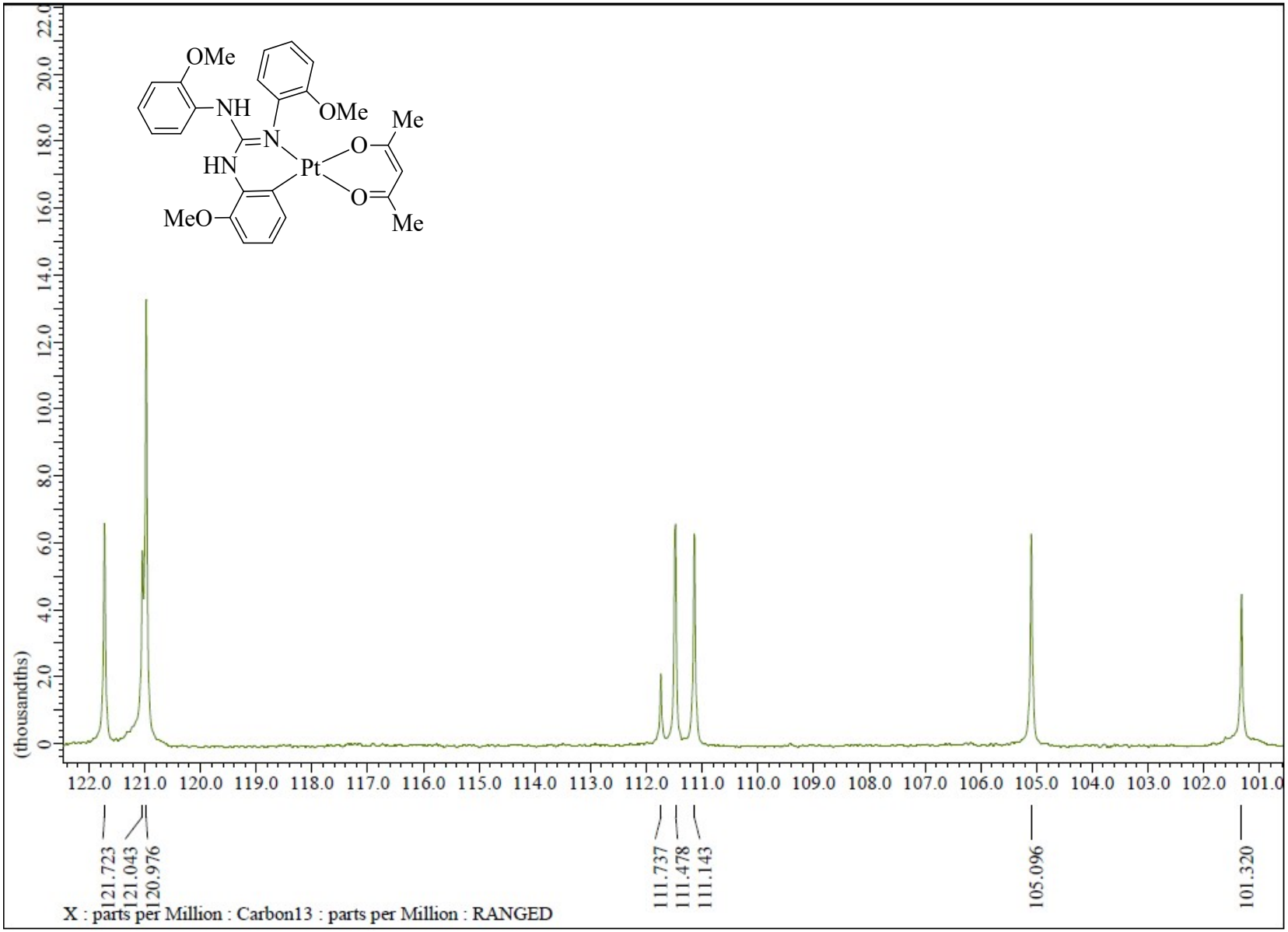

Fig. S77 ^{13}C NMR ($CDCl_3$, 100.5 MHz) spectrum of **10** in the indicated region.

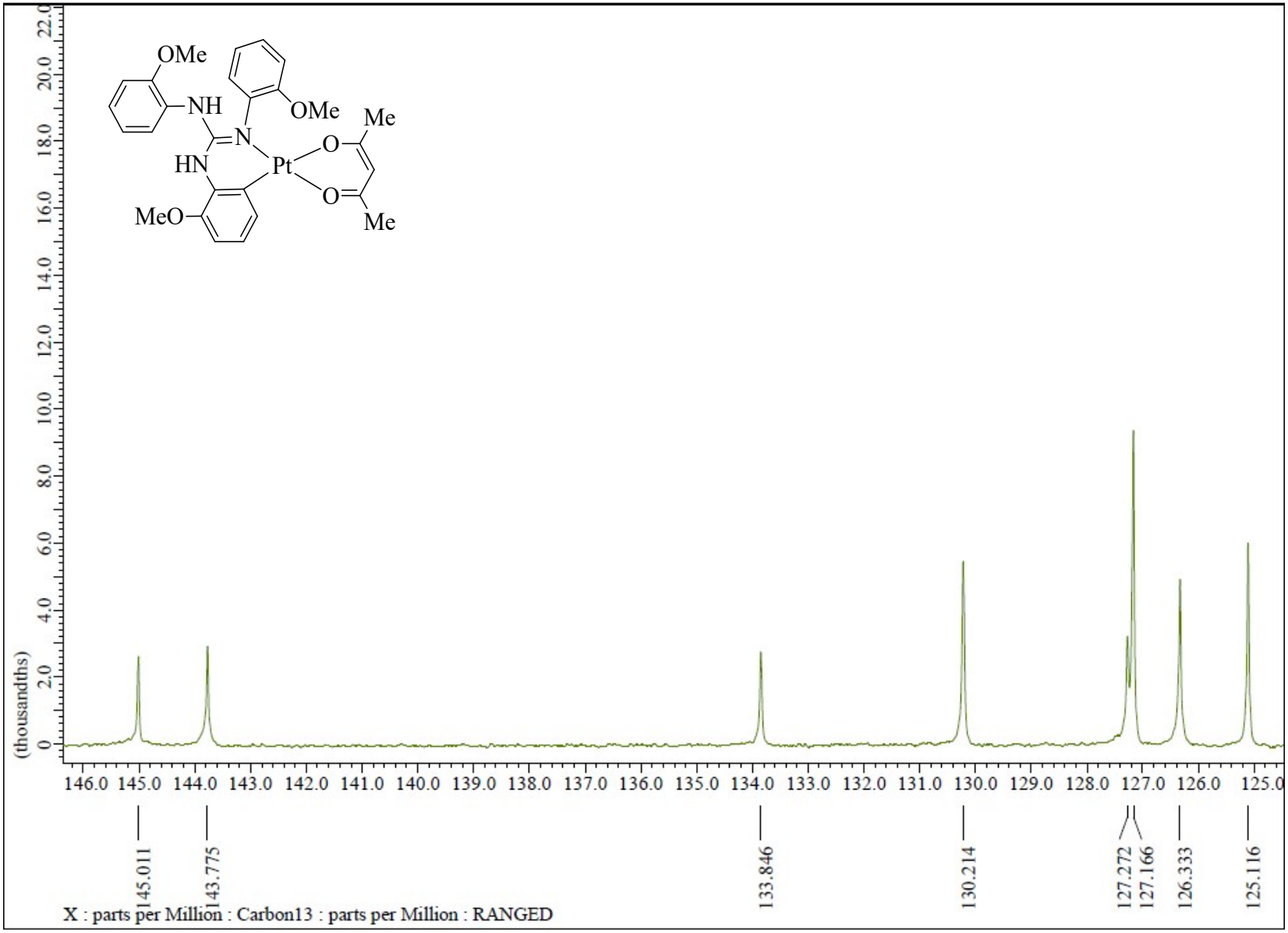

Fig. S78 ^{13}C NMR ($CDCl_3$, 100.5 MHz) spectrum of **10** in the indicated region.

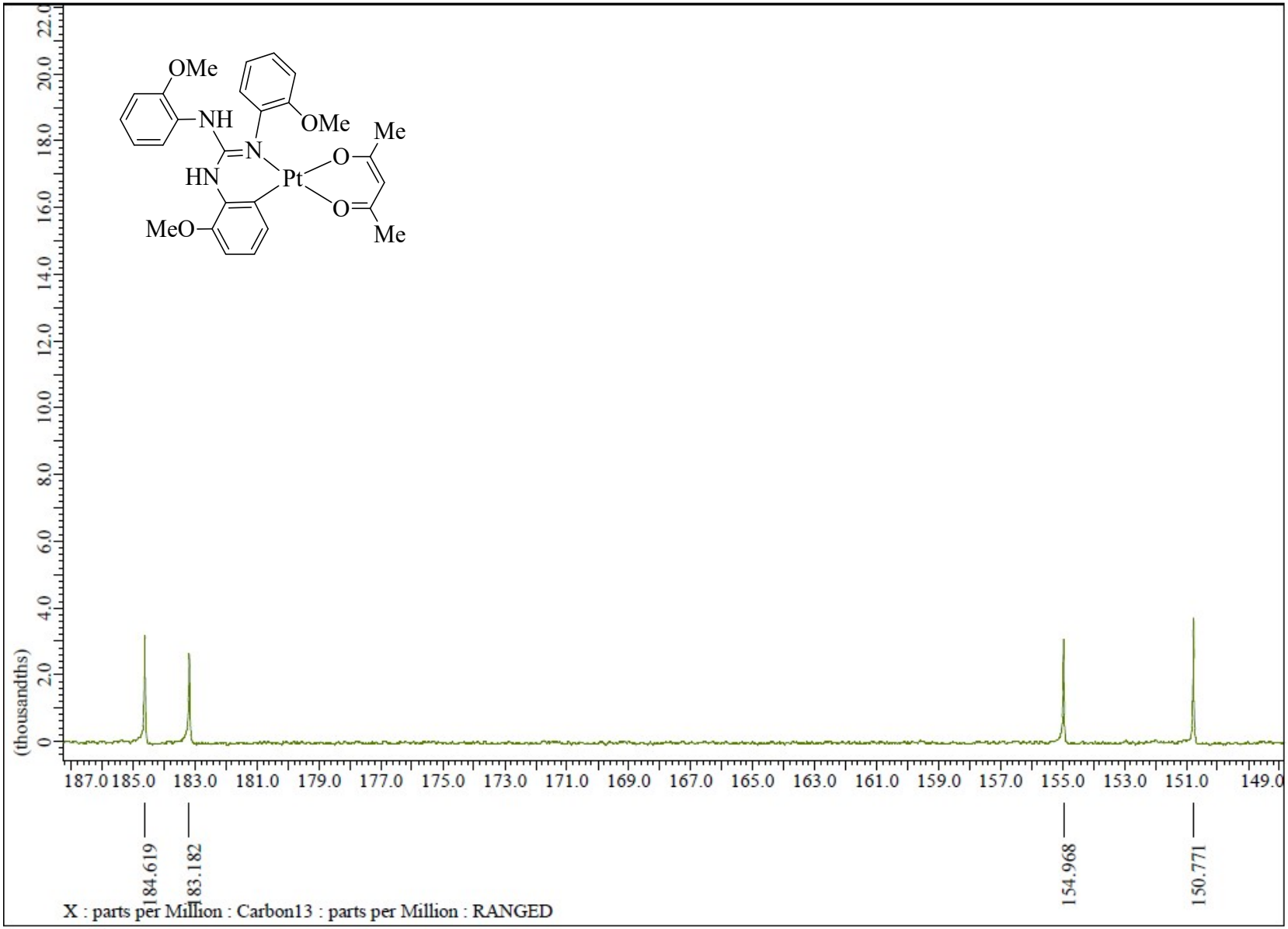

Fig. S79 ^{13}C NMR ($CDCl_3$, 100.5 MHz) spectrum of **10** in the indicated region.

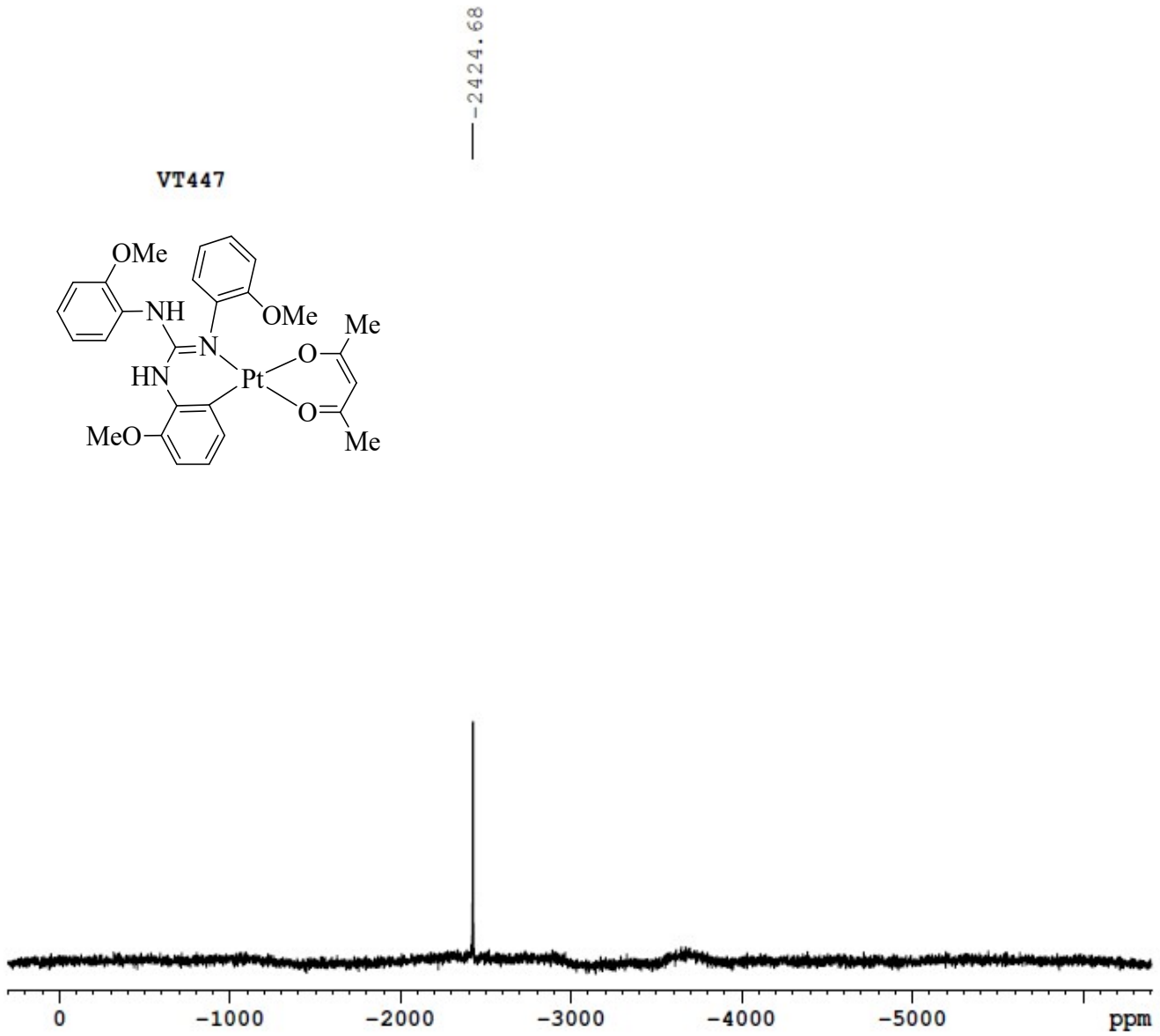


```
Current Data Parameters
NAME         11_Tirupati
EXPNO                  7
PROCNO                 1

F2 - Acquisition Parameters
Date_           20170712
Time               10.36
INSTRUM            spect
PROBHD   5 mm PABBO BB-
PULPROG               zg
TD                  5710
SOLVENT            CDCl3
NS                  1024
DS                     0
SWH          576923.063 Hz
FIDRES       101.037315 Hz
AQ            0.0049487 sec
RG                    18
DW                0.867 usec
DE                6.50 usec
TE                298.0 K
D1           1.00000000 sec
TD0                    1

======== CHANNEL f1 ========
NUC1                195Pt
P1                 9.50 usec
PL1                -2.00 dB
PL1W         48.79838562 W
SFO1         85.7741674 MHz

F2 - Processing parameters
SI                 32768
SF           86.0365790 MHz
WDW                   EM
SSB       0
LB                 1.00 Hz
GB        0
PC                 1.00
```

Fig. S80 $^{195}Pt\{^{1}H\}$ NMR ($CDCl_3$, 85.8 MHz) spectrum of **10**.

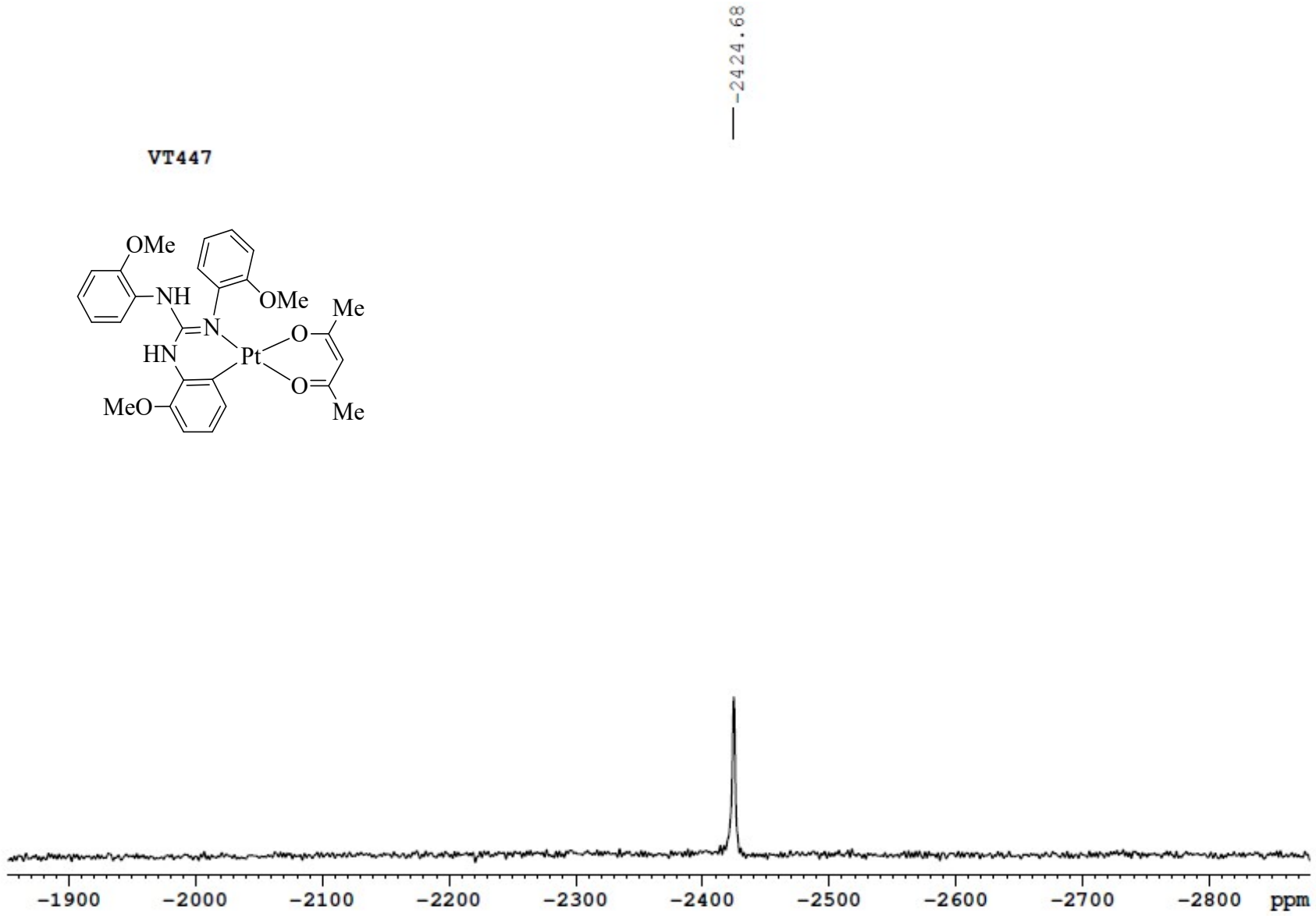

Fig. S81 $^{195}Pt\{^{1}H\}$ NMR ($CDCl_3$, 85.8 MHz) spectrum of **10** in the indicated region.

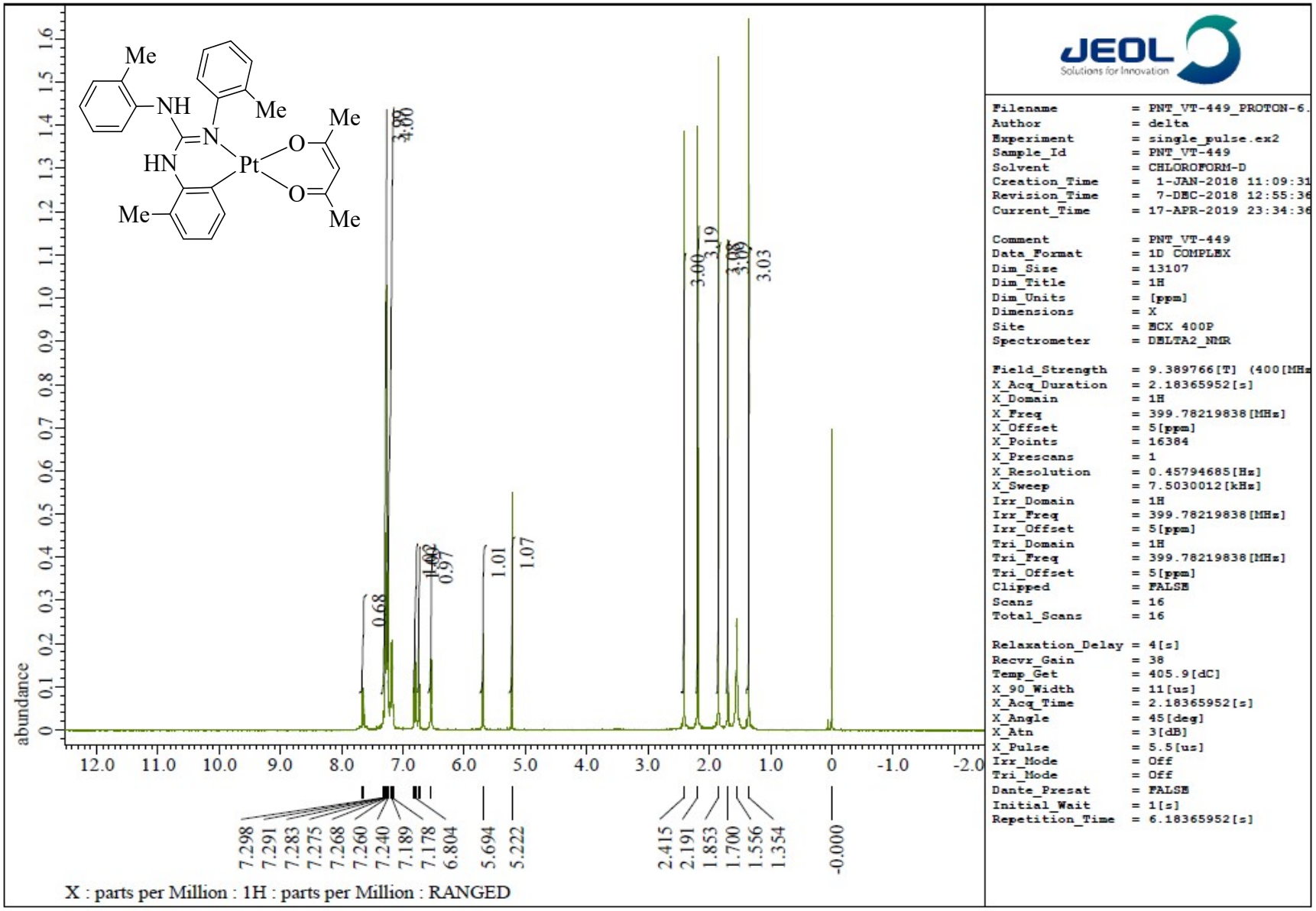

Fig. S82 ^{1}H NMR ($CDCl_3$, 400 MHz) spectrum of **11**.

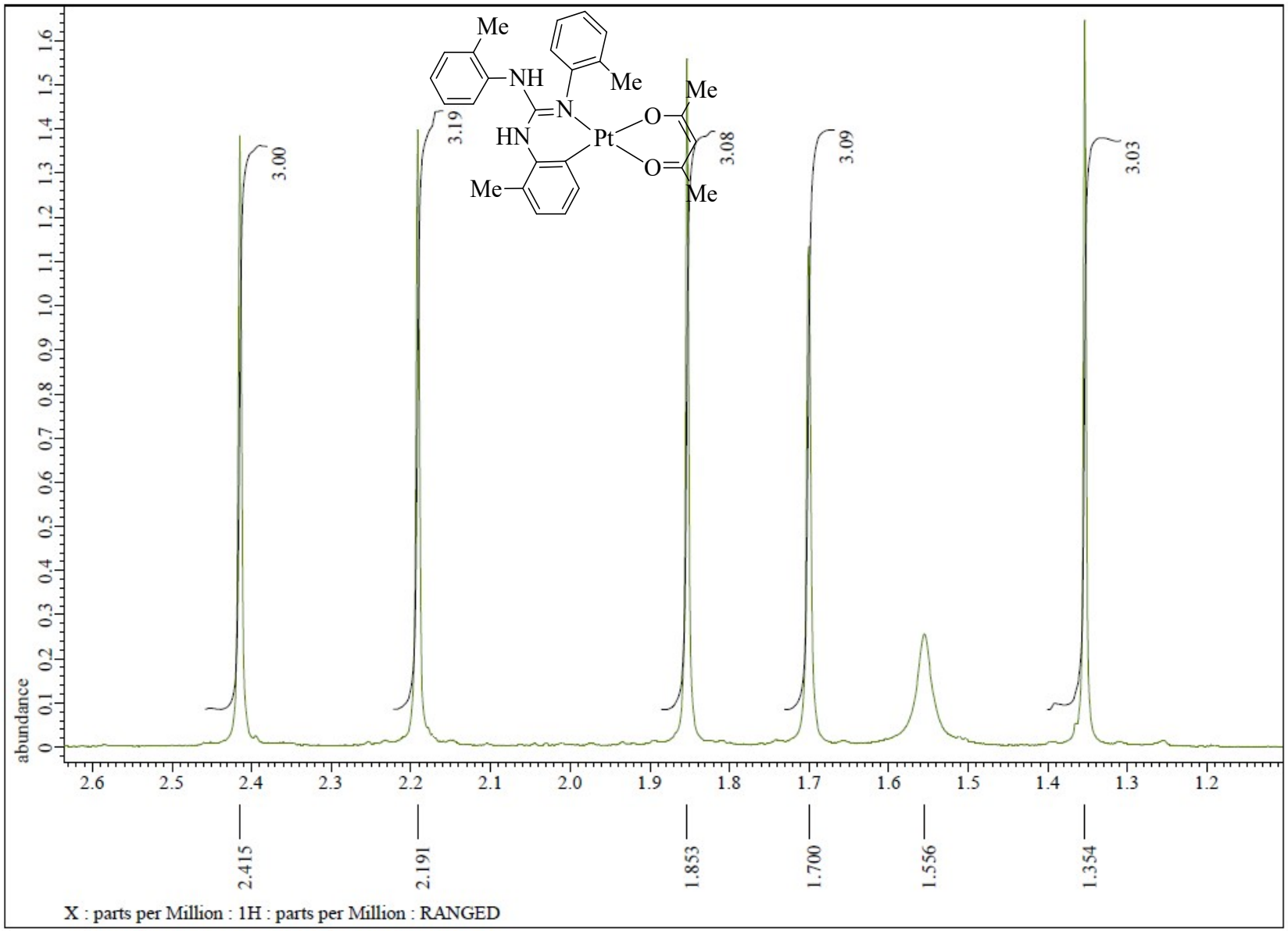

Fig. S83 ^{1}H NMR ($CDCl_3$, 400 MHz) spectrum of **11** in the indicated region.

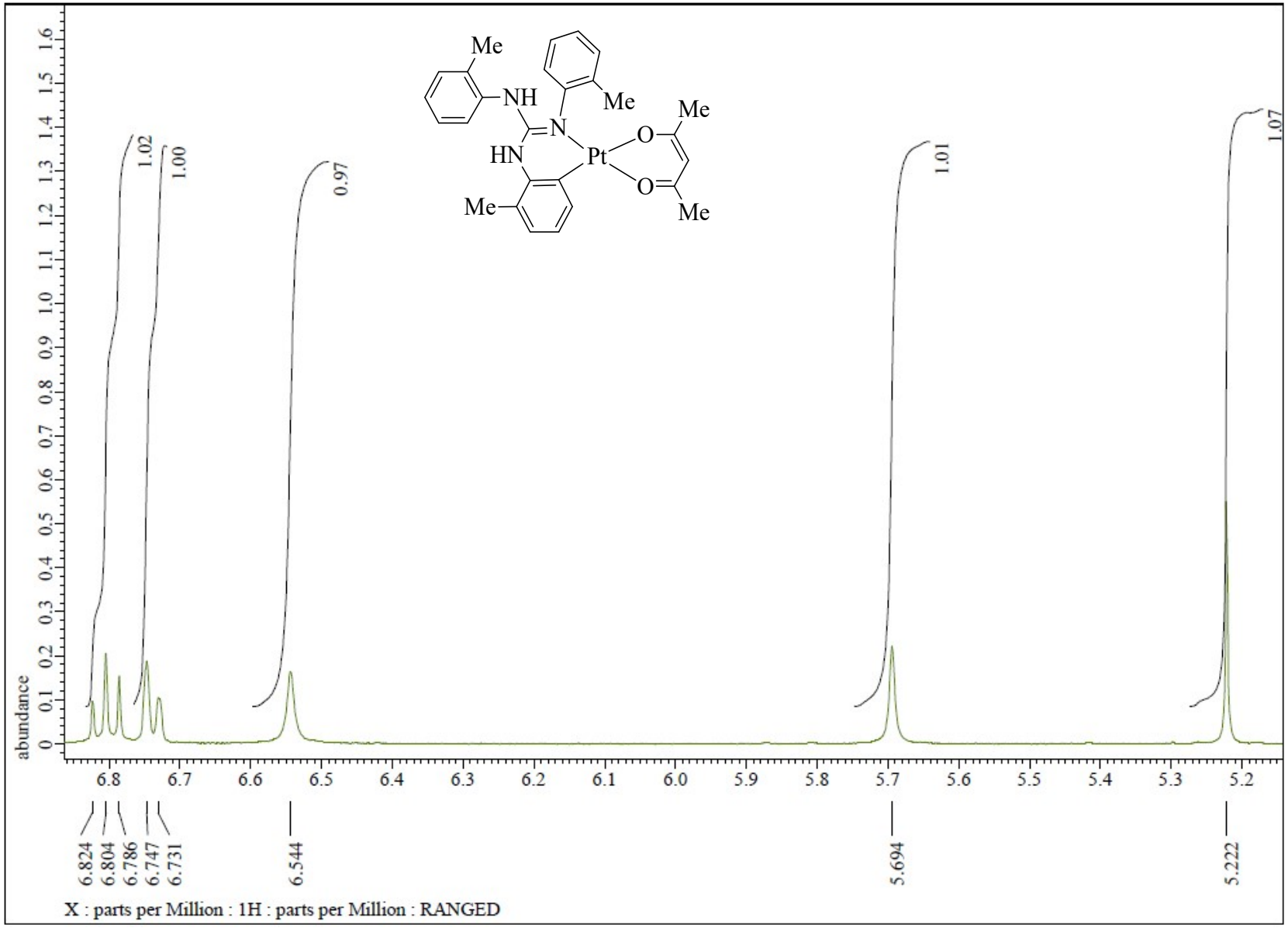

Fig. S84 ^{1}H NMR ($CDCl_3$, 400 MHz) spectrum of **11** in the indicated region.

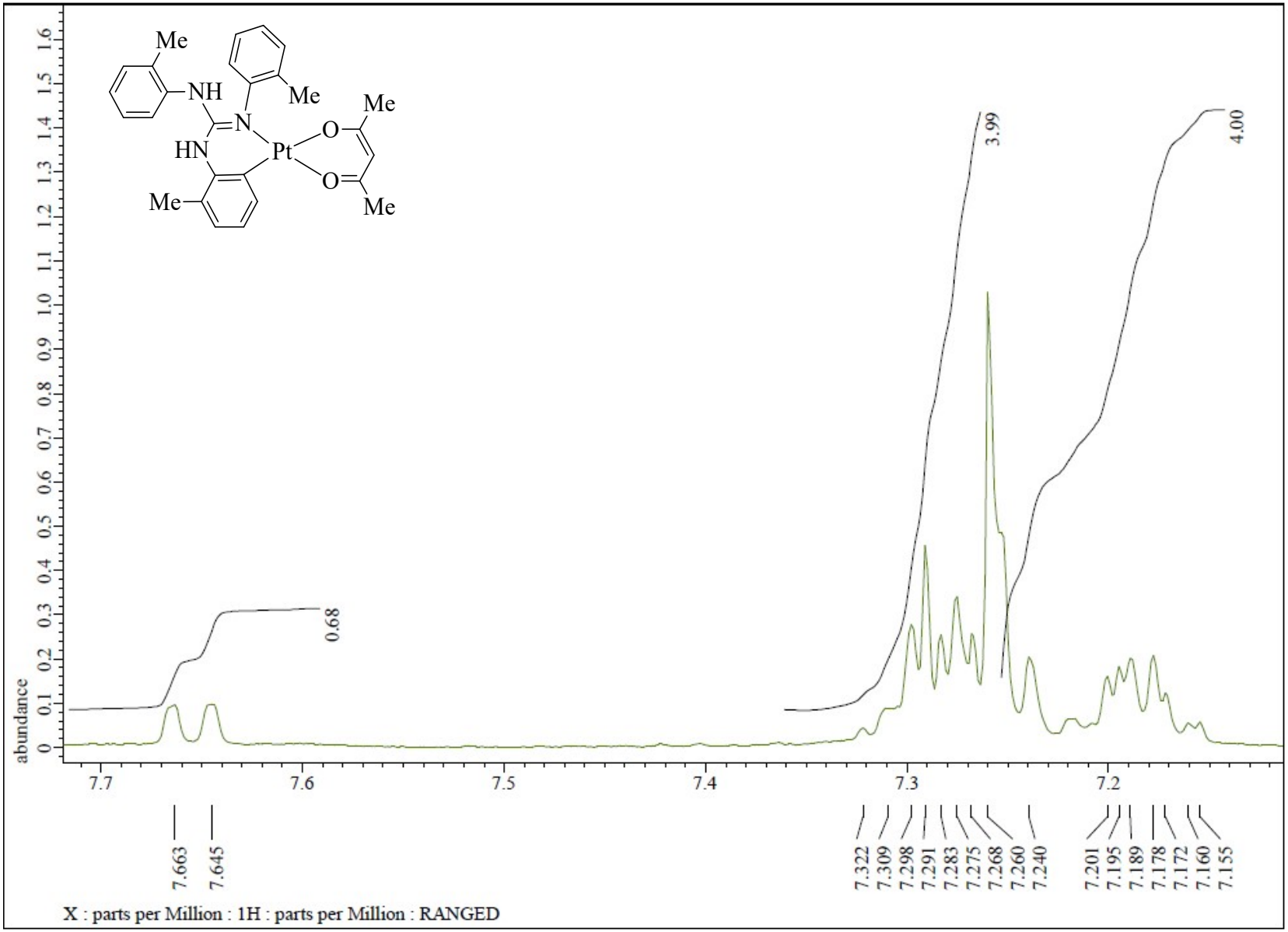

Fig. S85 ^{1}H NMR ($CDCl_3$, 400 MHz) spectrum of **11** in the indicated region.

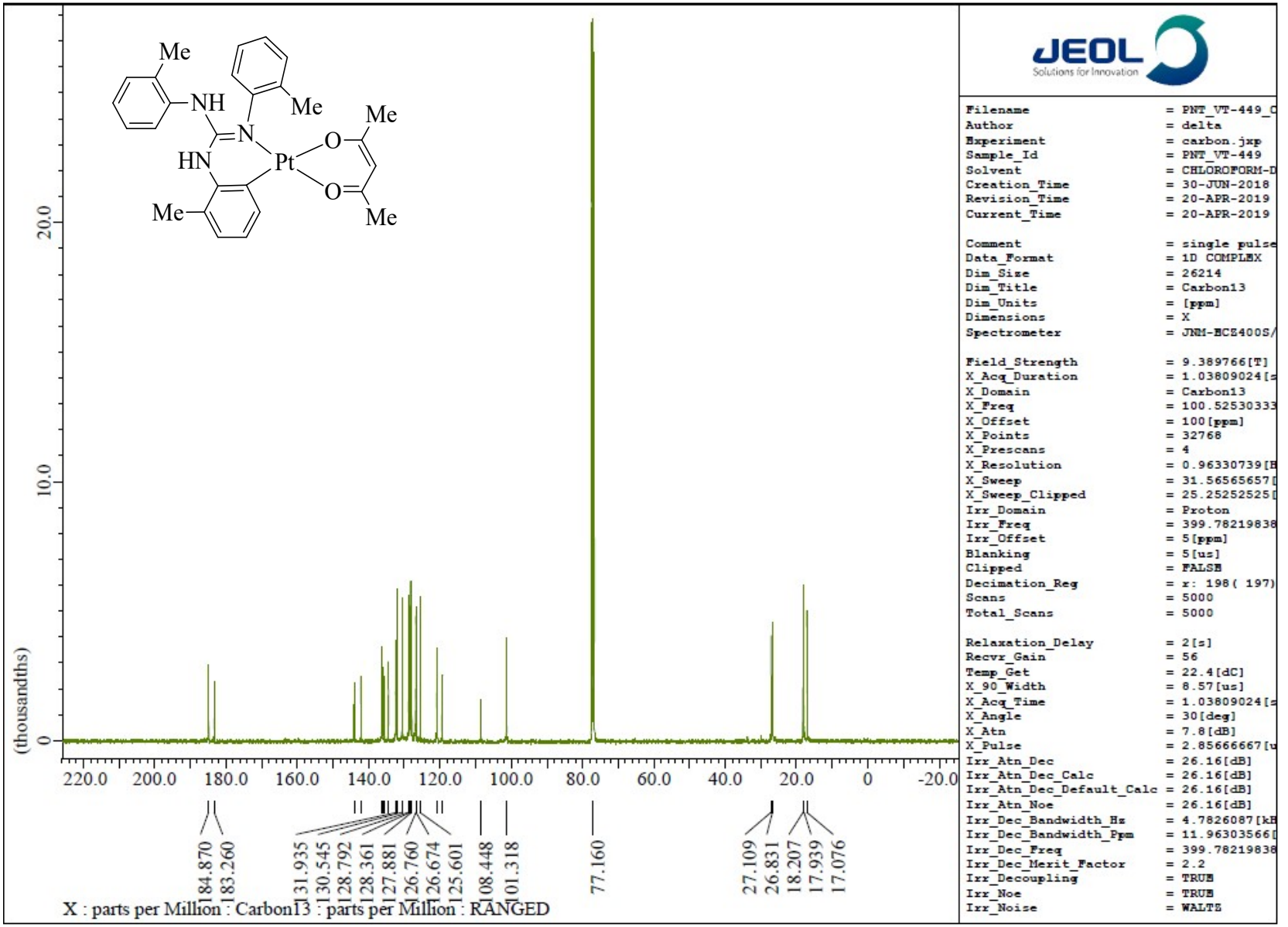

Fig. S86 $^{13}C\{^{1}H\}$ NMR ($CDCl_3$, 100.5 MHz) spectrum of **11**.

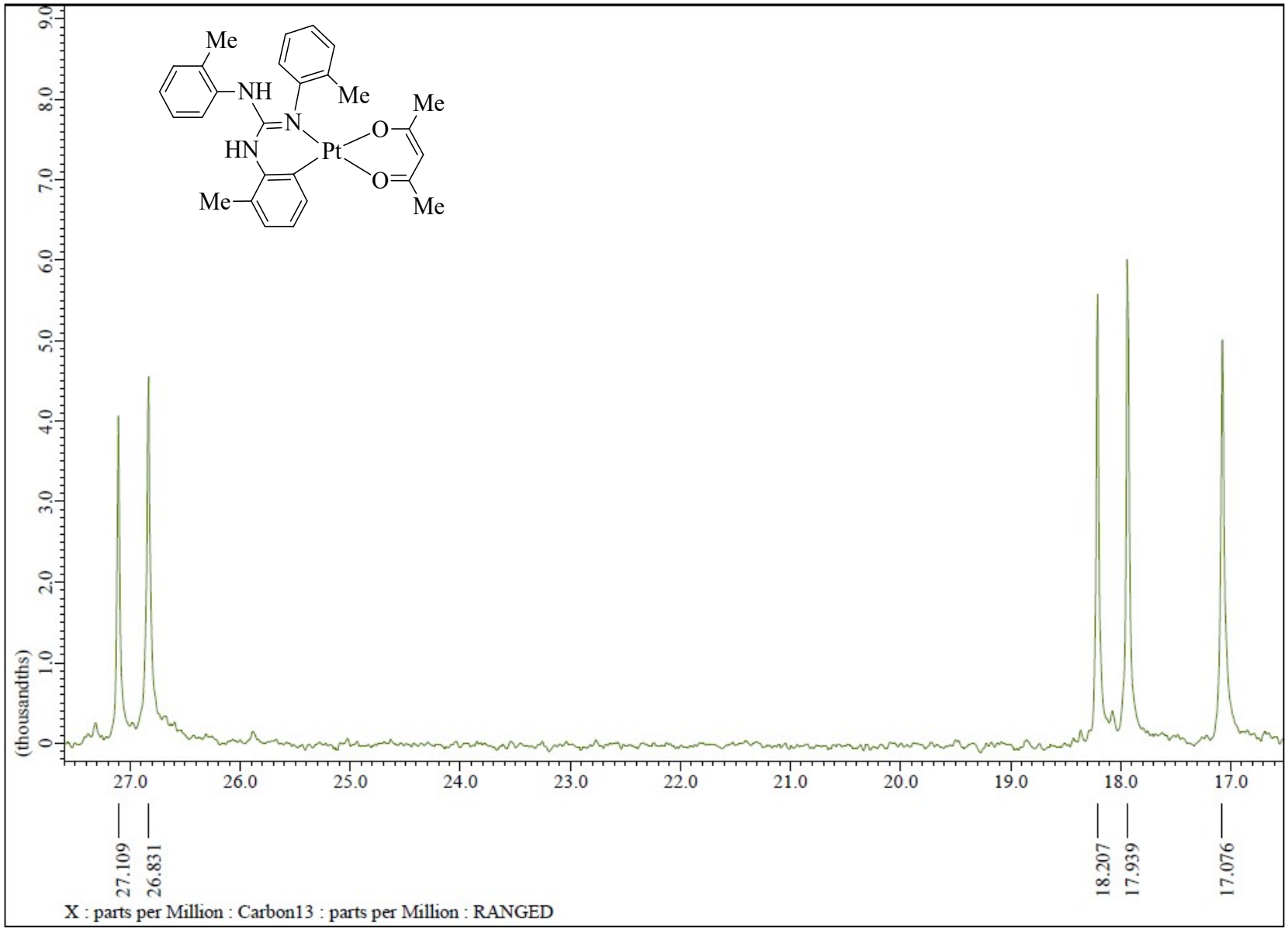

Fig. S87 $^{13}C\{^{1}H\}$ NMR ($CDCl_3$, 100.5 MHz) spectrum of **11** in the indicated region.

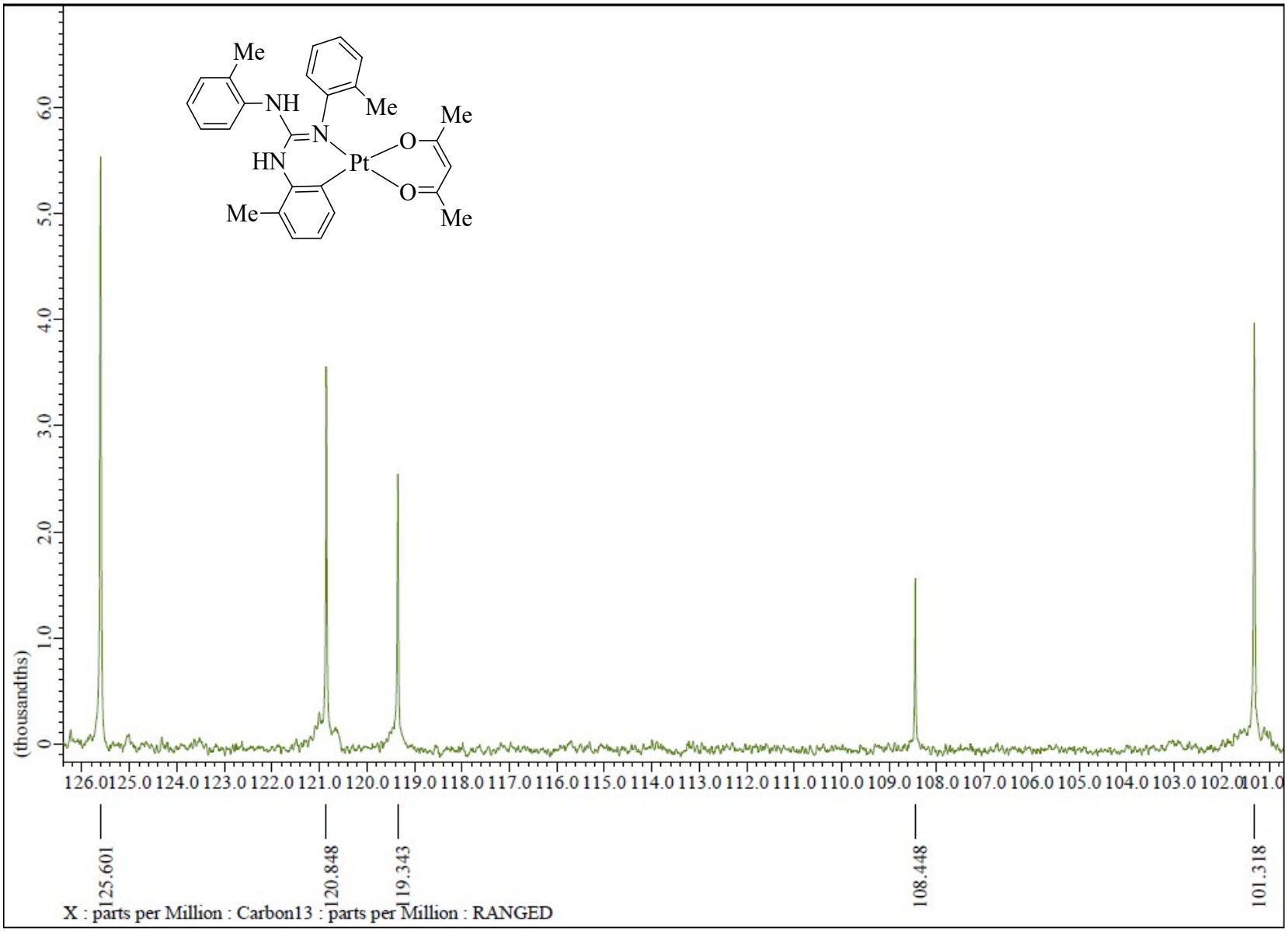

Fig. S88 $^{13}C\{^{1}H\}$ NMR ($CDCl_3$, 100.5 MHz) spectrum of **11** in the indicated region.

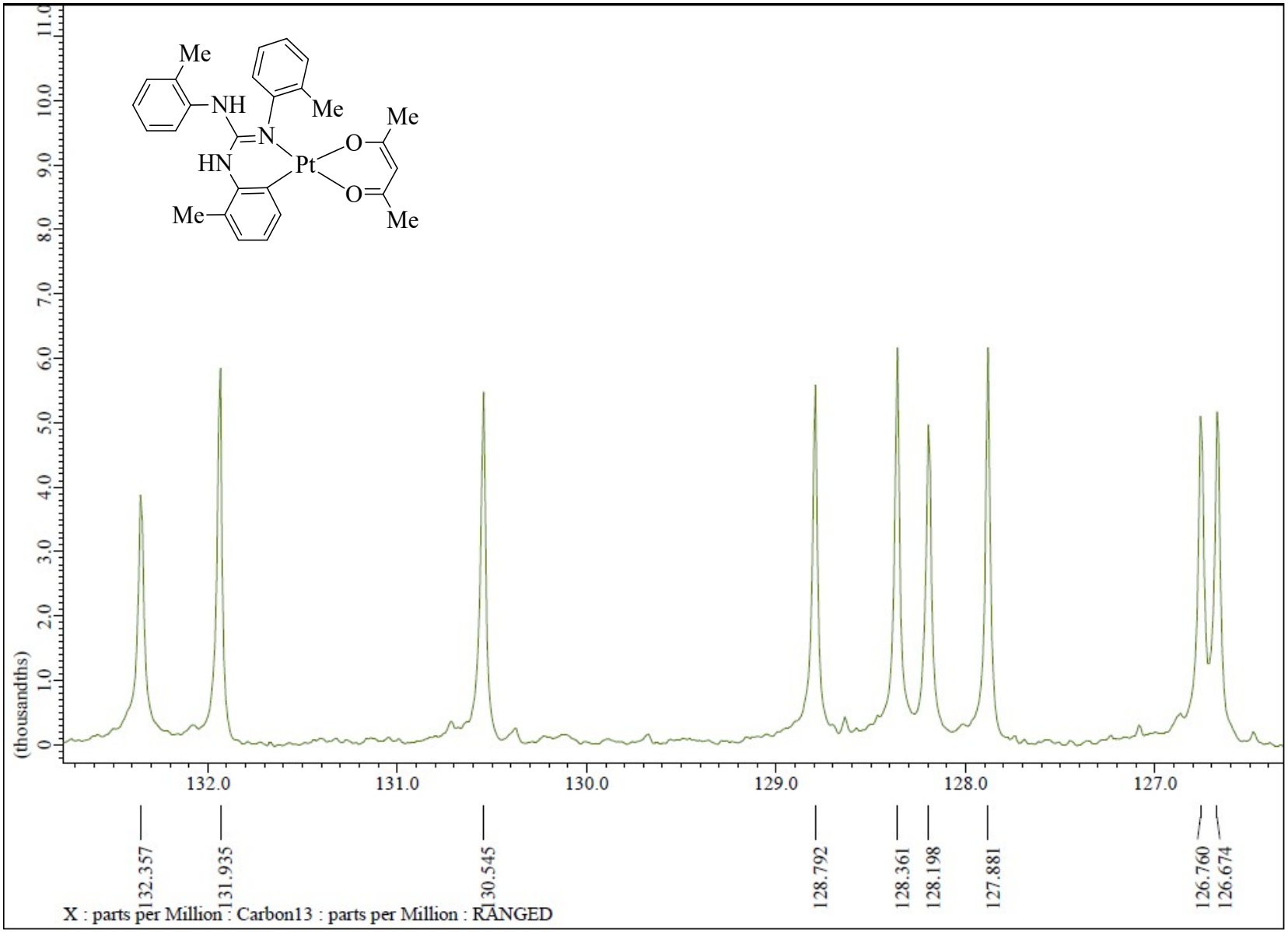

Fig. S89 $^{13}C\{^{1}H\}$ NMR ($CDCl_3$, 100.5 MHz) spectrum of **11** in the indicated region.

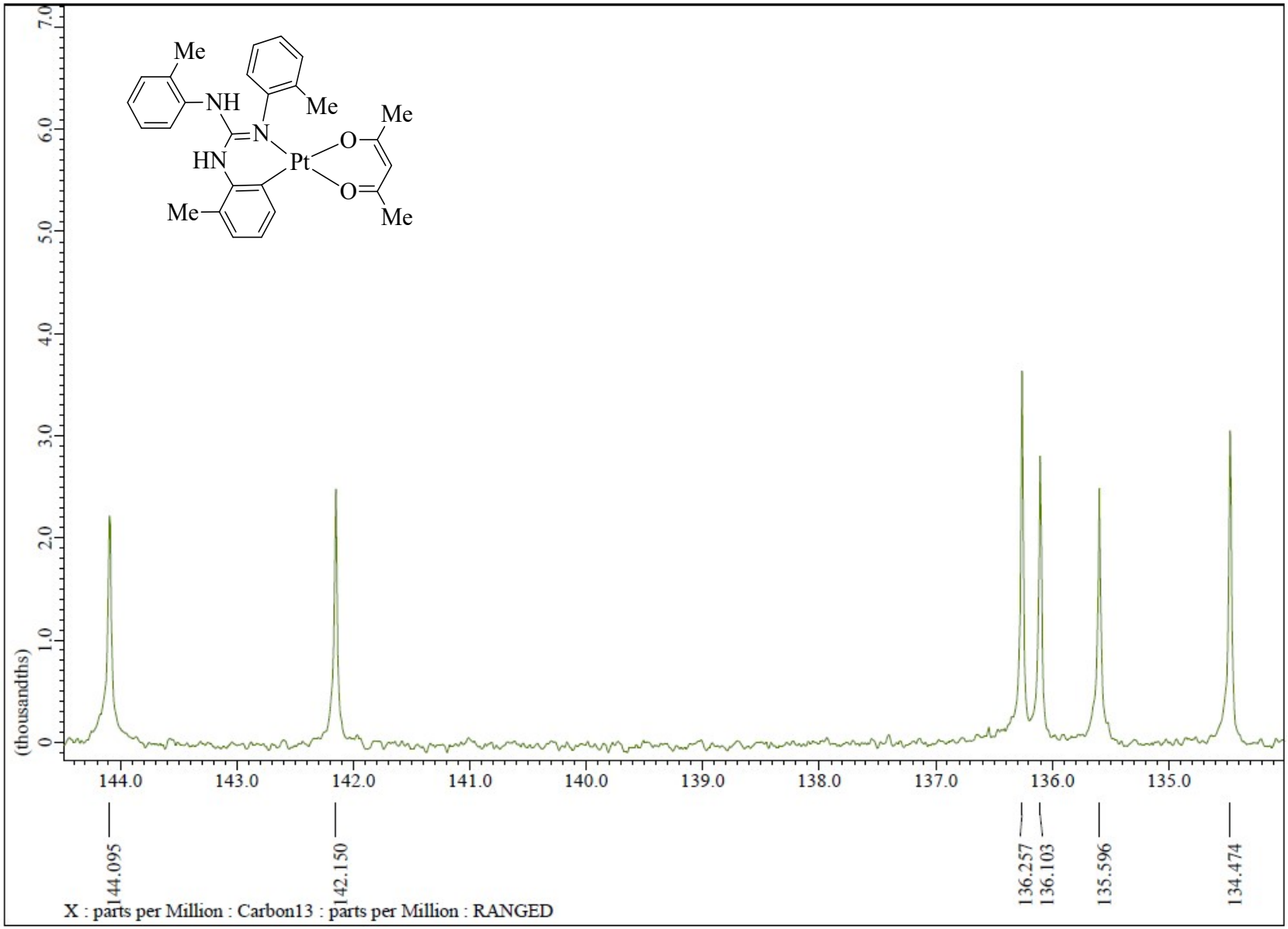

Fig. S90 $^{13}C\{^{1}H\}$ NMR ($CDCl_3$, 100.5 MHz) spectrum of **11** in the indicated region.

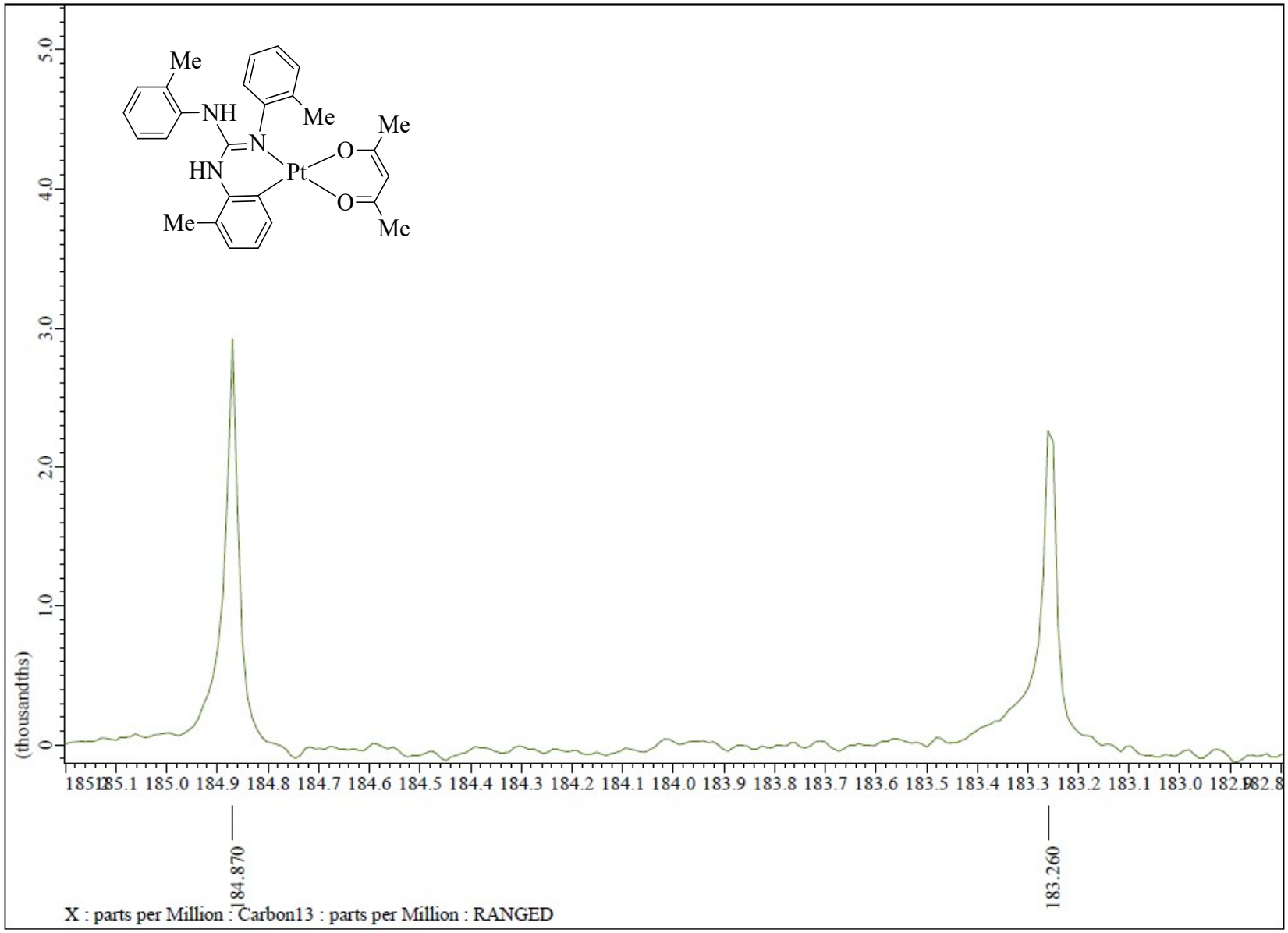

Fig. S91 $^{13}C\{^{1}H\}$ NMR ($CDCl_3$, 100.5 MHz) spectrum of **11** in the indicated region.

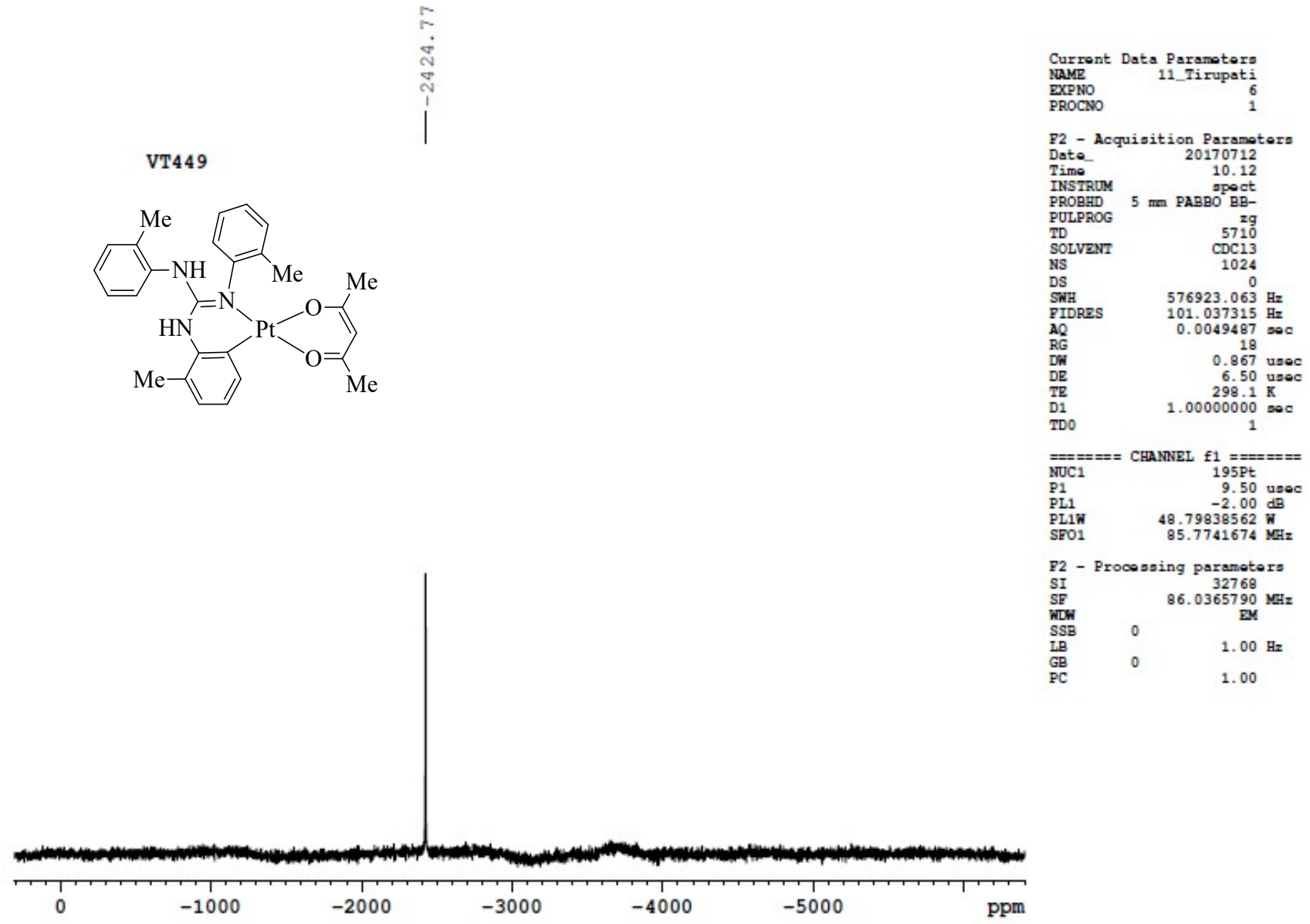

Fig. S92 $^{195}Pt\{^{1}H\}$ NMR ($CDCl_3$, 85.8 MHz) spectrum of **11**.

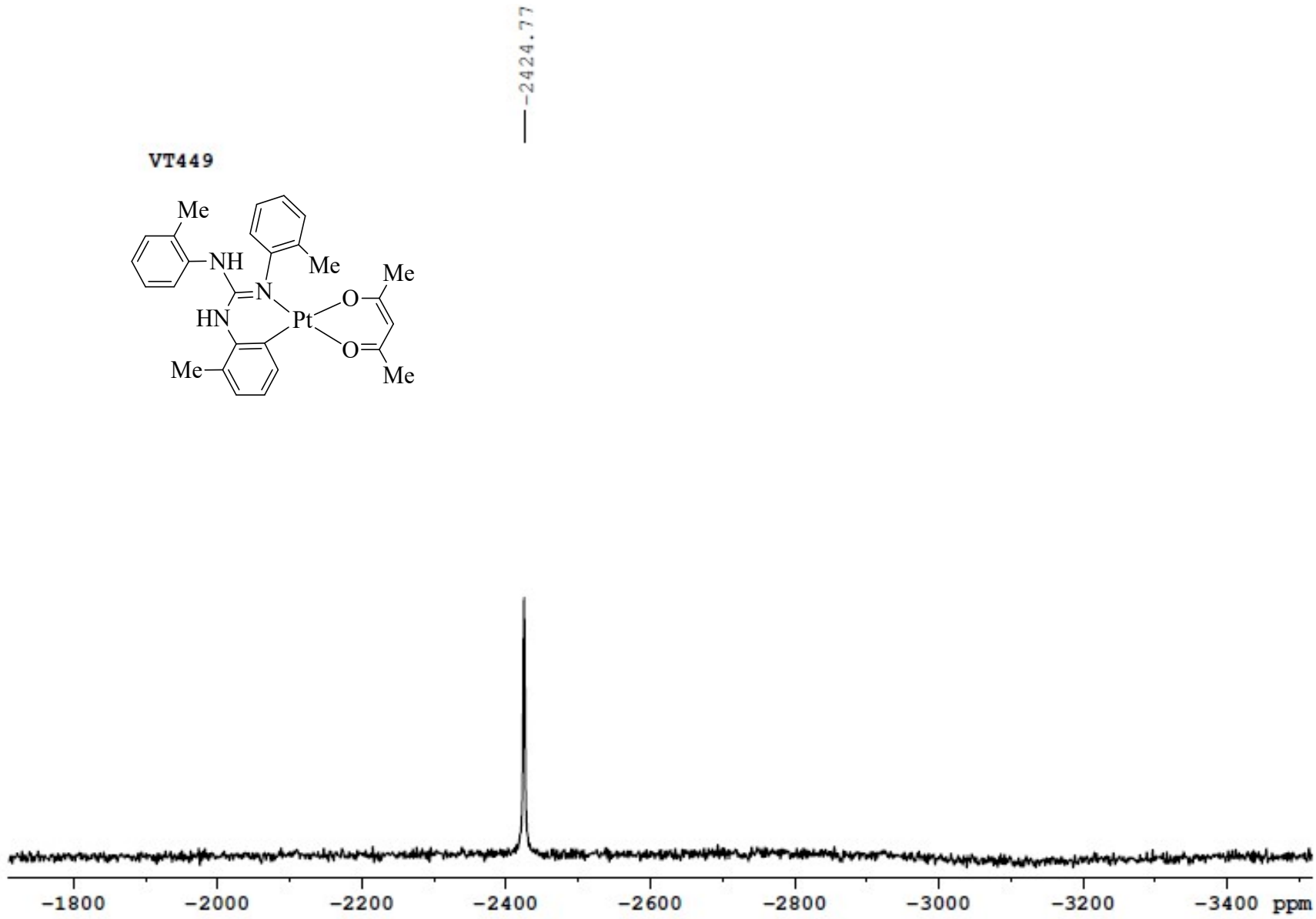

Fig. S93 $^{195}Pt\{^{1}H\}$ NMR ($CDCl_3$, 85.8 MHz) spectrum of **11** in the indicated region.

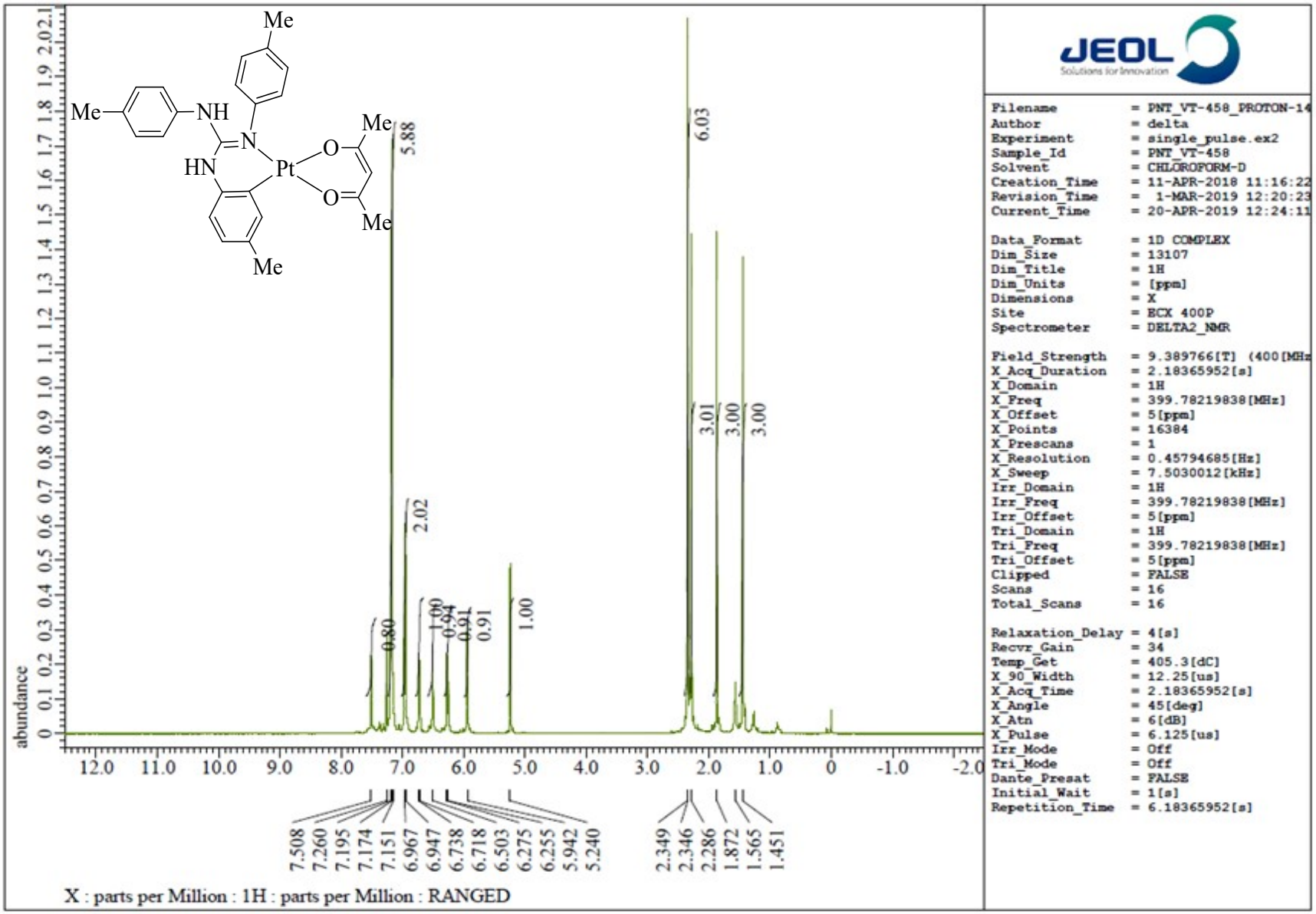

Fig. S94 ^{1}H NMR ($CDCl_3$, 400 MHz) spectrum of **12**.

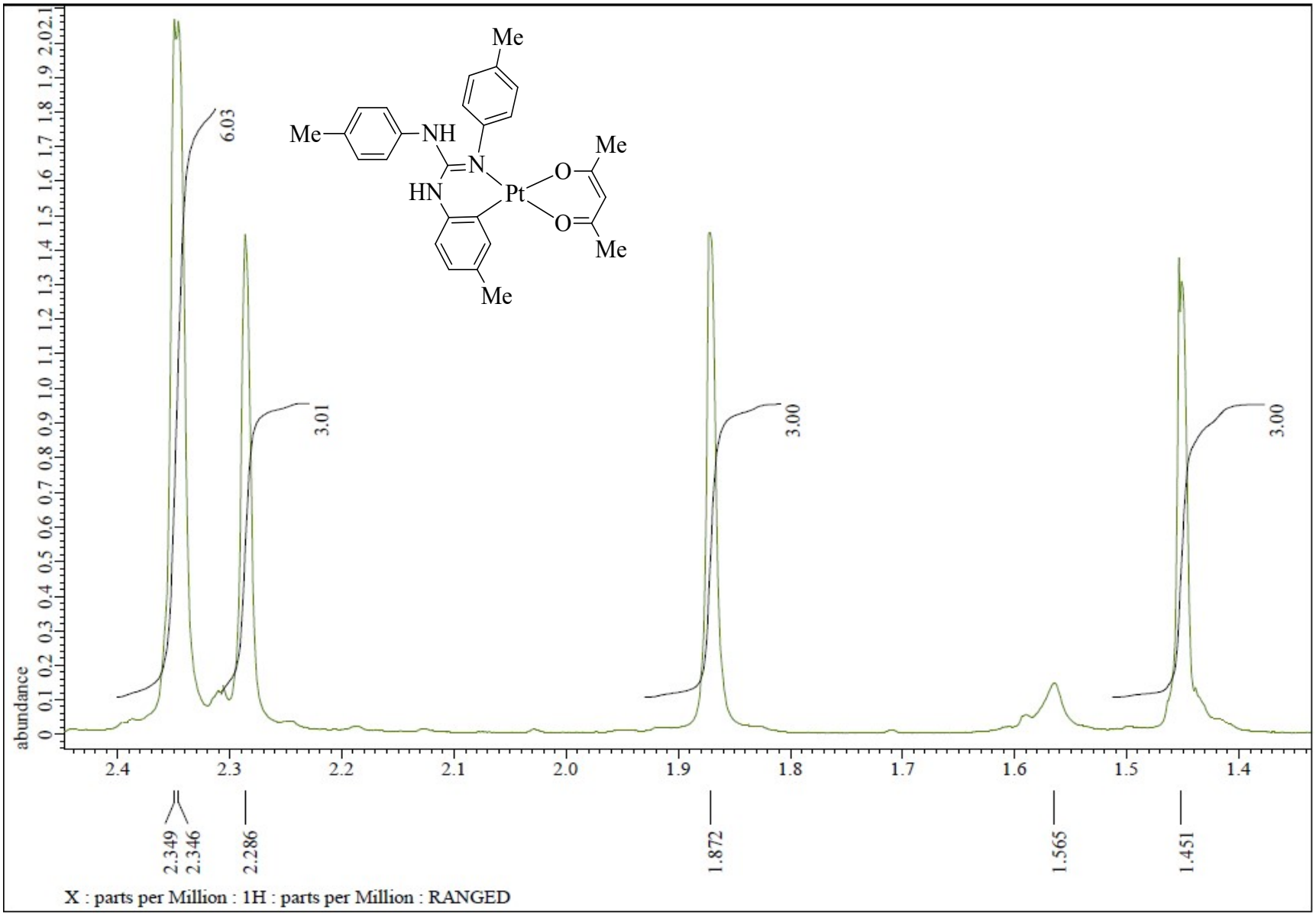

Fig. S95 ^{1}H NMR ($CDCl_3$, 400 MHz) spectrum of **12** in the indicated region.

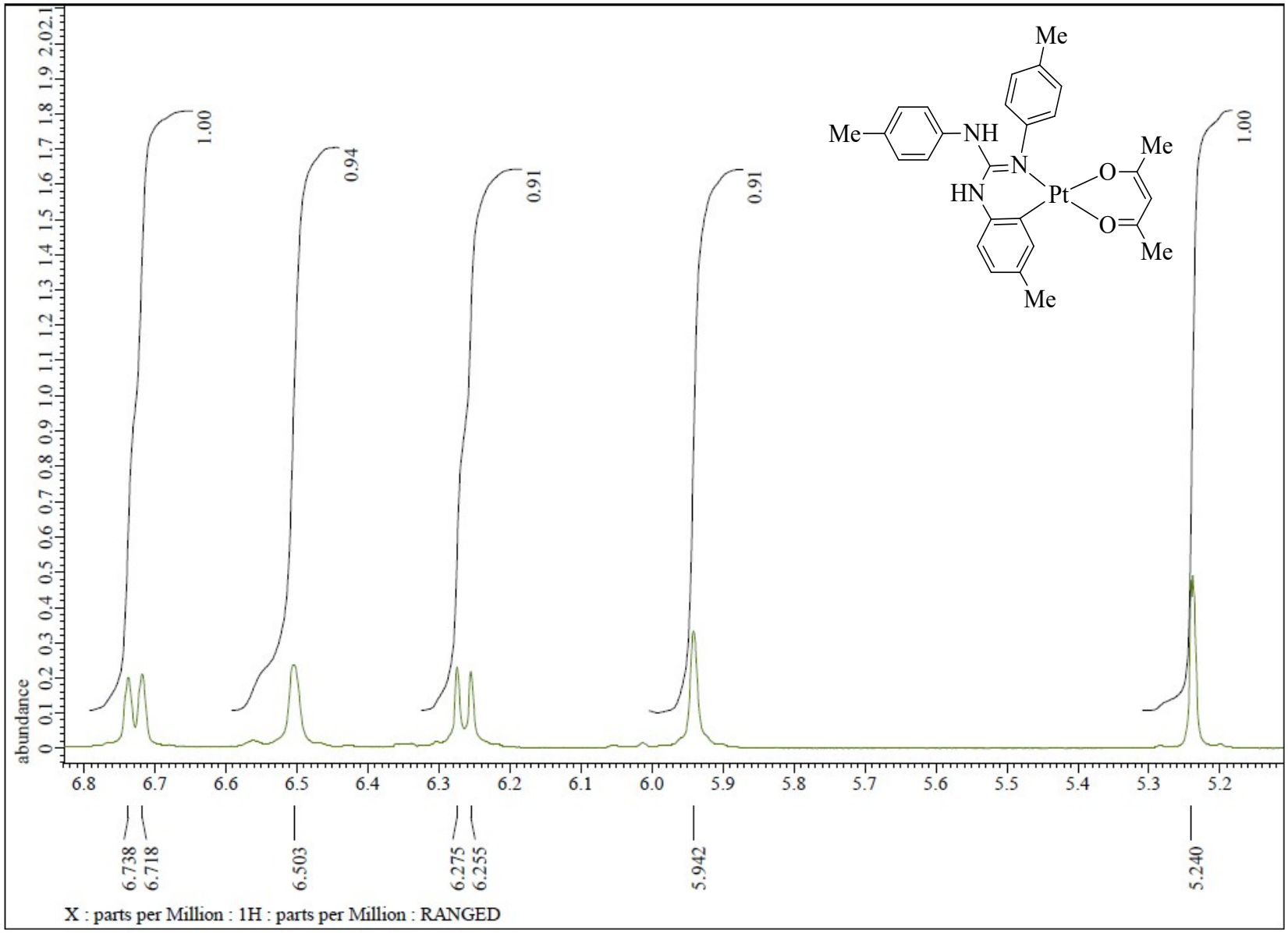

Fig. S96 ^{1}H NMR ($CDCl_3$, 400 MHz) spectrum of **12** in the indicated region.

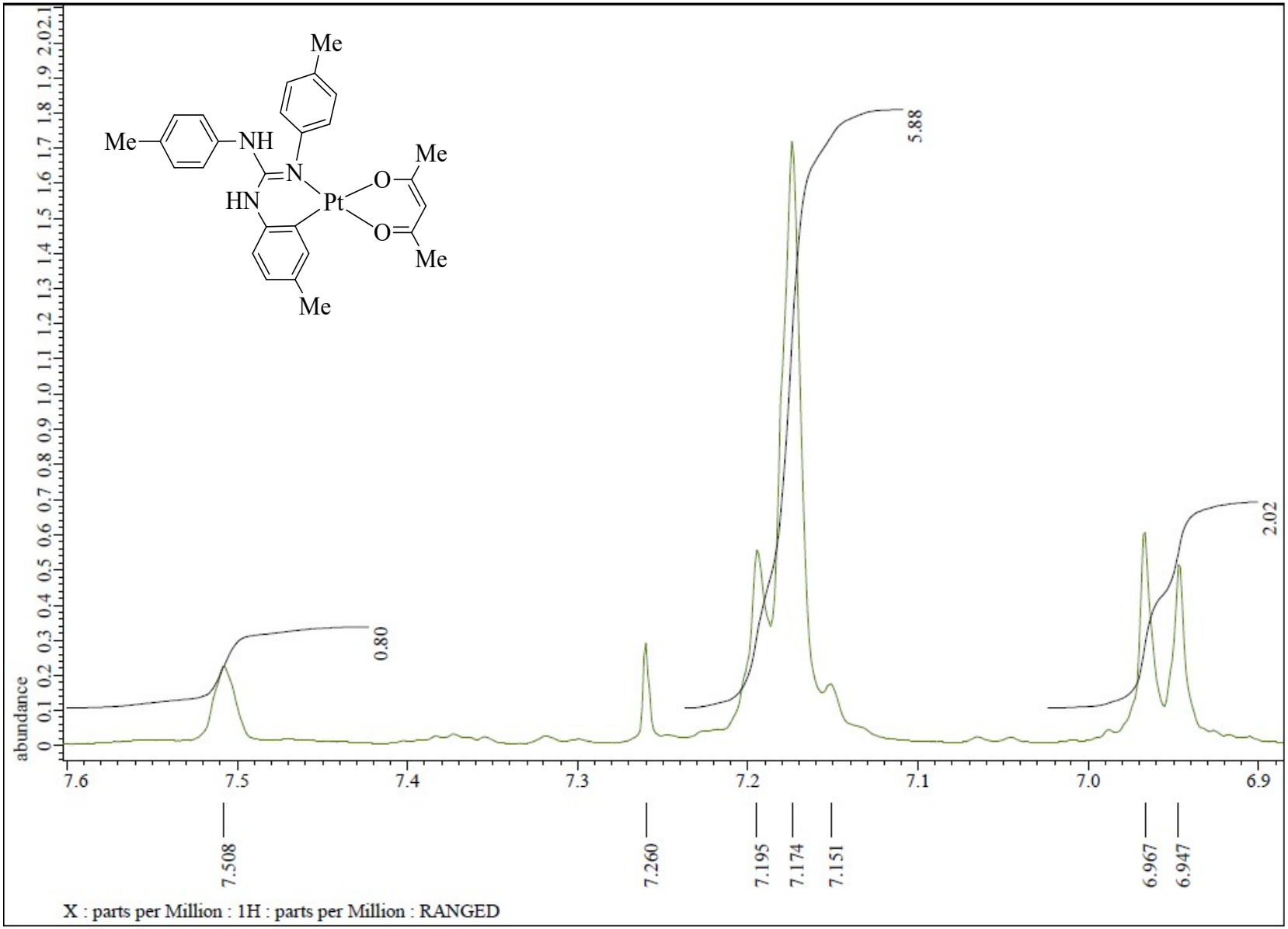

Fig. S97 ^{1}H NMR ($CDCl_3$, 400 MHz) spectrum of **12** in the indicated region.

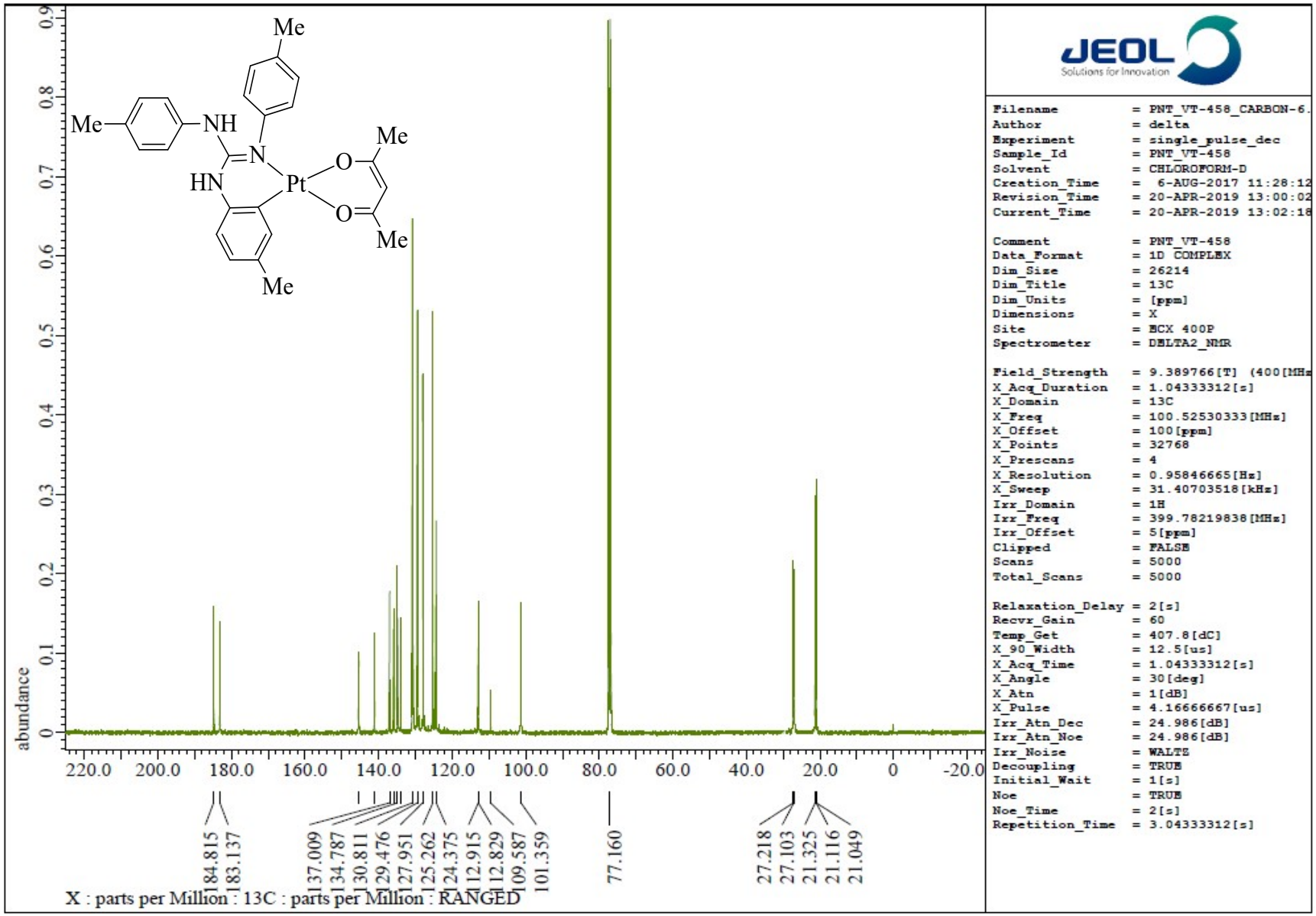

Fig. S98 $^{13}C\{^{1}H\}$ NMR ($CDCl_3$, 100.5 MHz) spectrum of **12**.

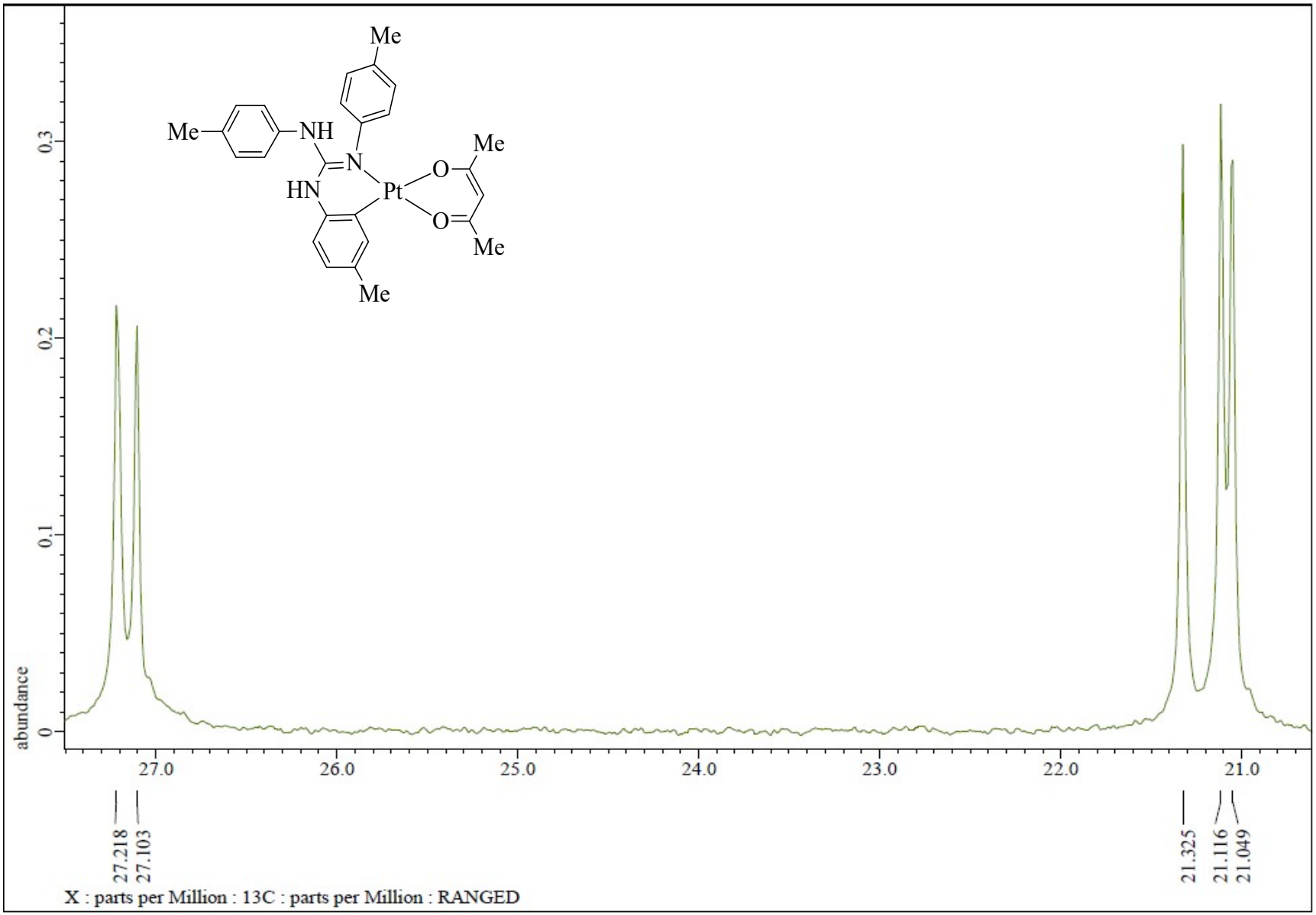

Fig. S99 $^{13}C\{^{1}H\}$ NMR ($CDCl_3$, 100.5 MHz) spectrum of **12** in the indicated region.

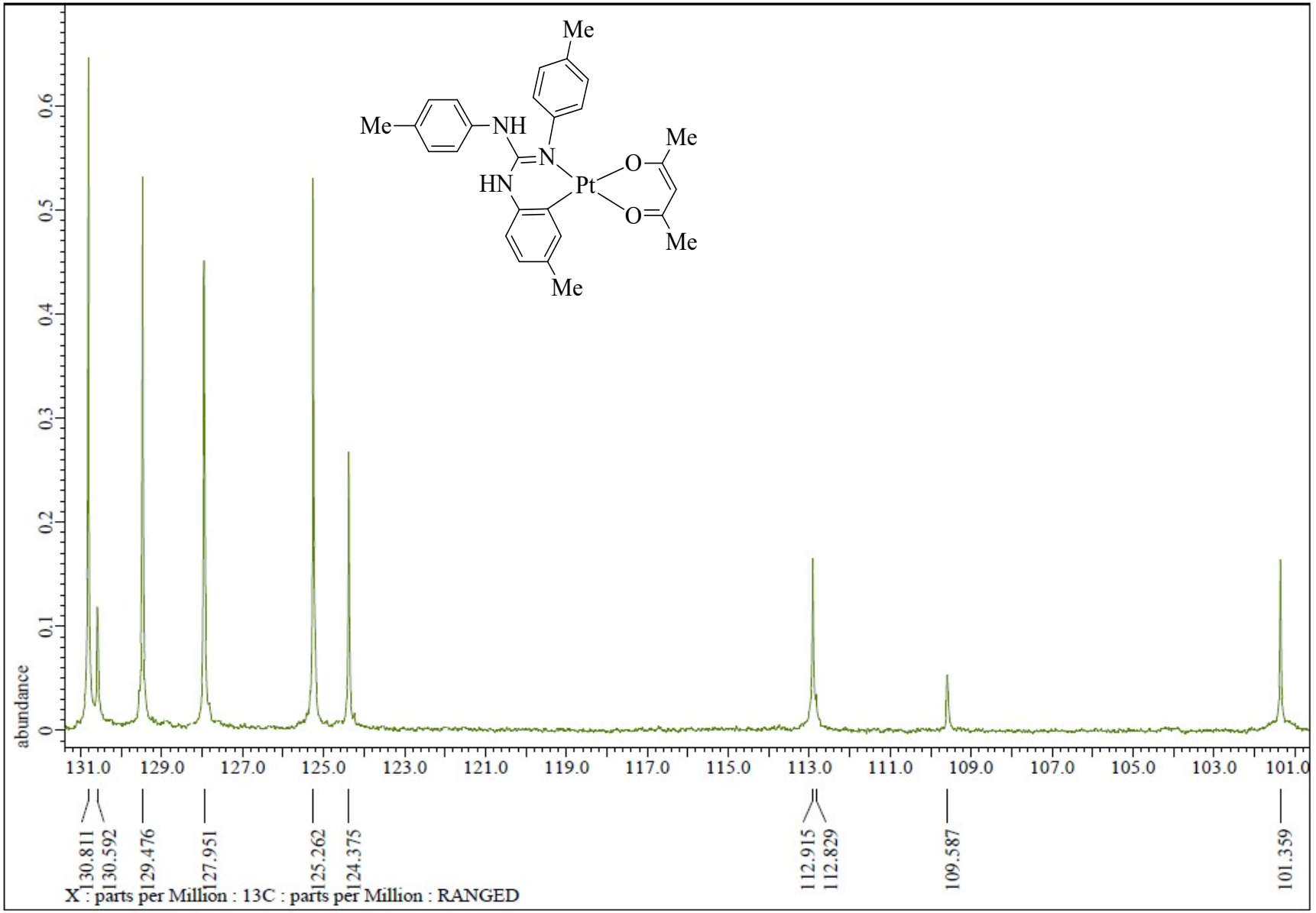

Fig. S100 $^{13}C\{^{1}H\}$ NMR ($CDCl_3$, 100.5 MHz) spectrum of **12** in the indicated region.

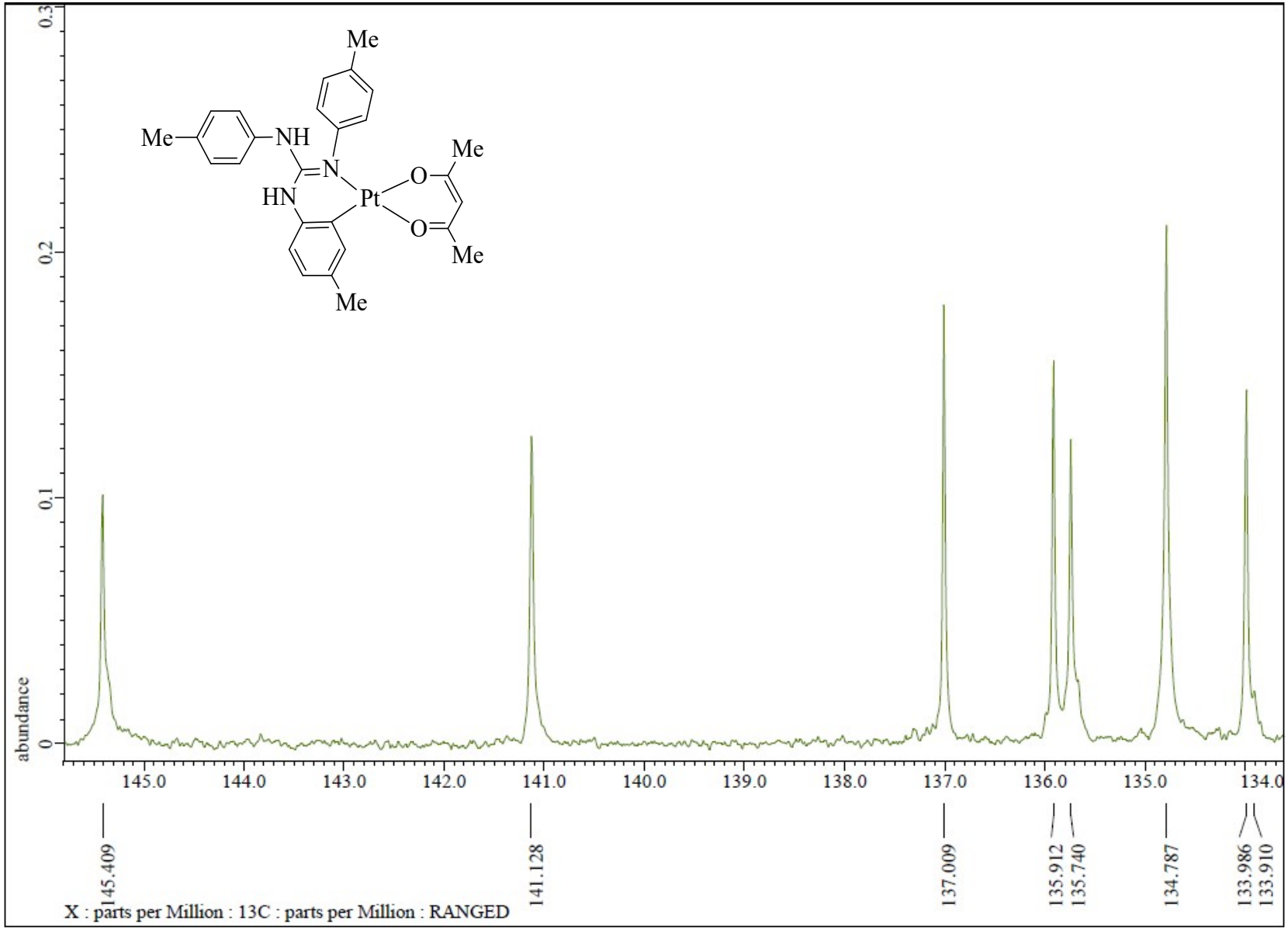

Fig. S101 $^{13}C\{^{1}H\}$ NMR ($CDCl_3$, 100.5 MHz) spectrum of **12** in the indicated region.

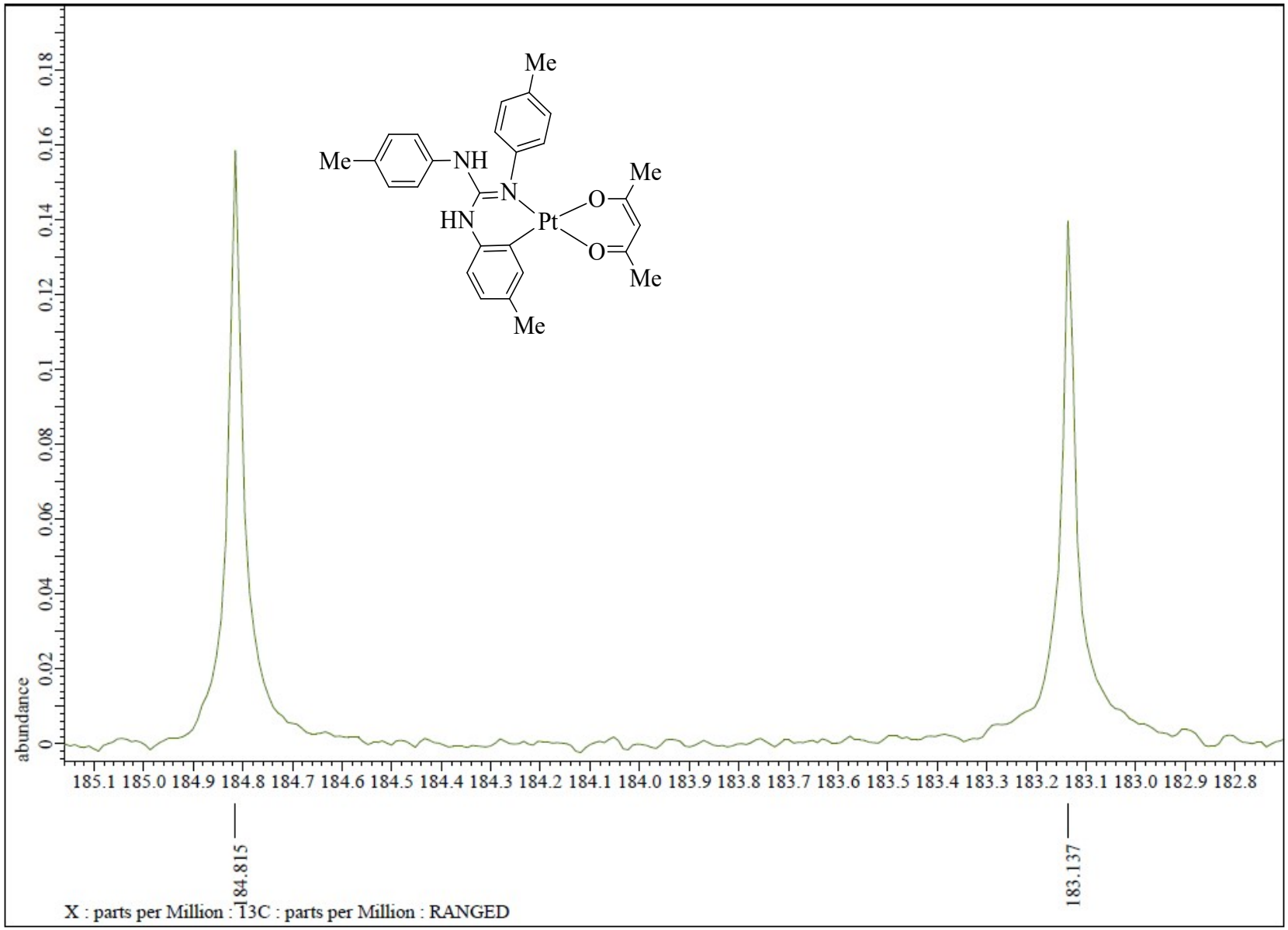

Fig. S102 $^{13}C\{^{1}H\}$ NMR ($CDCl_3$, 100.5 MHz) spectrum of **12** in the indicated region.

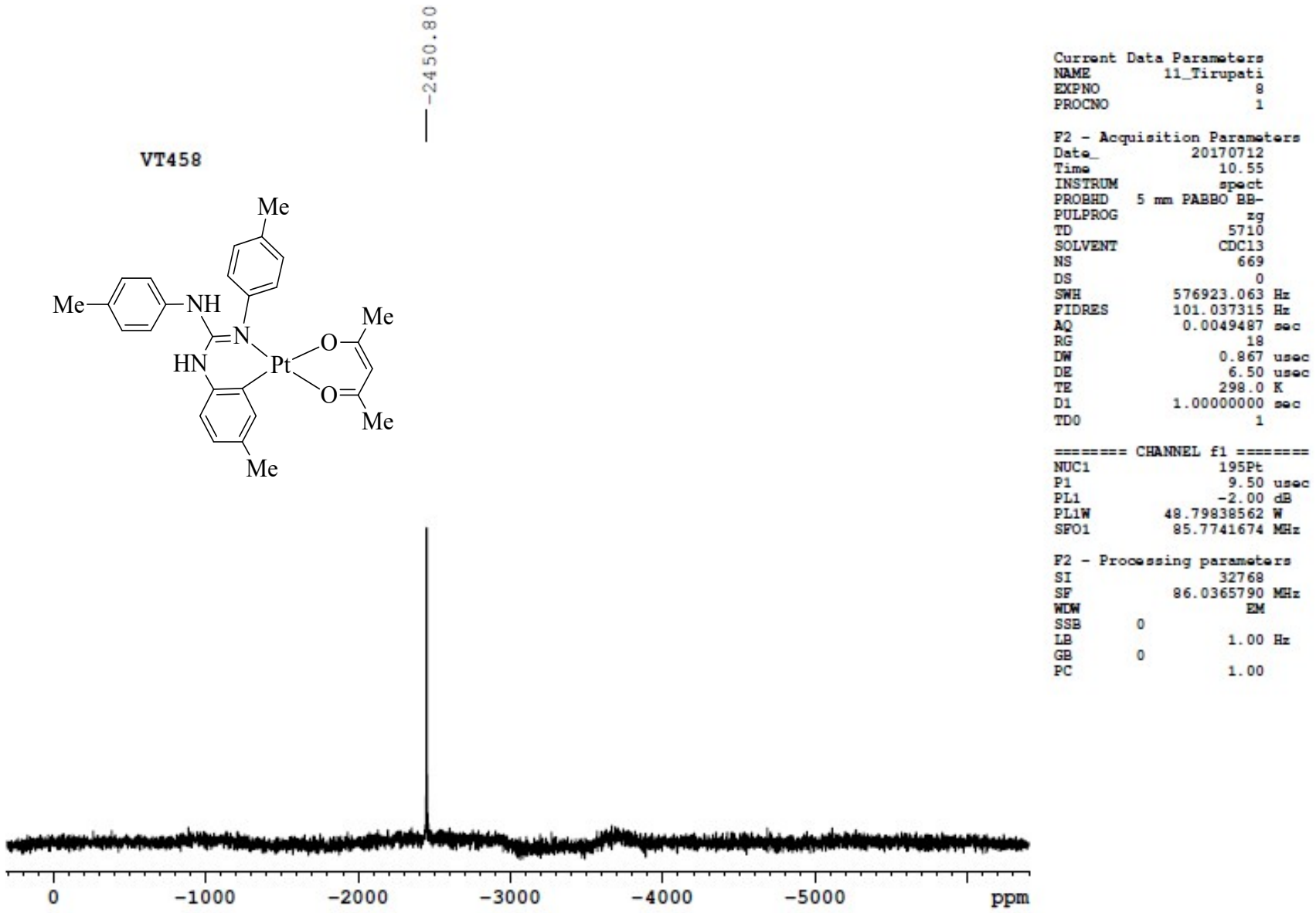

Fig. S103 $^{195}Pt\{^{1}H\}$ NMR ($CDCl_3$, 85.8 MHz) spectrum of **12**.

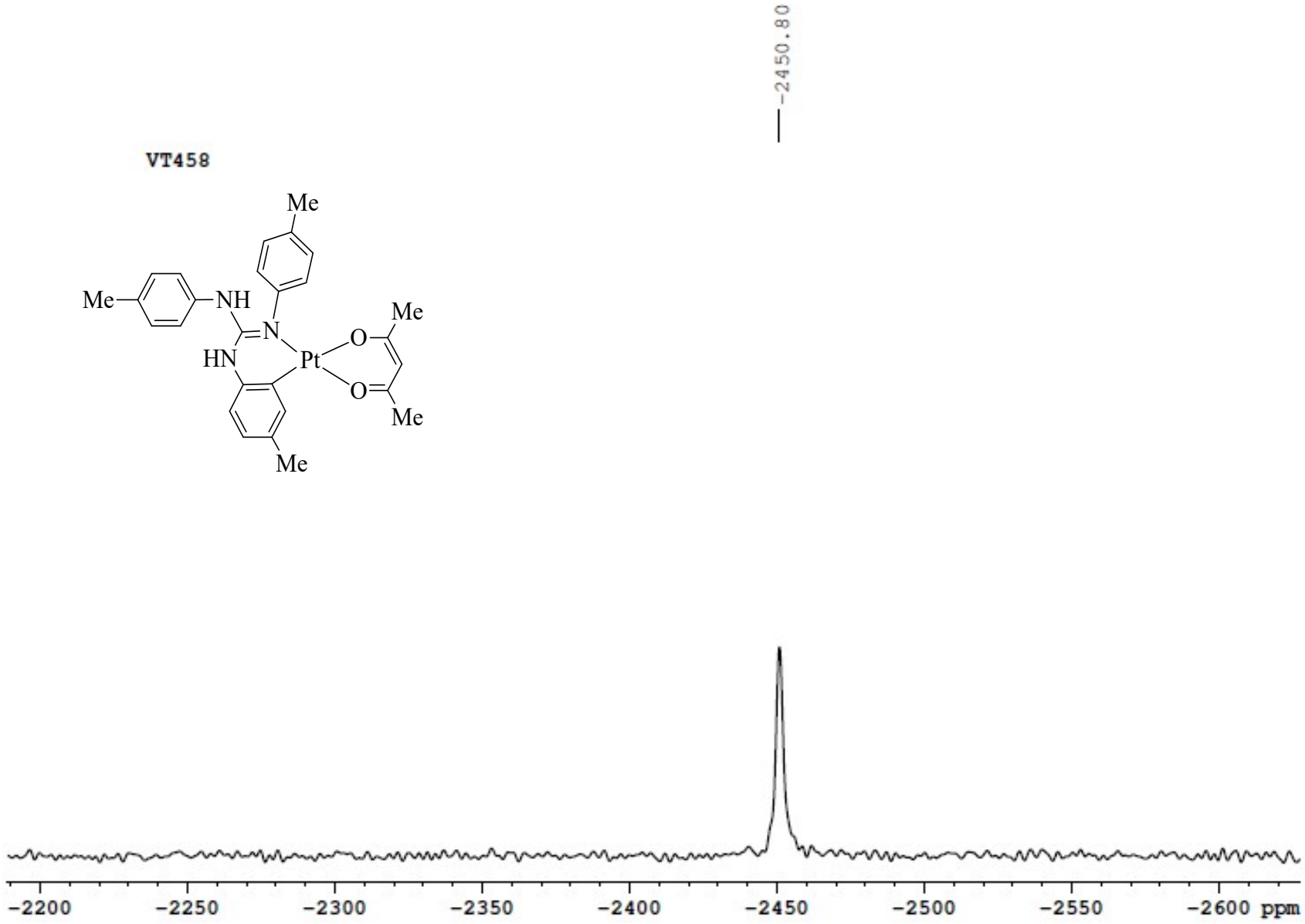

Fig. S104 $^{195}Pt\{^{1}H\}$ NMR ($CDCl_3$, 85.8 MHz) spectrum of **12** in the indicated region.

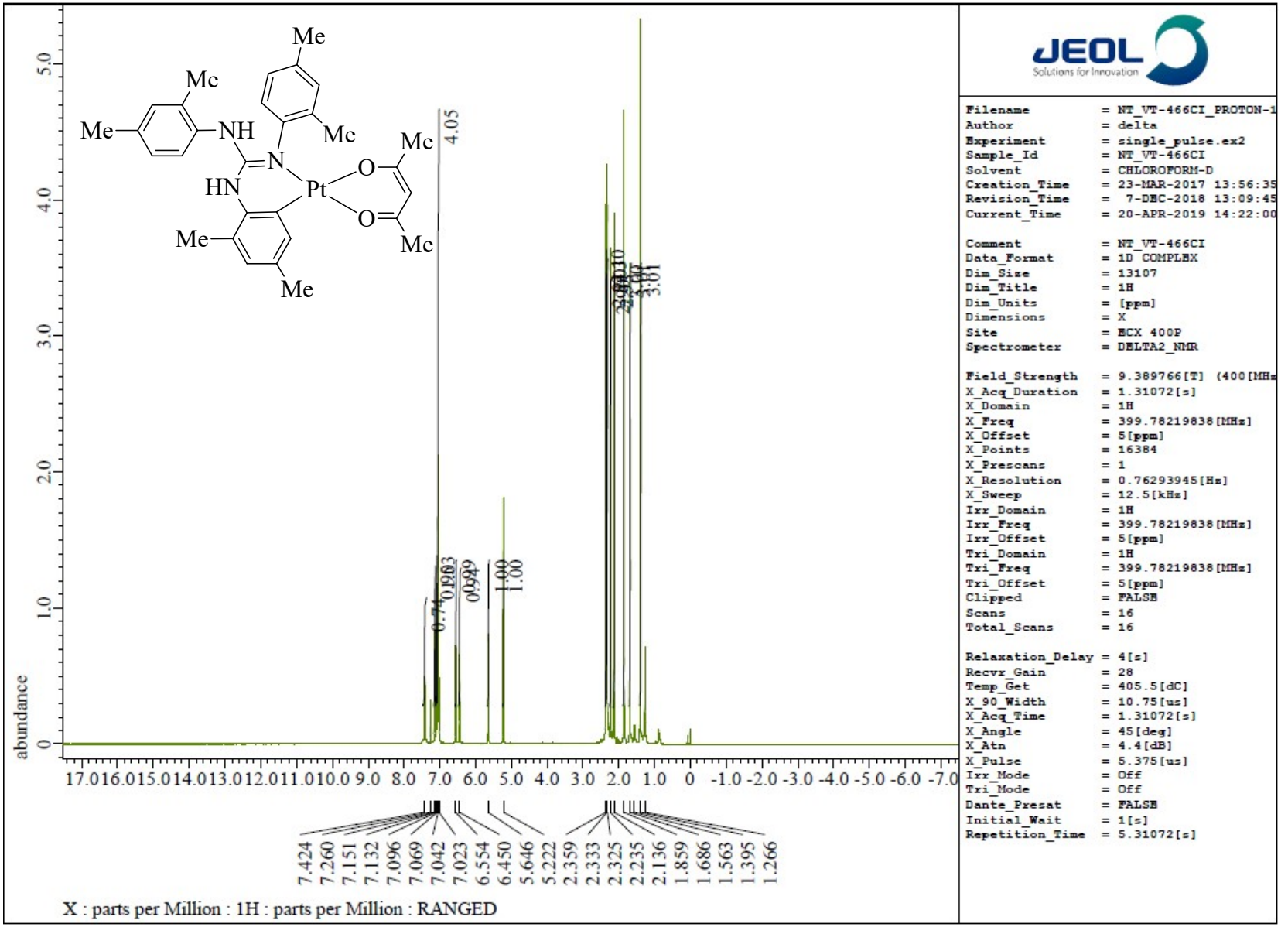

Fig. S105 ^{1}H NMR ($CDCl_3$, 400 MHz) spectrum of **13**.

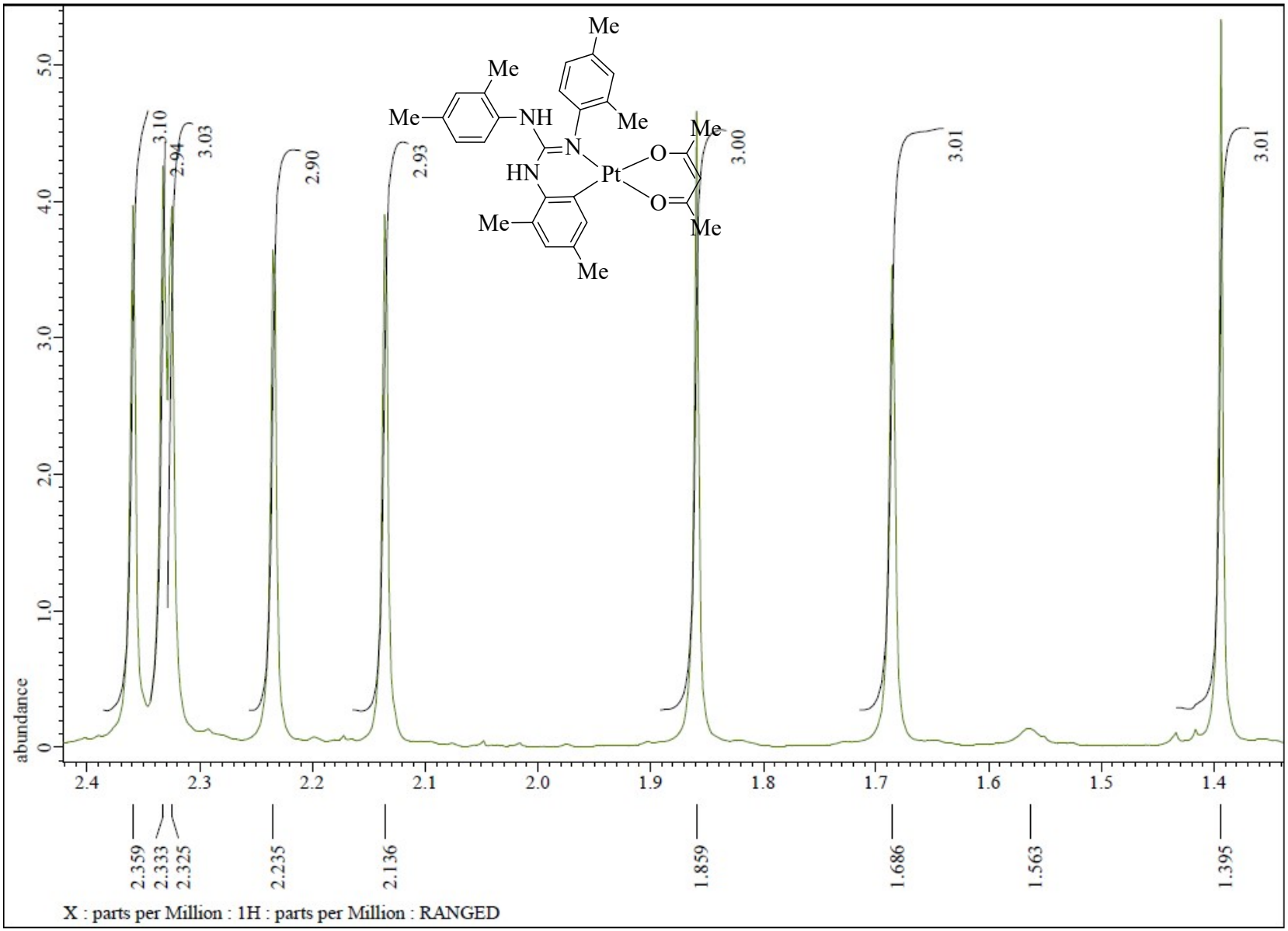

Fig. S106 ^{1}H NMR ($CDCl_3$, 400 MHz) spectrum of **13** in the indicated region.

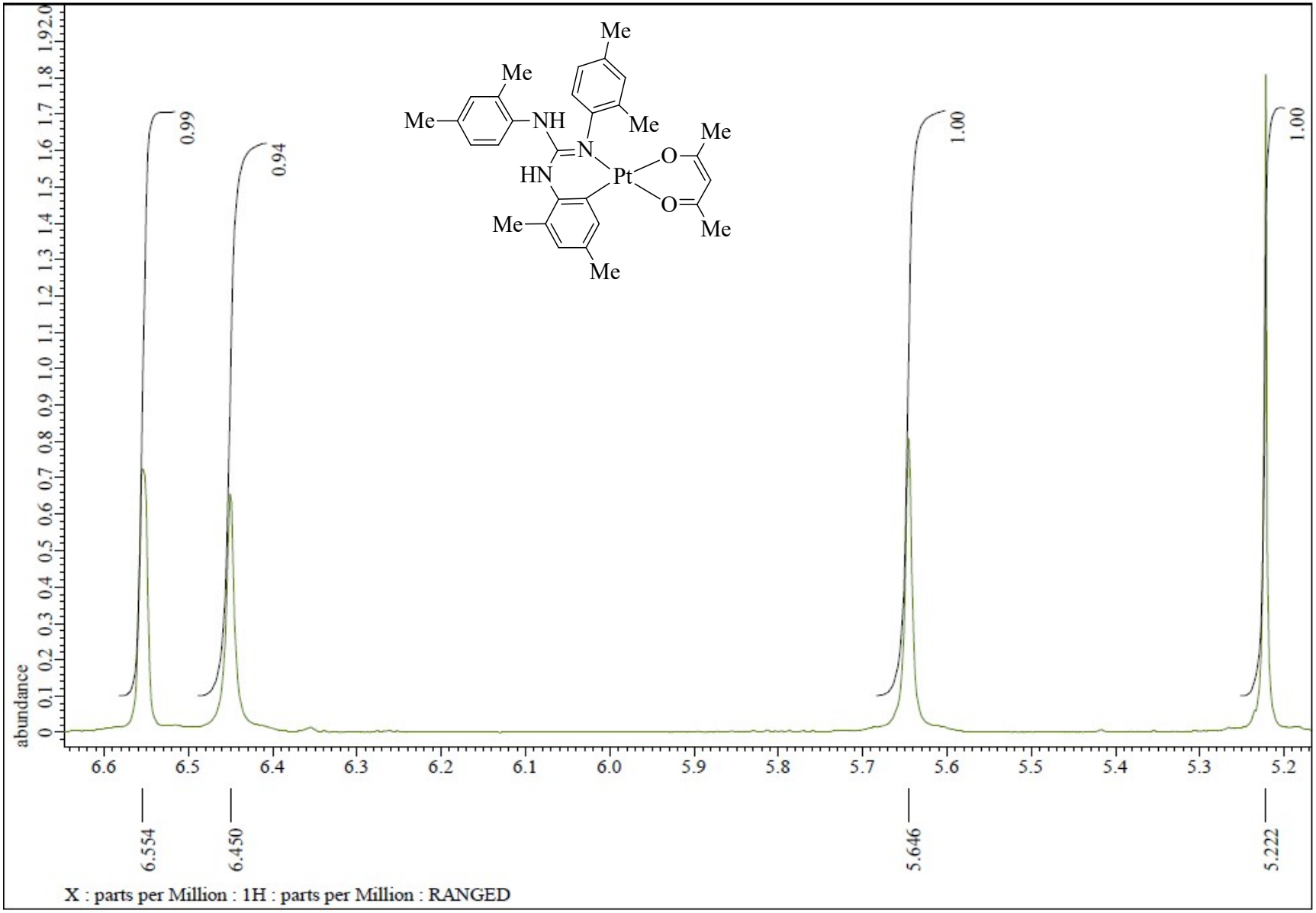

Fig. S107 ^{1}H NMR ($CDCl_3$, 400 MHz) spectrum of **13** in the indicated region.

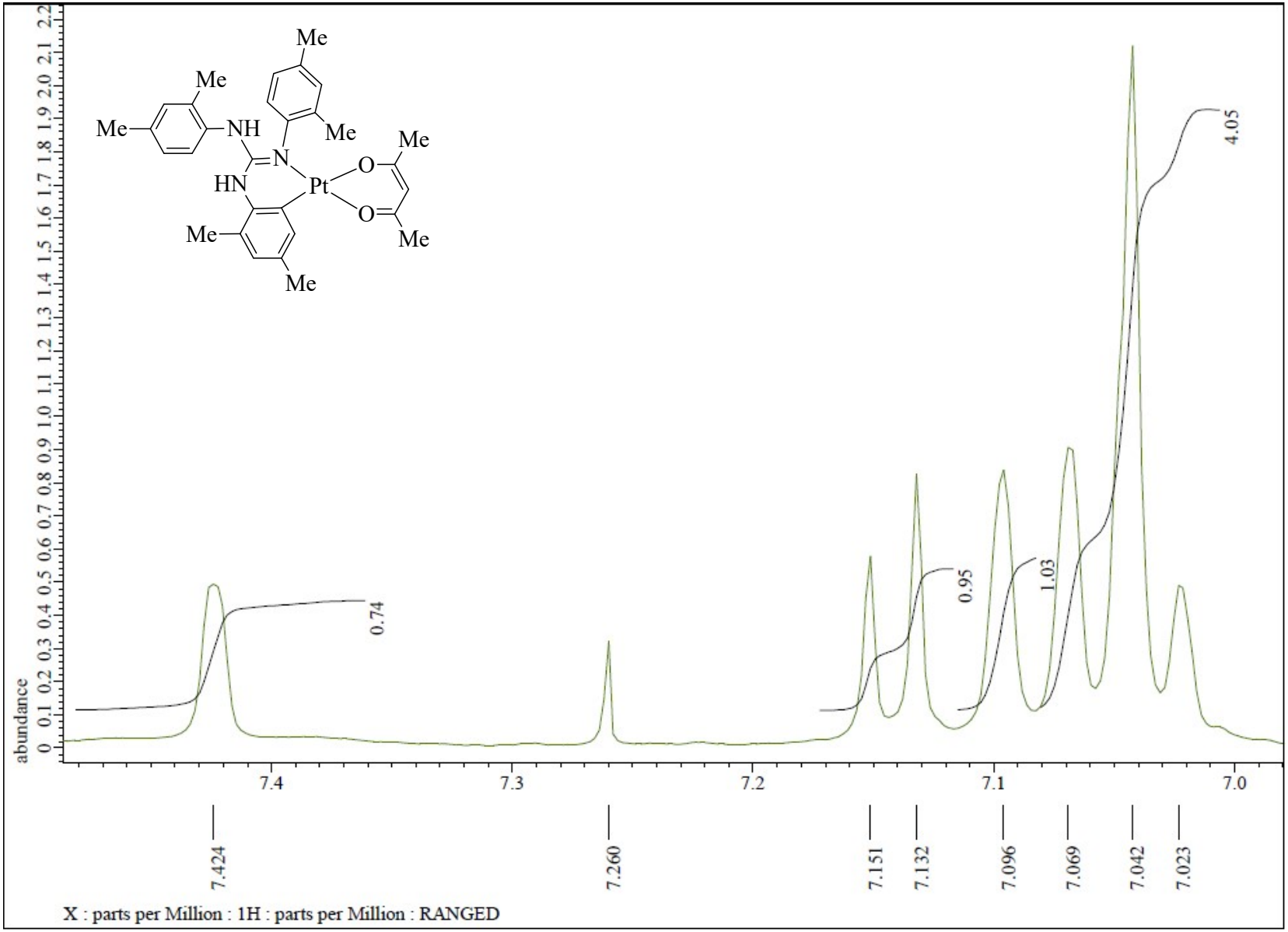

Fig. S108 ^{1}H NMR ($CDCl_3$, 400 MHz) spectrum of **13** in the indicated region.

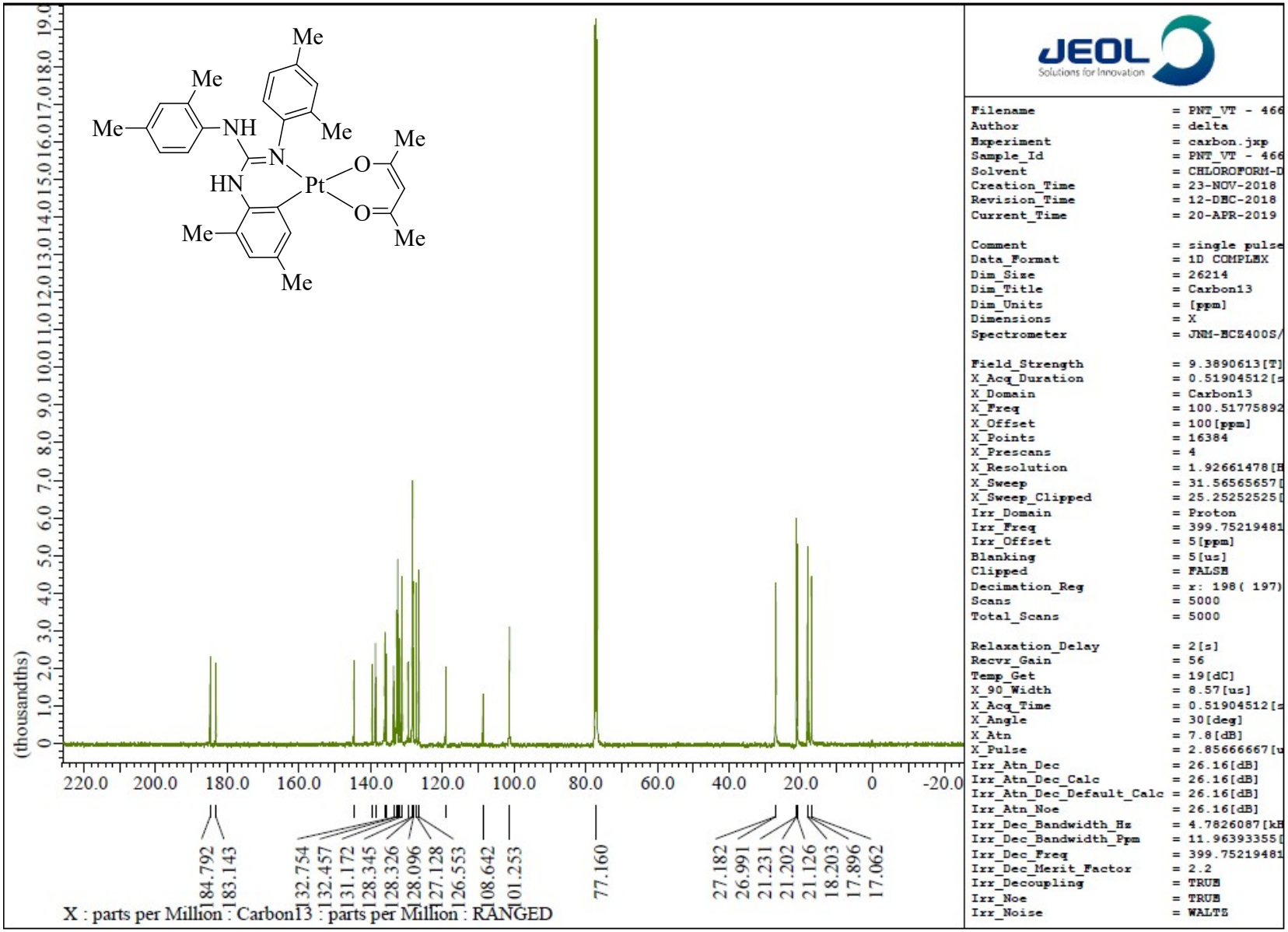

Fig. S109 $^{13}C\{^{1}H\}$ NMR ($CDCl_3$, 100.5 MHz) spectrum of **13**.

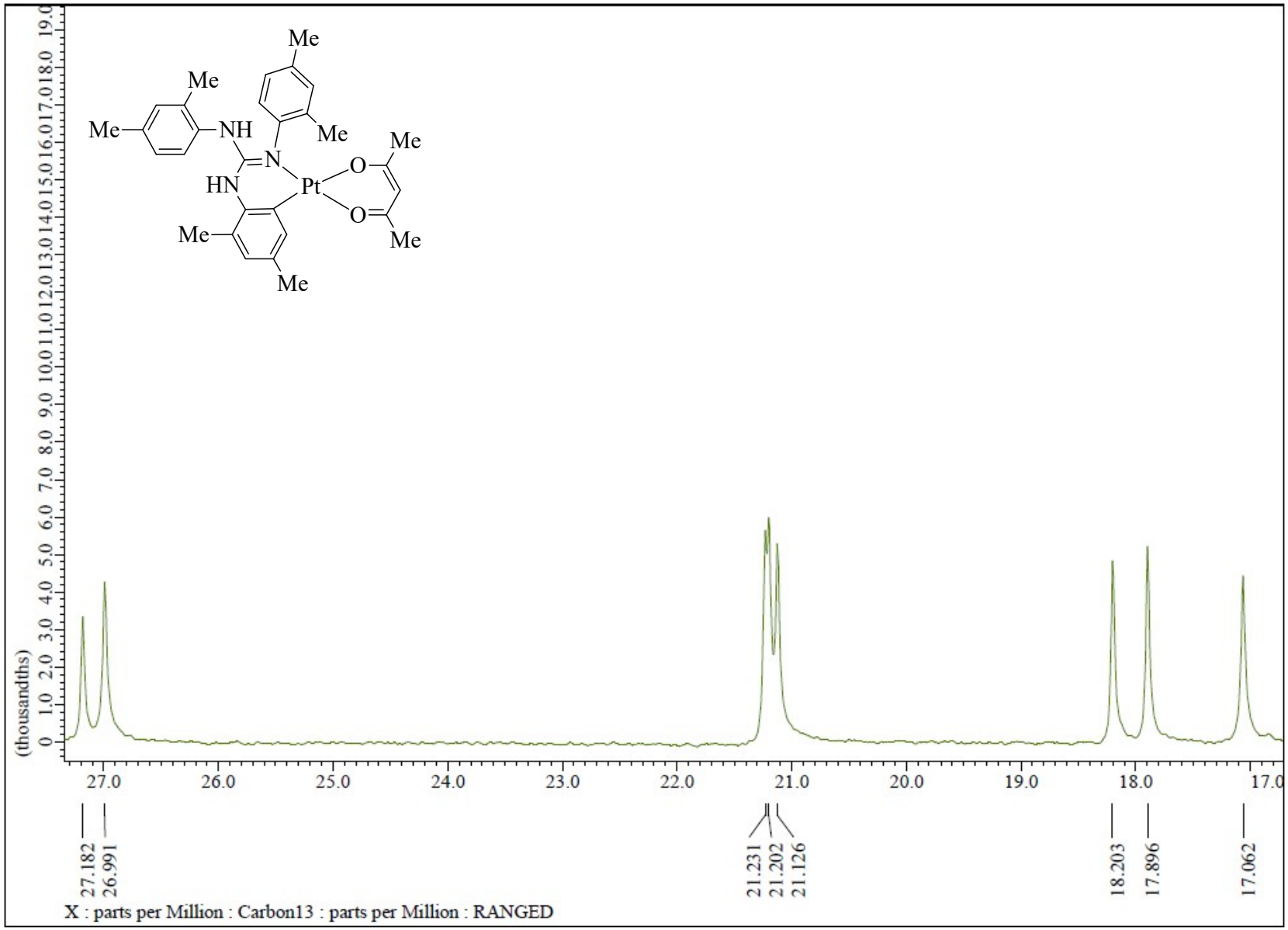

Fig. S110 $^{13}C\{^{1}H\}$ NMR ($CDCl_3$, 100.5 MHz) spectrum of **13** in the indicated region.

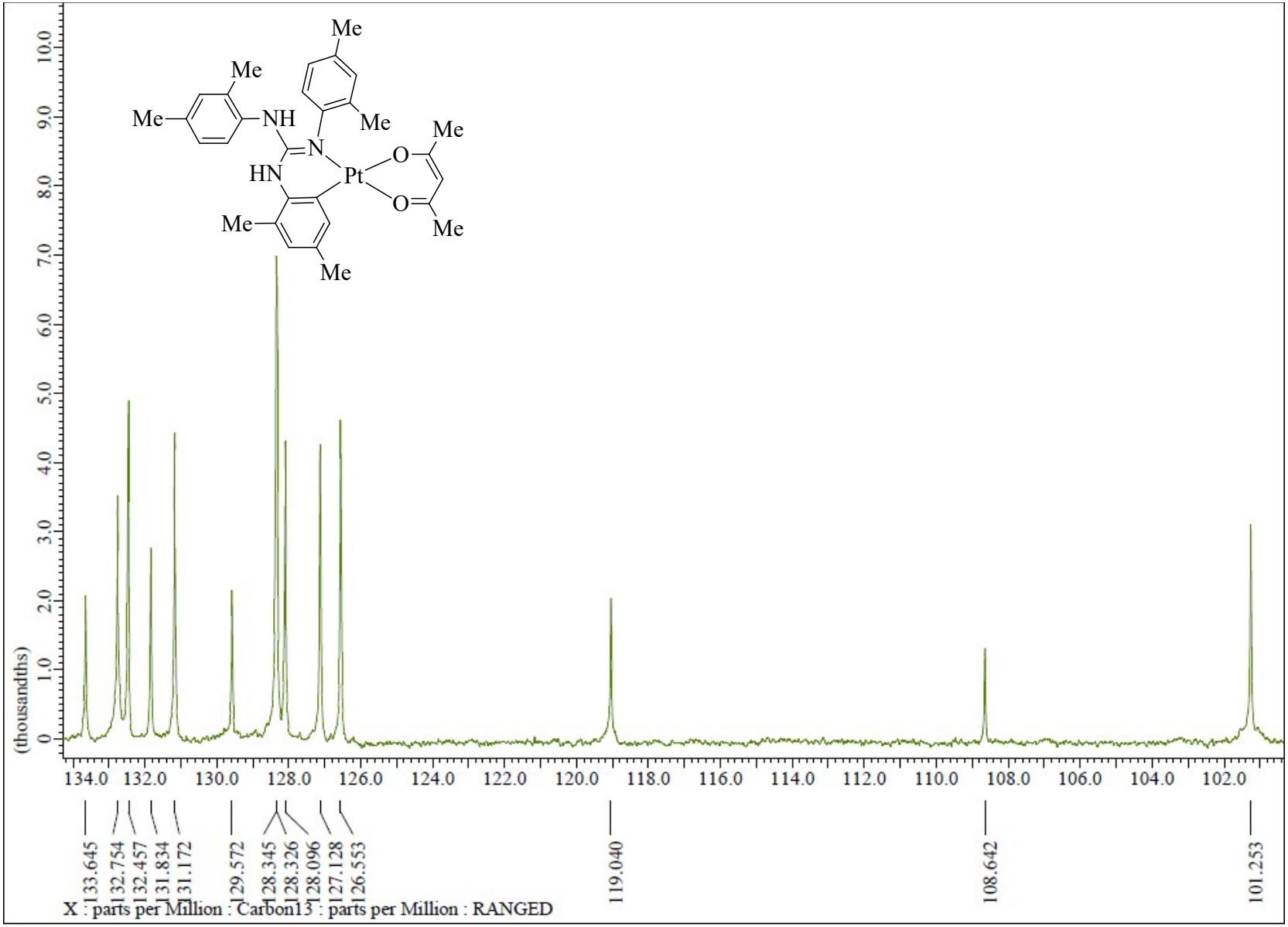

Fig. S111 $^{13}C\{^{1}H\}$ NMR ($CDCl_3$, 100.5 MHz) spectrum of **13** in the indicated region.

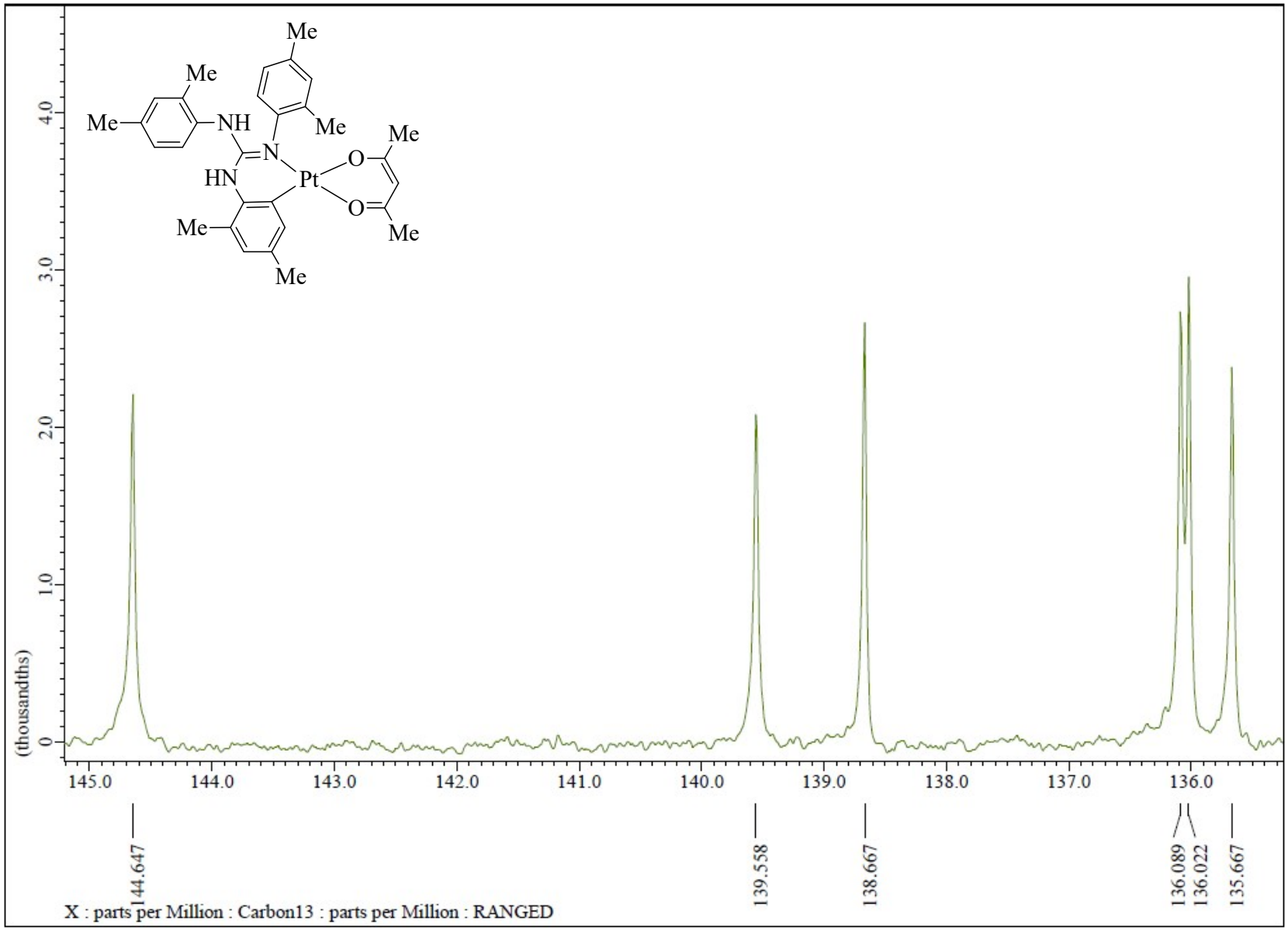

Fig. S112 $^{13}C\{^{1}H\}$ NMR ($CDCl_3$, 100.5 MHz) spectrum of **13** in the indicated region.

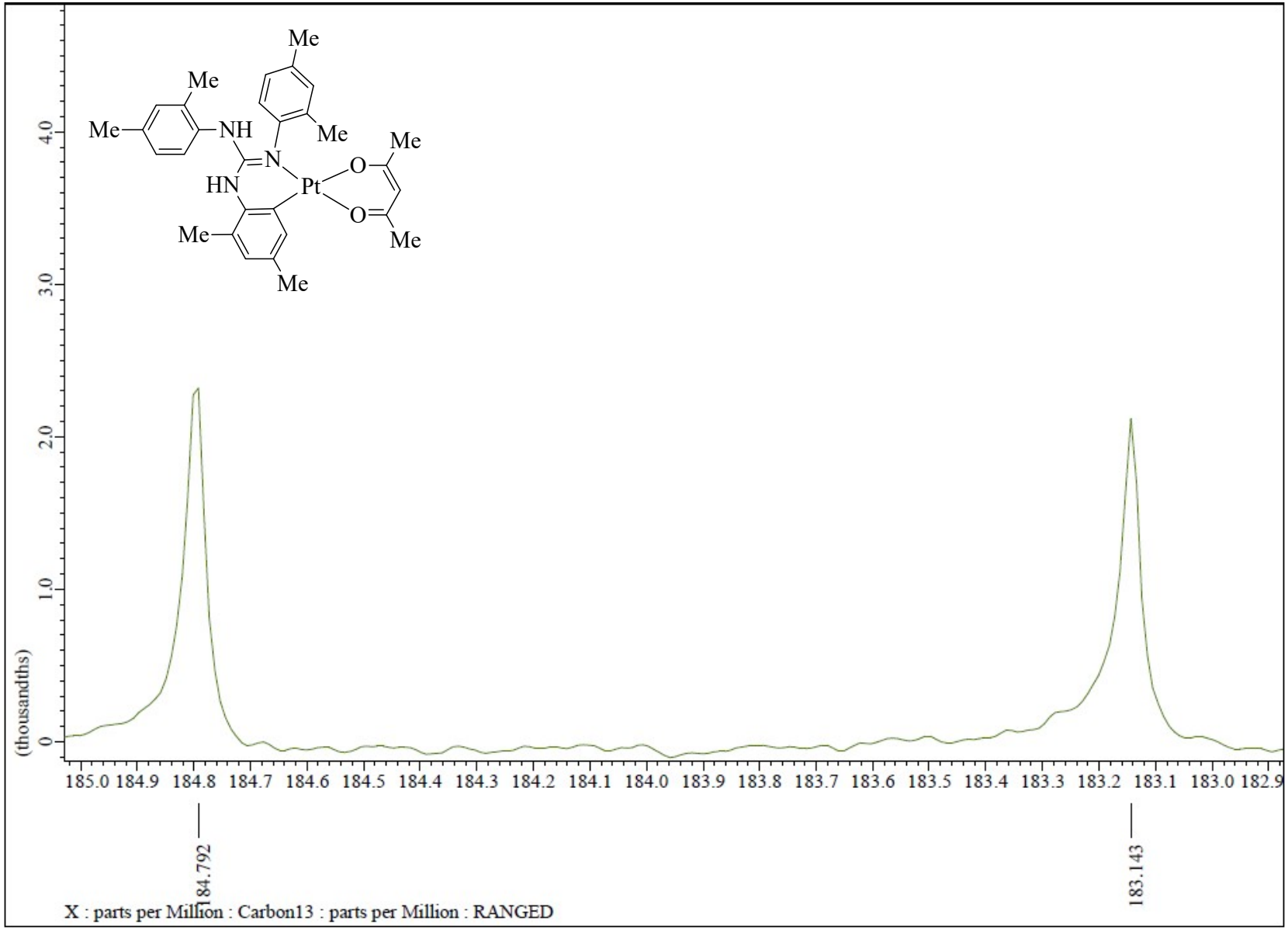

Fig. S113 $^{13}C\{^{1}H\}$ NMR ($CDCl_3$, 100.5 MHz) spectrum of **13** in the indicated region.

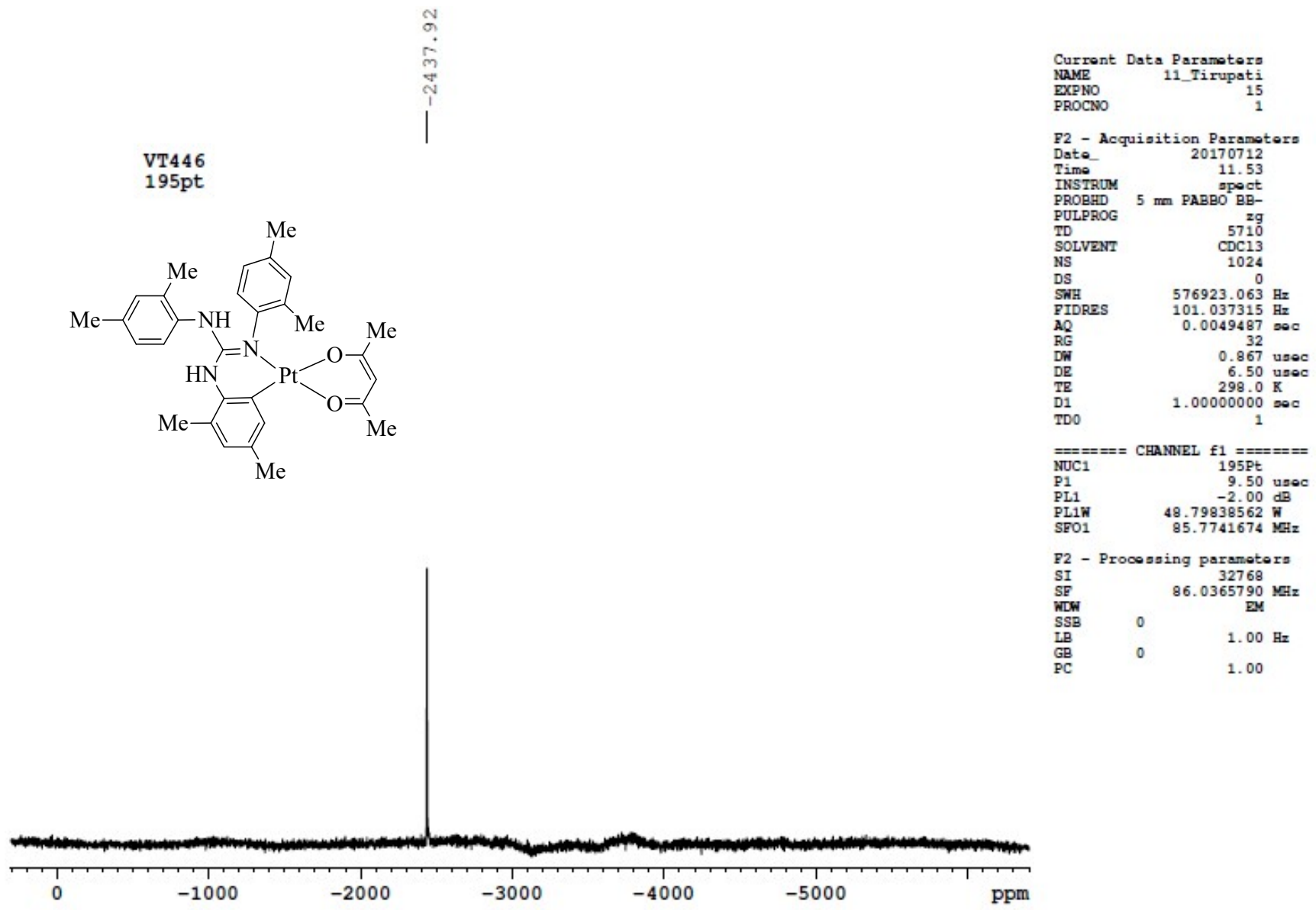

Fig. S114 $^{195}Pt\{^{1}H\}$ NMR ($CDCl_3$, 85.8 MHz) spectrum of **13**.

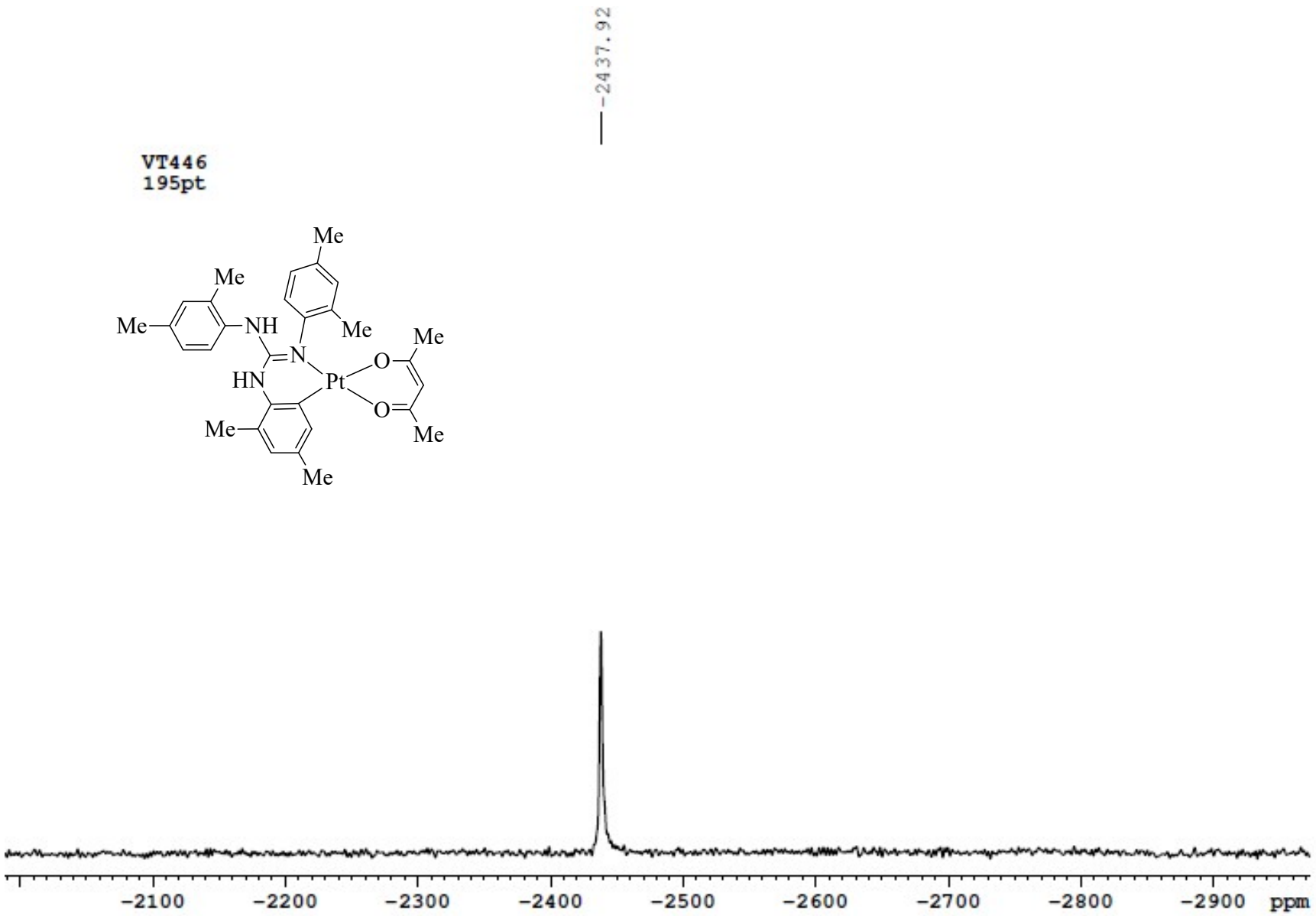

Fig. S115 $^{195}Pt\{^{1}H\}$ NMR ($CDCl_3$, 85.8 MHz) spectrum of **13** in the indicated region.

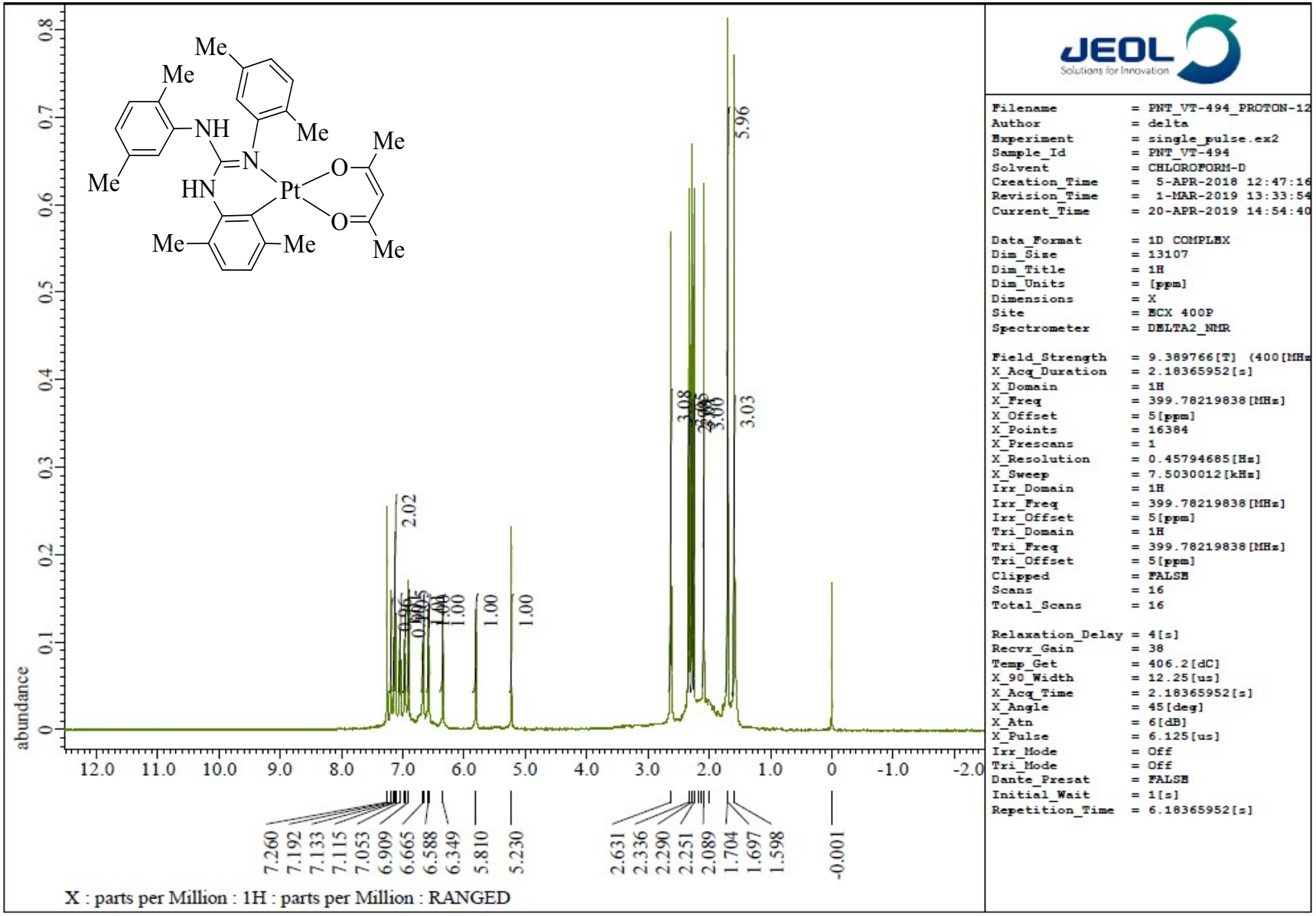

Fig. S116 ^{1}H NMR ($CDCl_3$, 400 MHz) spectrum of **14**.

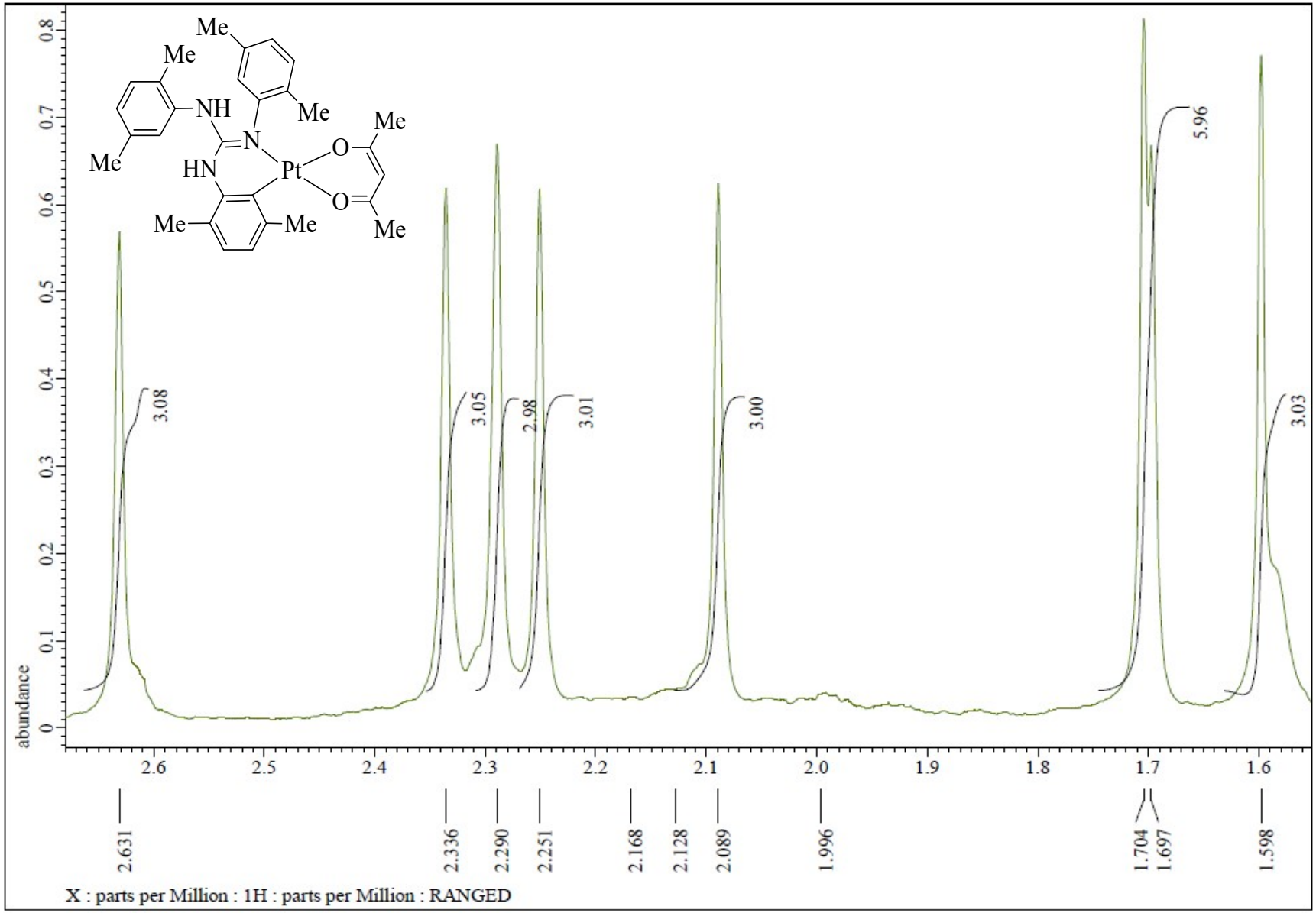

Fig. S117 ^{1}H NMR ($CDCl_3$, 400 MHz) spectrum of **14** in the indicated region.

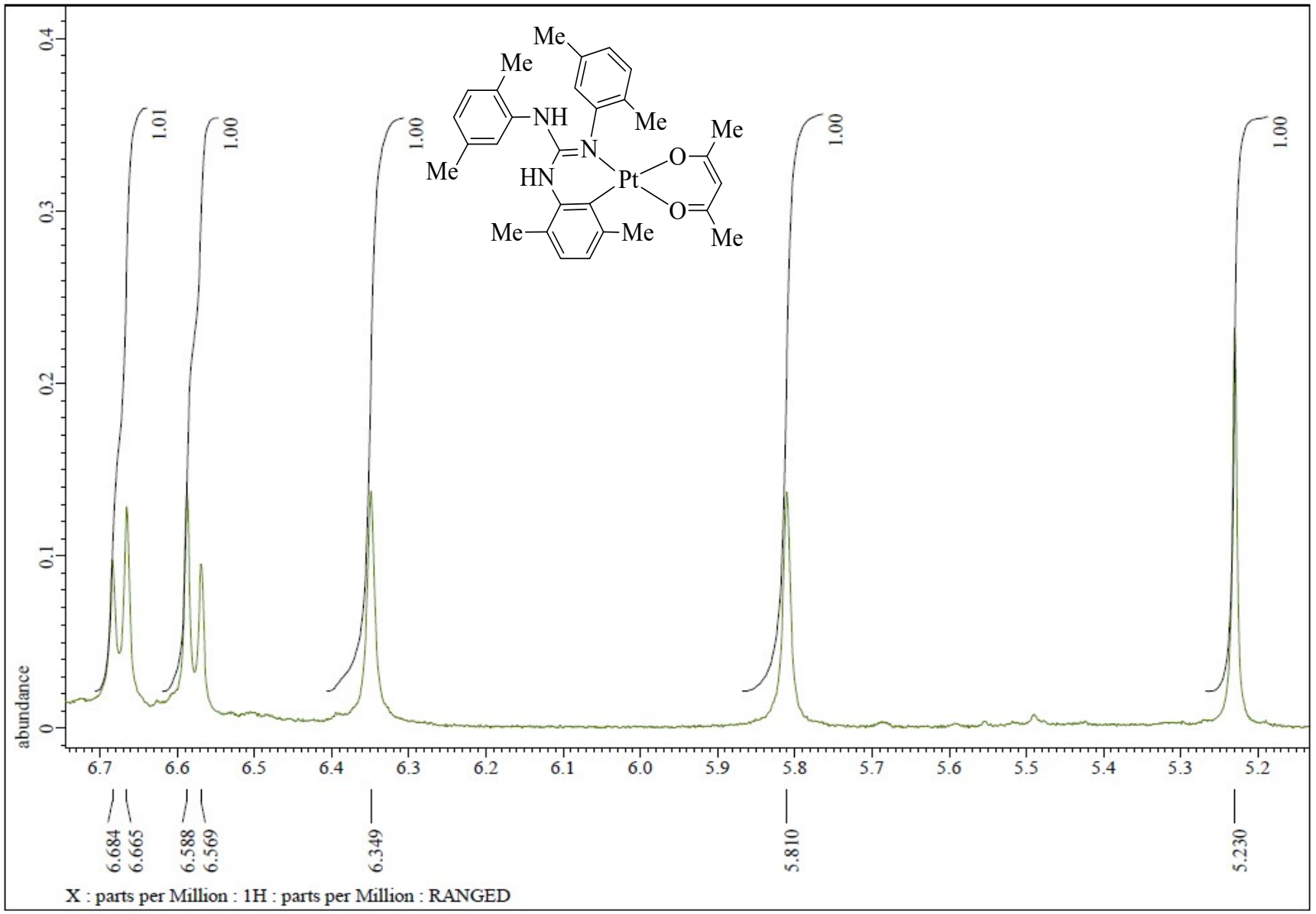

Fig. S118 ^{1}H NMR ($CDCl_3$, 400 MHz) spectrum of **14** in the indicated region.

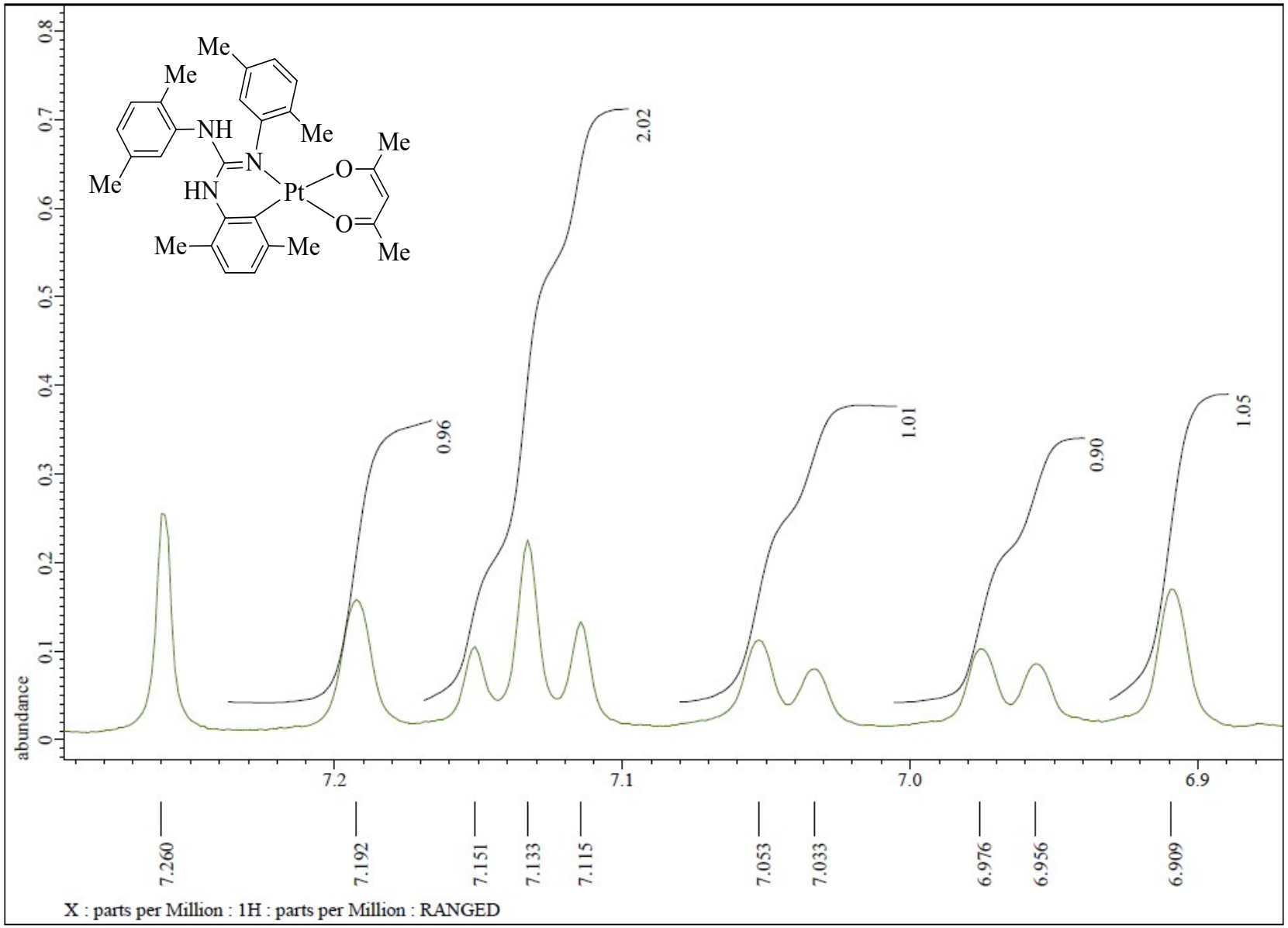

Fig. S119 ^{1}H NMR ($CDCl_3$, 400 MHz) spectrum of **14** in the indicated region.

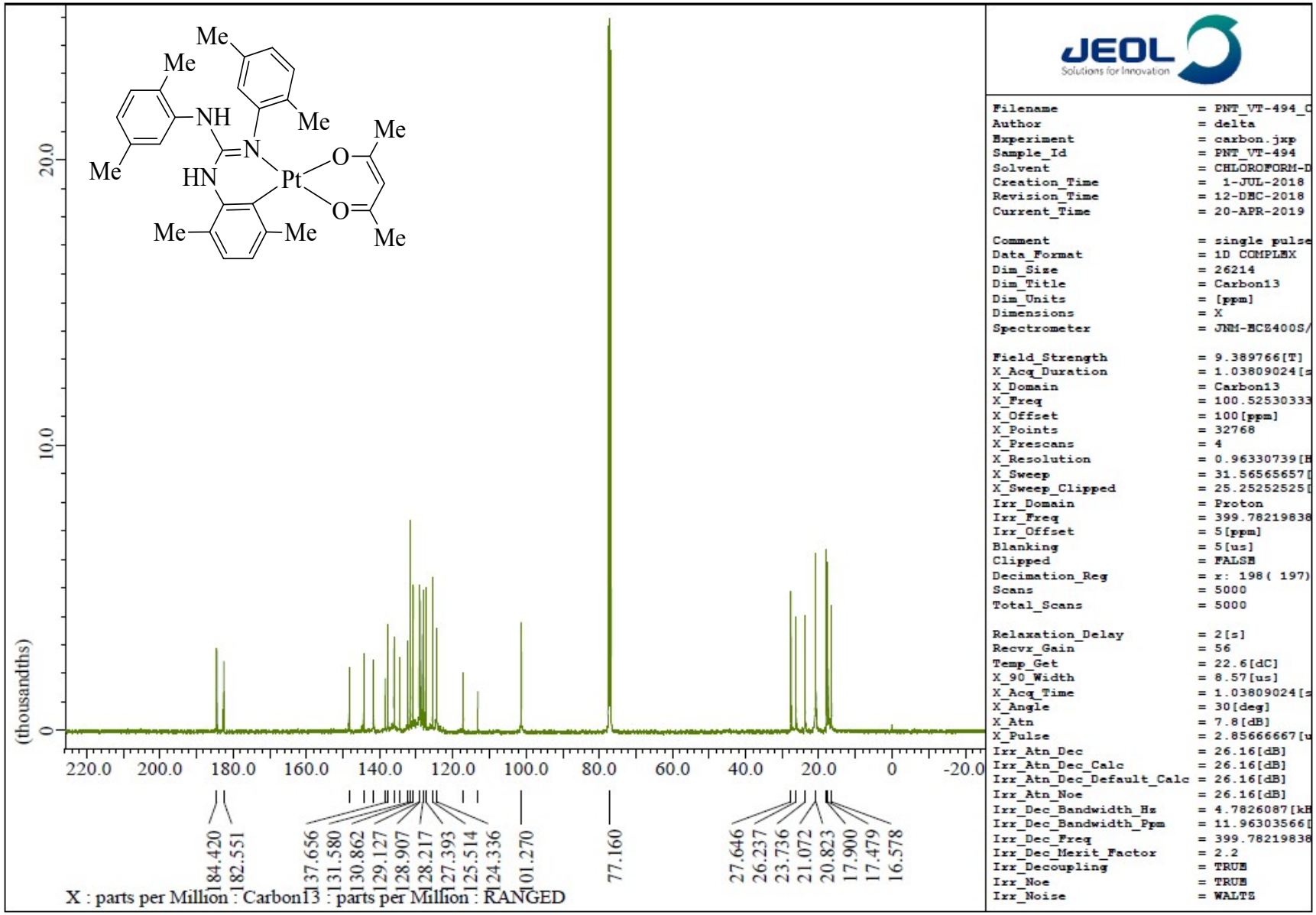

Fig. S120 $^{13}C\{^{1}H\}$ NMR ($CDCl_3$, 100.5 MHz) spectrum of **14**.

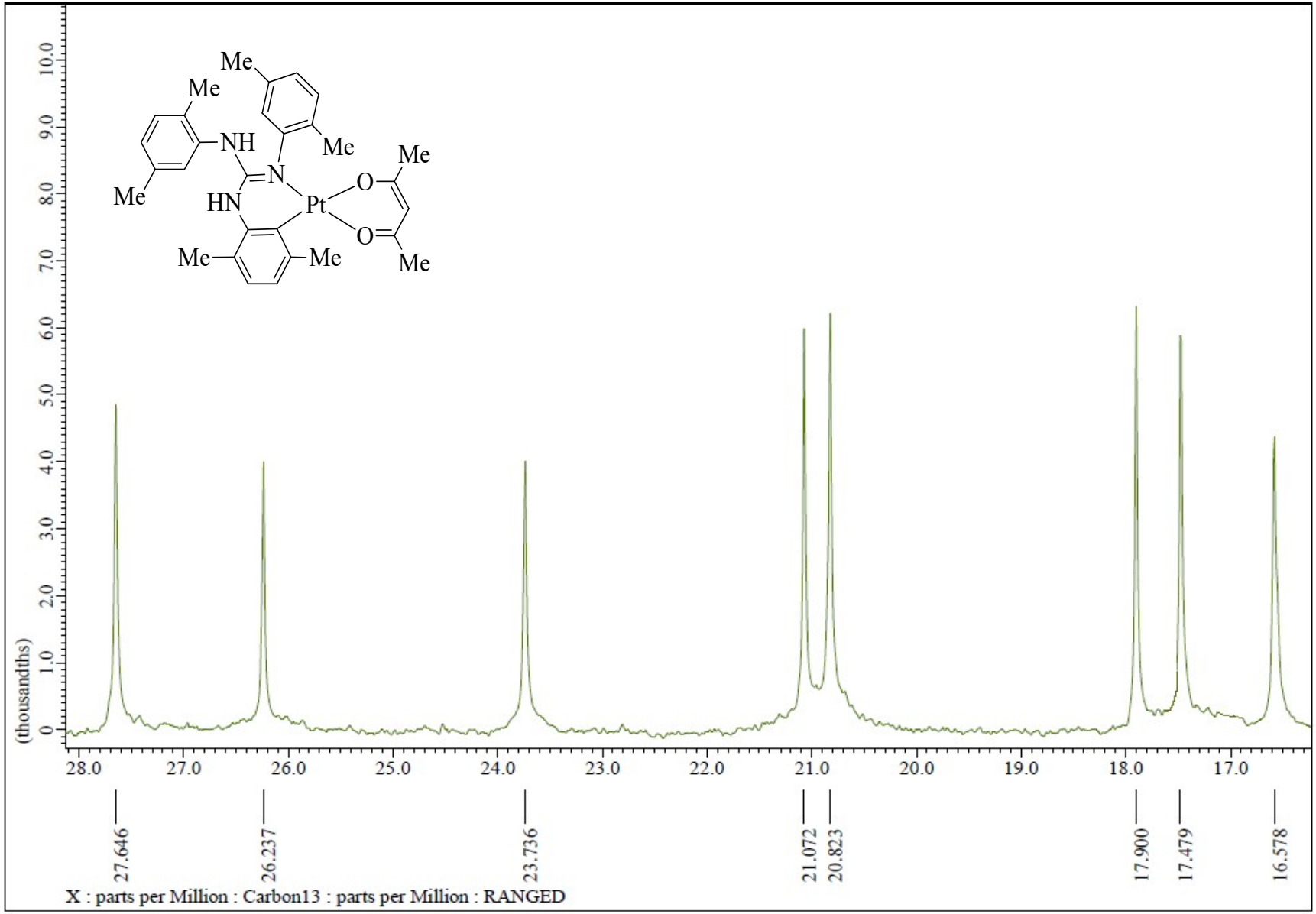

Fig. S121 $^{13}C\{^{1}H\}$ NMR ($CDCl_3$, 100.5 MHz) spectrum of **14** in the indicated region.

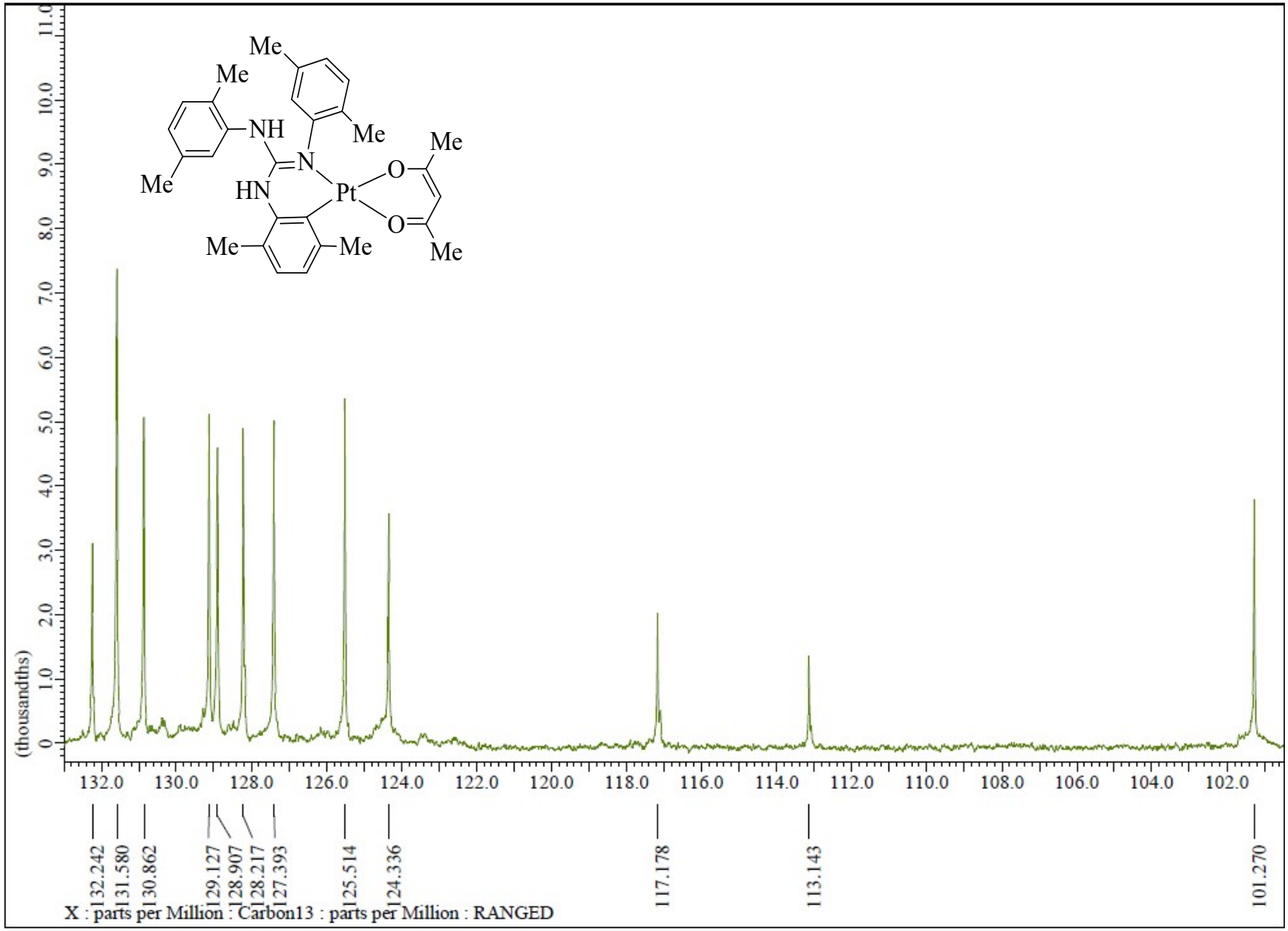

Fig. S122 $^{13}C\{^{1}H\}$ NMR ($CDCl_3$, 100.5 MHz) spectrum of **14** in the indicated region.

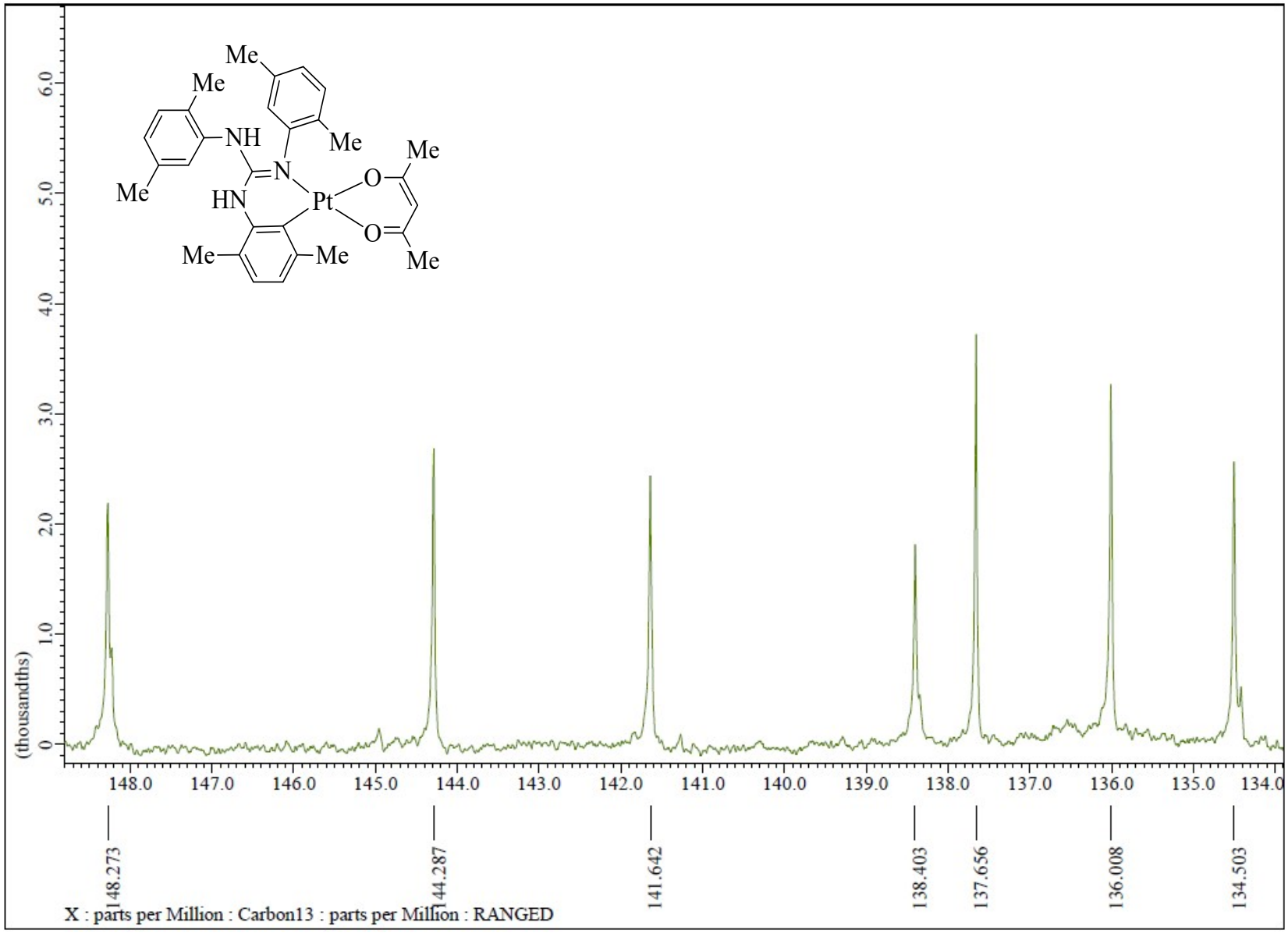

Fig. S123 $^{13}C\{^{1}H\}$ NMR ($CDCl_3$, 100.5 MHz) spectrum of **14** in the indicated region.

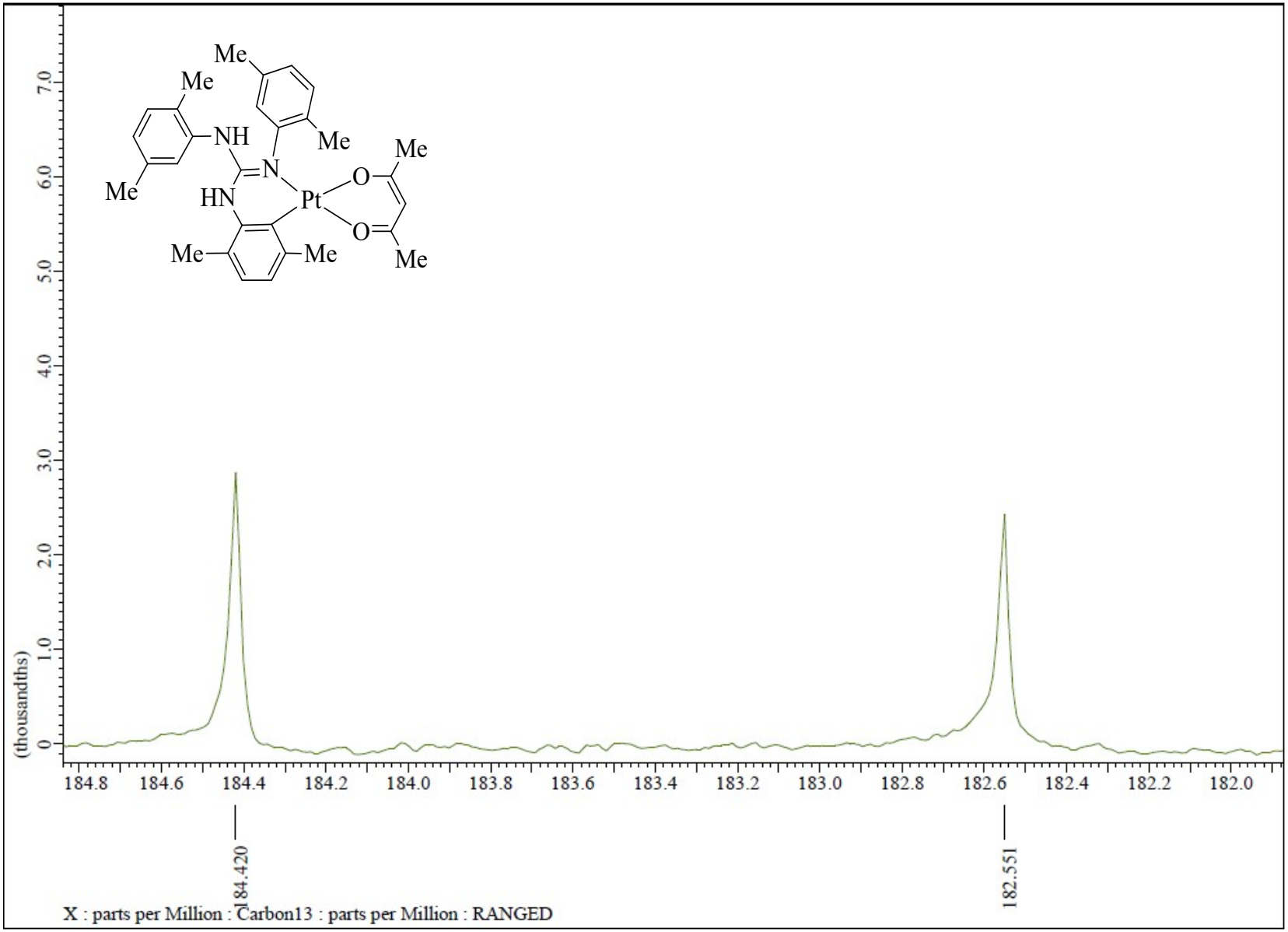

Fig. S124 $^{13}C\{^{1}H\}$ NMR ($CDCl_3$, 100.5 MHz) spectrum of **14** in the indicated region.

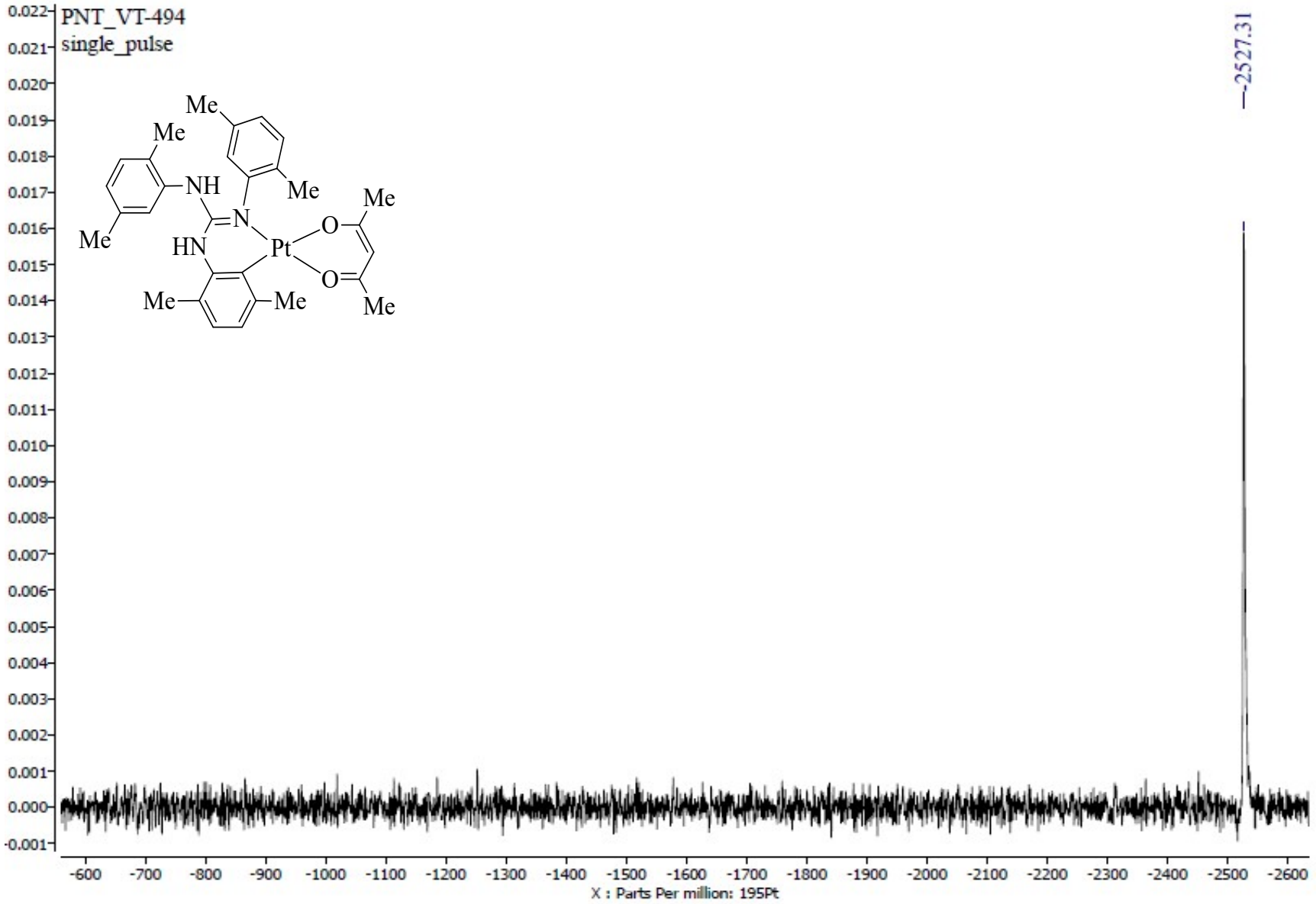

Fig. S125 $^{195}Pt\{^{1}H\}$ NMR ($CDCl_3$, 85.8 MHz) spectrum of **14**.

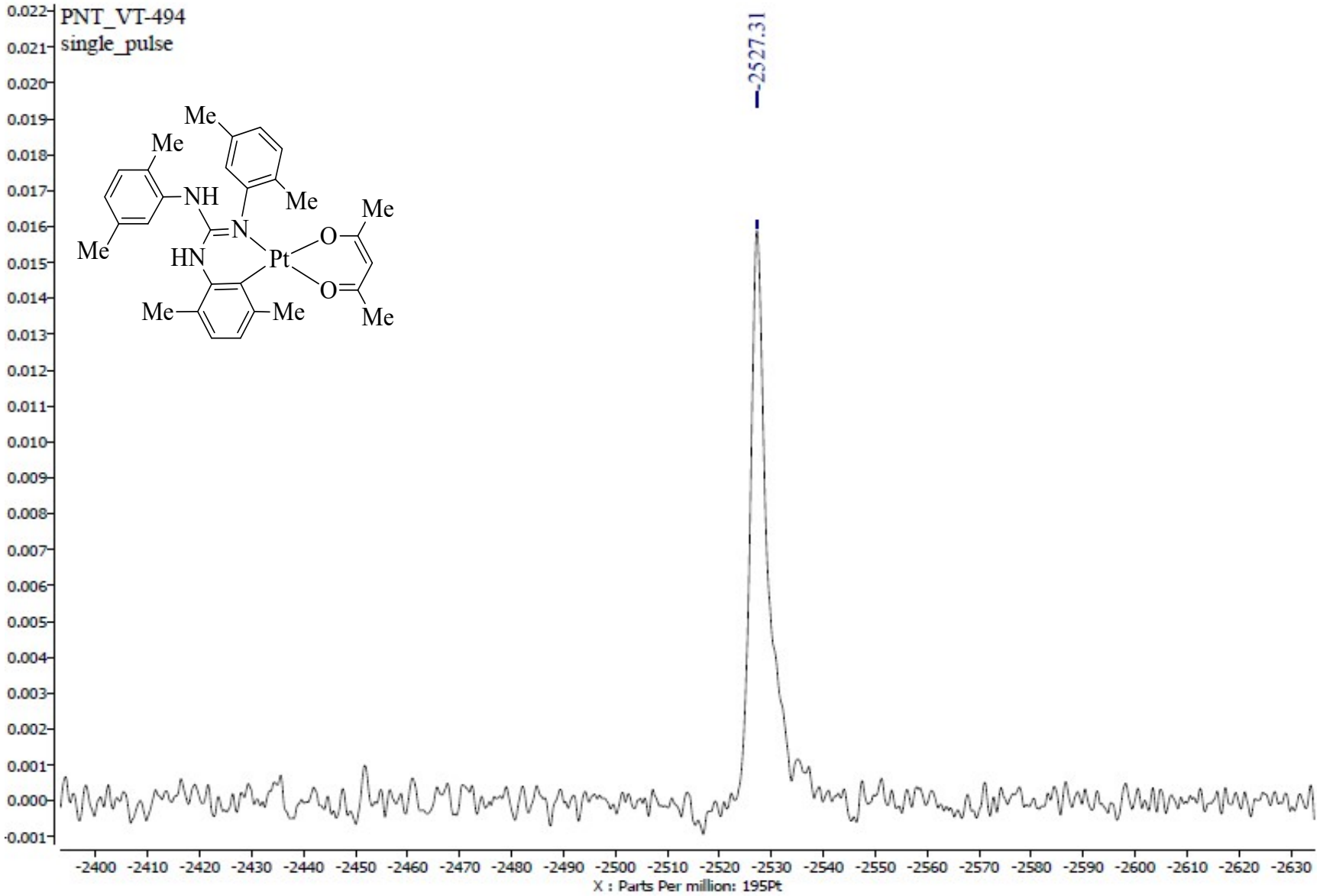

Fig. S126 $^{195}Pt\{^{1}H\}$ NMR ($CDCl_3$, 85.8 MHz) spectrum of **14** in the indicated region.

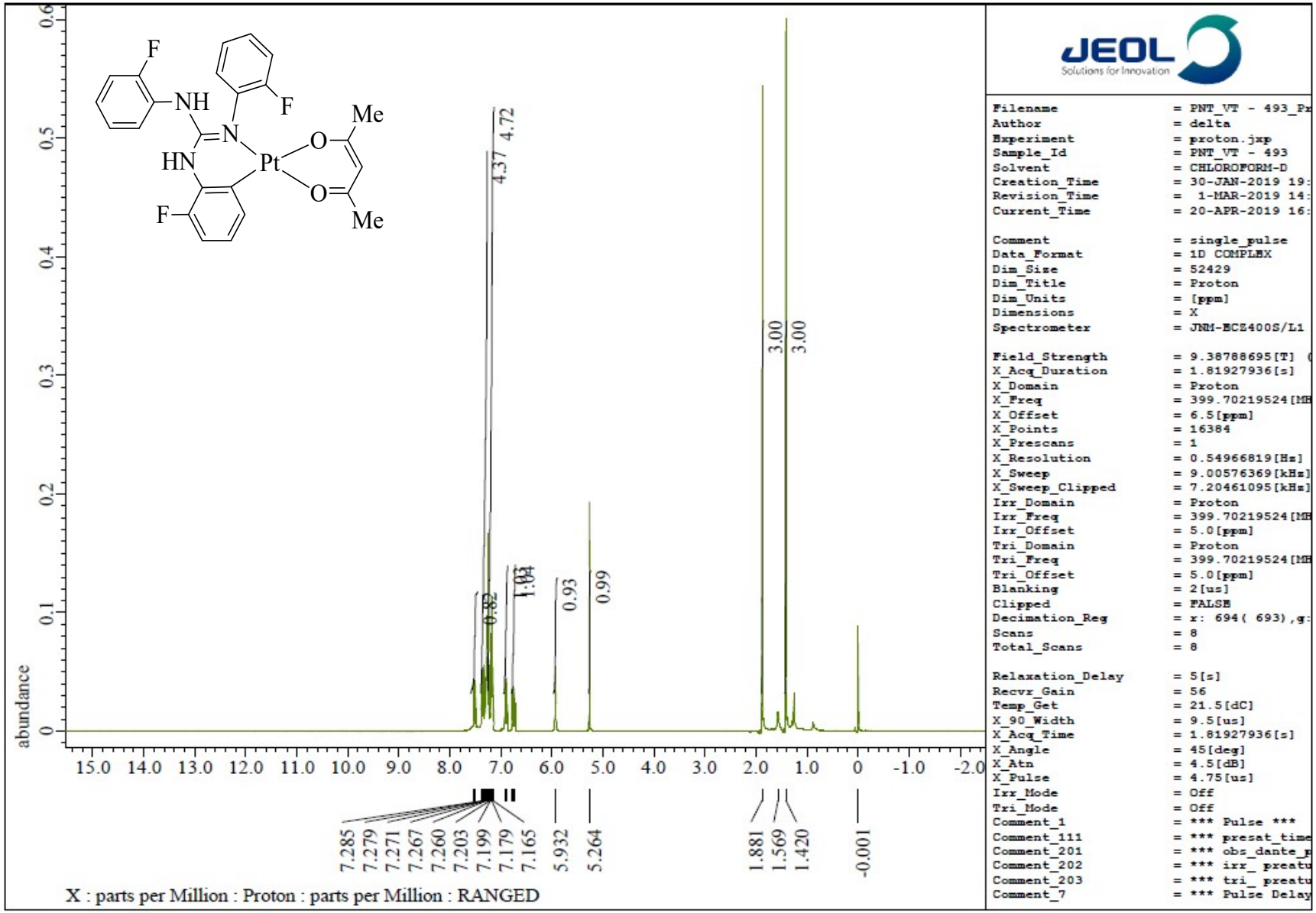

Fig. S127 ^{1}H NMR ($CDCl_3$, 400 MHz) spectrum of **15**.

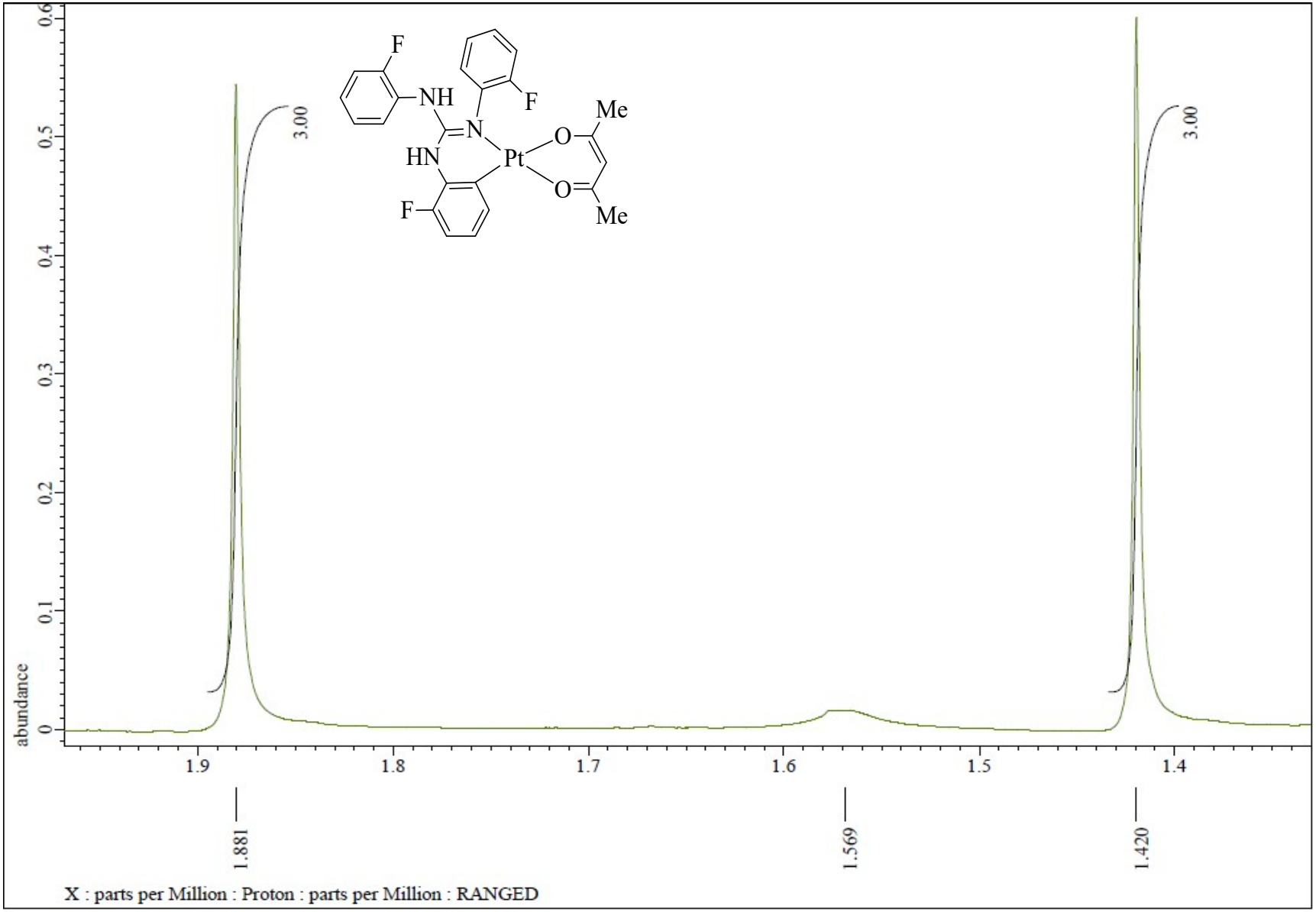

Fig. S128 ^{1}H NMR ($CDCl_3$, 400 MHz) spectrum of **15** in the indicated region.

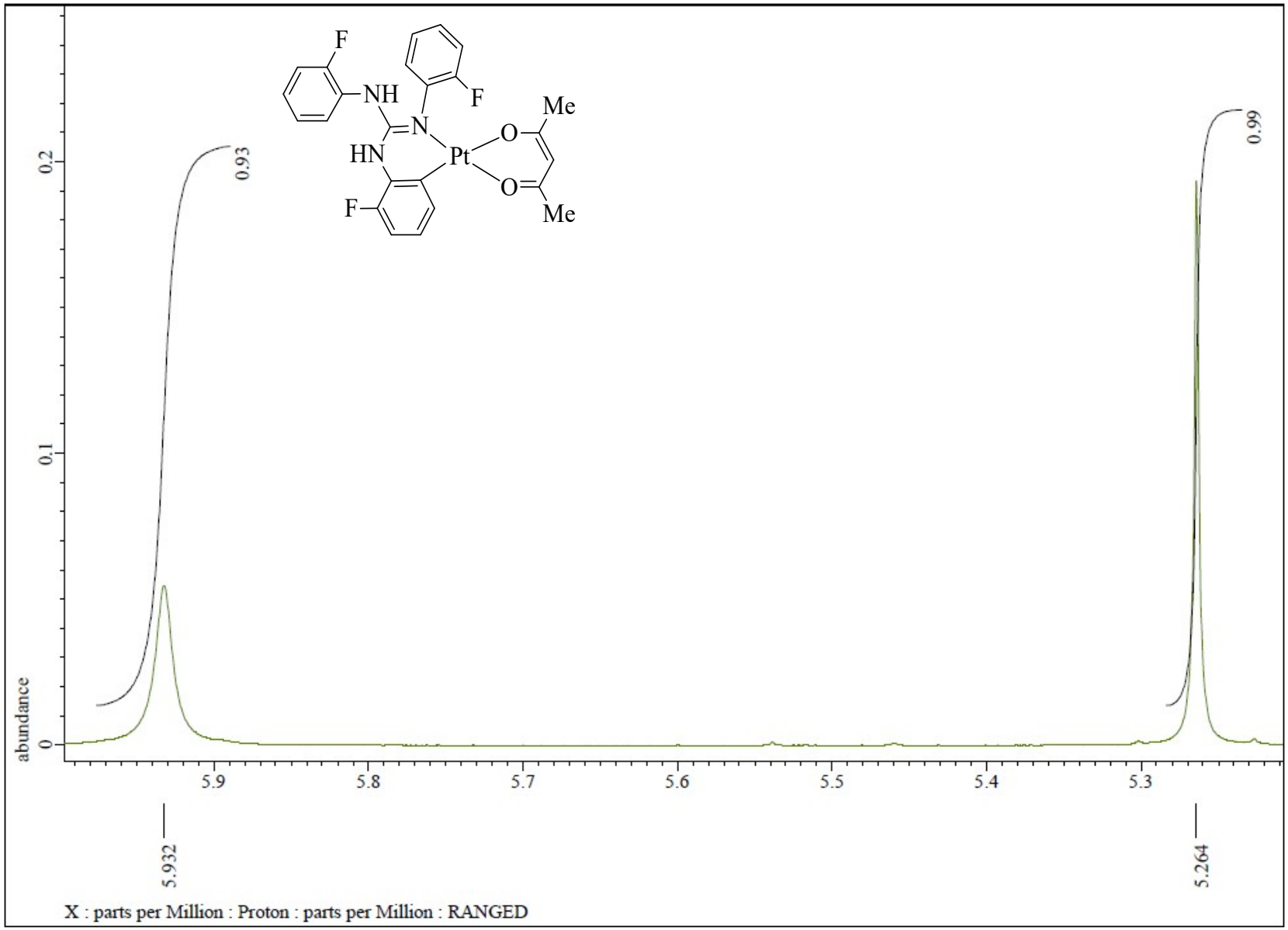

Fig. S129 ^{1}H NMR ($CDCl_3$, 400 MHz) spectrum of **15** in the indicated region.

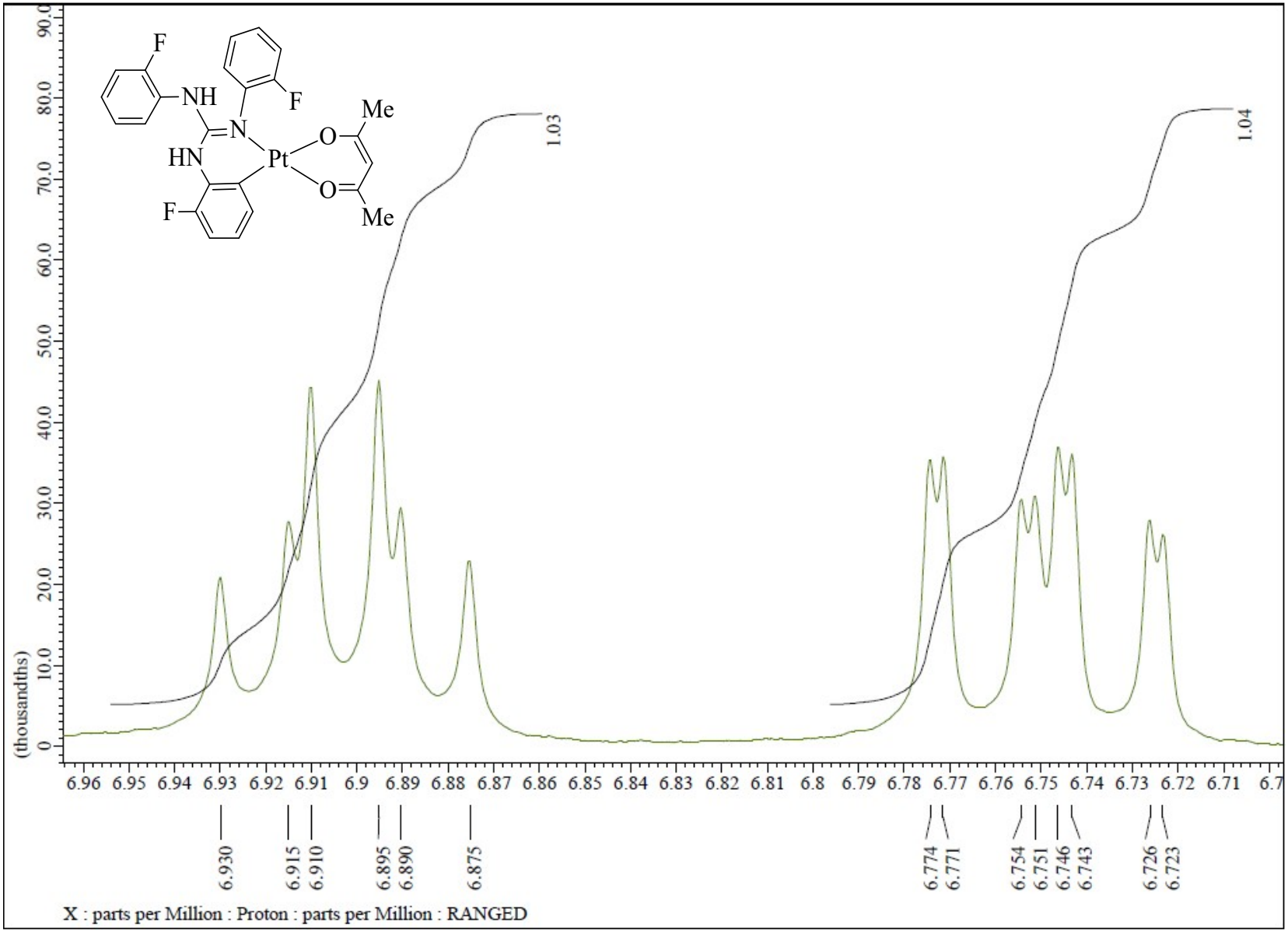

Fig. S130 ^{1}H NMR ($CDCl_3$, 400 MHz) spectrum of **15** in the indicated region.

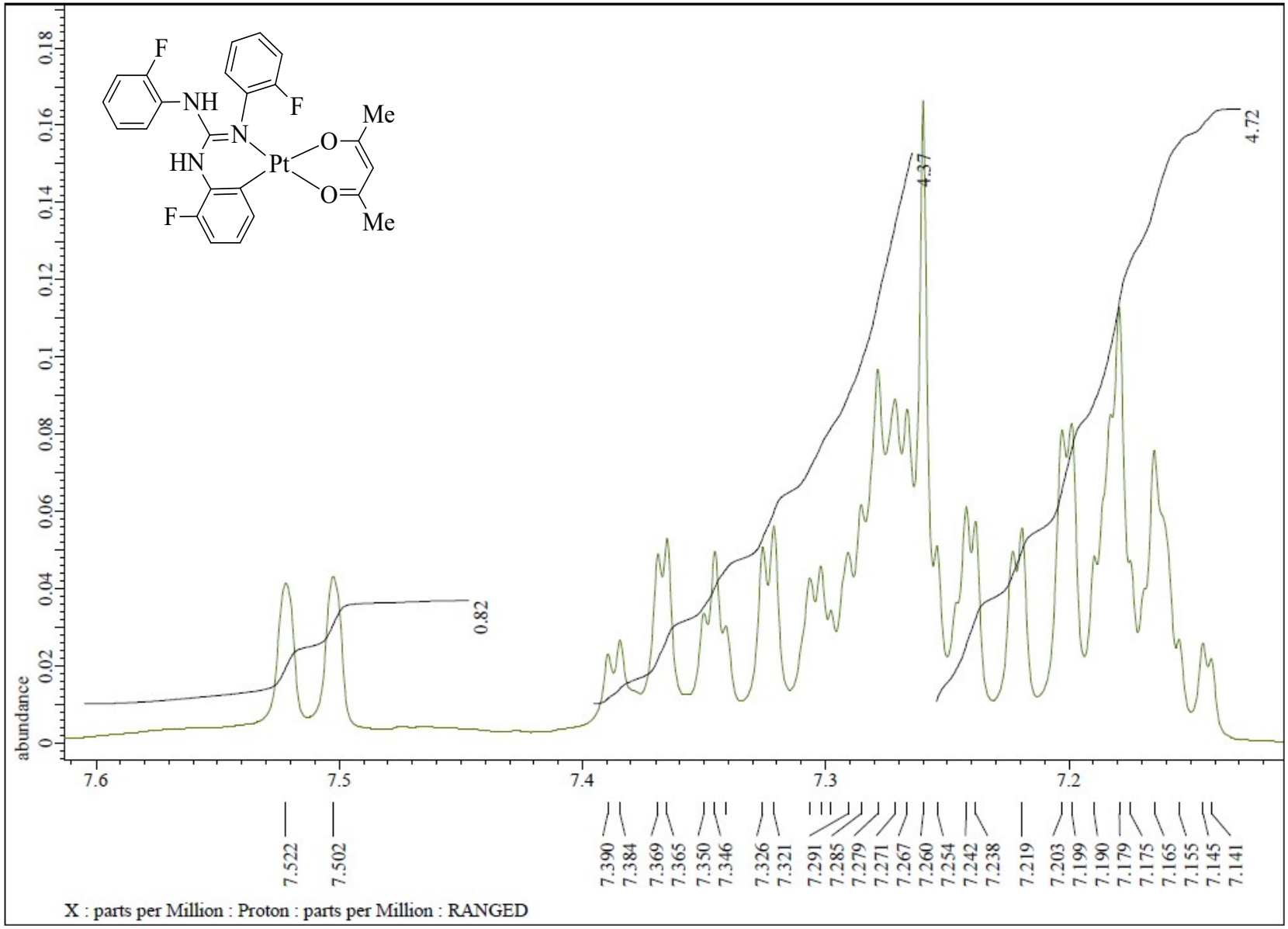

Fig. S131 ^{1}H NMR ($CDCl_3$, 400 MHz) spectrum of **15** in the indicated region.

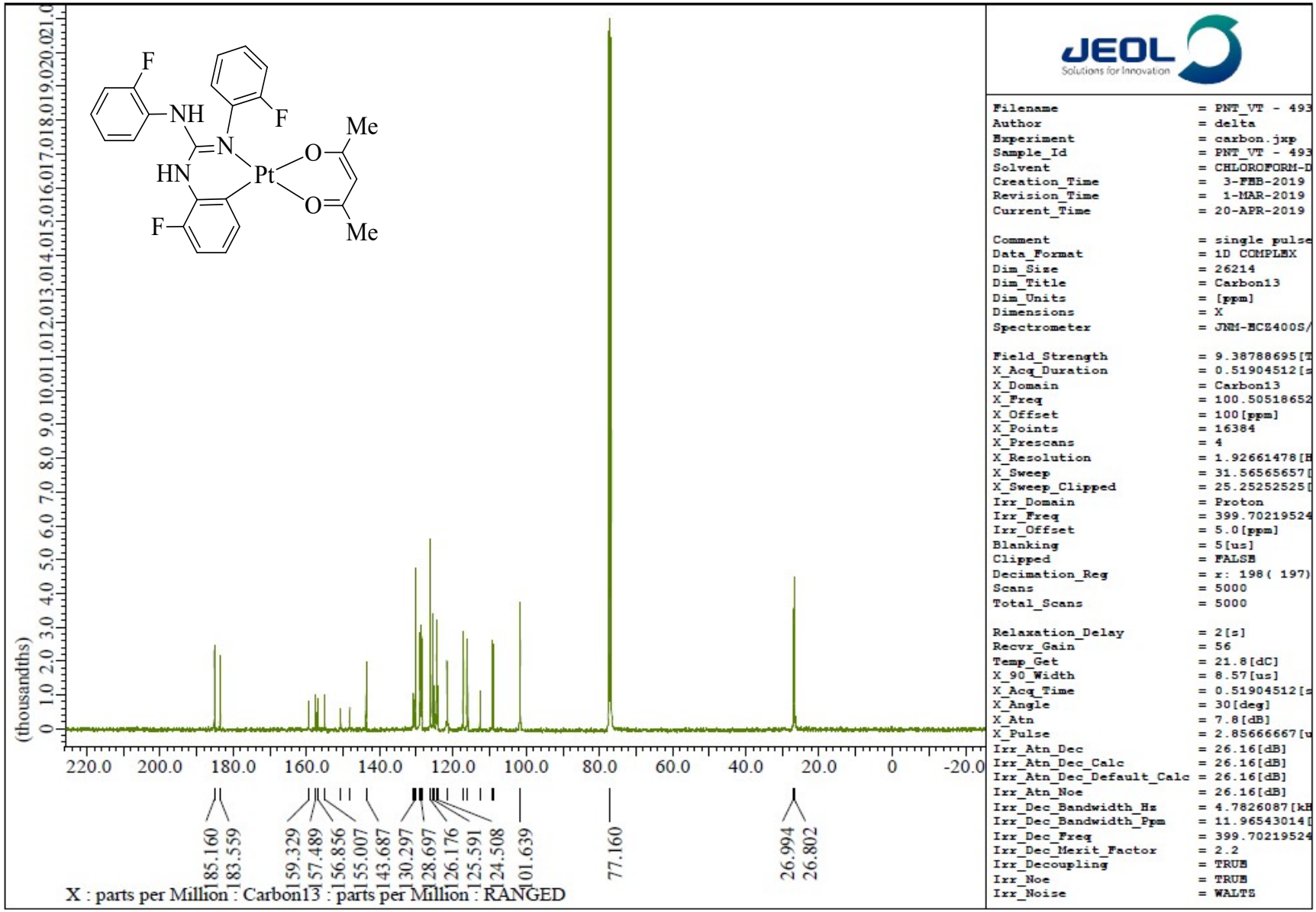

Fig. S132 $^{13}C\{^{1}H\}$ NMR ($CDCl_3$, 100.5 MHz) spectrum of **15**.

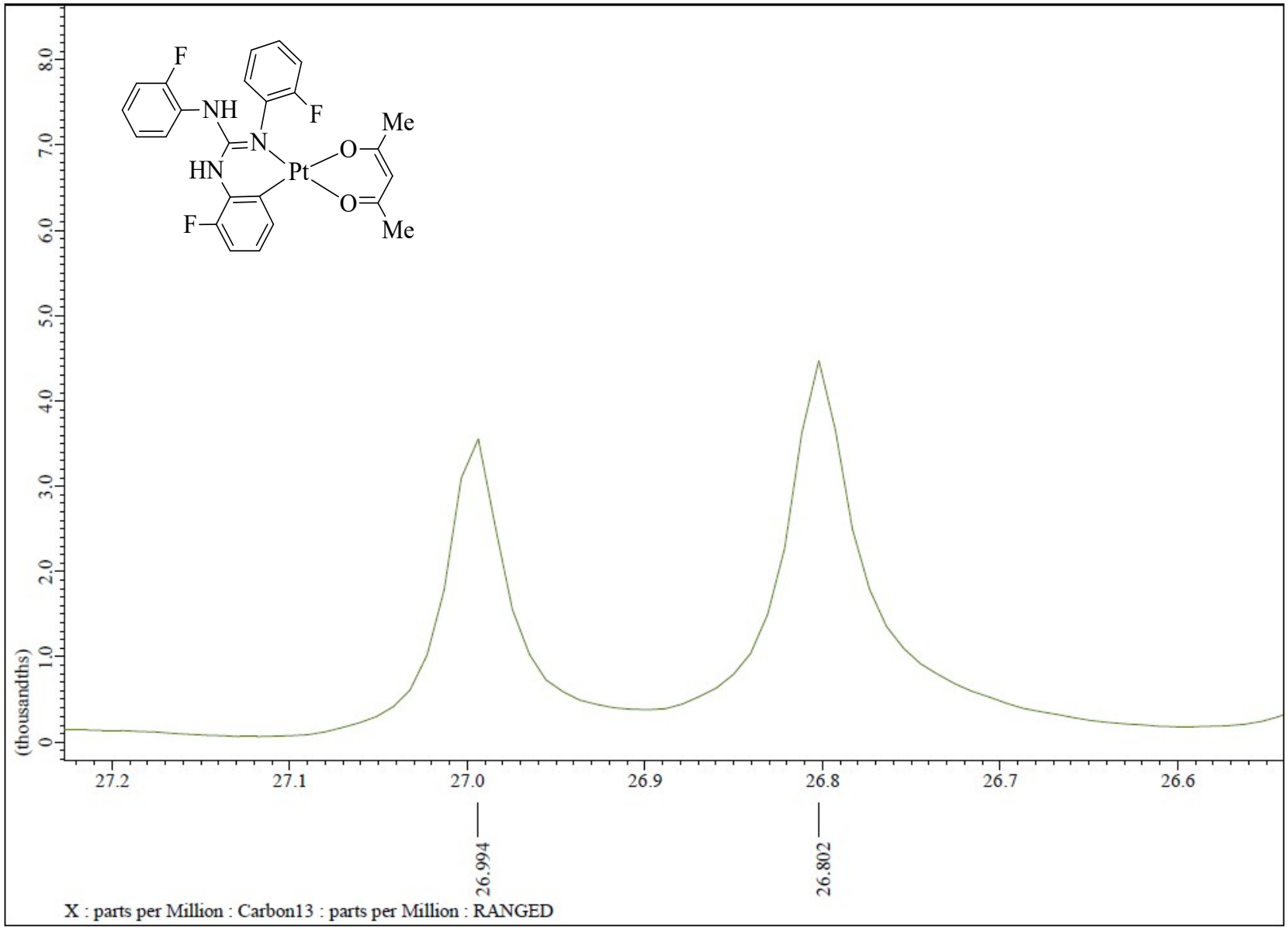

Fig. S133 $^{13}C\{^{1}H\}$ NMR ($CDCl_3$, 100.5 MHz) spectrum of **15** in the indicated region.

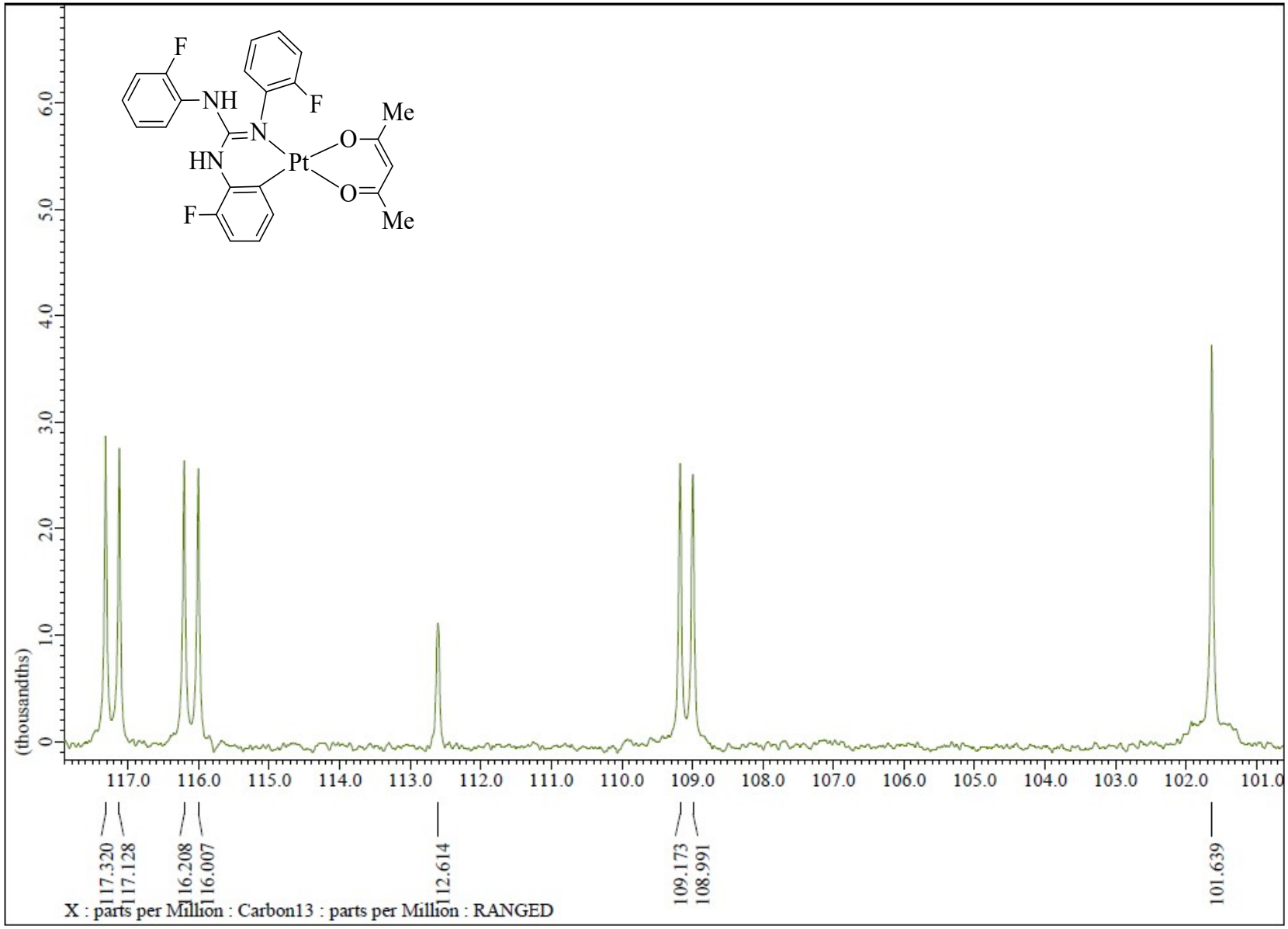

Fig. S134 $^{13}C\{^{1}H\}$ NMR ($CDCl_3$, 100.5 MHz) spectrum of **15** in the indicated region.

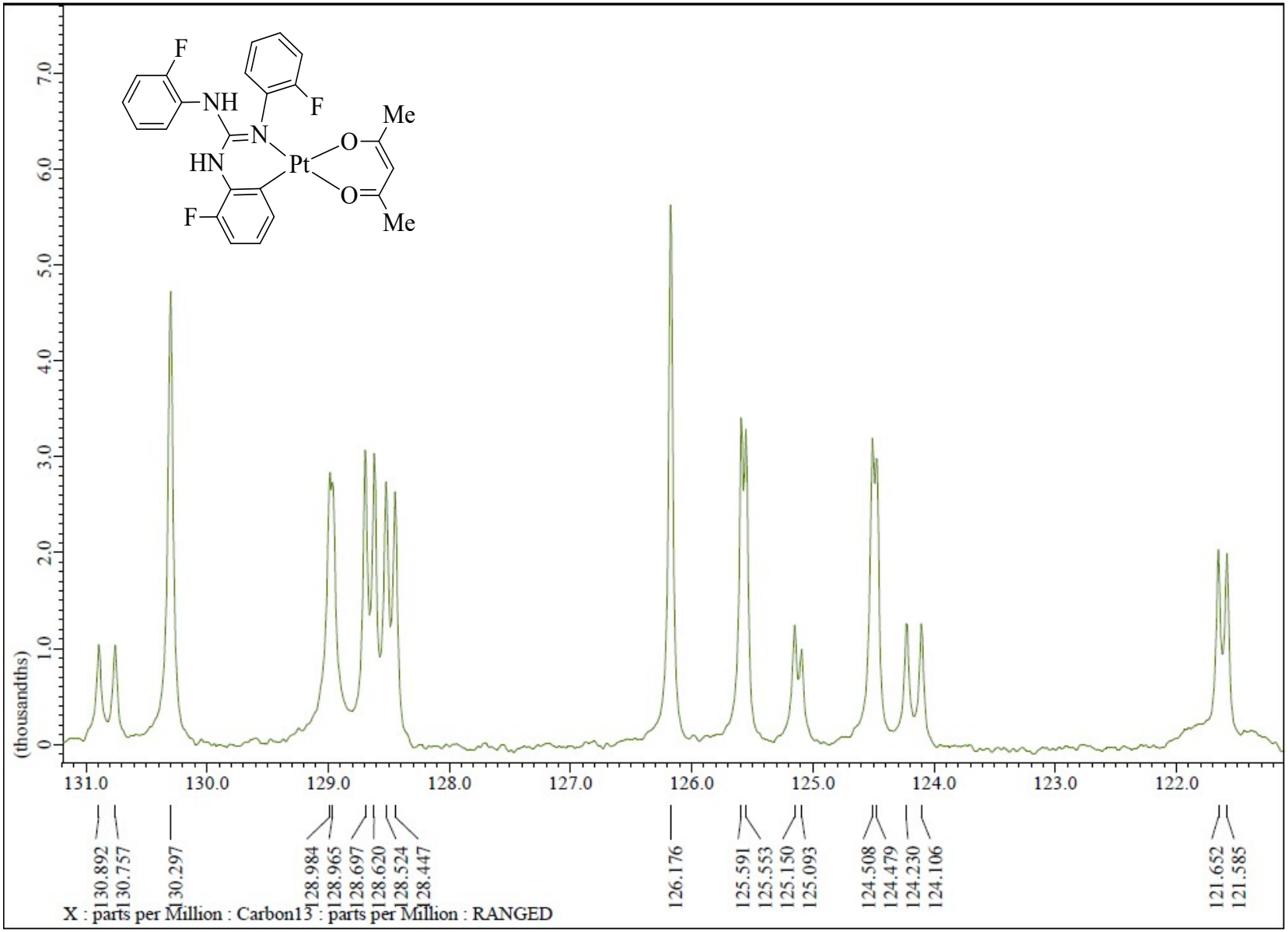

Fig. S135 $^{13}C\{^{1}H\}$ NMR ($CDCl_3$, 100.5 MHz) spectrum of **15** in the indicated region.

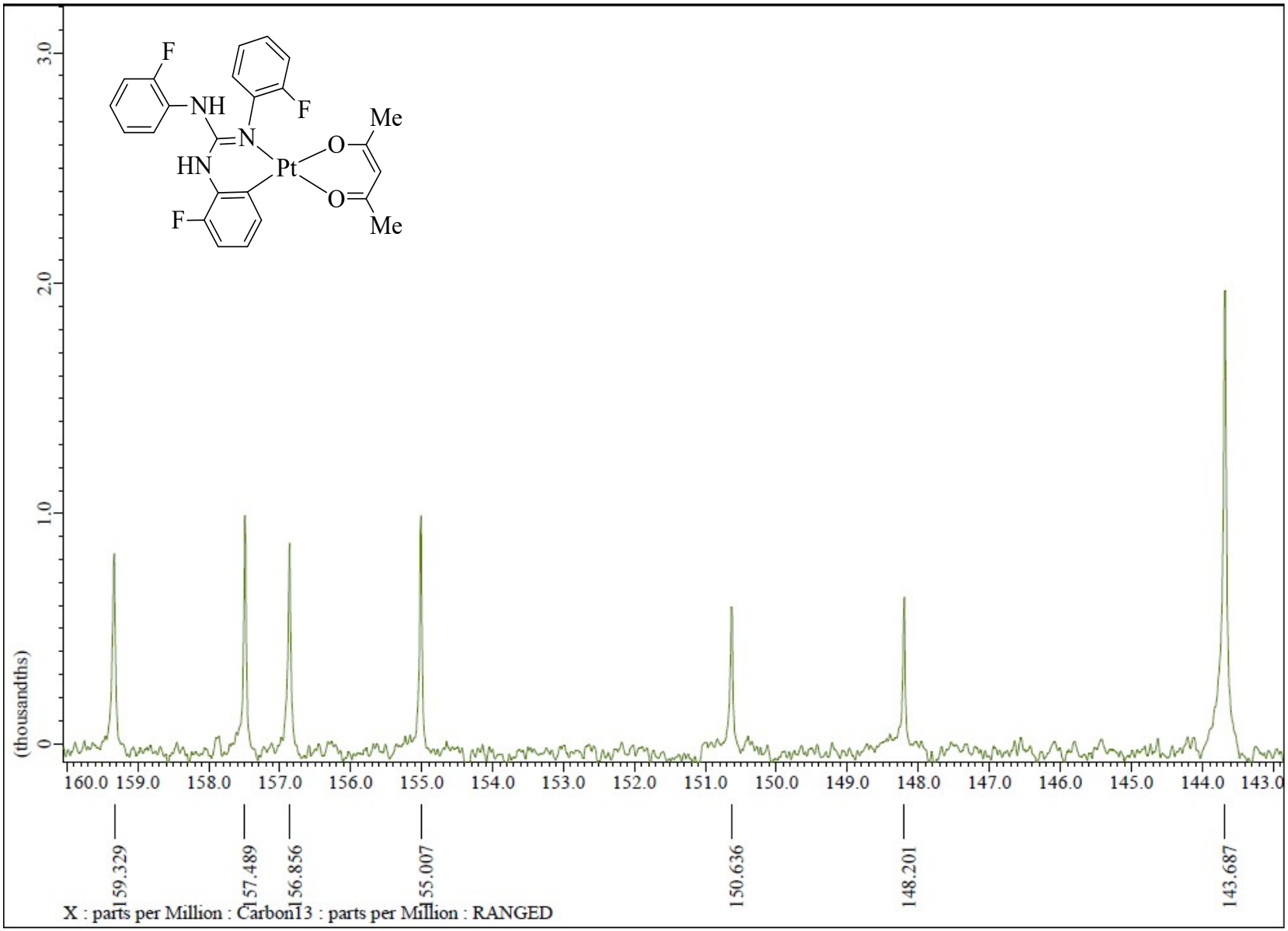

Fig. S136 $^{13}C\{^{1}H\}$ NMR ($CDCl_3$, 100.5 MHz) spectrum of **15** in the indicated region.

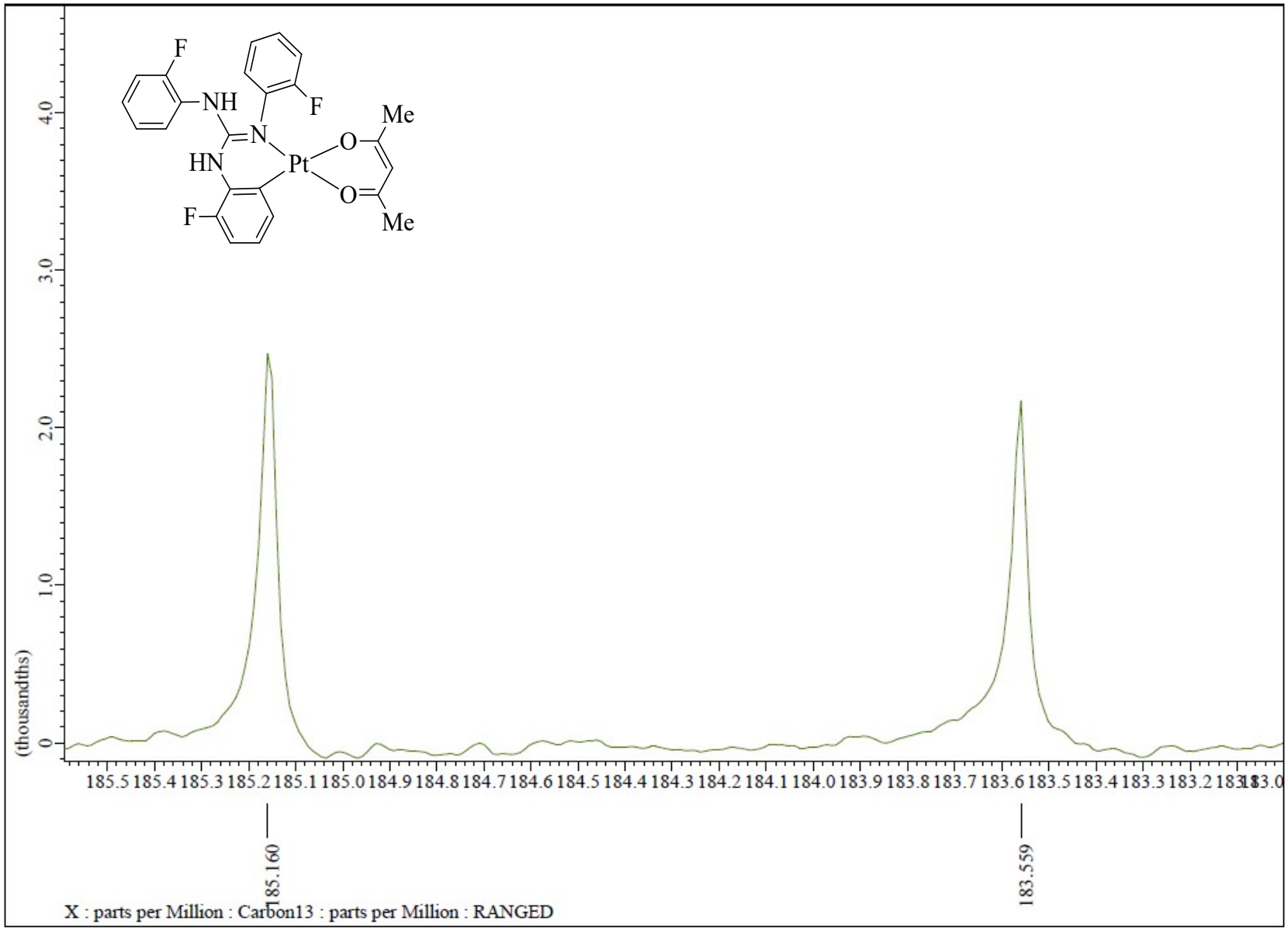

Fig. S137 $^{13}C\{^{1}H\}$ NMR ($CDCl_3$, 100.5 MHz) spectrum of **15** in the indicated region.

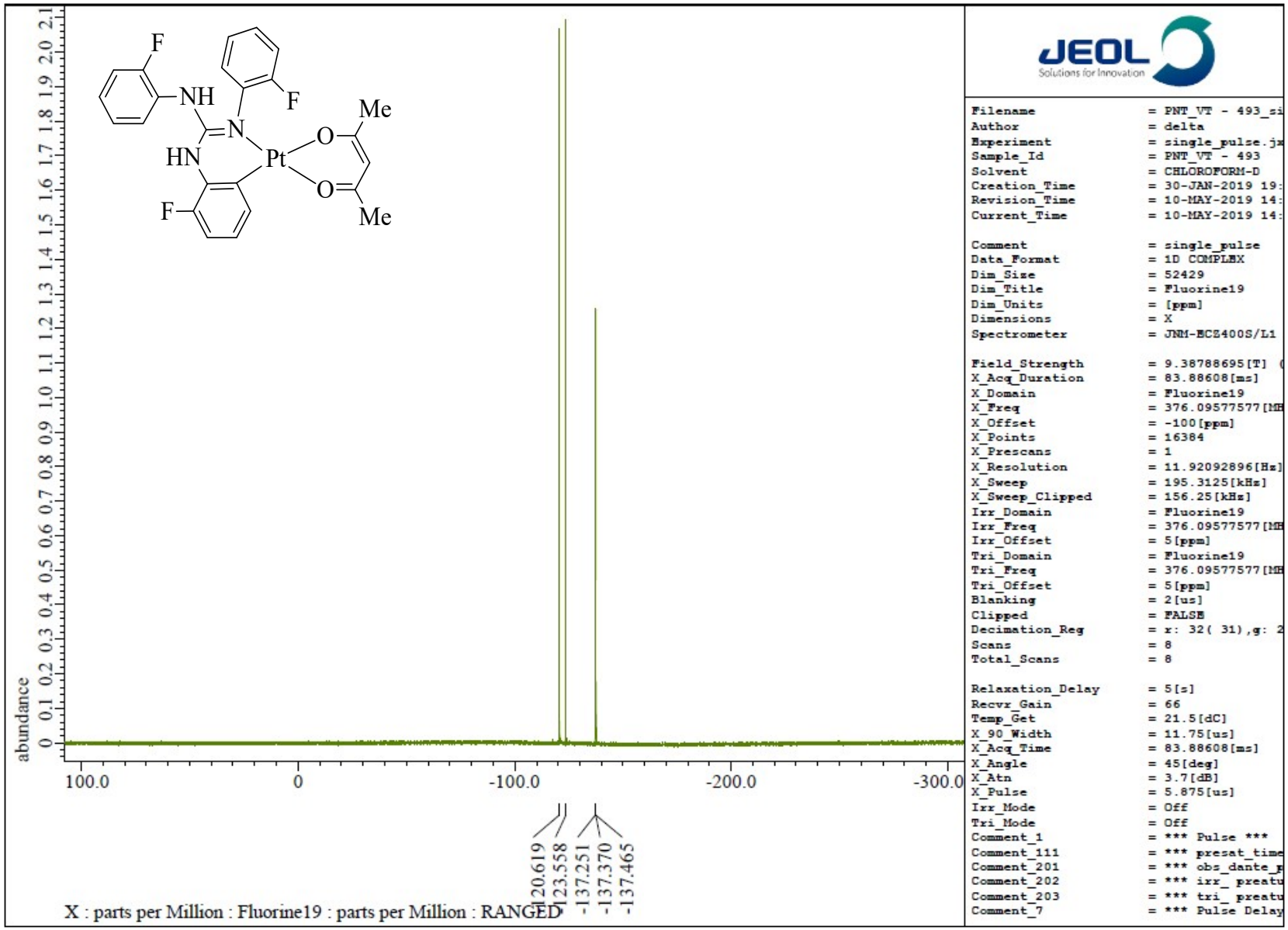

Fig. S138 $^{19}F\{^{1}H\}$ NMR ($CDCl_3$, 376.31 MHz) spectrum of **15**.

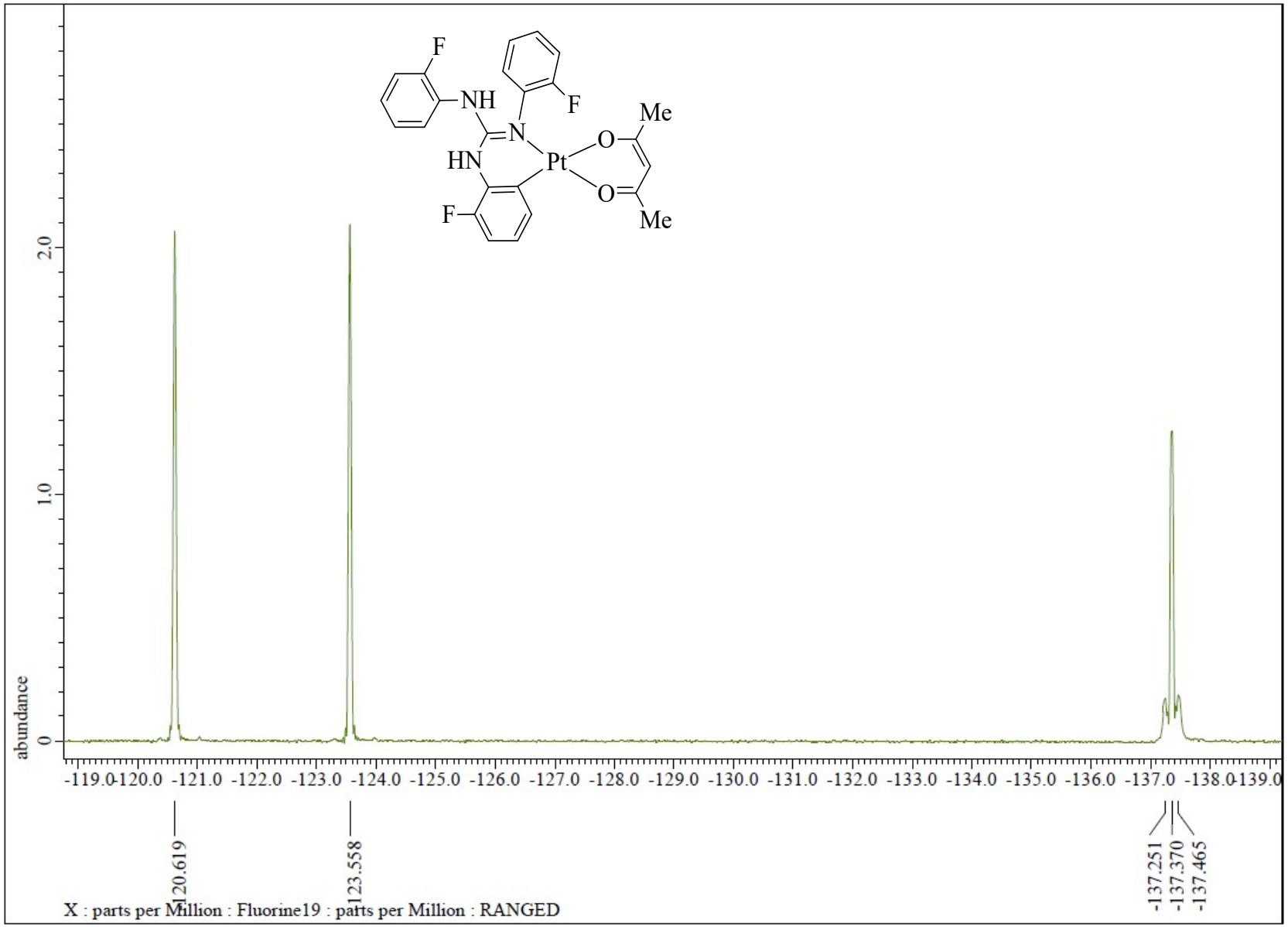

Fig. S139 $^{19}F\{^{1}H\}$ NMR ($CDCl_3$, 376.31 MHz) spectrum of **15** in the indicated region.

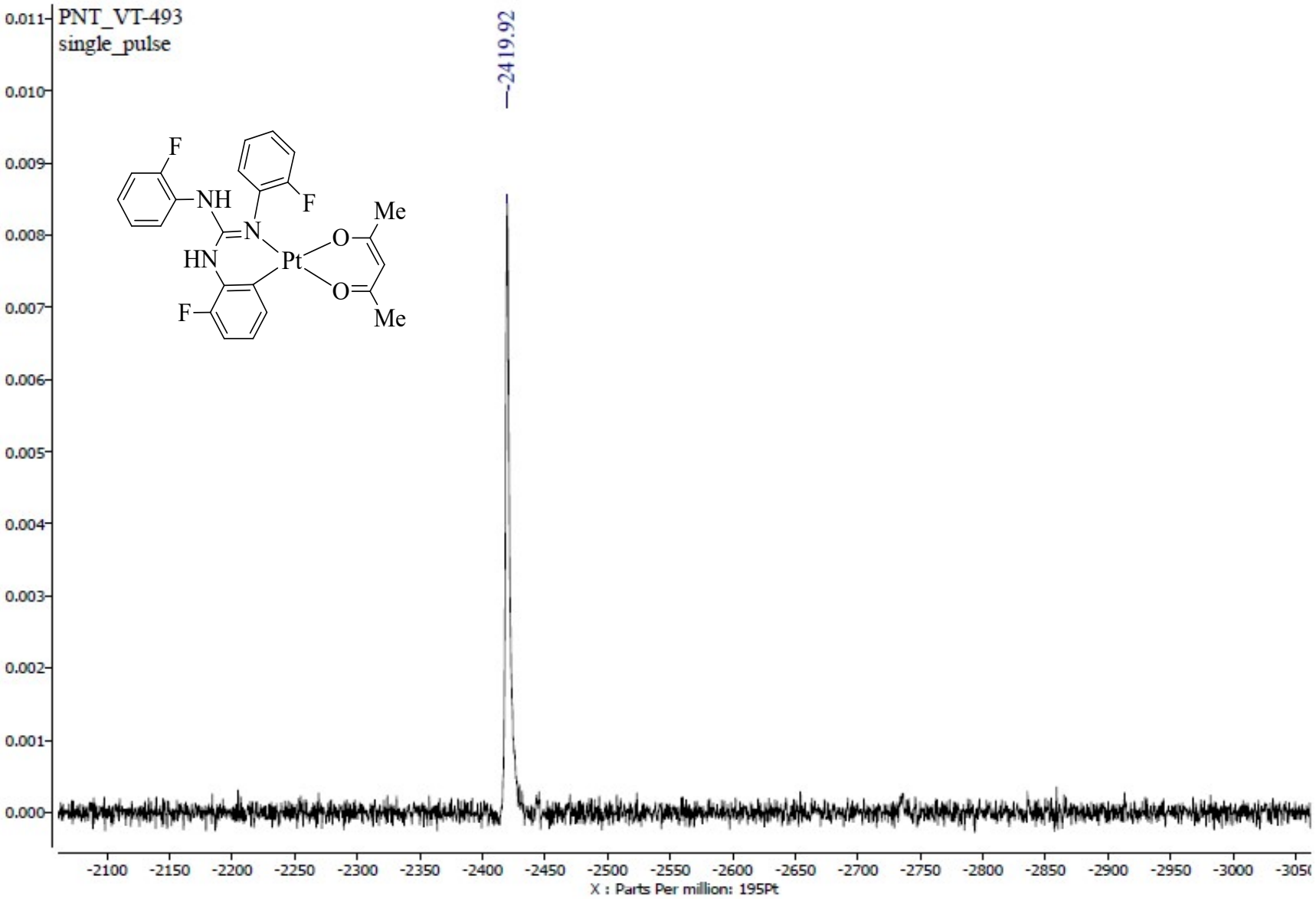

Fig. S140 $^{195}Pt\{^{1}H\}$ NMR ($CDCl_3$, 85.8 MHz) spectrum of **15**.

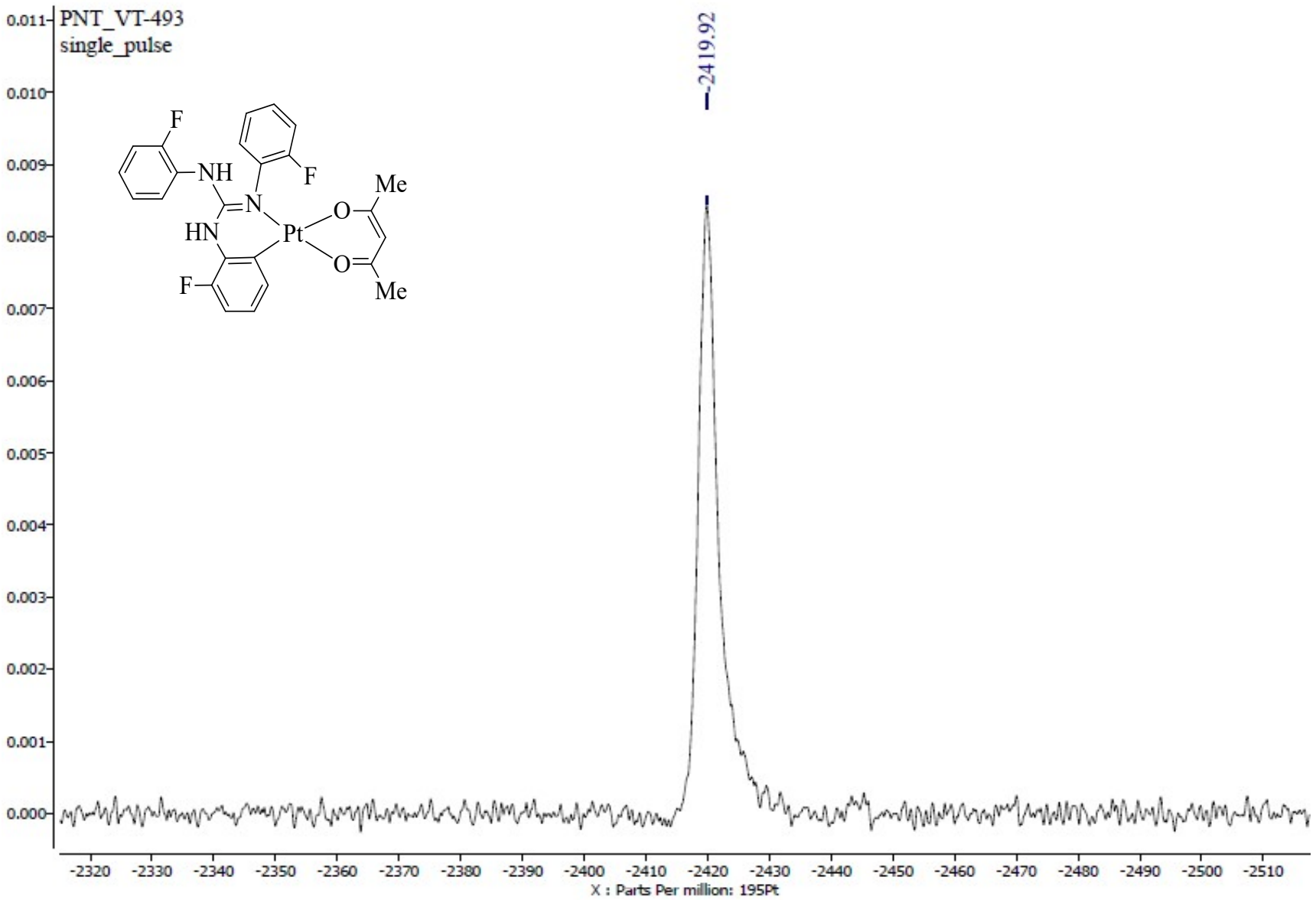

Fig. S141 $^{195}Pt\{^{1}H\}$ NMR ($CDCl_3$, 85.8 MHz) spectrum of **15**.

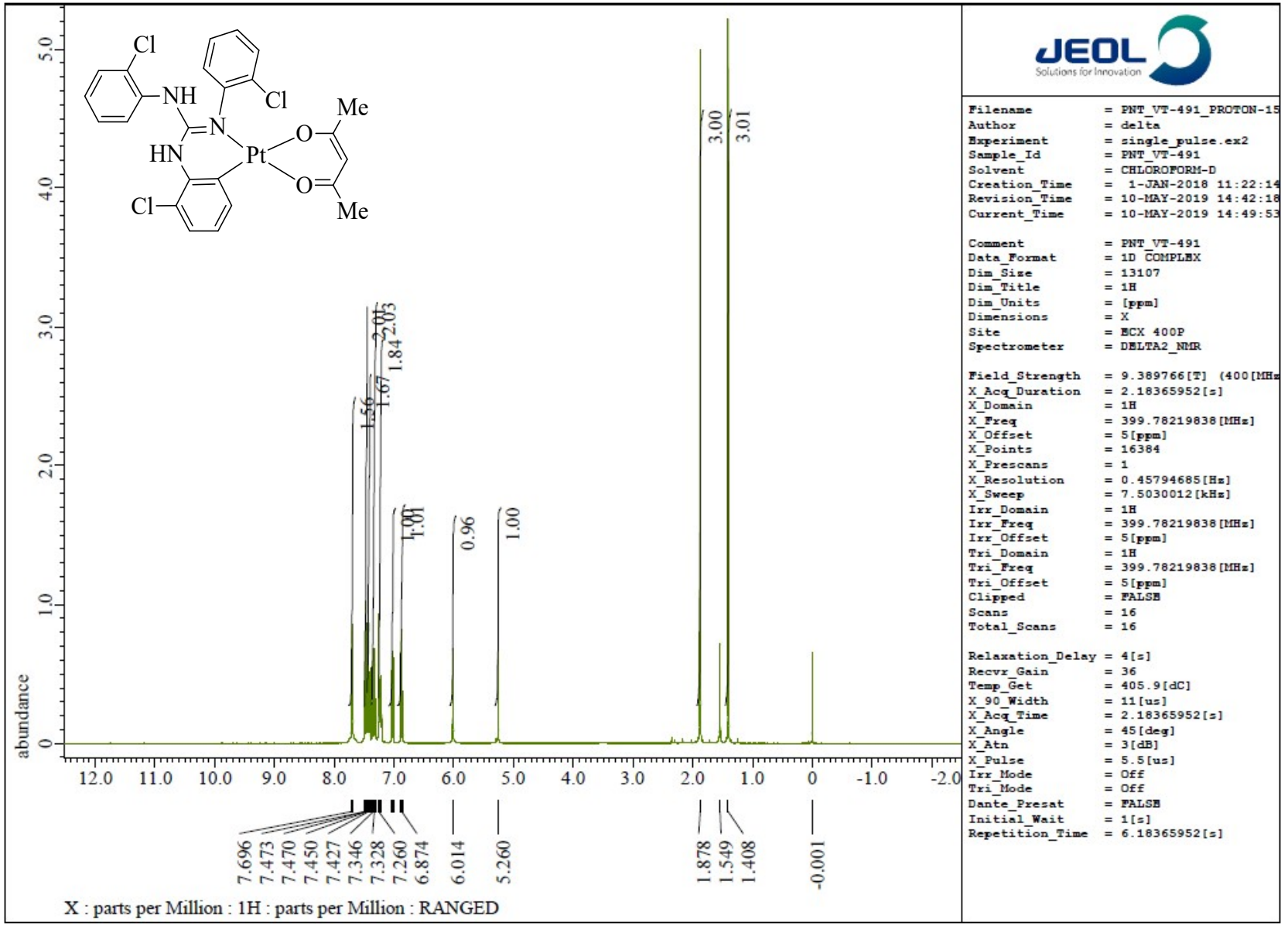

Fig. S142 ^{1}H NMR ($CDCl_3$, 400 MHz) spectrum of **16**.

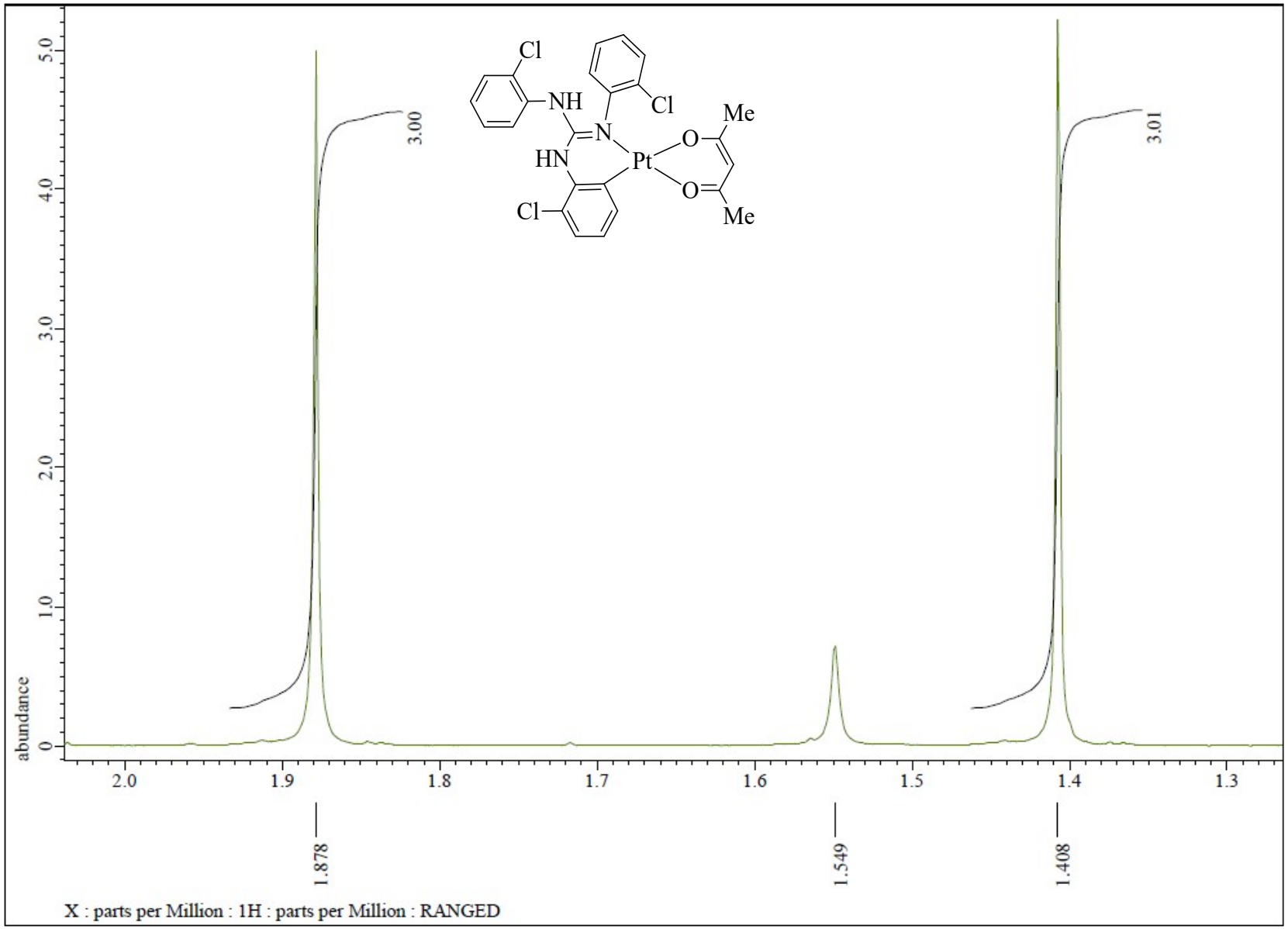

Fig. S143 ^{1}H NMR ($CDCl_3$, 400 MHz) spectrum of **16** in the indicated region.

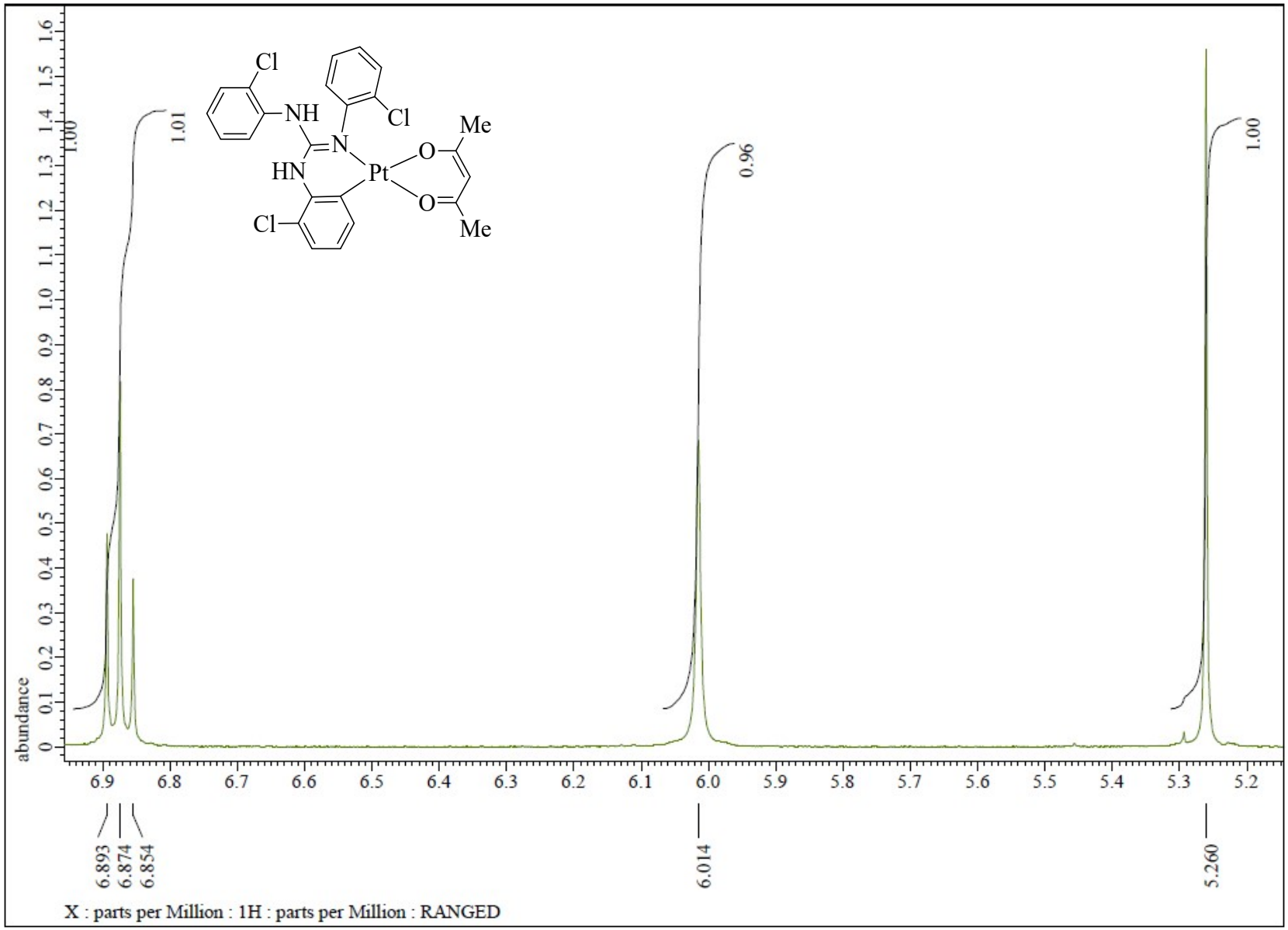

Fig. S144 ^{1}H NMR ($CDCl_3$, 400 MHz) spectrum of **16** in the indicated region.

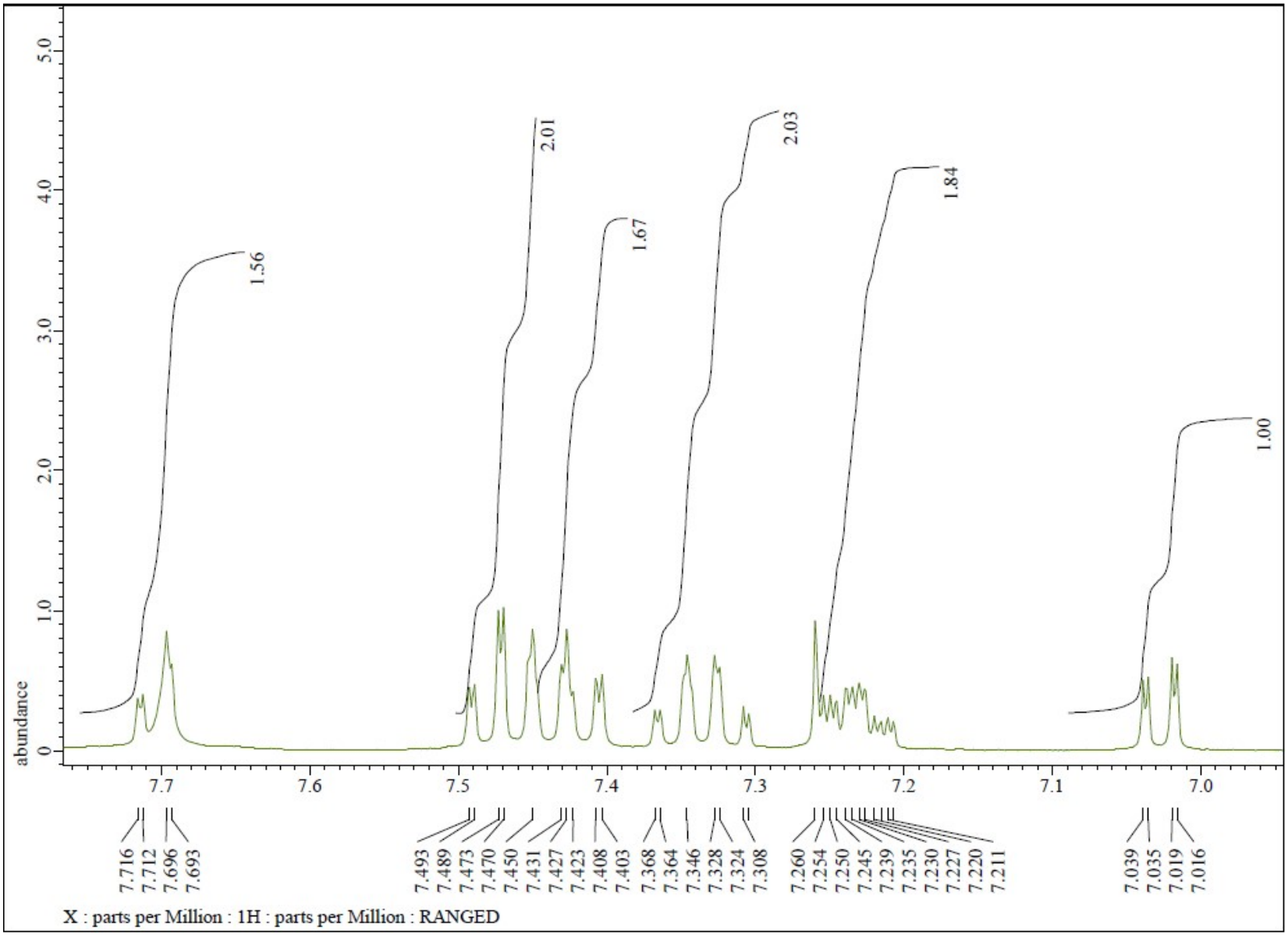

Fig. S145 ^{1}H NMR ($CDCl_3$, 400 MHz) spectrum of **16** in the indicated region.

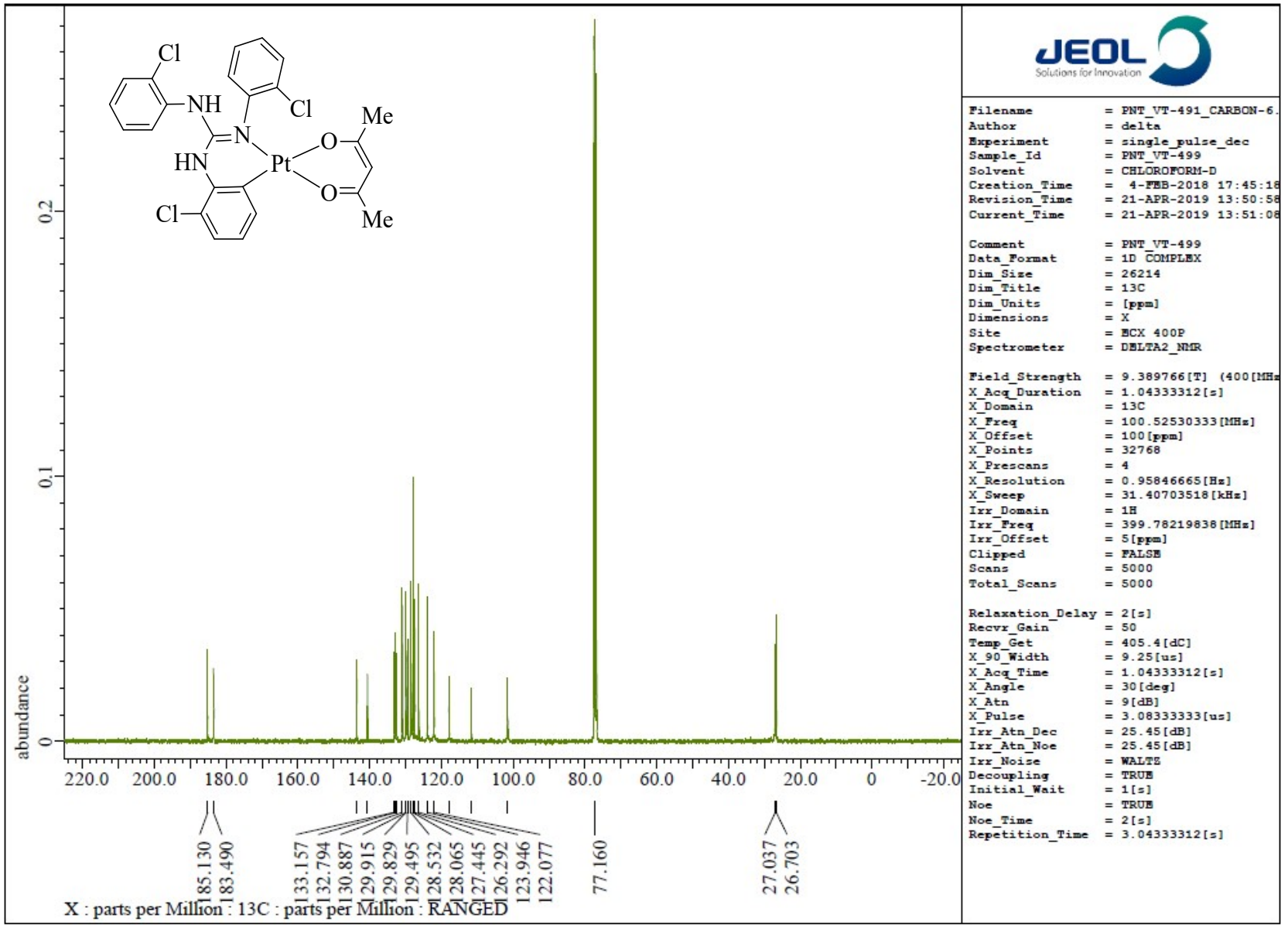

Fig. S146 $^{13}C\{^{1}H\}$ NMR ($CDCl_3$, 100.5 MHz) spectrum of **16**.

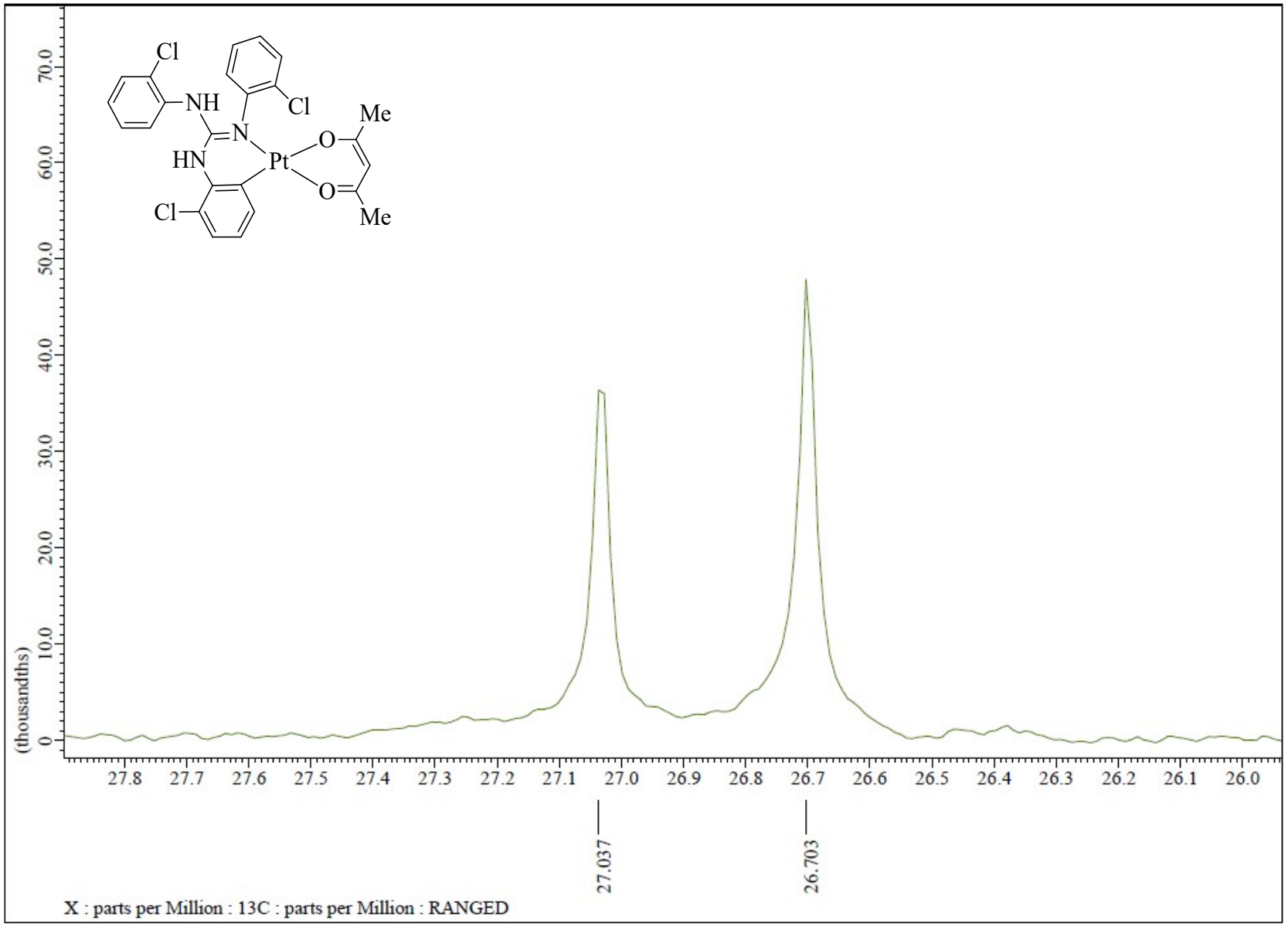

Fig. S147 $^{13}C\{^{1}H\}$ NMR ($CDCl_3$, 100.5 MHz) spectrum of **16** in the indicated region.

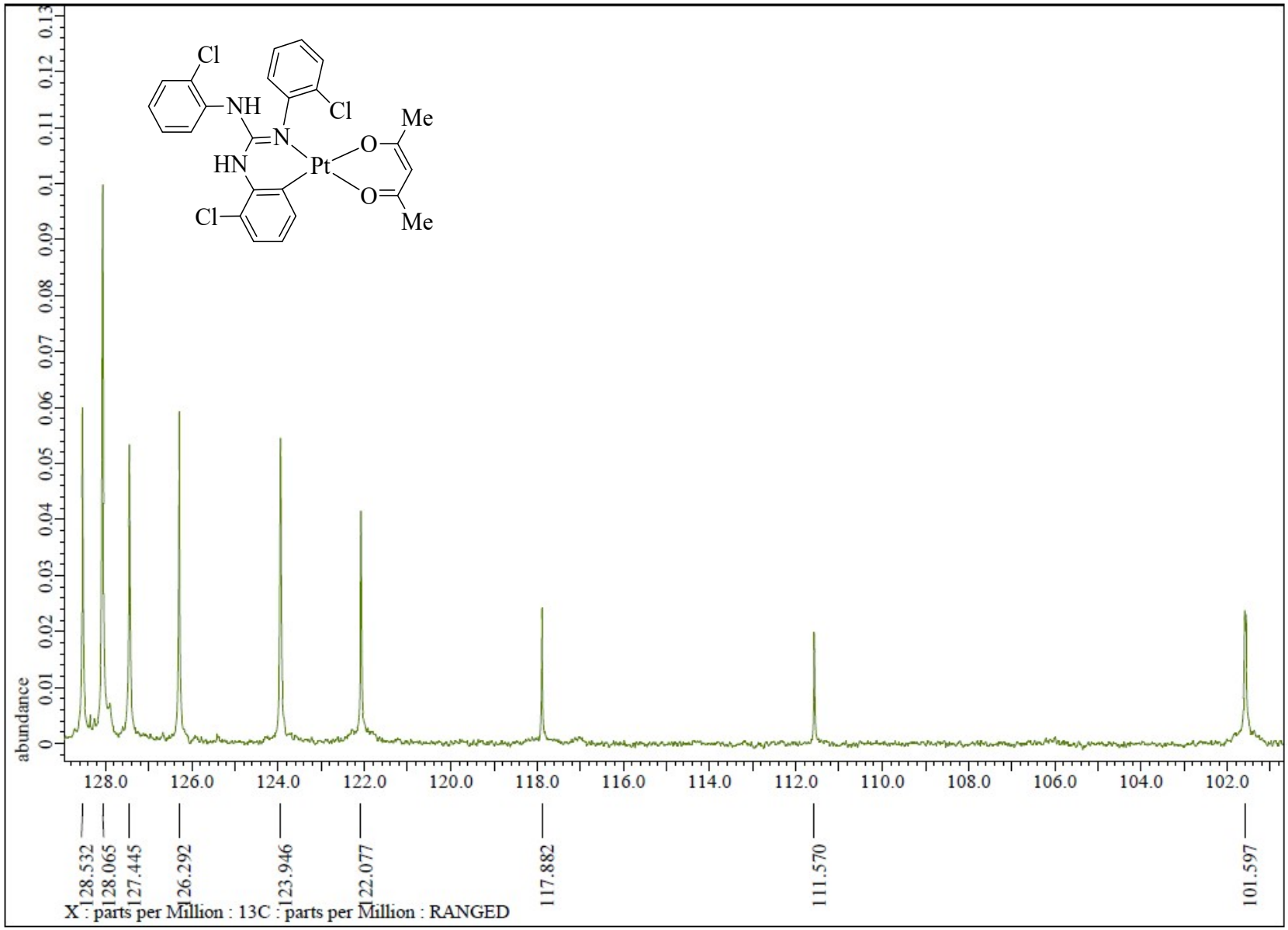

Fig. S148 $^{13}C\{^{1}H\}$ NMR ($CDCl_3$, 100.5 MHz) spectrum of **16** in the indicated region.

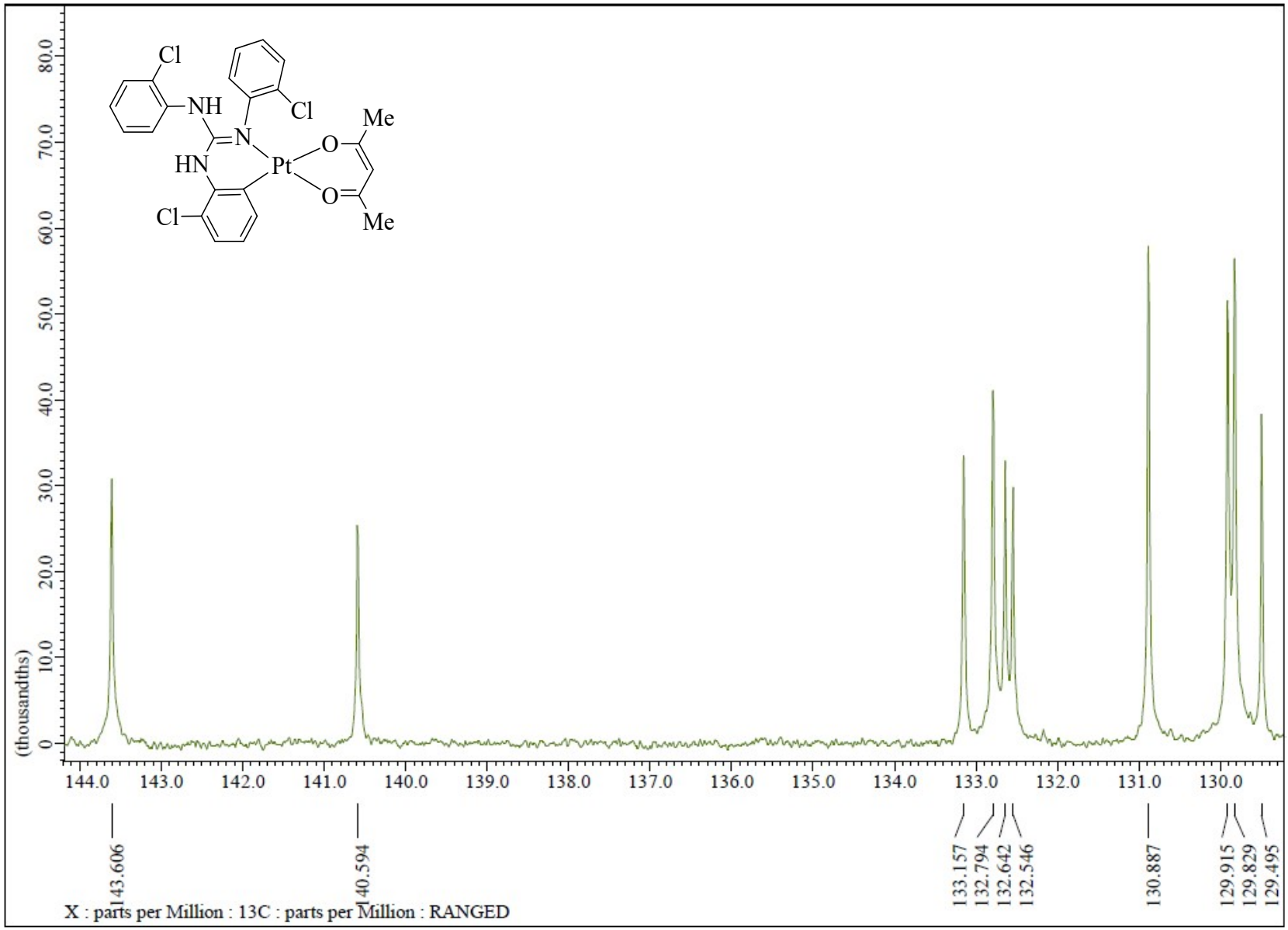

Fig. S149 $^{13}C\{^{1}H\}$ NMR ($CDCl_3$, 100.5 MHz) spectrum of **16** in the indicated region.

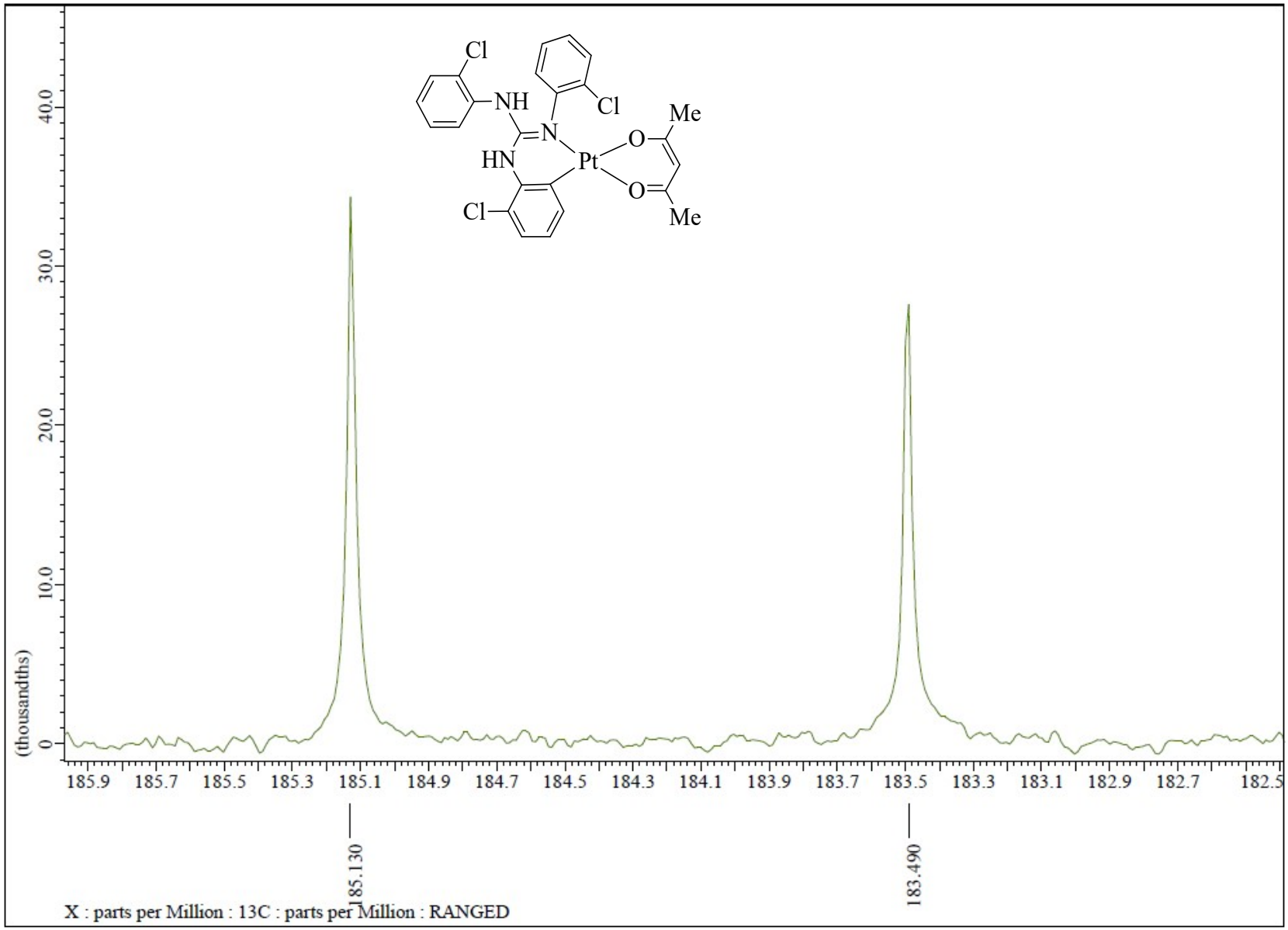

Fig. S150 $^{13}C\{^{1}H\}$ NMR ($CDCl_3$, 100.5 MHz) spectrum of **16** in the indicated region.

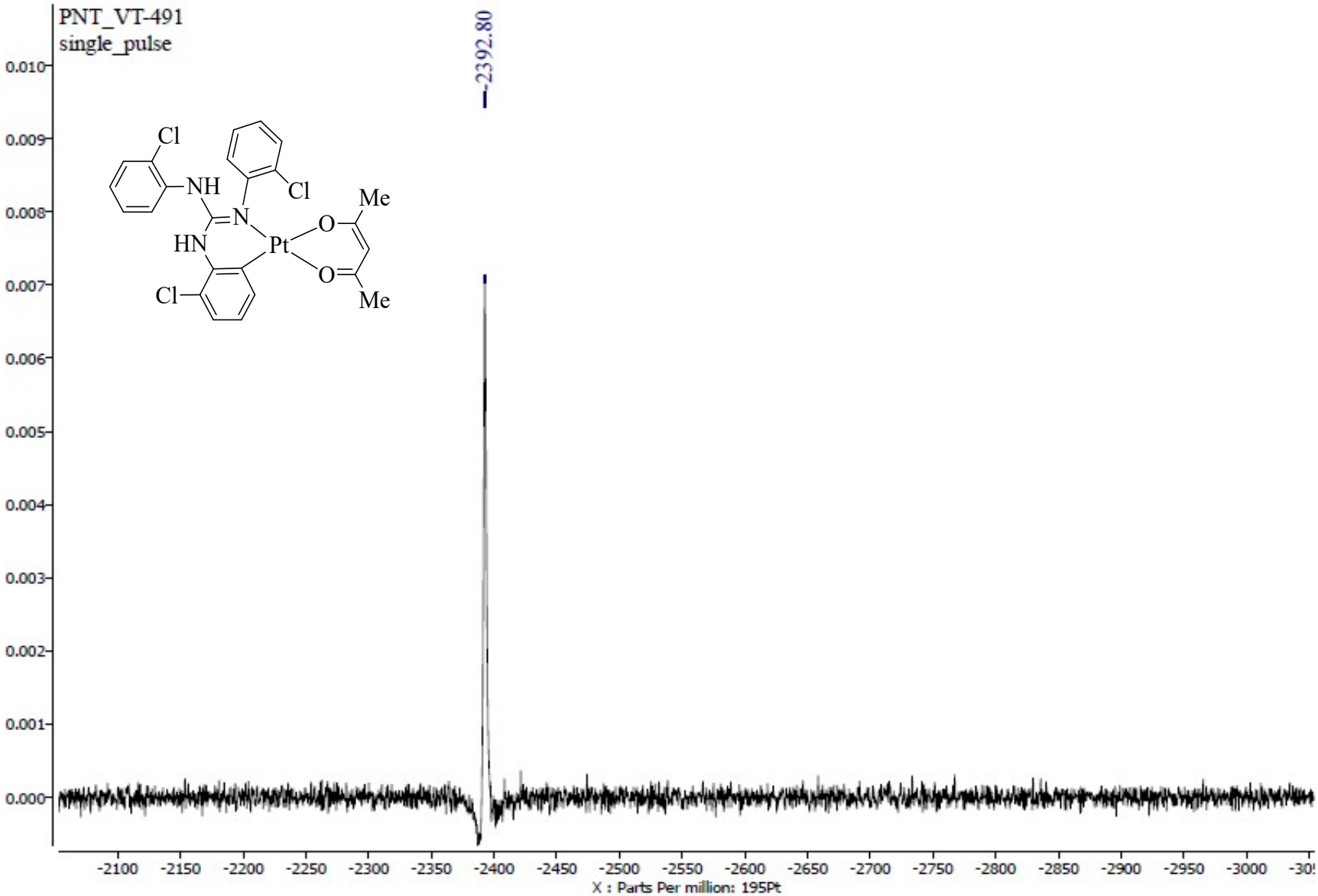

Fig. S151 $^{195}Pt\{^{1}H\}$ NMR ($CDCl_3$, 85.8 MHz) spectrum of **16**.

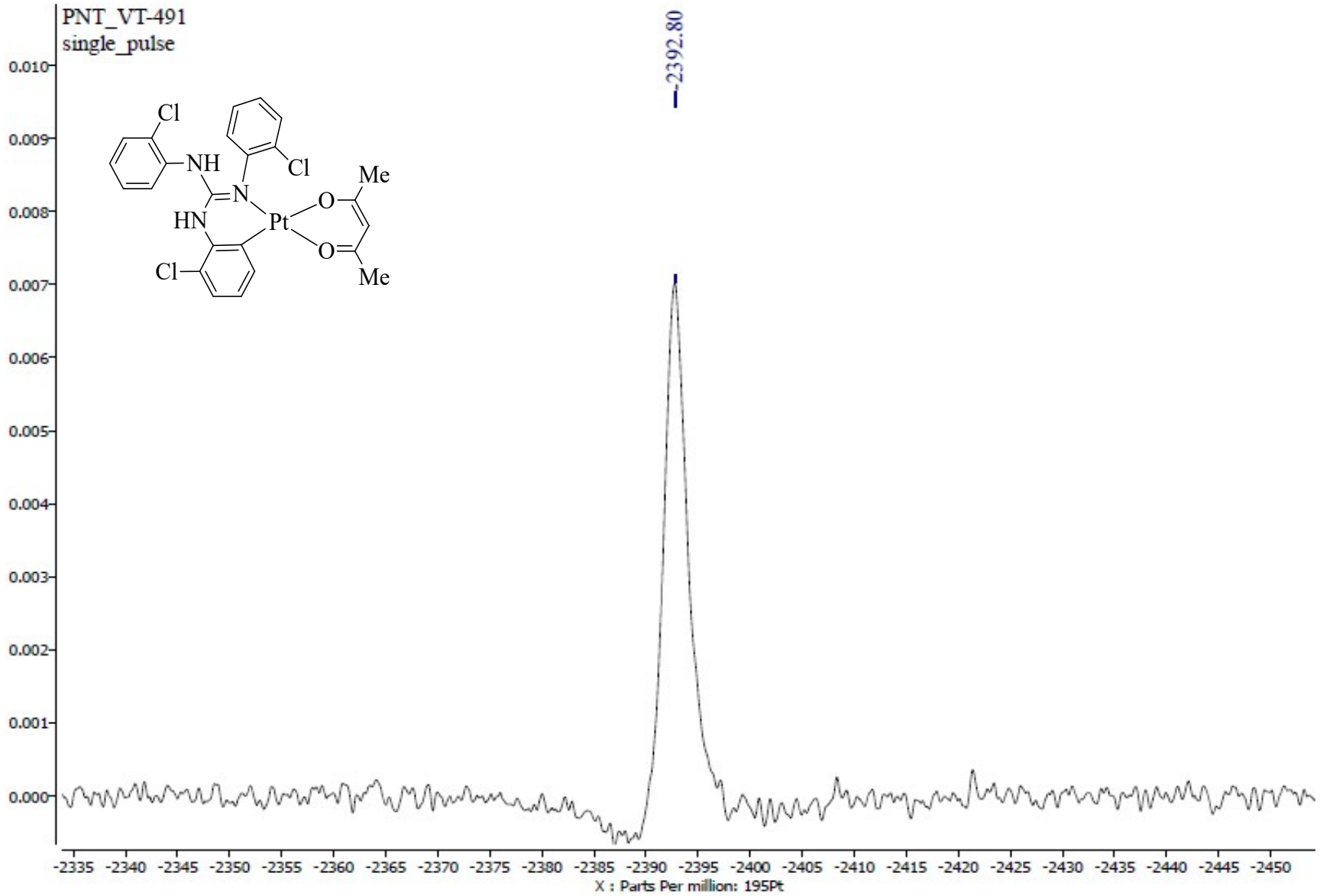

Fig. S152 $^{195}Pt\{^{1}H\}$ NMR ($CDCl_3$, 85.8 MHz) spectrum of **16** in the indicated region.

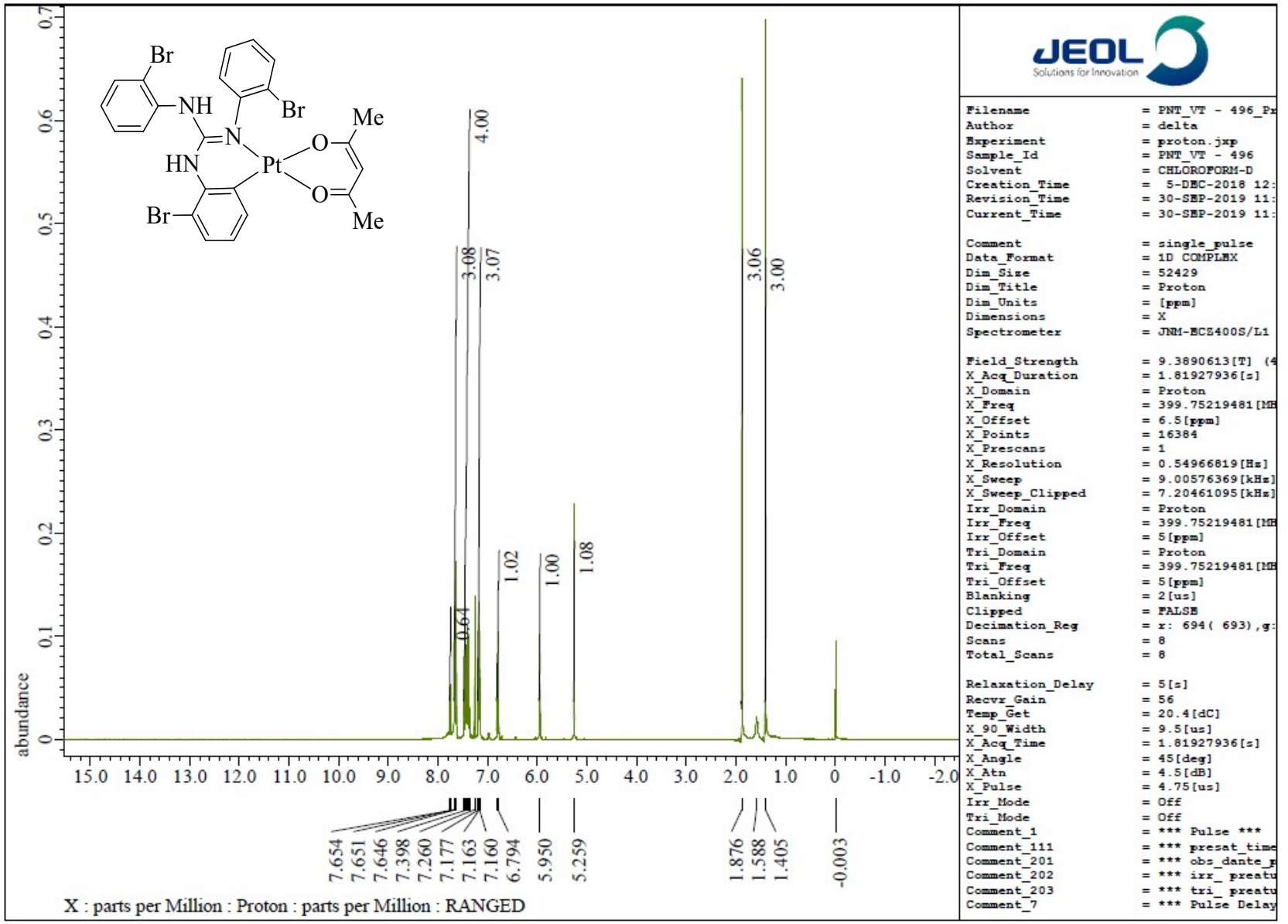

Fig. S153 ^{1}H NMR ($CDCl_3$, 400 MHz) spectrum of **17**.

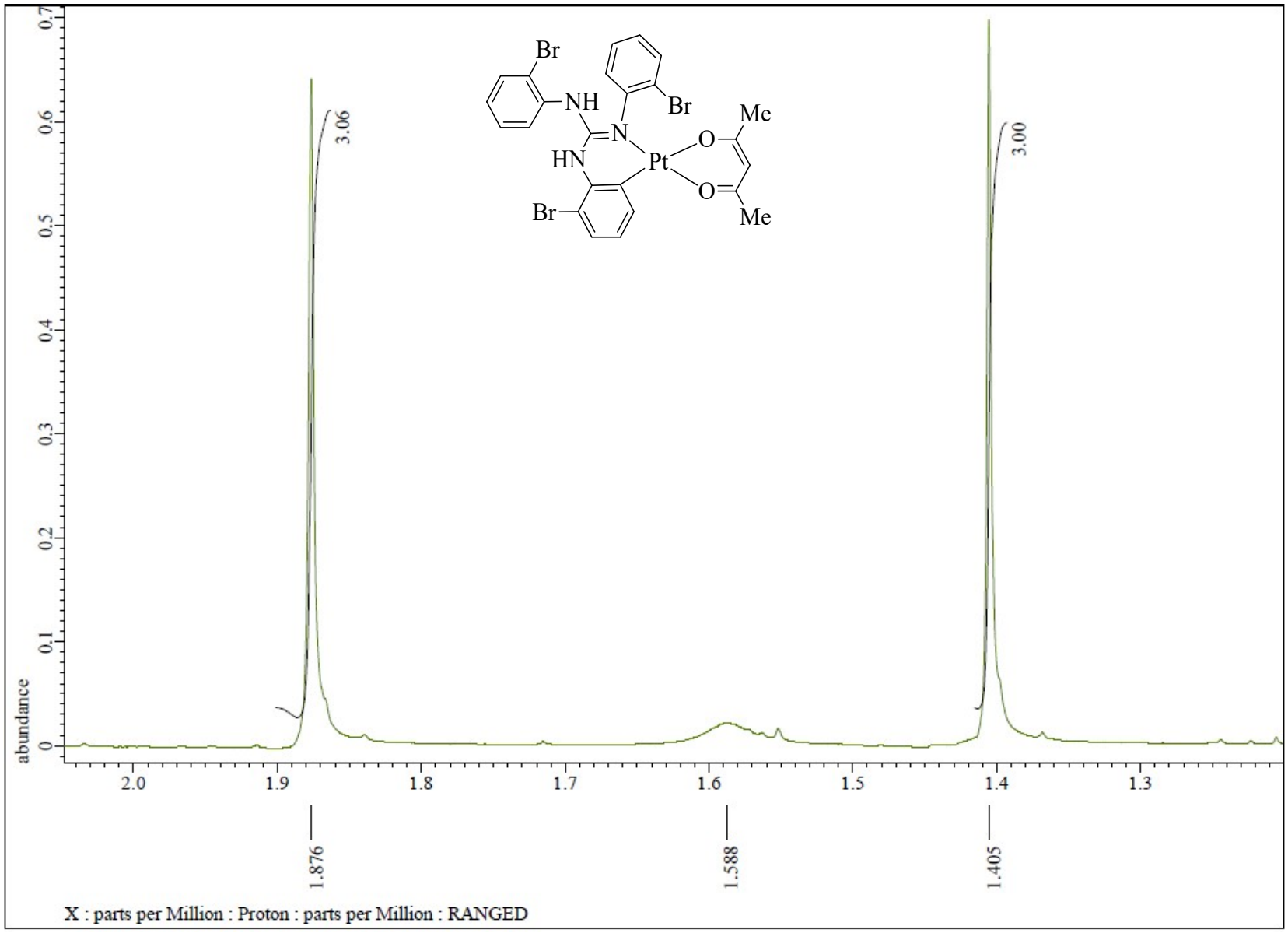

Fig. S154 ^{1}H NMR ($CDCl_3$, 400 MHz) spectrum of **17** in the indicated region.

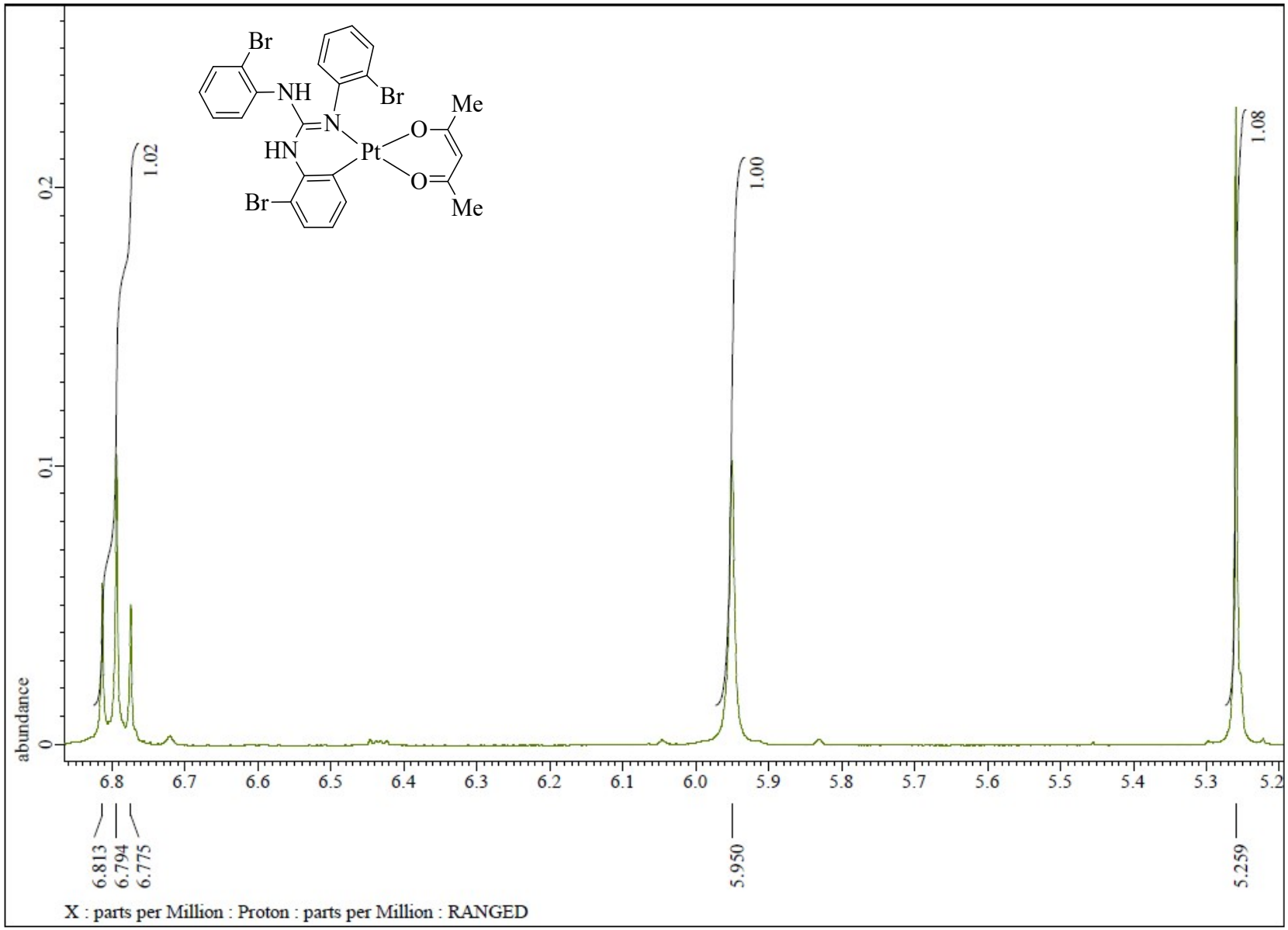

Fig. S155 ^{1}H NMR ($CDCl_3$, 400 MHz) spectrum of **17** in the indicated region.

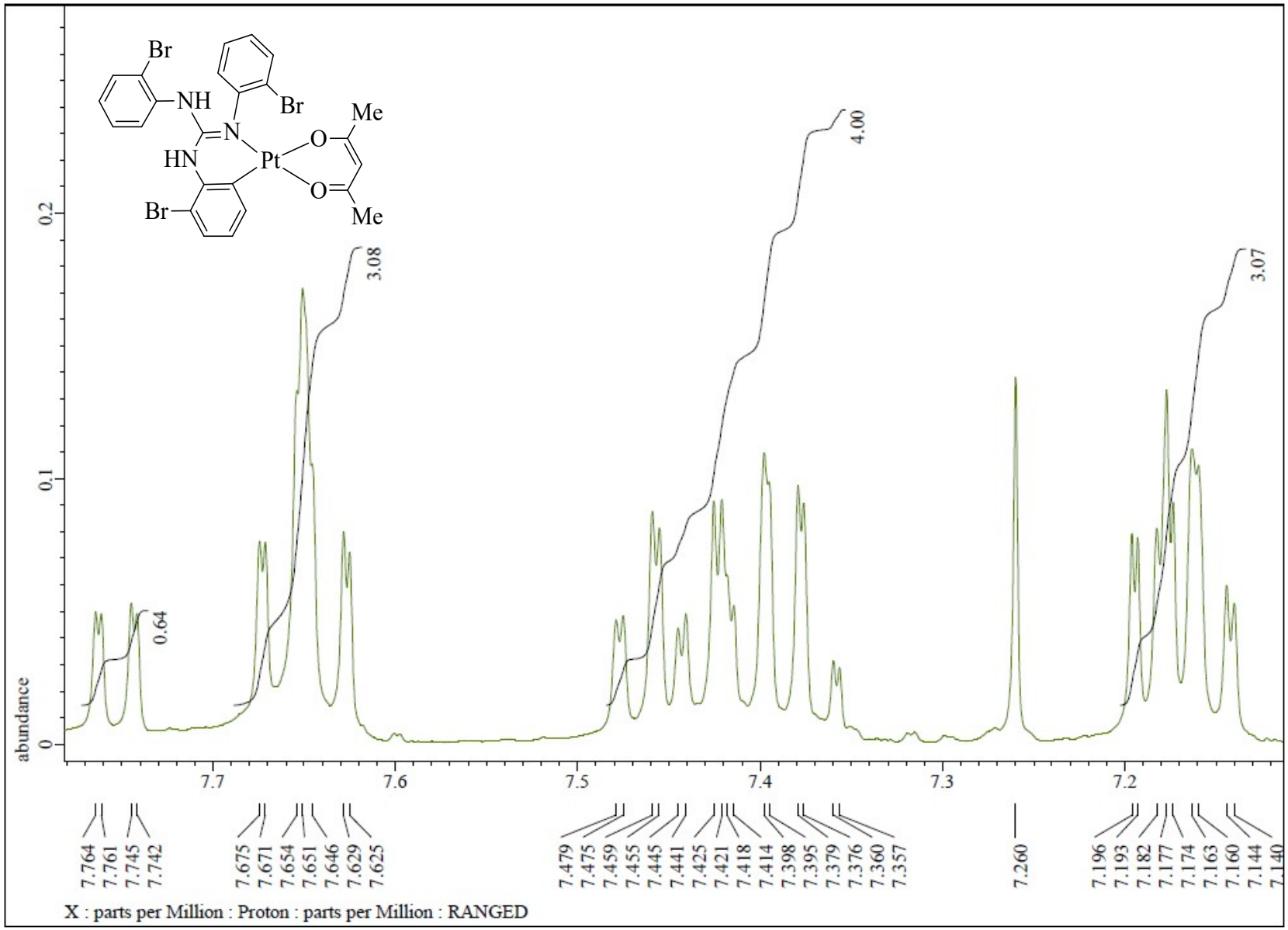

Fig. S156 ^{1}H NMR ($CDCl_3$, 400 MHz) spectrum of **17** in the indicated region.

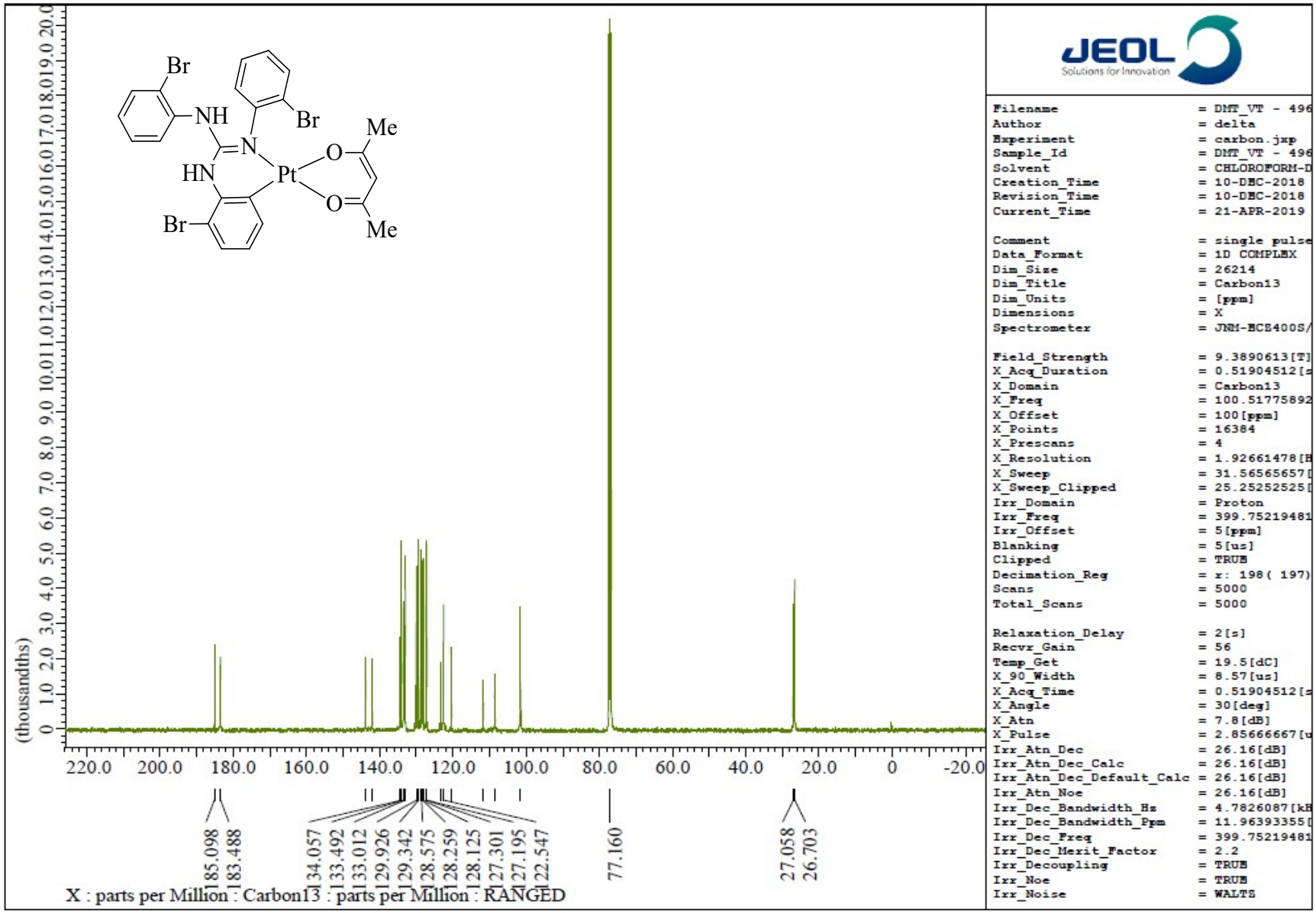

Fig. S157 $^{13}C\{^{1}H\}$ NMR ($CDCl_3$, 100.5 MHz) spectrum of **17**.

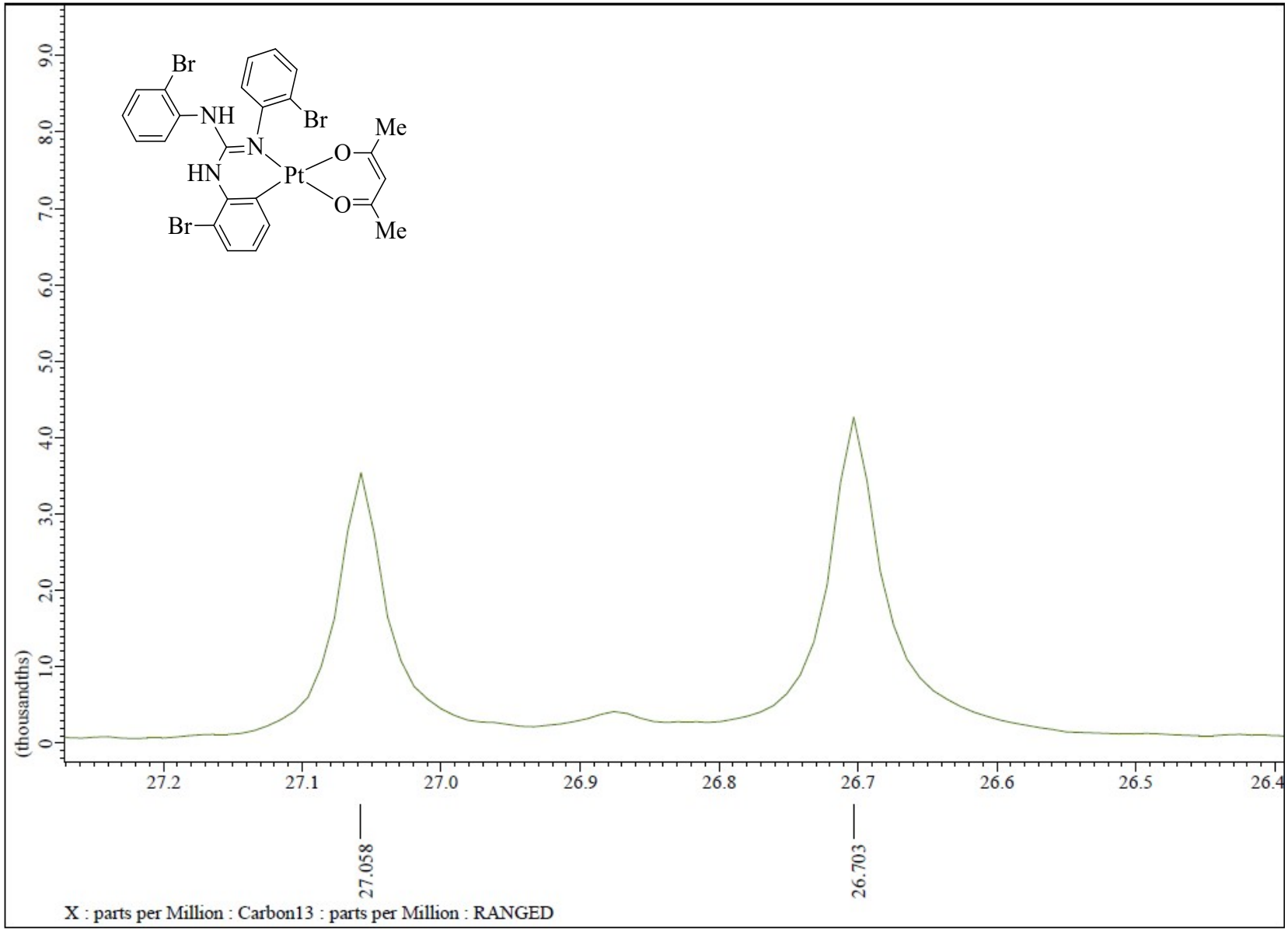

Fig. S158 $^{13}C\{^{1}H\}$ NMR ($CDCl_3$, 100.5 MHz) spectrum of **17** in the indicated region.

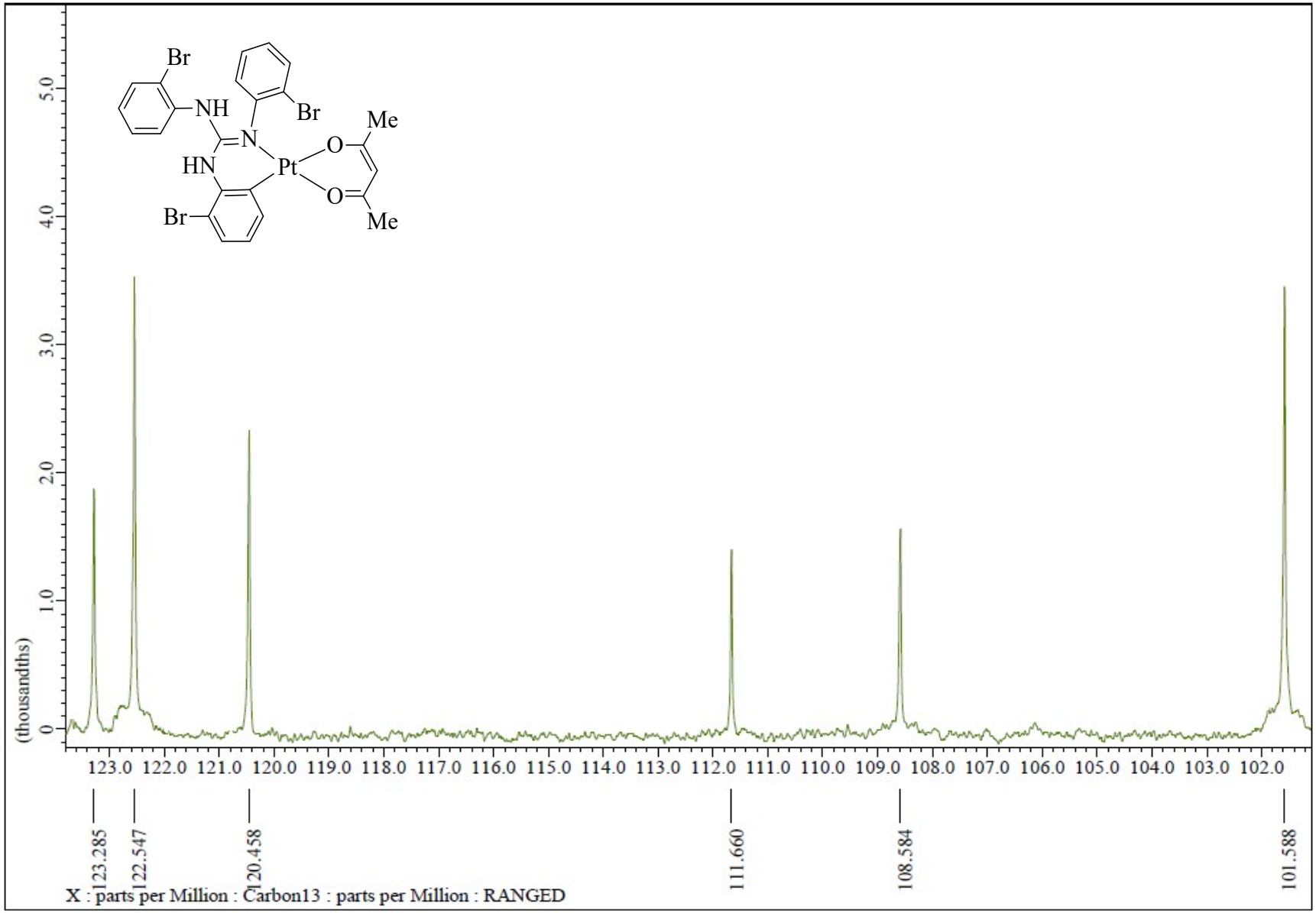

Fig. S159 $^{13}C\{^{1}H\}$ NMR ($CDCl_3$, 100.5 MHz) spectrum of **17** in the indicated region.

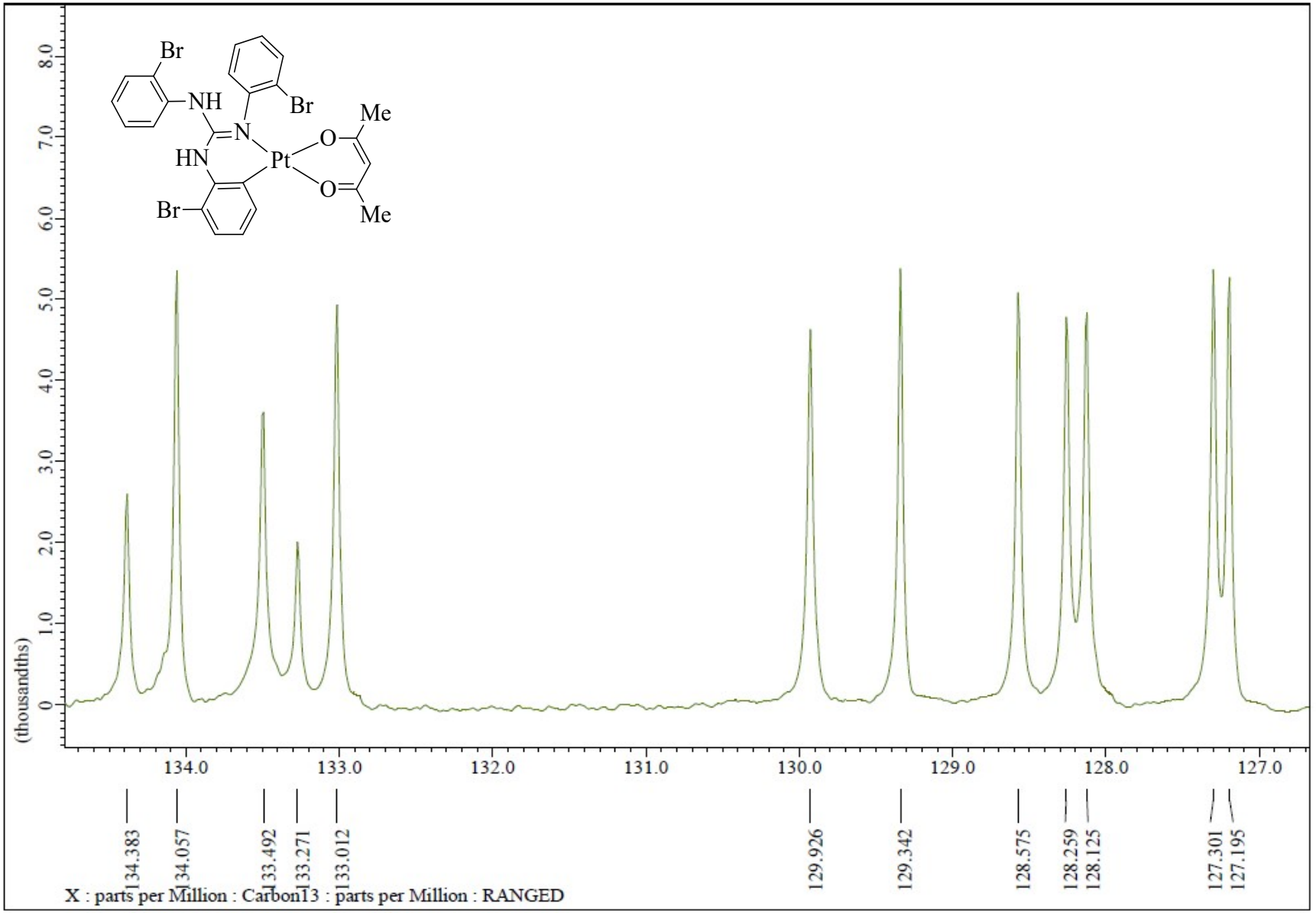

Fig. S160 $^{13}C\{^{1}H\}$ NMR ($CDCl_3$, 100.5 MHz) spectrum of **17** in the indicated region.

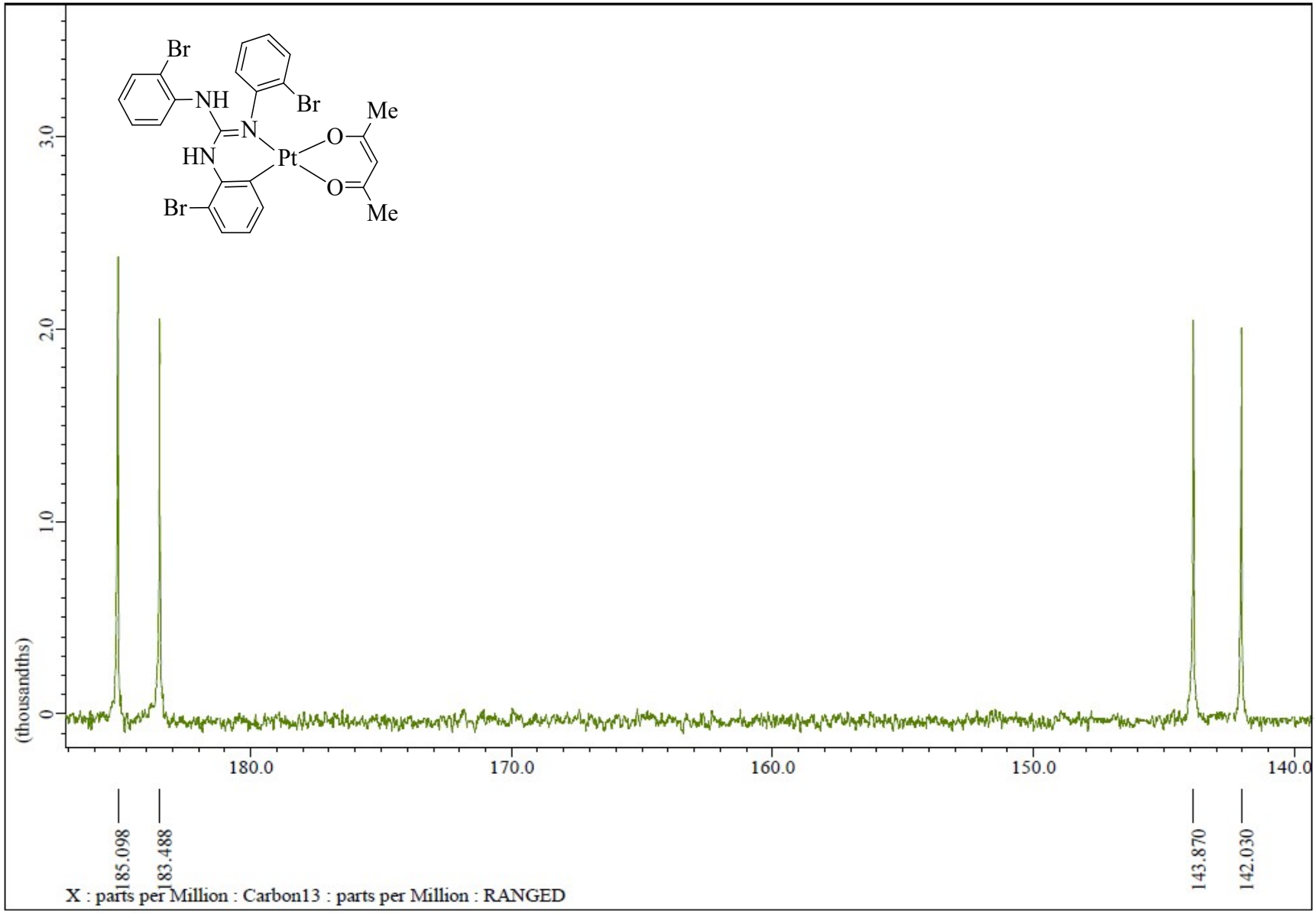

Fig. S161 $^{13}C\{^{1}H\}$ NMR ($CDCl_3$, 100.5 MHz) spectrum of **17** in the indicated region.

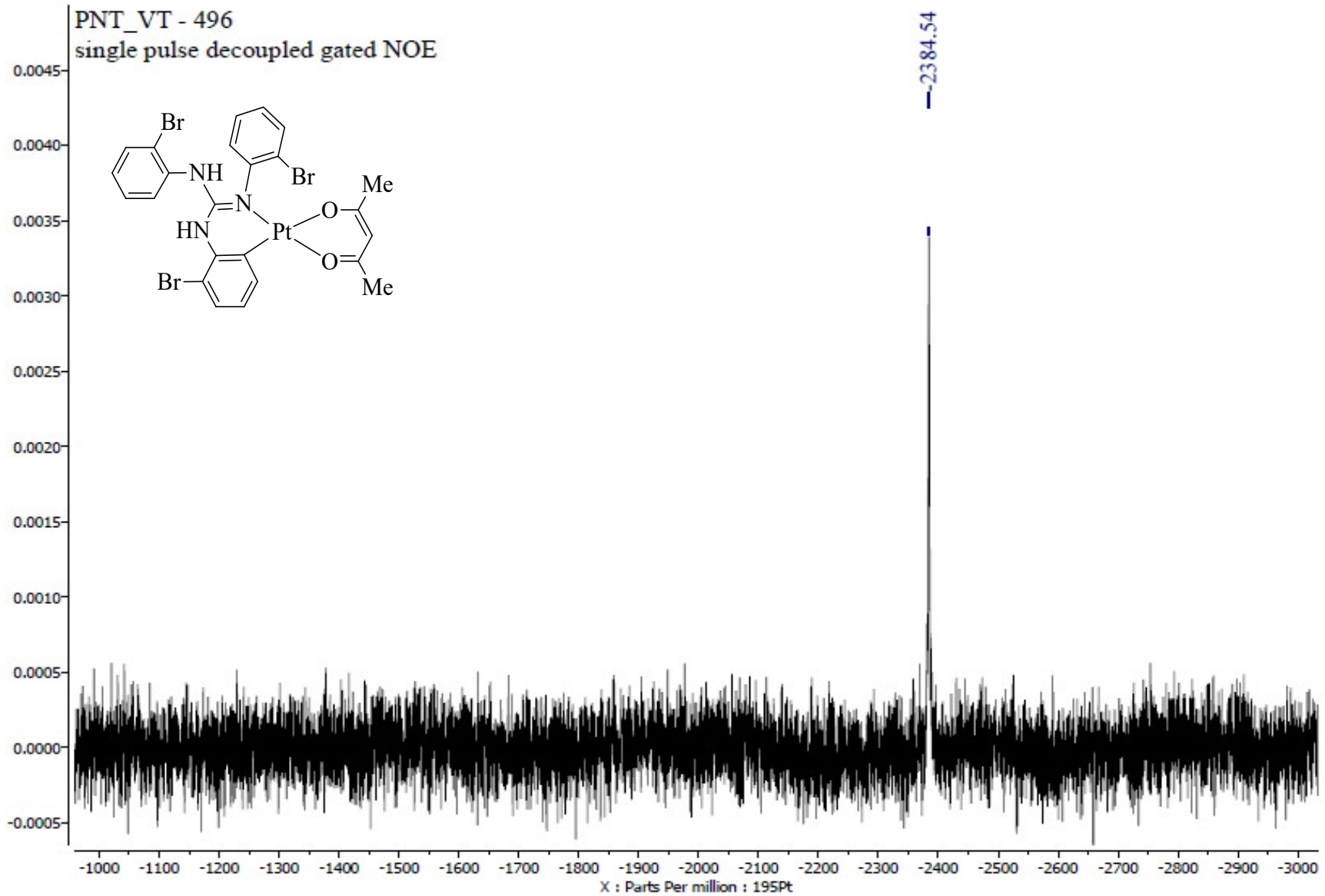

Fig. S162 $^{195}Pt\{^{1}H\}$ NMR ($CDCl_3$, 85.8 MHz) spectrum of **17**.

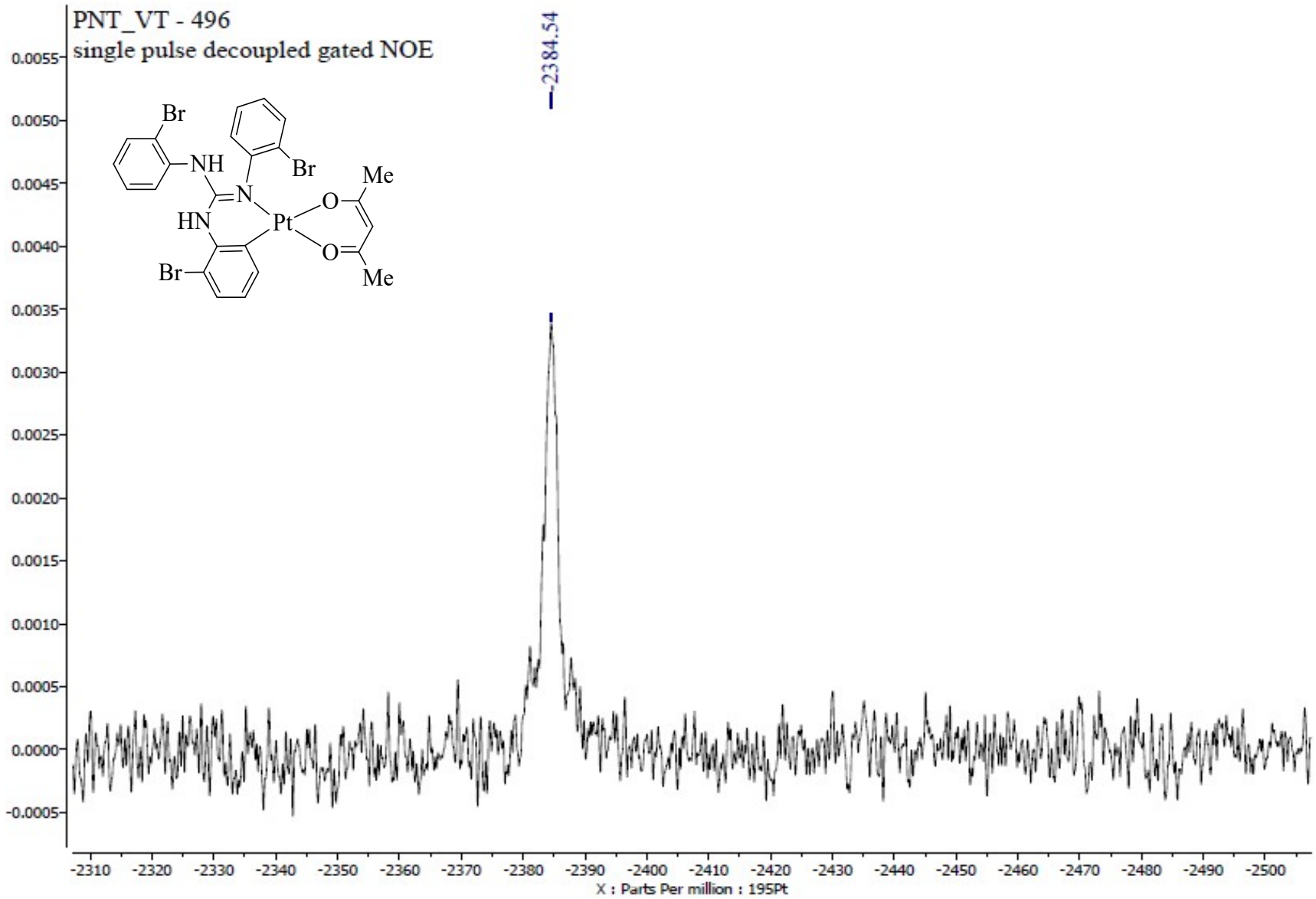

Fig. S163 $^{195}Pt\{^{1}H\}$ NMR ($CDCl_3$, 85.8 MHz) spectrum of **17** in the indicated region.

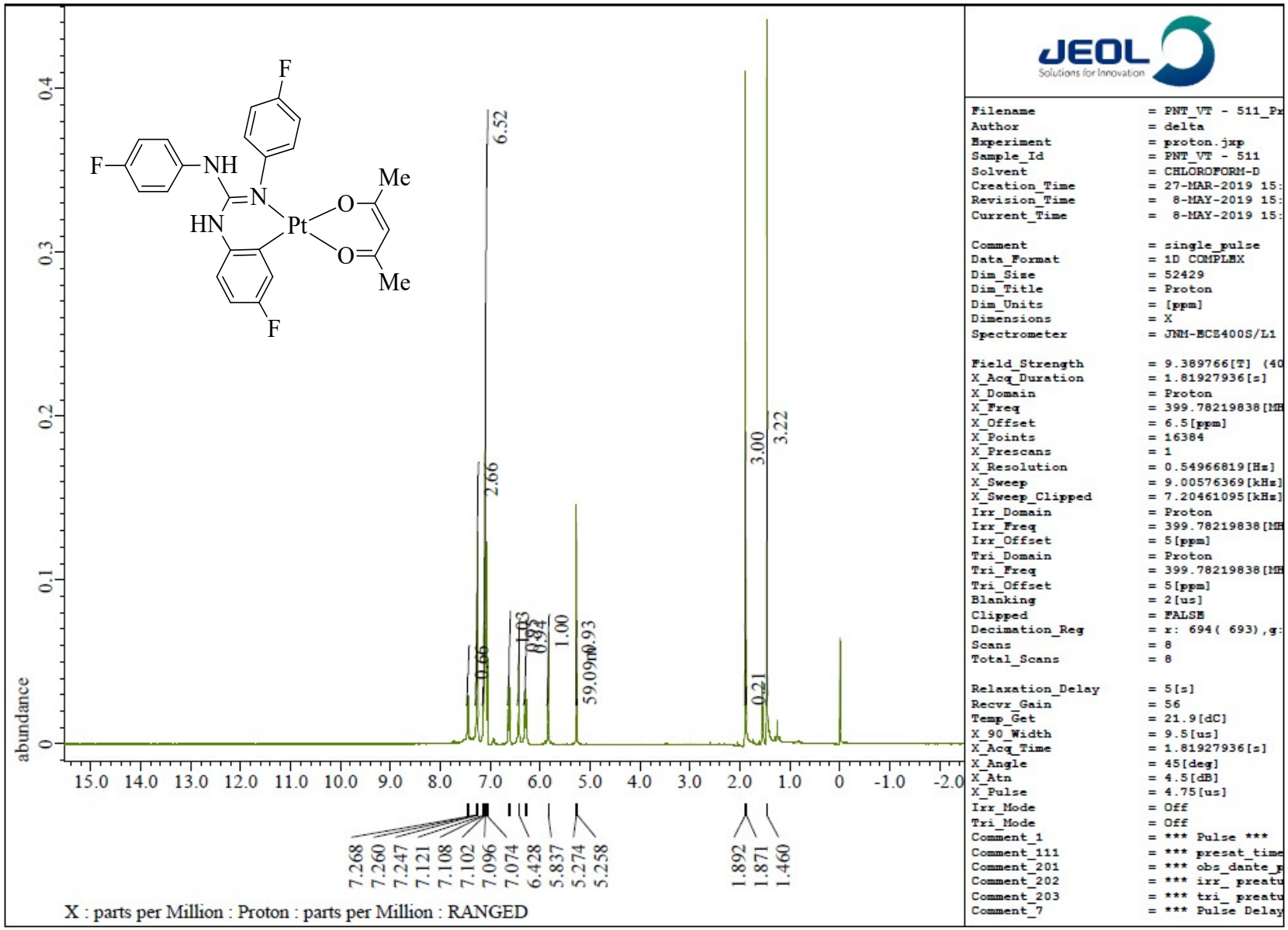

Fig. S164 ^{1}H NMR ($CDCl_3$, 400 MHz) spectrum of **18**.

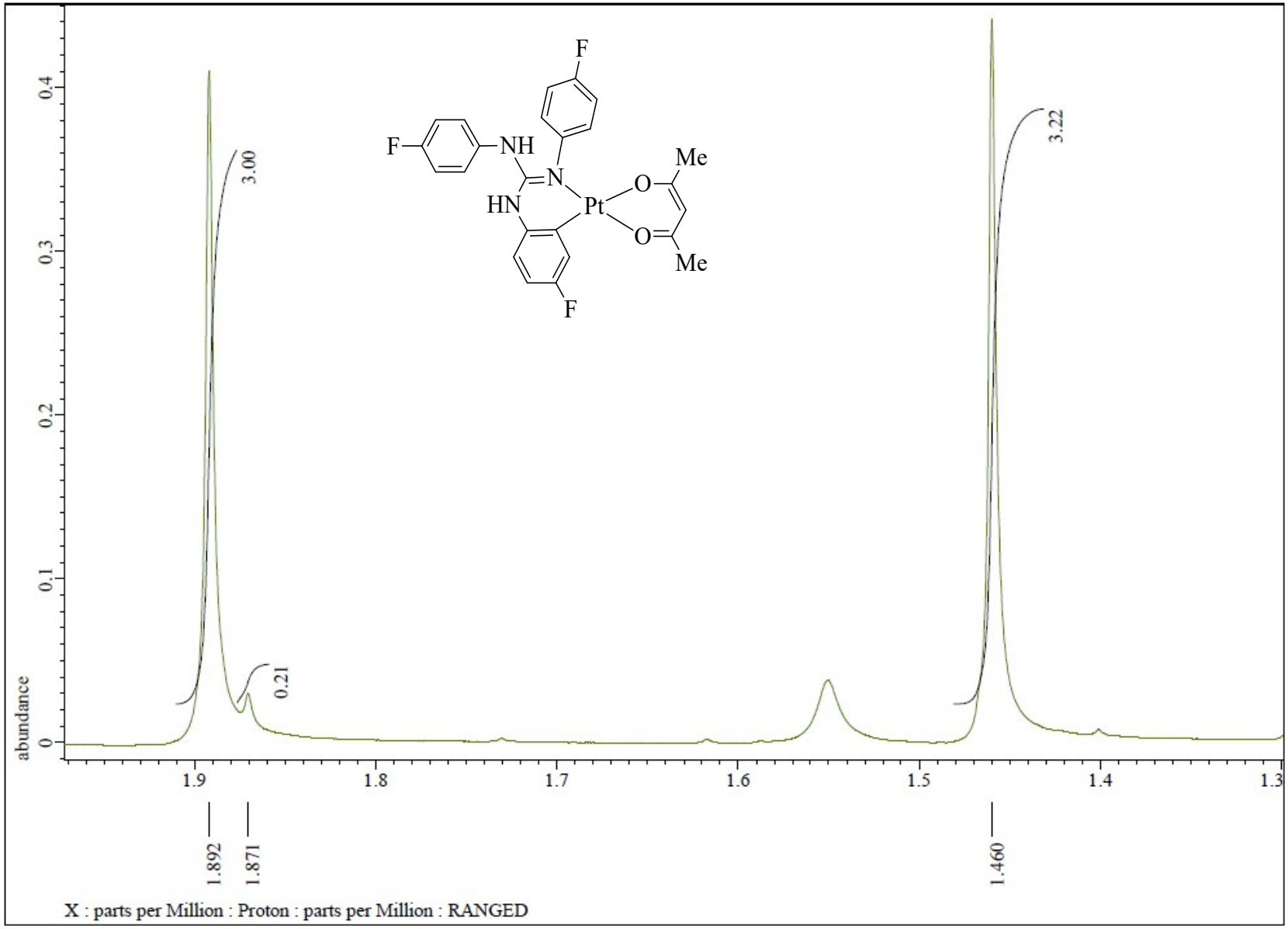

Fig. S165 ^{1}H NMR ($CDCl_3$, 400 MHz) spectrum of **18** in the indicated region.

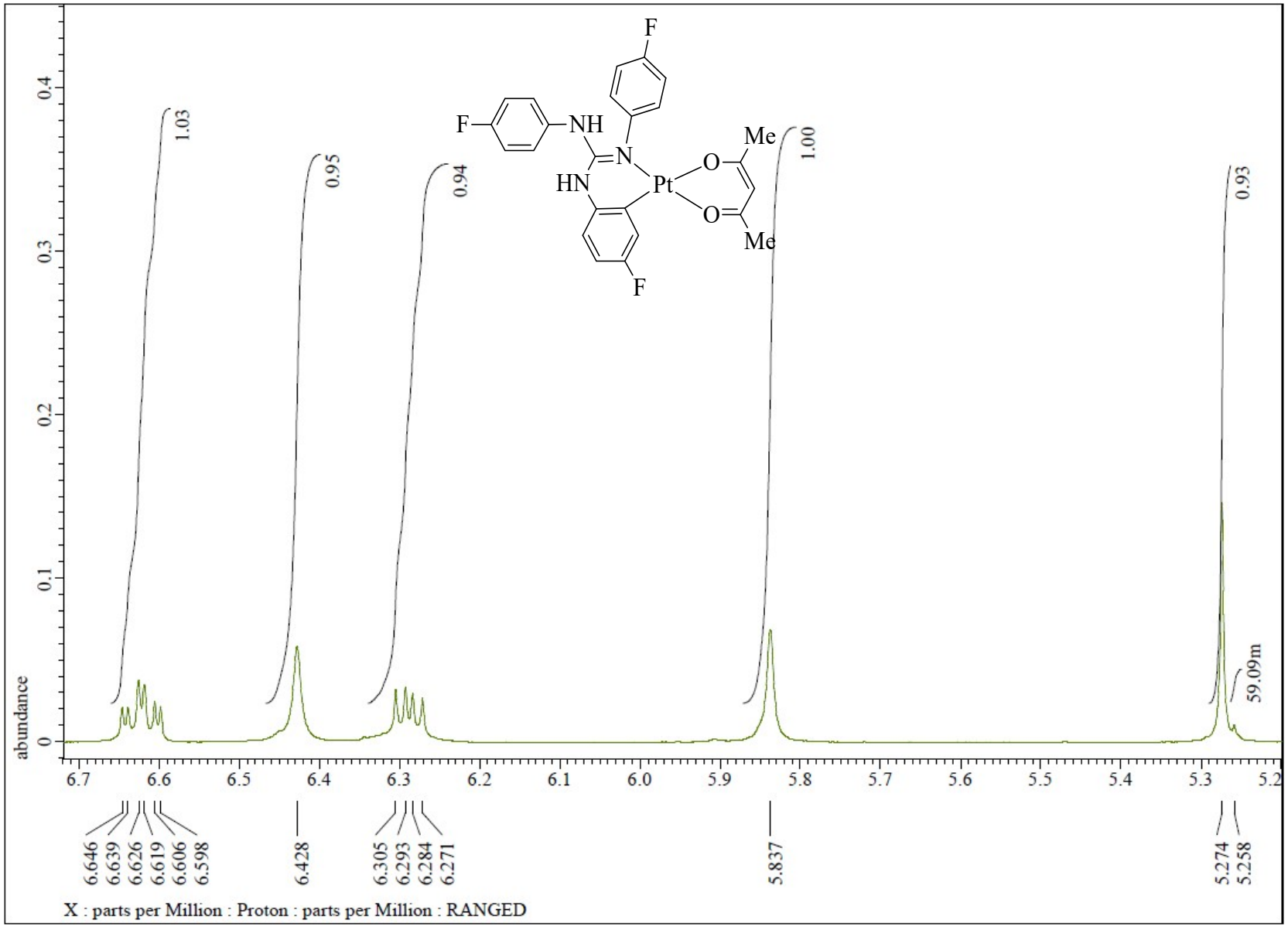

Fig. S166 ^{1}H NMR ($CDCl_3$, 400 MHz) spectrum of **18** in the indicated region.

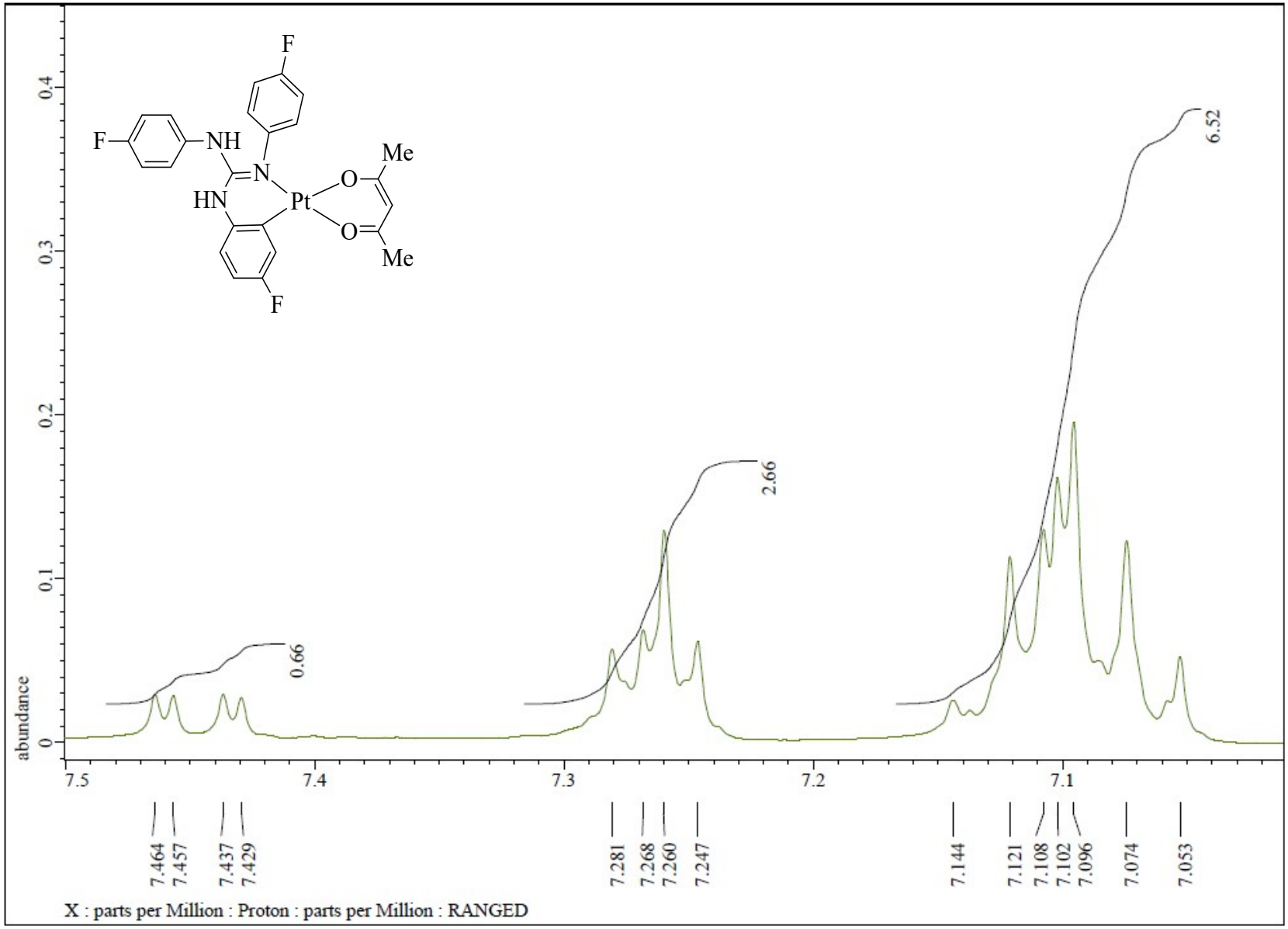

Fig. S167 ^{1}H NMR ($CDCl_3$, 400 MHz) spectrum of **18** in the indicated region.

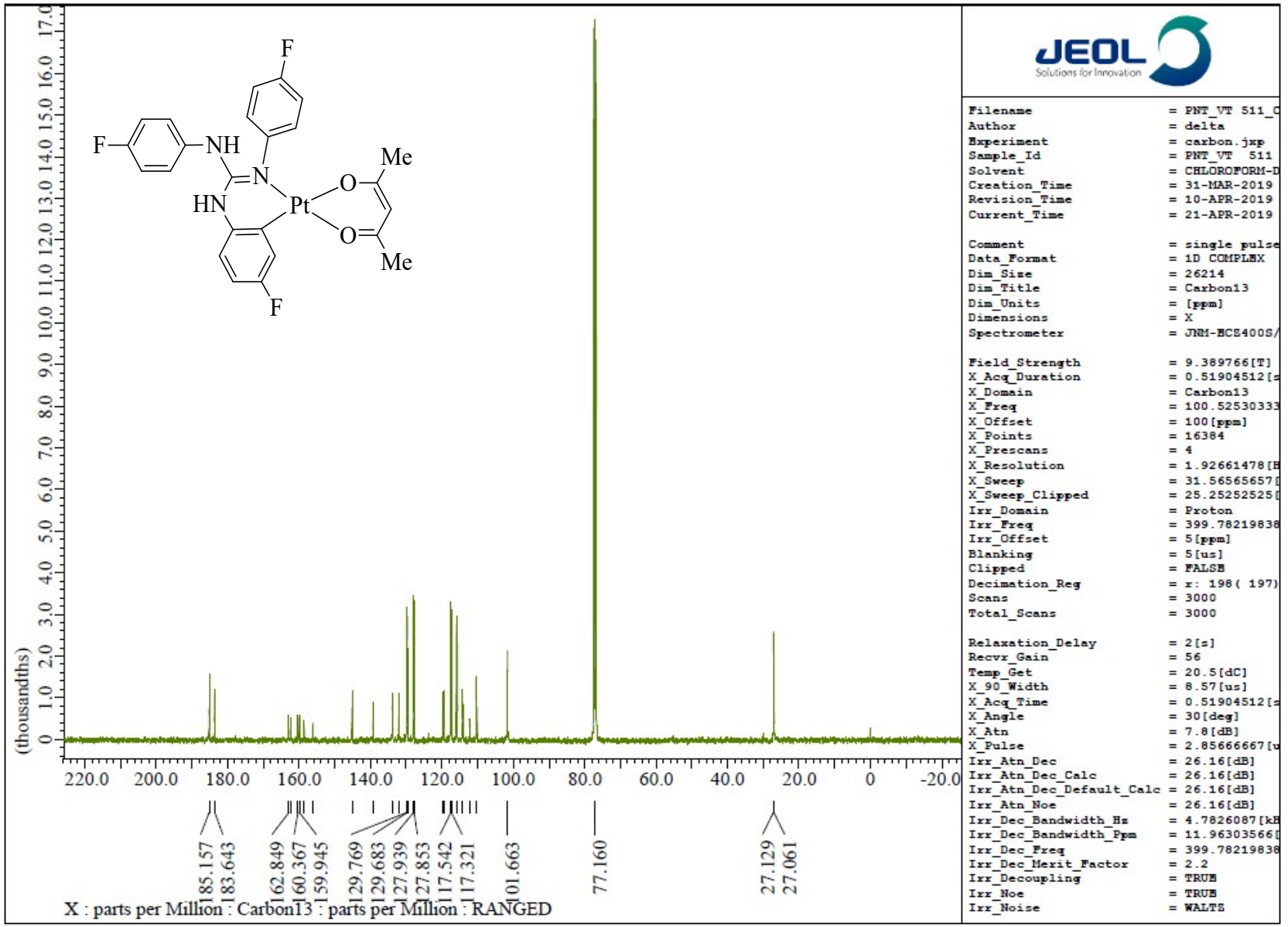

Fig. S168 $^{13}C\{^{1}H\}$ NMR ($CDCl_3$, 100.5 MHz) spectrum of **18**.

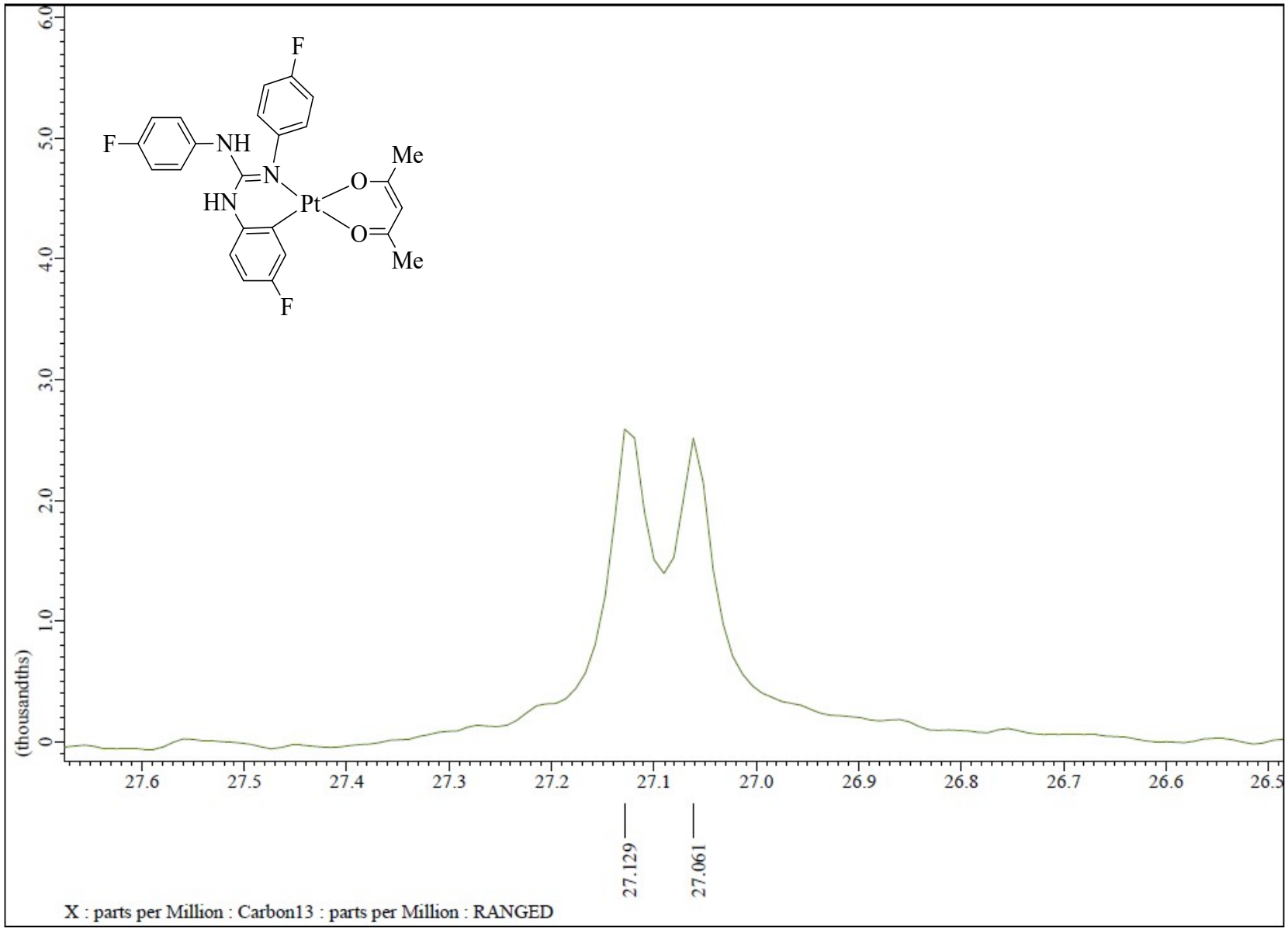

Fig. S169 $^{13}C\{^{1}H\}$ NMR ($CDCl_3$, 100.5 MHz) spectrum of **18** in the indicated region.

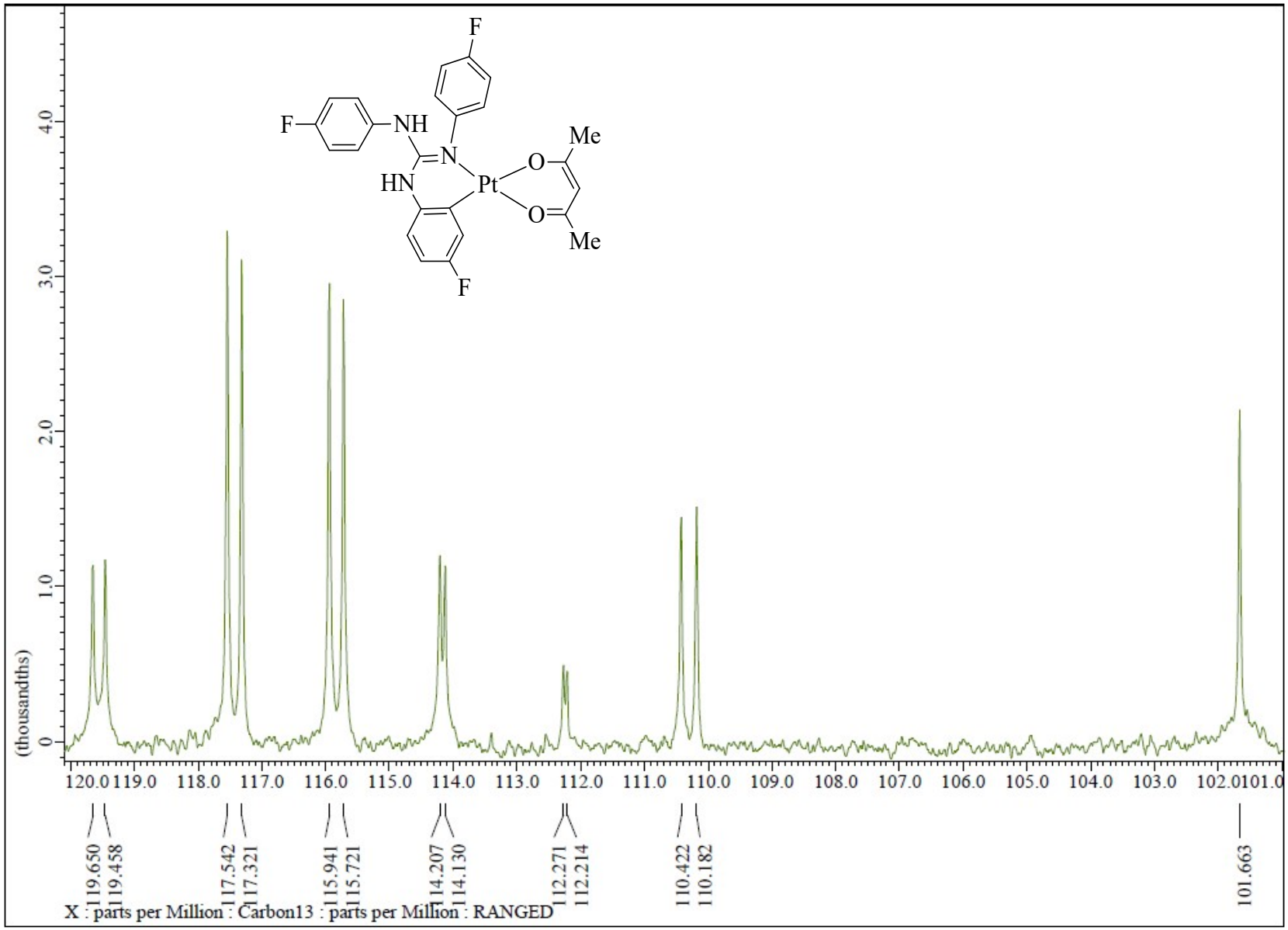

Fig. S170 $^{13}C\{^{1}H\}$ NMR ($CDCl_3$, 100.5 MHz) spectrum of **18** in the indicated region.

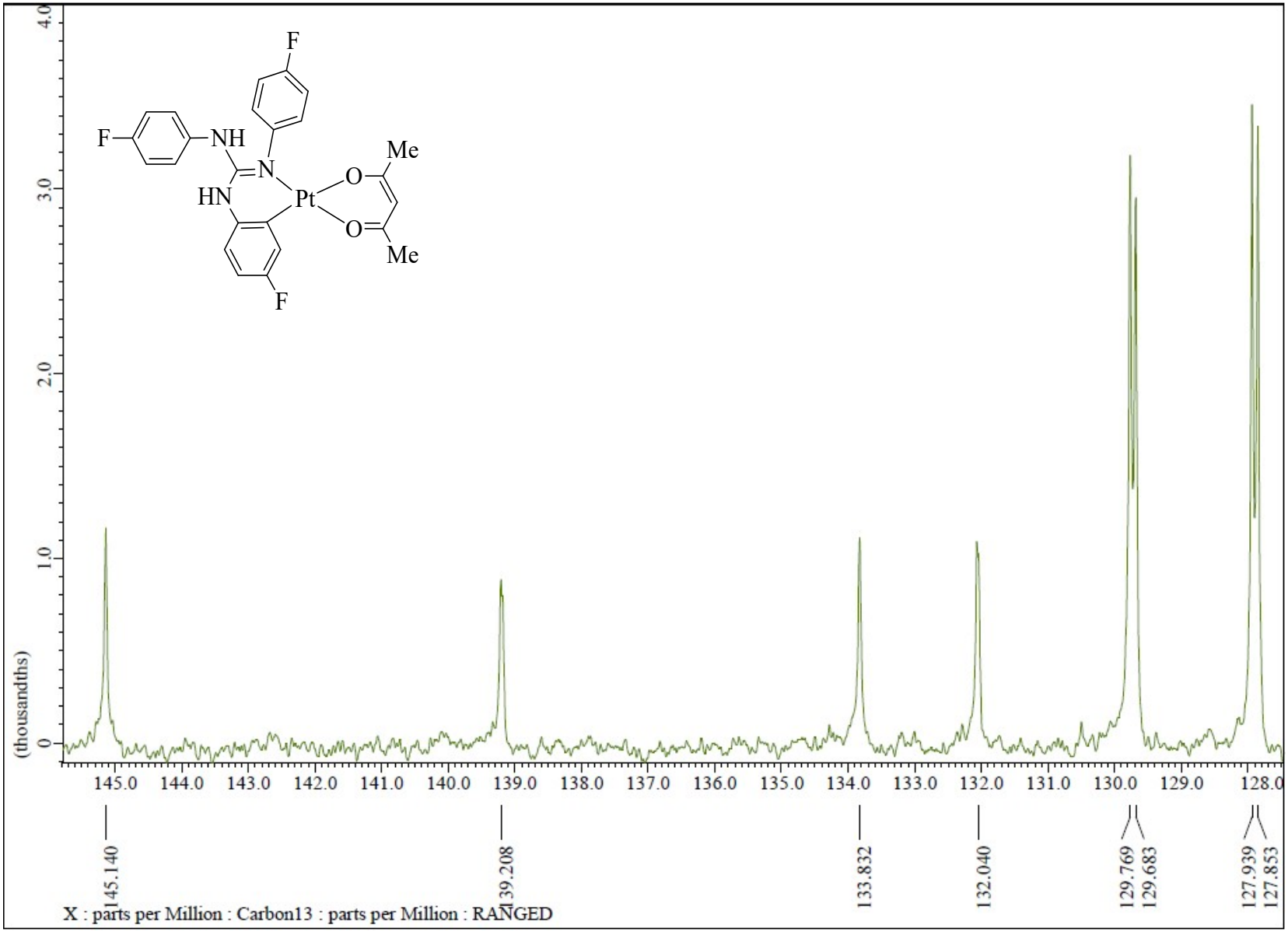

Fig. S171 $^{13}C\{^{1}H\}$ NMR ($CDCl_3$, 100.5 MHz) spectrum of **18** in the indicated region.

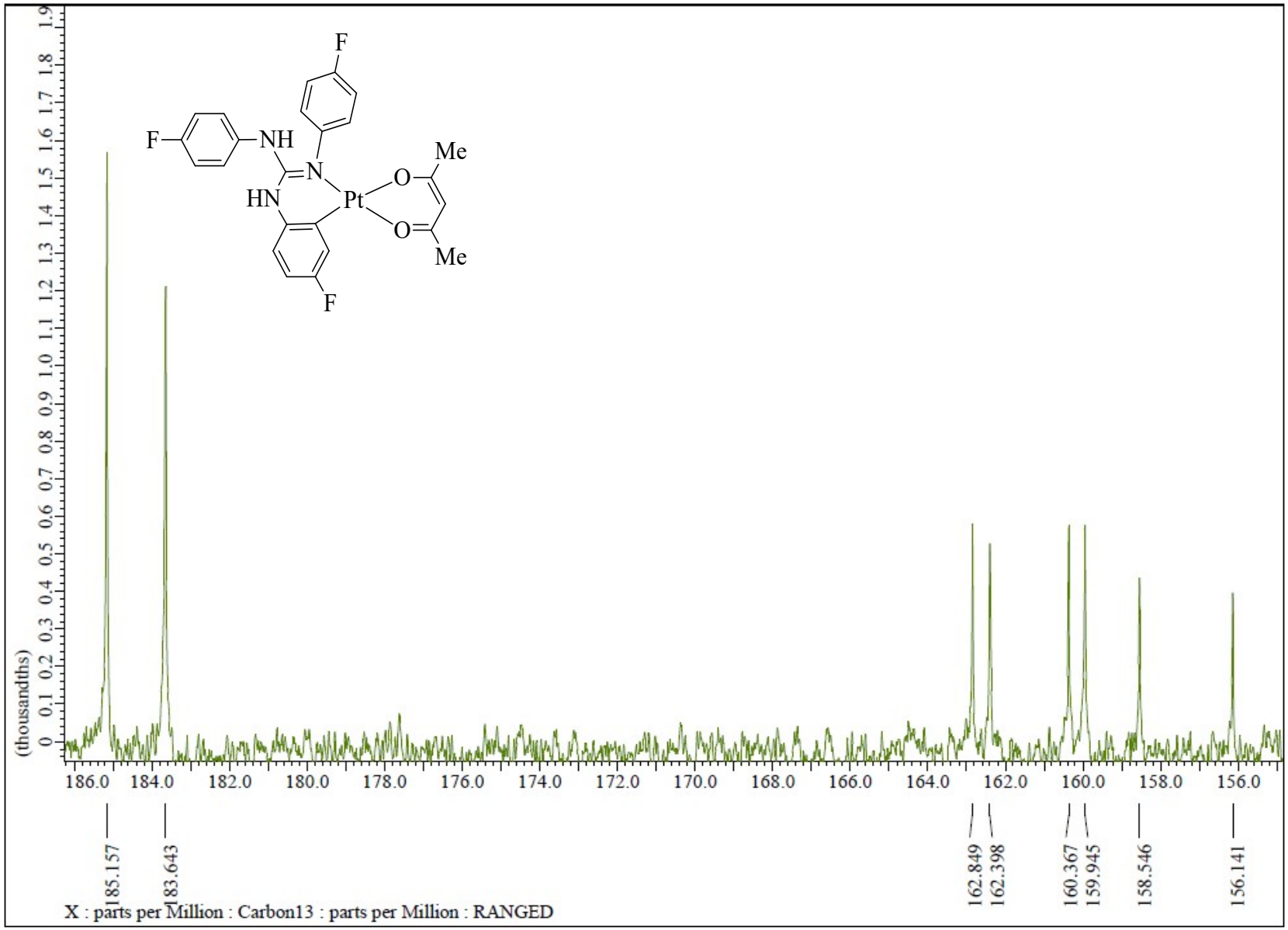

Fig. S172 $^{13}C\{^{1}H\}$ NMR ($CDCl_3$, 100.5 MHz) spectrum of **18** in the indicated region.

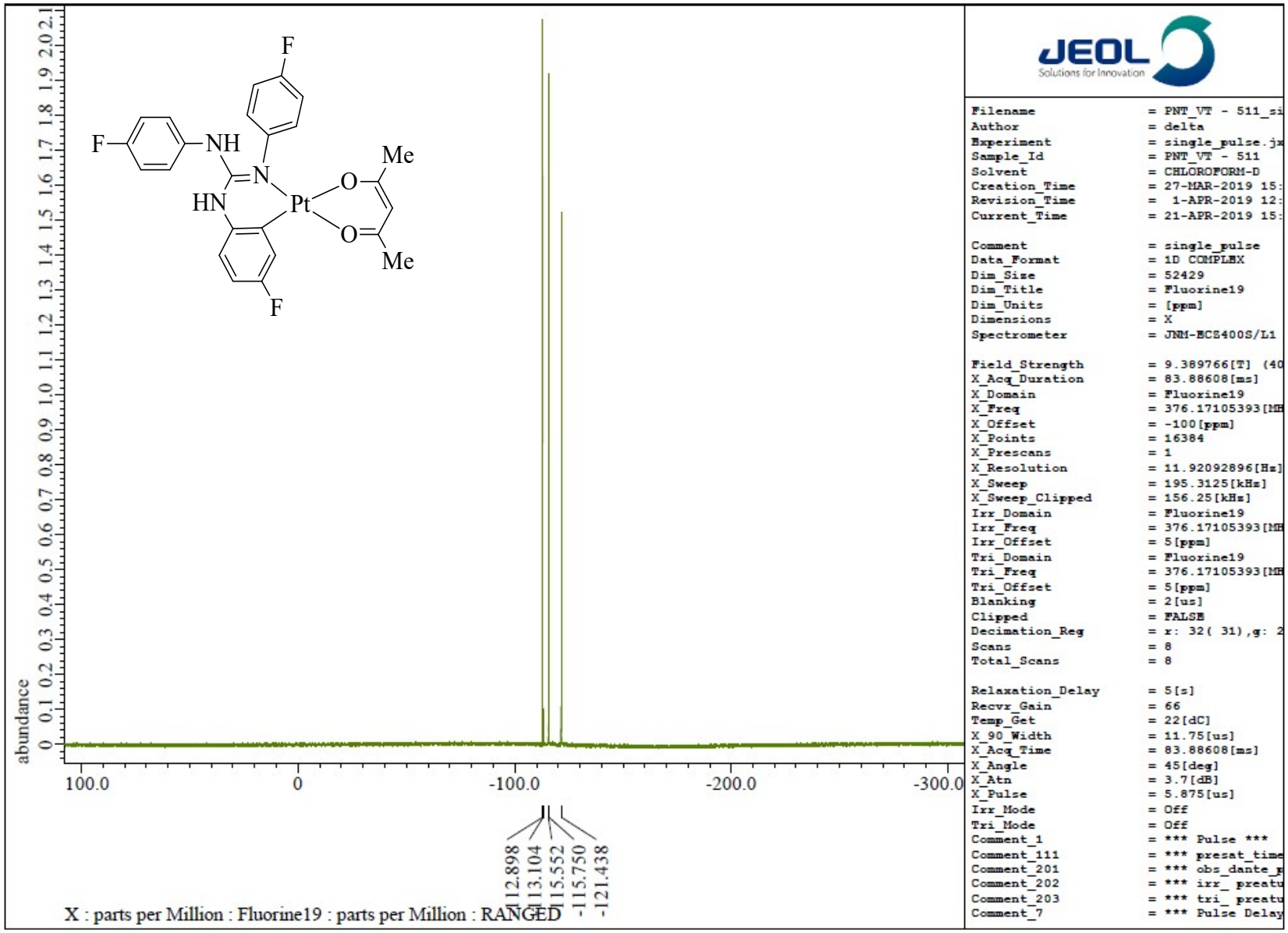

Fig. S173 $^{19}F\{^{1}H\}$ NMR ($CDCl_3$, 376.31 MHz) spectrum of **18**.

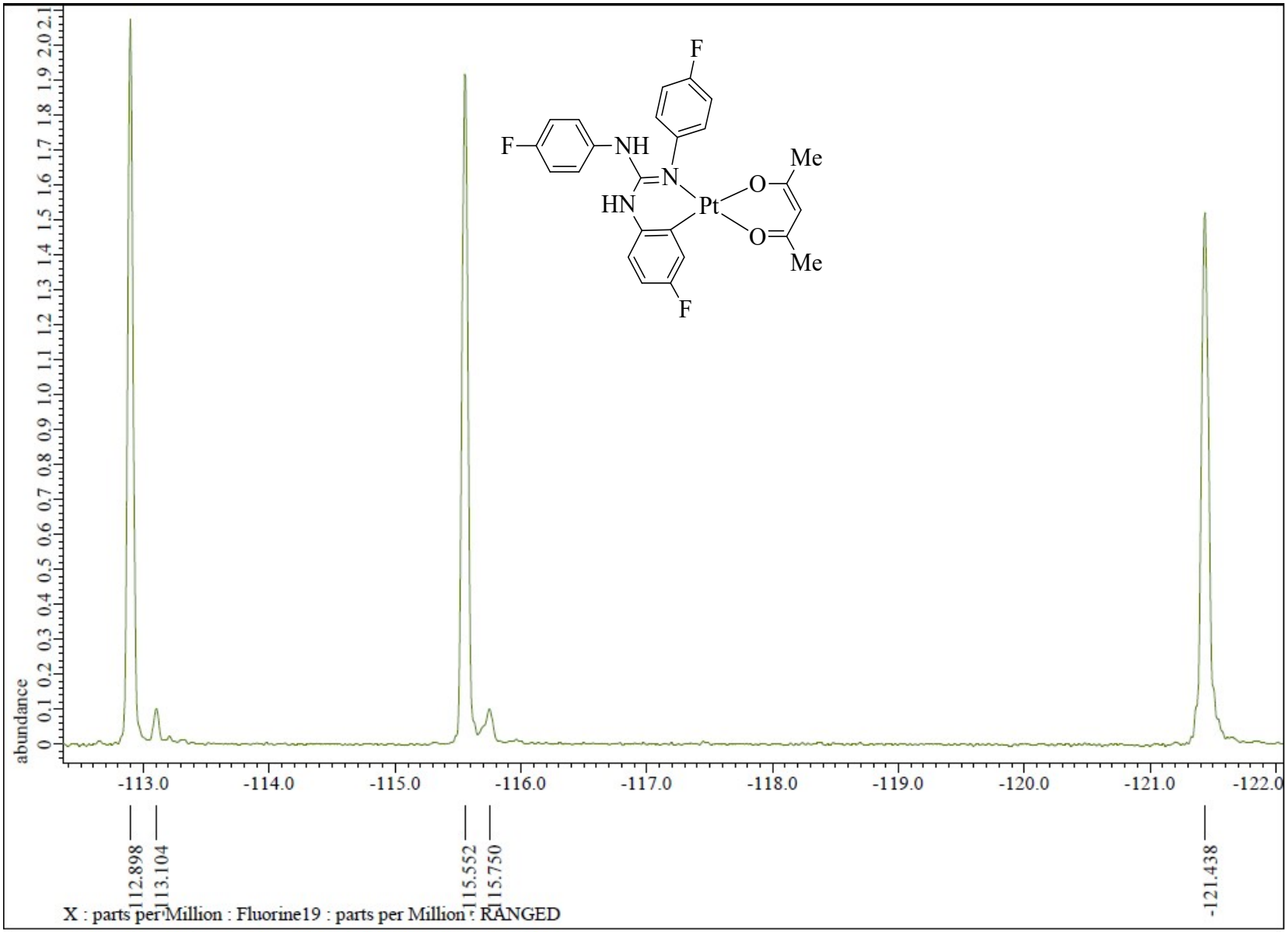

Fig. S174 $^{19}F\{^{1}H\}$ NMR ($CDCl_3$, 376.31 MHz) spectrum of **18** in the indicated region.

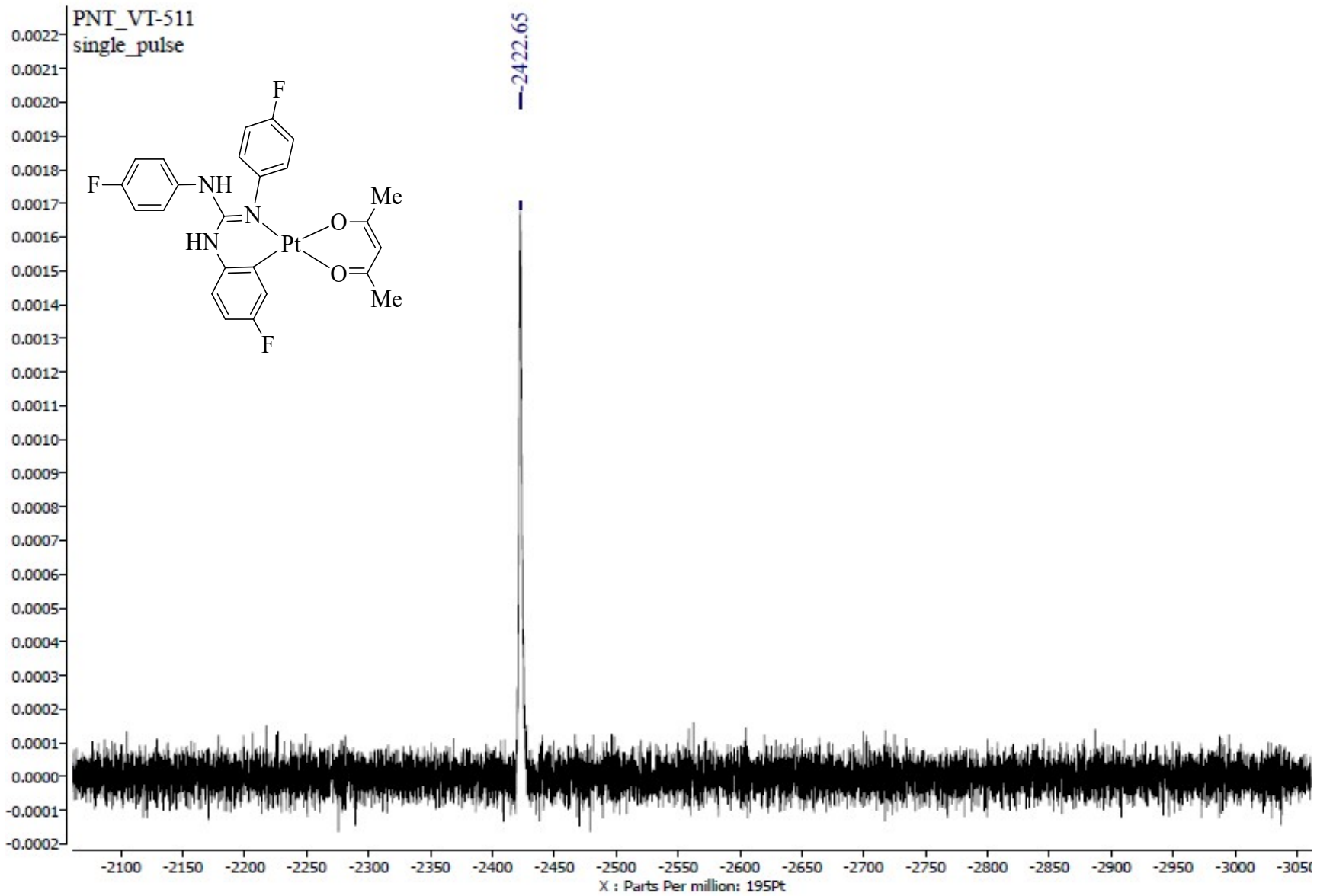

Fig. S175 $^{195}Pt\{^{1}H\}$ NMR ($CDCl_3$, 85.8 MHz) spectrum of **18**.

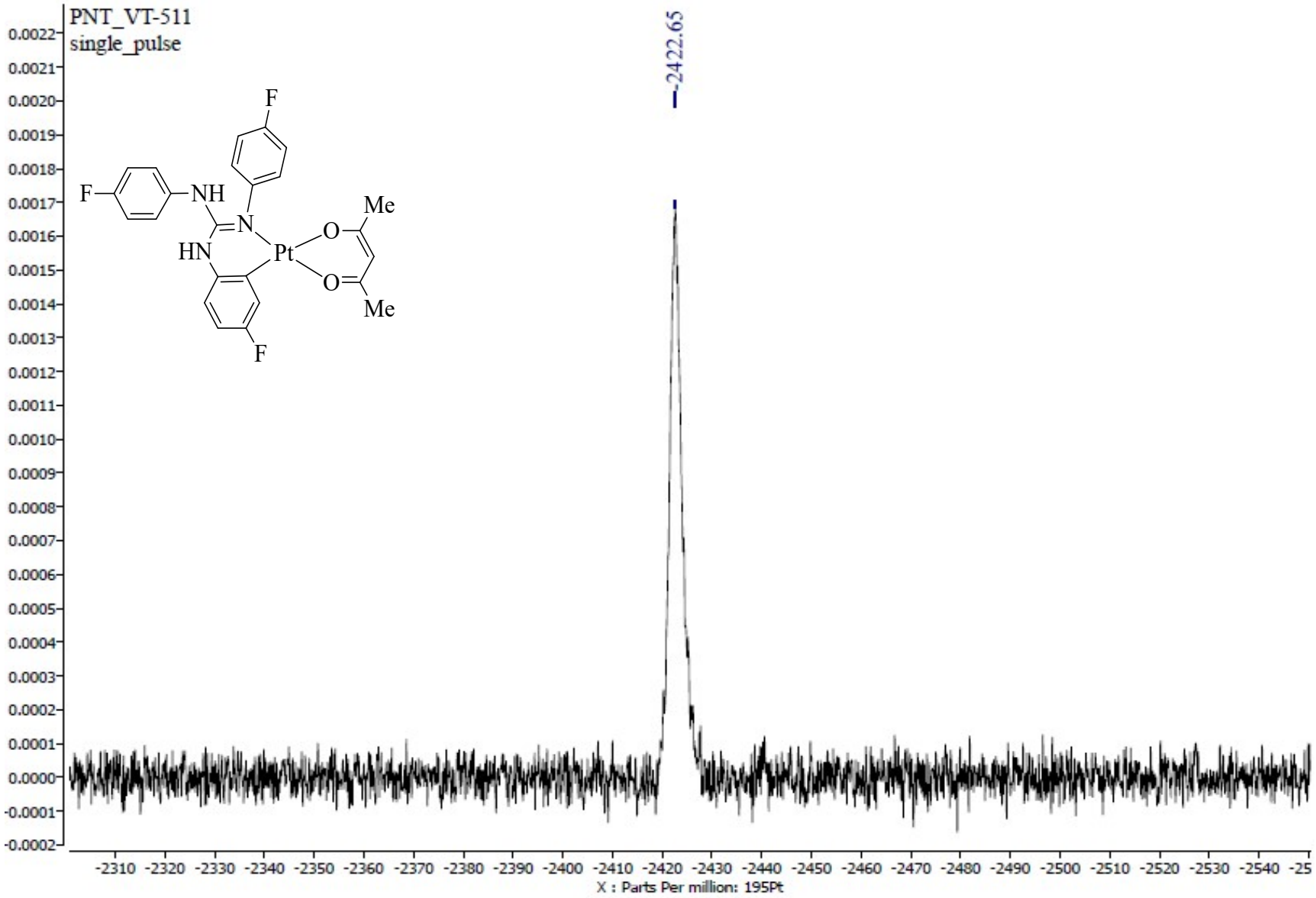

Fig. S176 $^{195}Pt\{^{1}H\}$ NMR ($CDCl_3$, 85.8 MHz) spectrum of **18** in the indicated region.

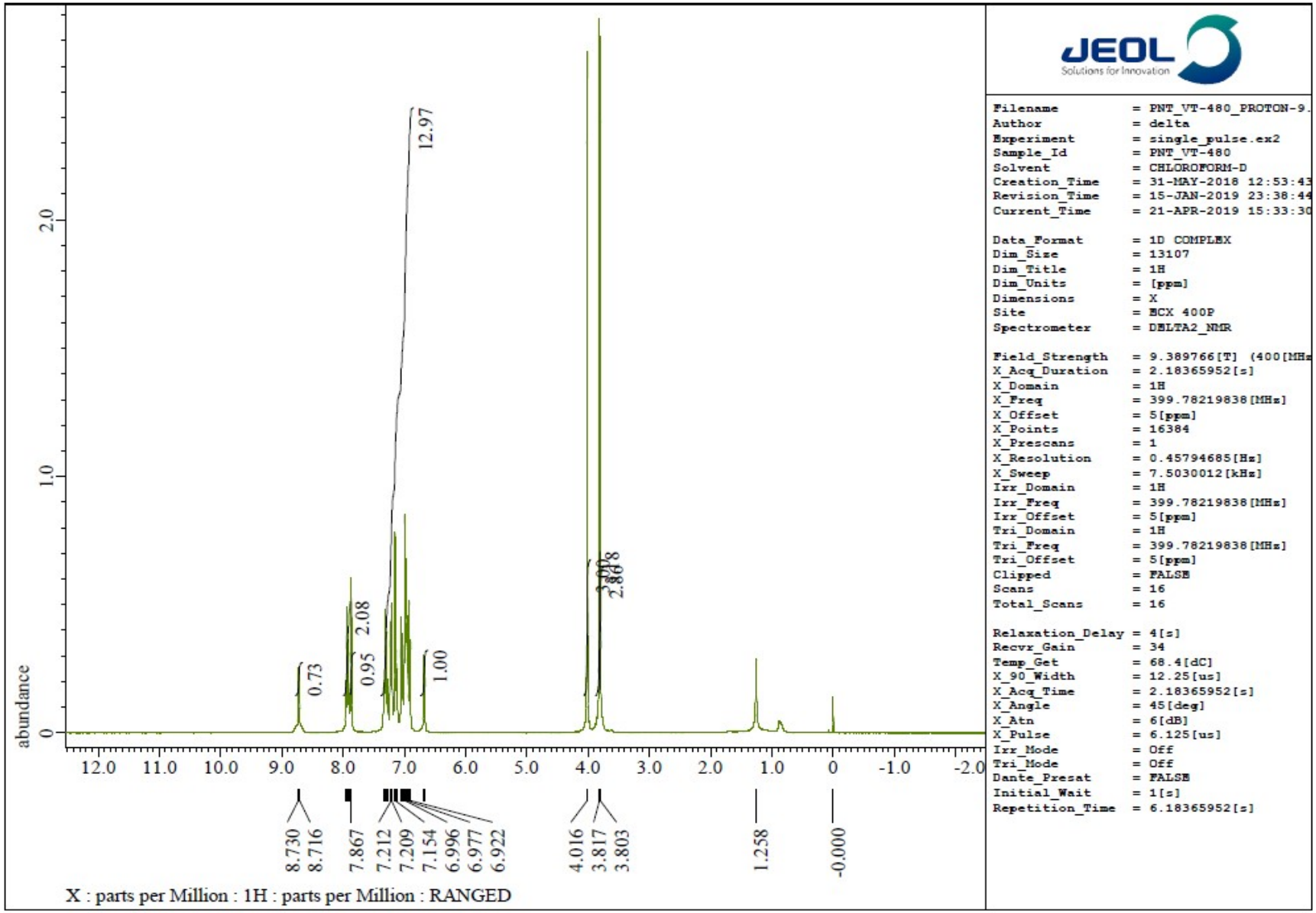

Fig. S177 ^{1}H NMR ($CDCl_3$, 400 MHz) spectrum of **19**.

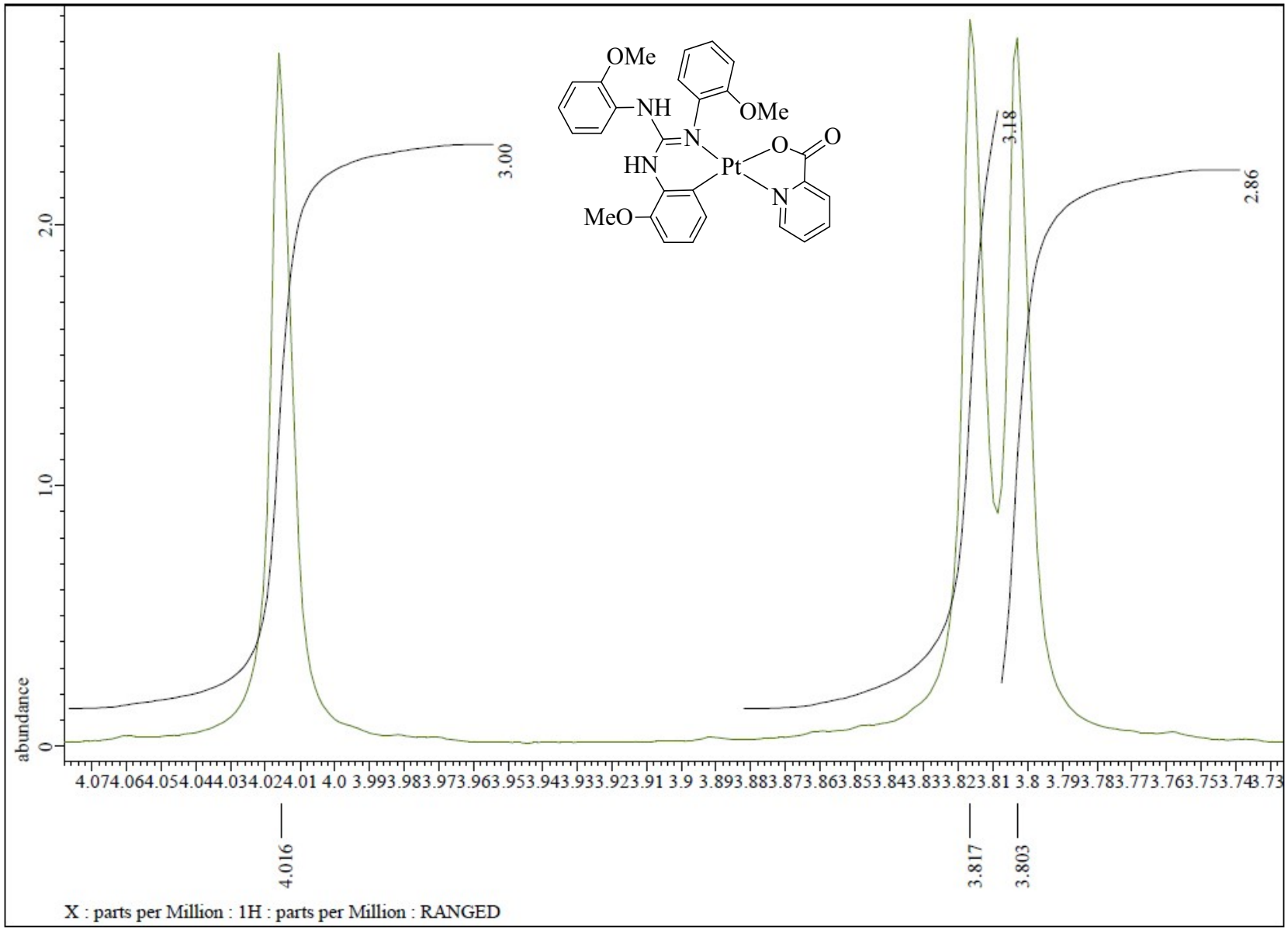

Fig. S178 ^{1}H NMR ($CDCl_3$, 400 MHz) spectrum of **19** in the indicated region.

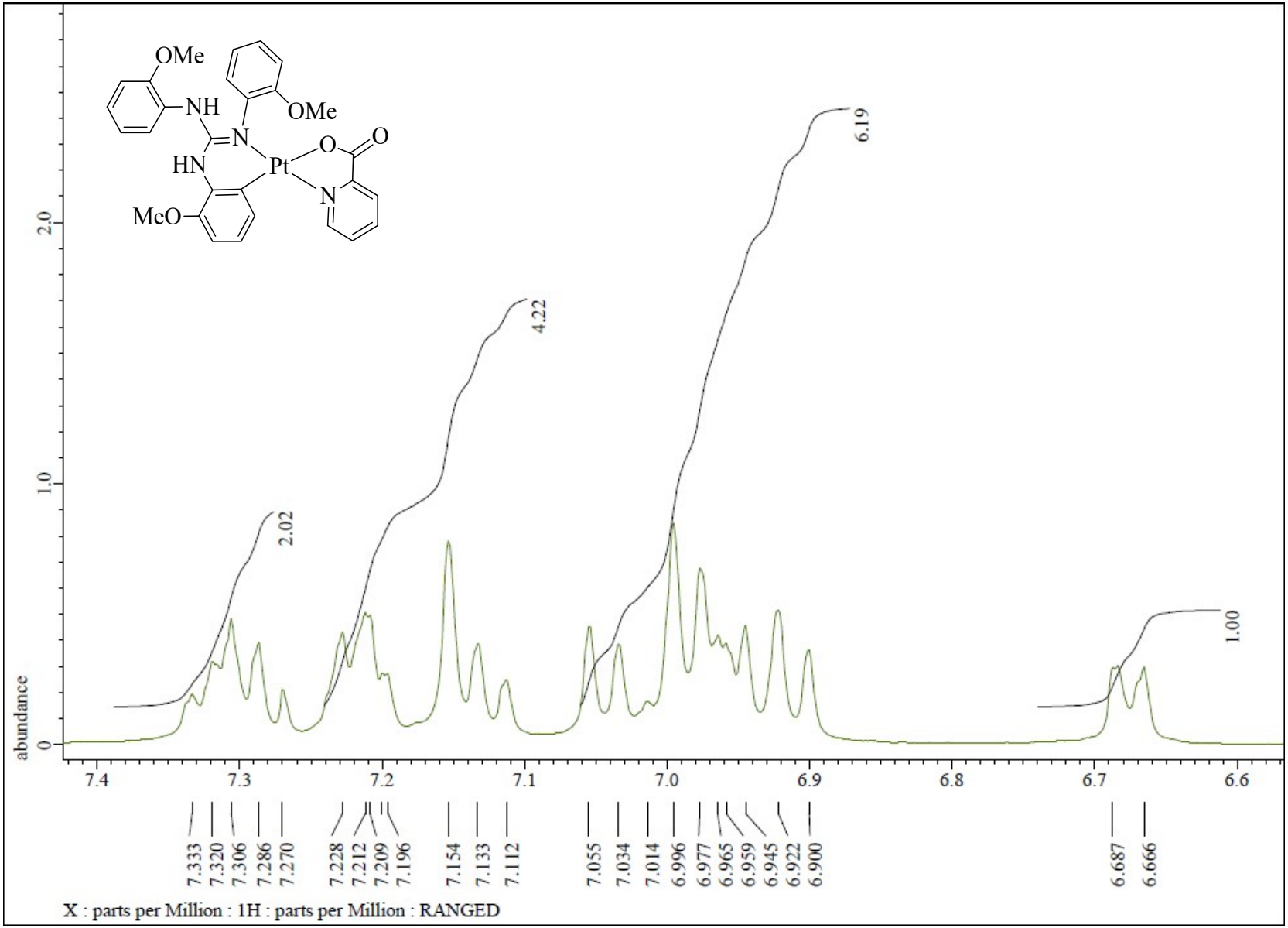

Fig. S179 ^{1}H NMR ($CDCl_3$, 400 MHz) spectrum of **19** in the indicated region.

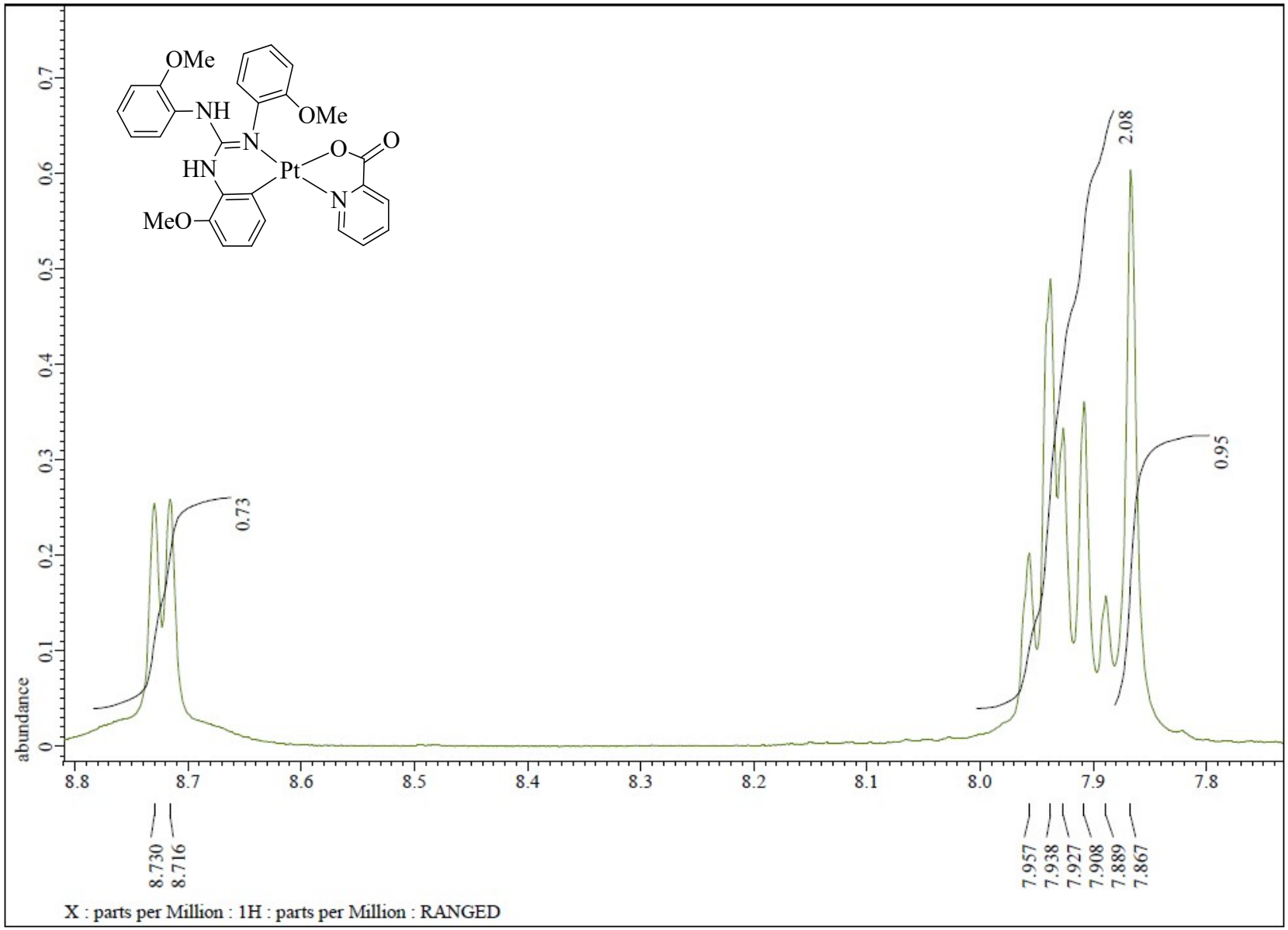

Fig. S180 ^{1}H NMR ($CDCl_3$, 400 MHz) spectrum of **19** in the indicated region.

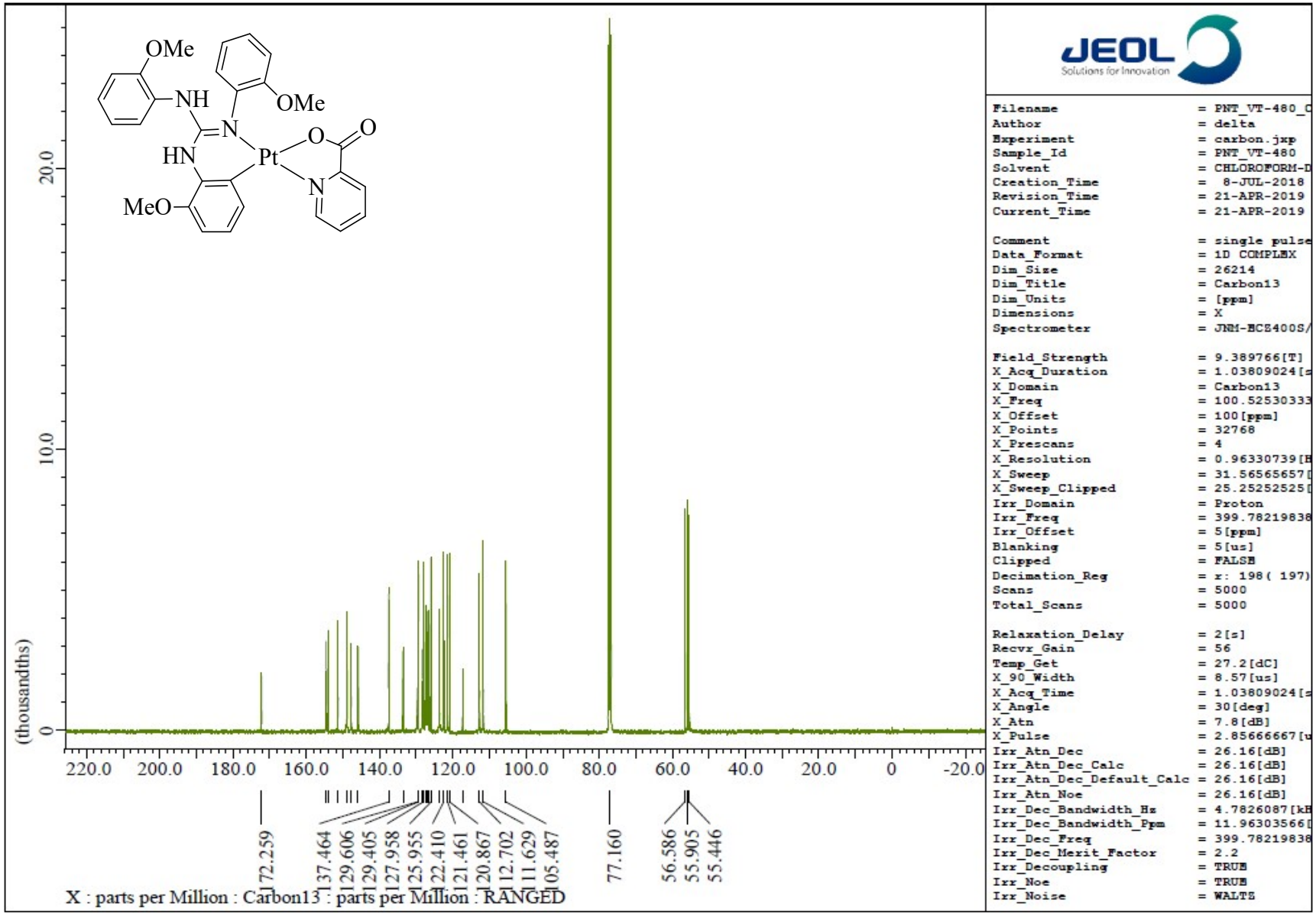

Fig. S181 $^{13}C\{^{1}H\}$NMR ($CDCl_3$, 100.5 MHz) spectrum of **19**.

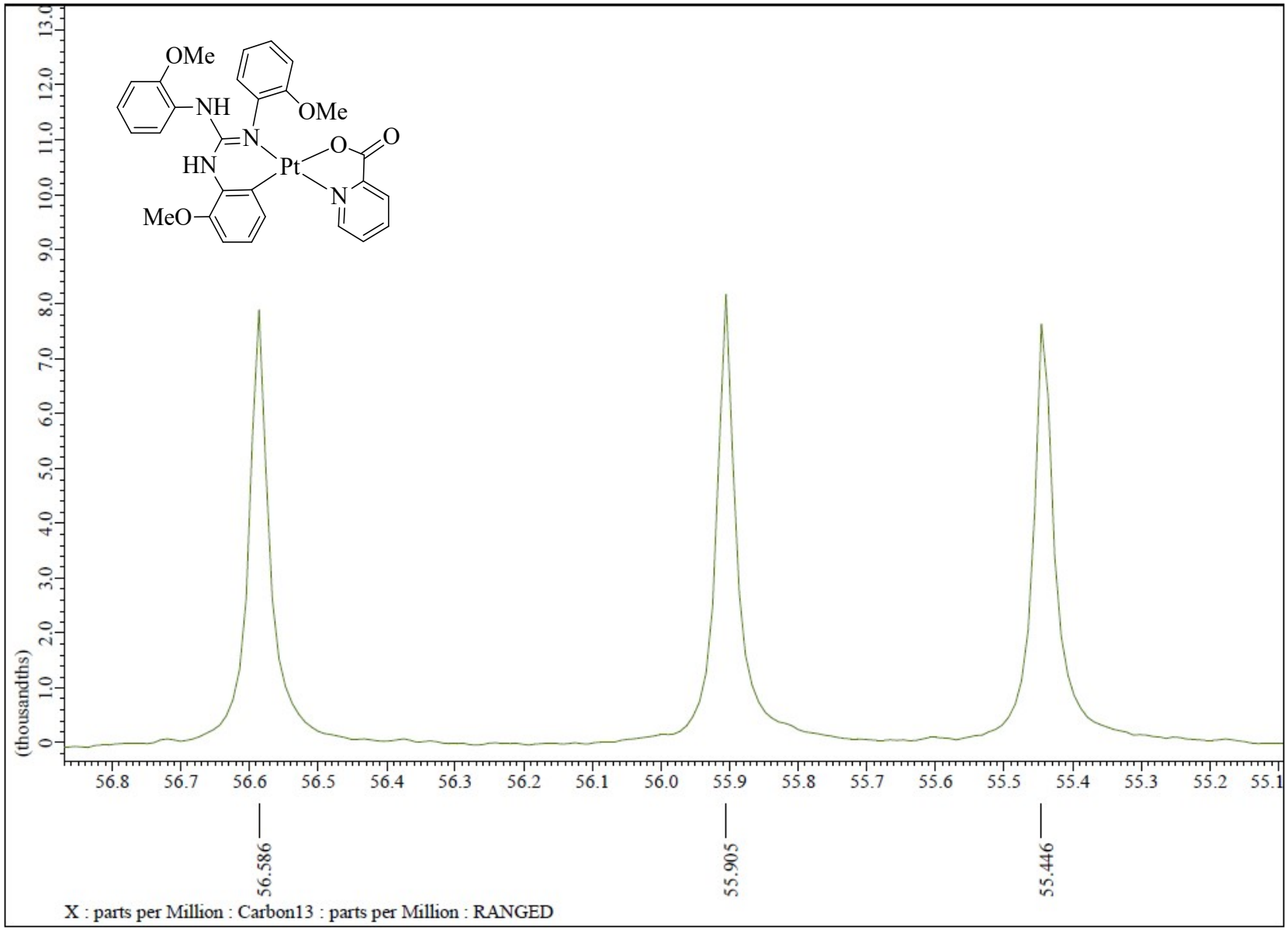

Fig. S182 $^{13}C\{^{1}H\}$ NMR ($CDCl_3$, 100.5 MHz) spectrum of **19** in the indicated region.

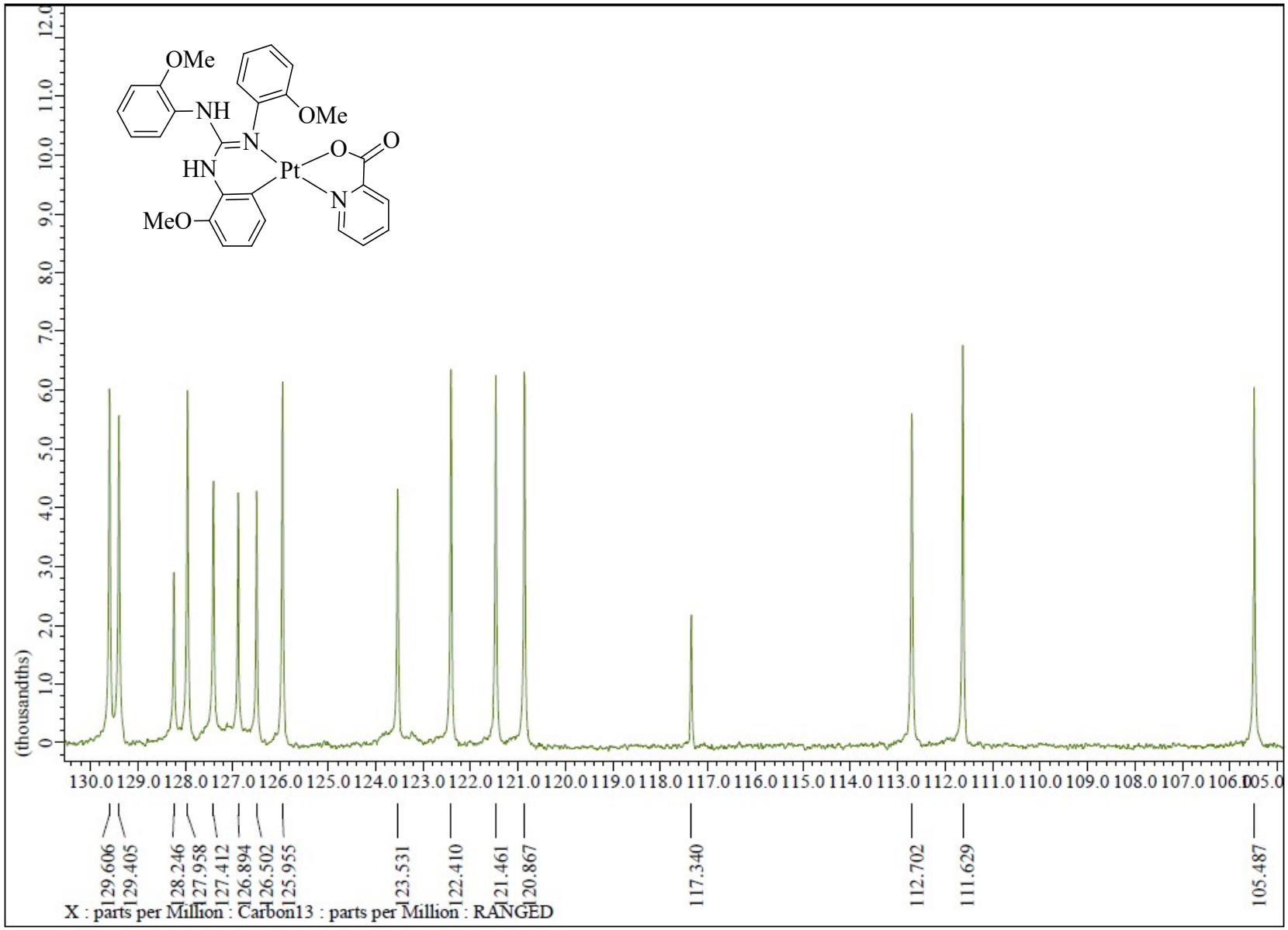

Fig. S183 $^{13}C\{^{1}H\}$ NMR ($CDCl_3$, 100.5 MHz) spectrum of **19** in the indicated region.

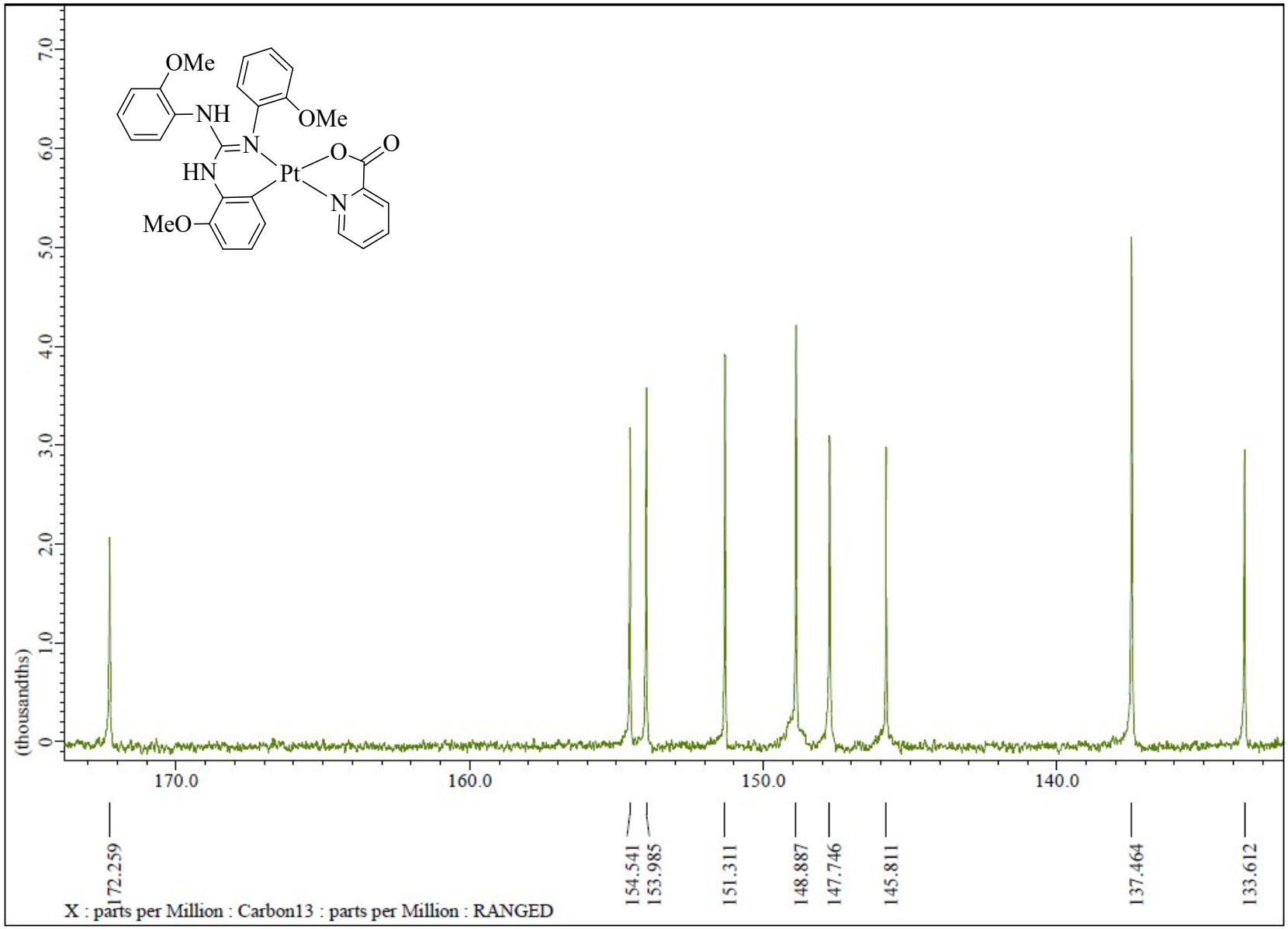

Fig. S184 $^{13}C\{^{1}H\}$ NMR ($CDCl_3$, 100.5 MHz) spectrum of **19** in the indicated region.

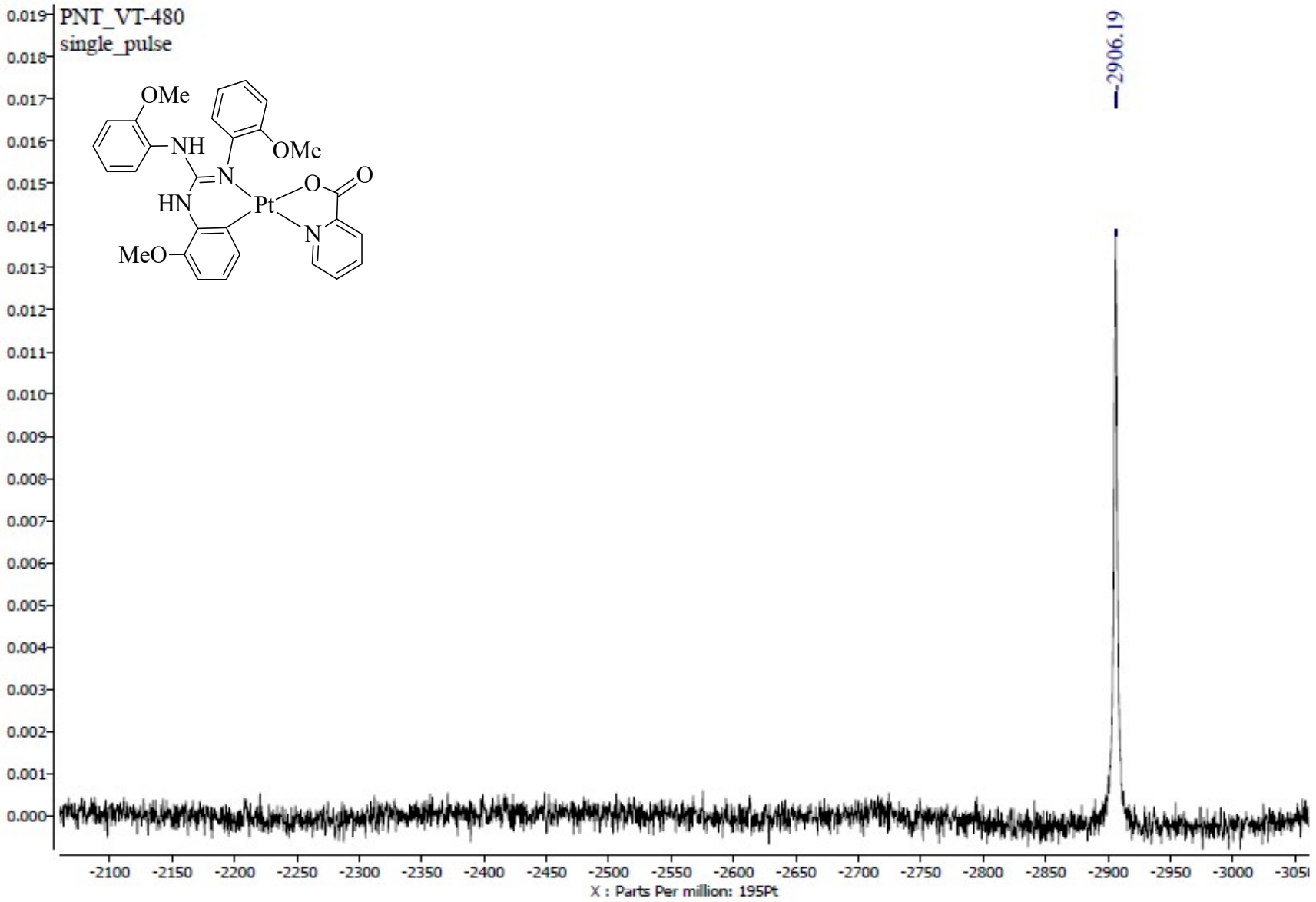

Fig. S185 $^{195}Pt\{^{1}H\}$ NMR ($CDCl_3$, 85.8 MHz) spectrum of **19**.

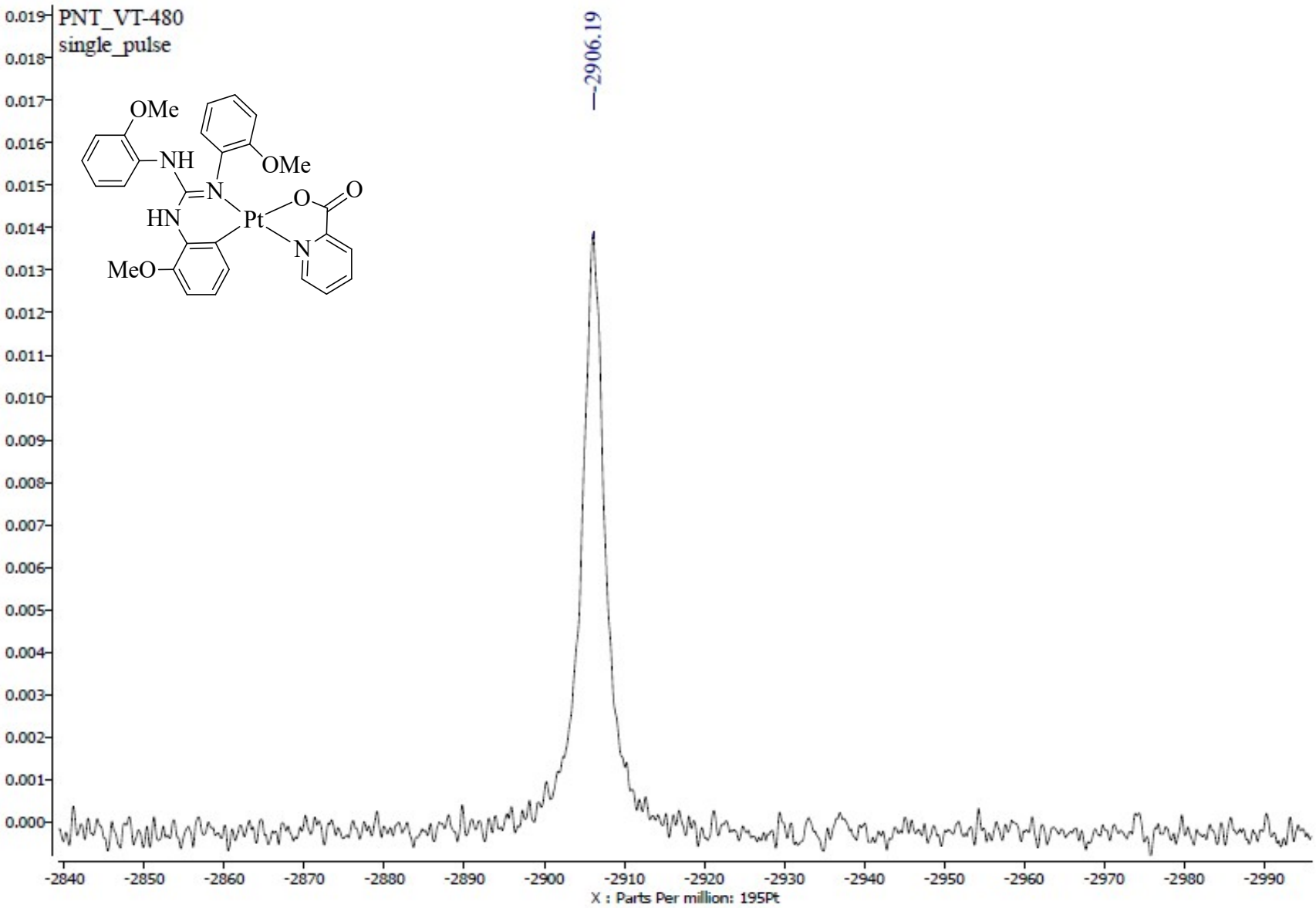

Fig. S186 $^{195}Pt\{^{1}H\}$ NMR ($CDCl_3$, 85.8 MHz) spectrum of **19** in the indicated region.

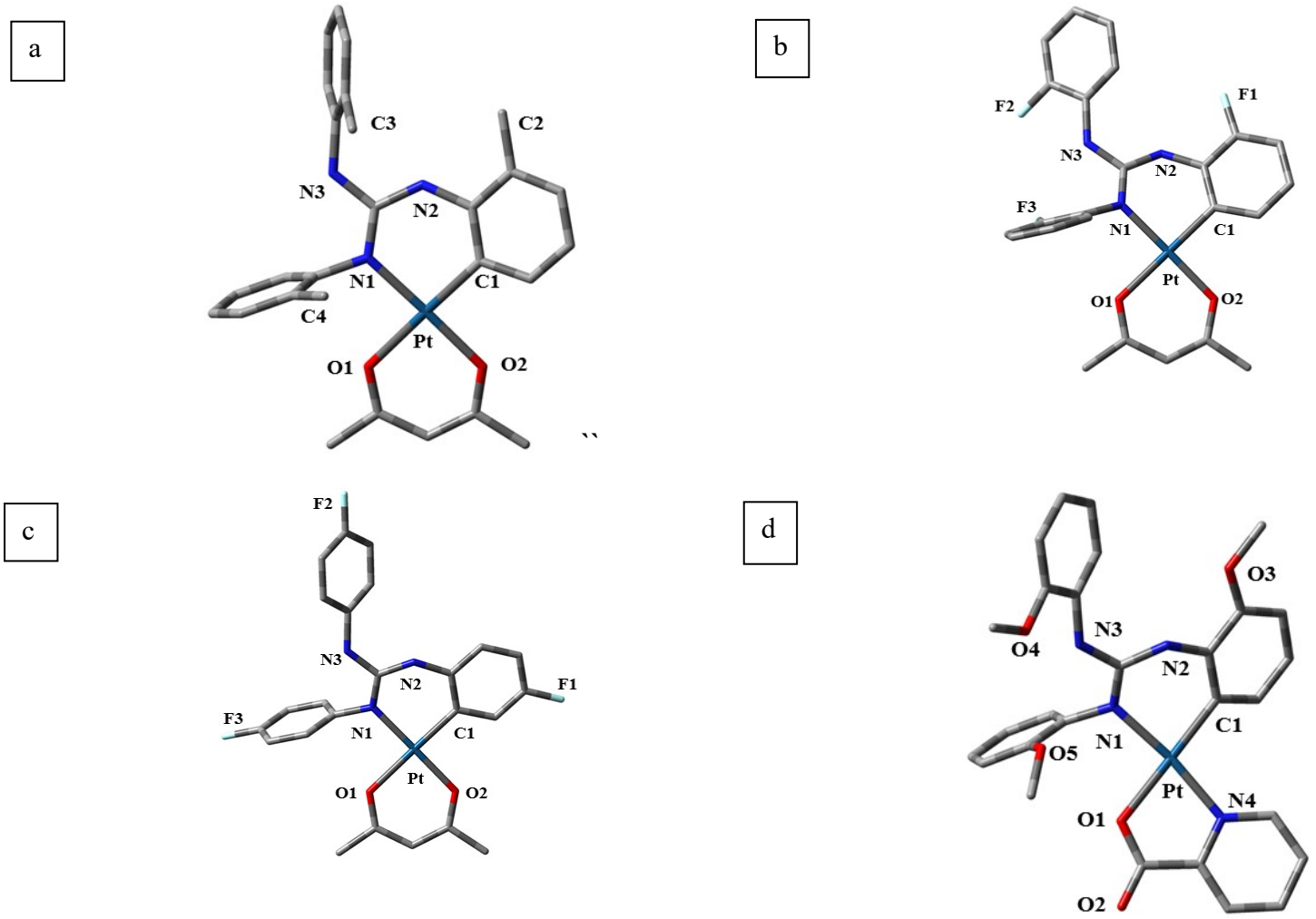

Fig. S187 Optimized geometries of **11** (a), **15** (b), **18** (c) and **19** (d). All the hydrogen atoms have been deleted for the sake of clarity.

Table S9 Selected bond angles (°) and bond lengths (Å) of **11**, **15**, **18** and **19** in ground state.

Bond Lengths (Å)	**11**	**15**	**18**	**19**
Pt-N1	2.047	2.053	2.050	2.045
Pt-C1	2.004	1.995	1.999	2.009
Pt-O1	2.157	2.144	2.147	2.147
Pt-O2/N4	2.056	2.046	2.048	2.068
Bond Angles (°)				
N1-Pt-C1	91.78	91.10	91.18	86.87
N1-Pt-O1	89.27	88.75	89.61	92.45
O1-Pt-O2	89.07	90.34	89.76	79.18
C1-Pt-O2	89.87	89.81	89.45	101.55

Table S10 Total energies in hartrees (a.u.) of **11**, **15**, **18** and **19** in ground state.

Conformer	E (gas phase) (hartree)	E (dichloromethane) (hartree)
11	-1480.2726165	-1478.8011715
15	-1660.0225111	-1659.1726203
18	-1660.0200515	-1658.8768318
19	-1796.9522634	-1795.5061360

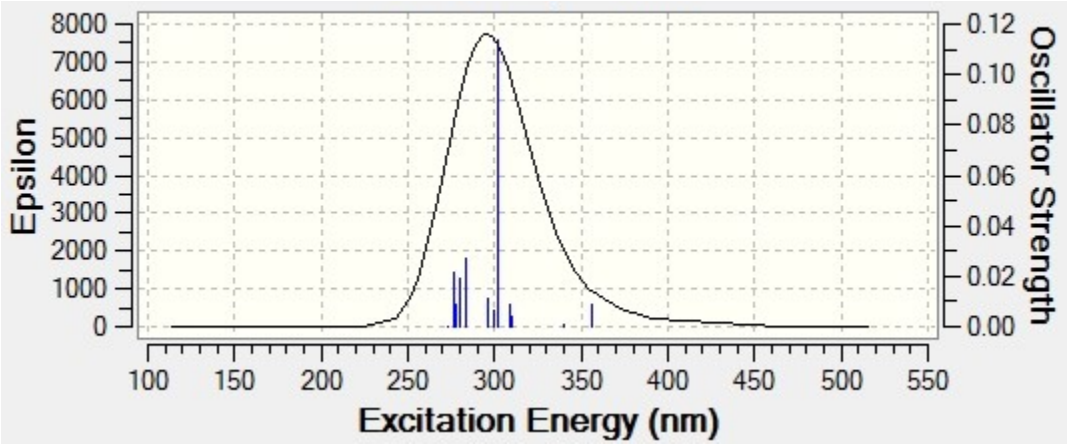

Fig. S188. TD-DFT predicated absorption spectra of **11**.

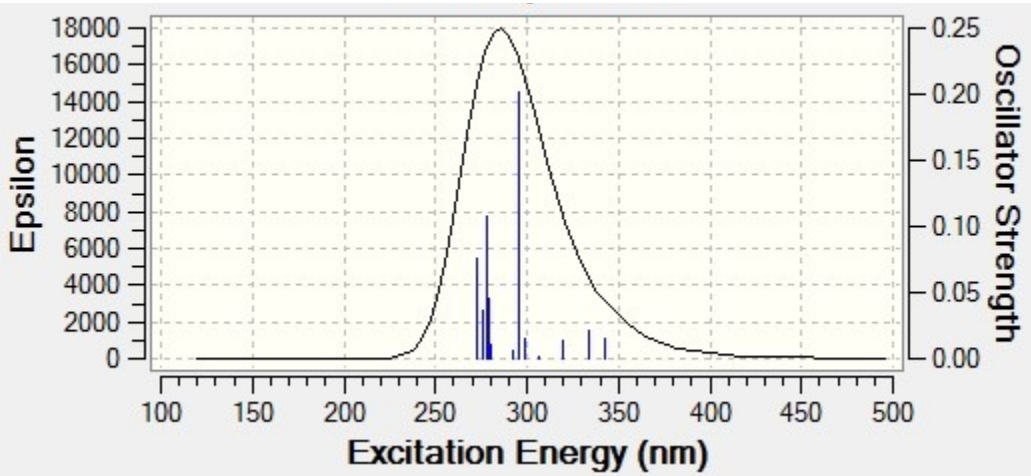

Fig. S189. TD-DFT predicated absorption spectra of **15**.

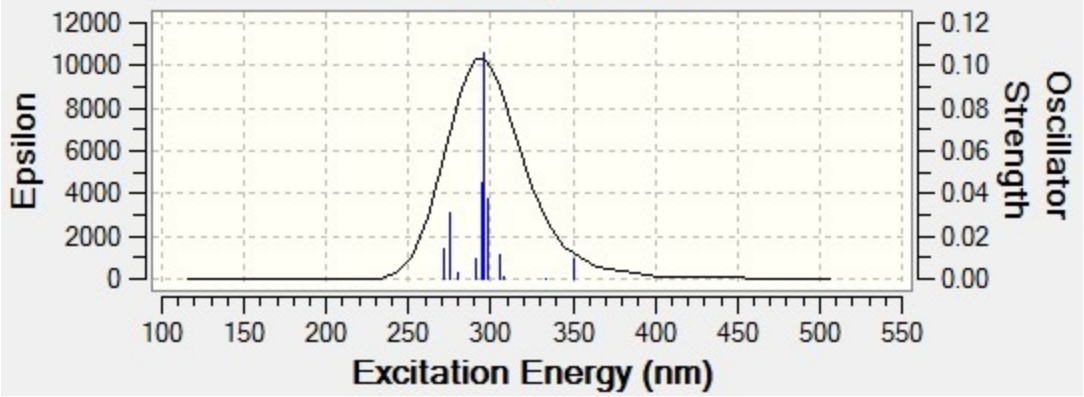

Fig. S190. TD-DFT predicated absorption spectra of **18**.

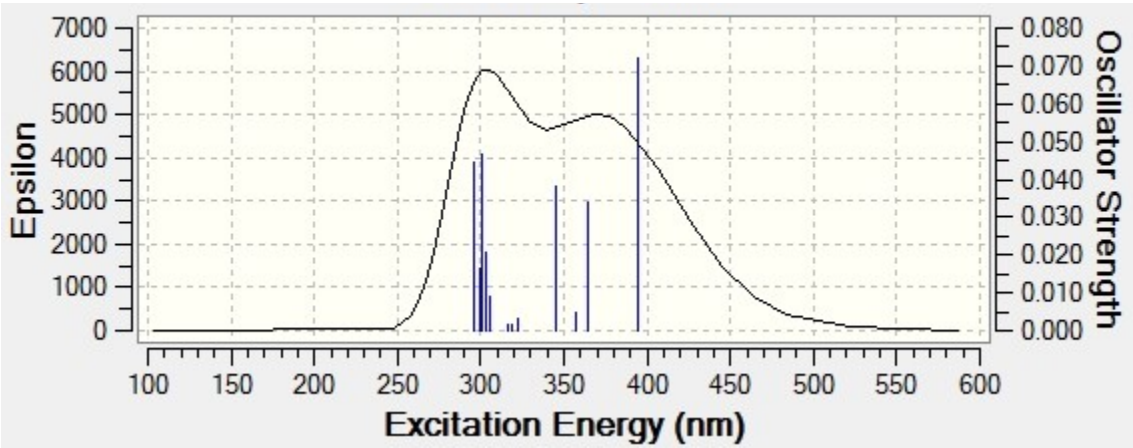

Fig. S191. TD-DFT predicated absorption spectra of **19**.

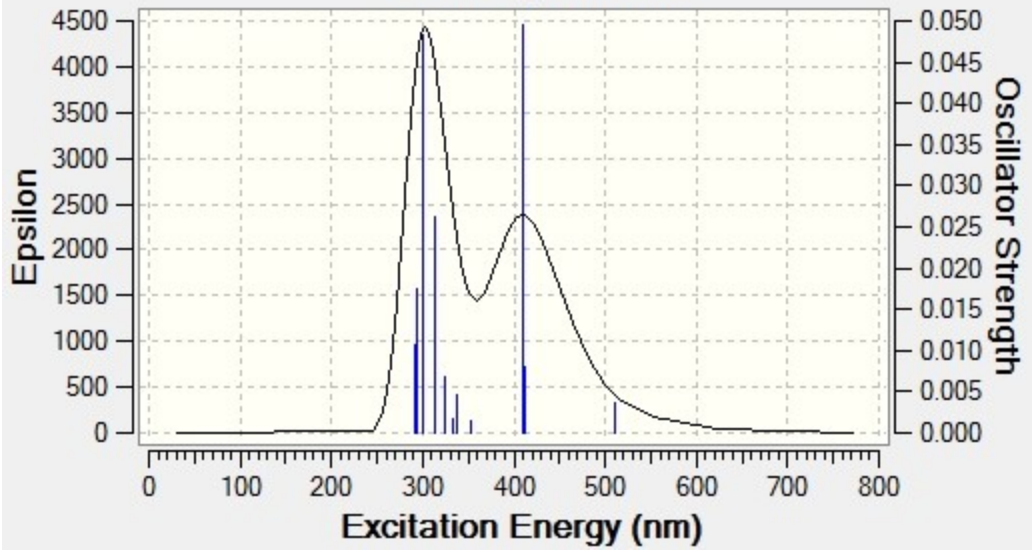

Fig S192 TD-DFT predicated emission spectra of **11**.

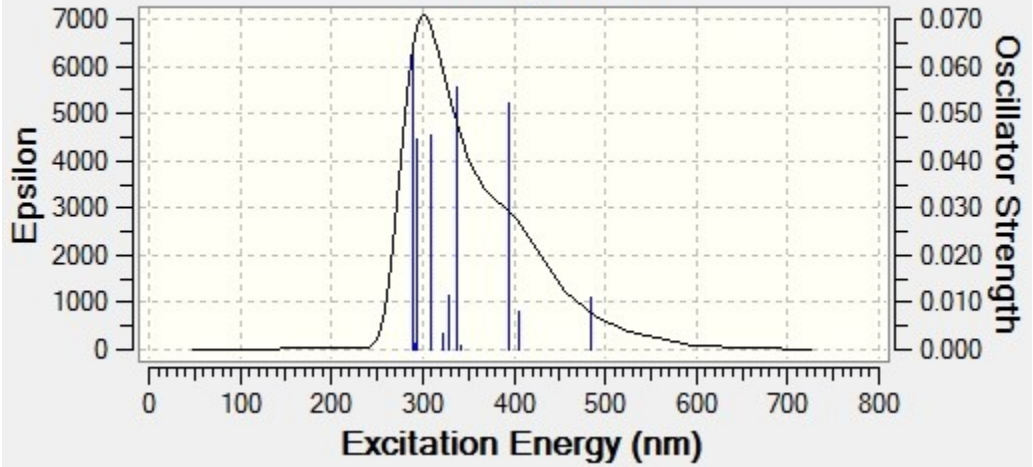

Fig. S193 TD-DFT predicated emission spectra of **15**.

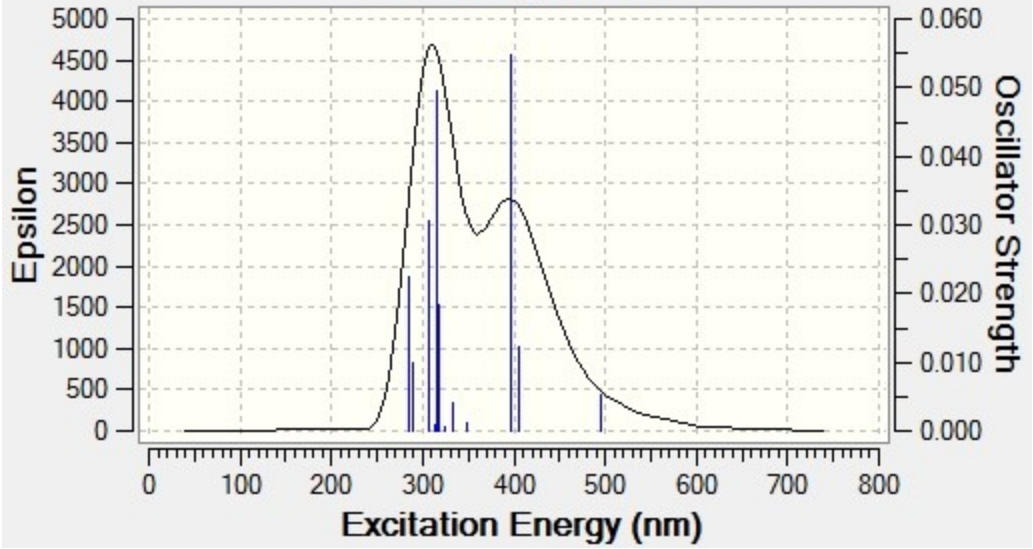

Fig. S194. TD-DFT predicated emission spectra of **18**.

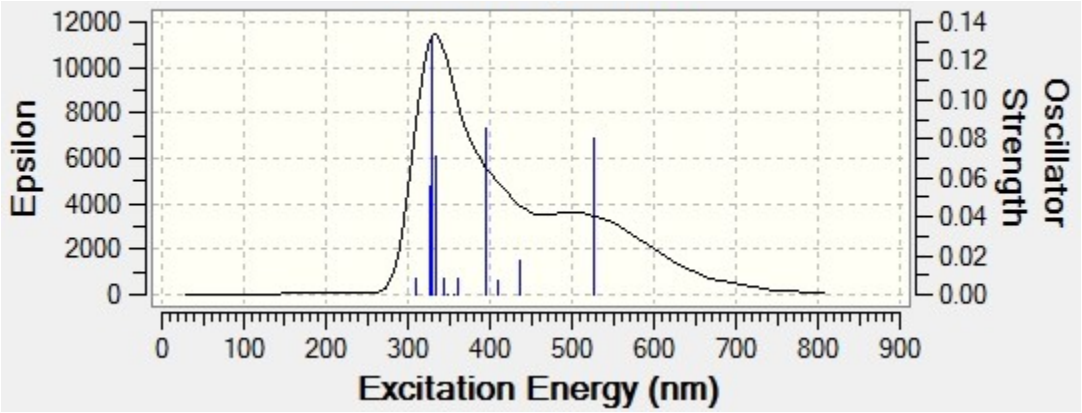

Fig. S195 TD-DFT predicated emission spectra of **19**.

Table S11 The energies (nm), oscillator strength (*f*), type of transition and the contribution of the main orbitals involved in the absorption spectra (in %) for **11**, **15**, **18** and **19** using TD-DFT.

Energy (nm)	Oscillator strength (*f*)	Transitions	Energy (nm)	Oscillator strength (*f*)	Transitions
11			**18**		
302	**0.1137**	**HOMO–1→LUMO (83%)**	298	0.0379	HOMO→ LUMO +1 (27%)
283	0.0271	HOMO→LUMO + 3 (67%)	**296**	**0.1063**	**HOMO–1→LUMO (59%)**
279	0.0192	HOMO–3→LUMO (26%) HOMO–2→LUMO (47%)	294	0.0447	HOMO→ LUMO +2 (29%)
276	0.0217	HOMO→LUMO + 5 (39%)	275	0.0309	HOMO→ LUMO +5 (71%)
15			**19**		
295	**0.2017**	**HOMO–1→LUMO (89%)**	**395**	**0.0721**	**HOMO→LUMO (91%)**
278	0.107	HOMO→LUMO +4 (53%)	365	0.0337	HOMO–2→LUMO (61%)
272	0.0757	HOMO–3→LUMO +1 (23%)	346	0.0379	HOMO–1→LUMO (66%)
			301	0.0468	HOMO→ LUMO +2 (62%)
			296	0.0447	HOMO–7→LUMO (28%), HOMO–6→LUMO (28%)

Table S12 Some of the selected energies (nm), oscillator strength (*f*), type of transition and the contribution of the main orbitals involved in the emission spectra (in %) for **11**, **15**, **18** and **19** using TD-DFT.

Energy (nm)	Oscillator strength (*f*)	Transitions	Energy (nm)	Oscillator strength (*f*)	Transitions
11			**18**		
512	**0.0037**	LUMO → HOMO (22%)	494	0.0052	LUMO → HOMO (23%)
410	**0.0494**	**LUMO → HOMO–1 (93%)**	**396**	**0.0548**	**LUMO → HOMO–1 (82%)**
313	0.0263	LUMO → HOMO–5 (47%)	316	0.0496	LUMO+2 → HOMO (34%) LUMO+3 → HOMO (54%)
301	0.0483	LUMO+3 → HOMO (36%)	306	0.0306	LUMO → HOMO–8 (21%) LUMO → HOMO–7 (18%) LUMO → HOMO–6 (18%)
			284	0.0224	LUMO+5 → HOMO (34%)
15			**19**		
484	0.0109	LUMO → HOMO (27%)	**525**	**0.0808**	**LUMO → HOMO (96%)**
394	**0.052**	**LUMO → HOMO–1 (92%)**	396	0.0995	LUMO → HOMO (91%)
337	0.0556	LUMO+1 → HOMO (90%)	333	0.0725	LUMO+2 → HOMO (51%) LUMO+3 → HOMO (31%)
309	0.0455	LUMO → HOMO–8 (34%) LUMO → HOMO–4 (33%)	330	0.13	LUMO+2 → HOMO (68%)
292	0.0446	LUMO+4 → HOMO (48%)	327	0.0568	LUMO+2 → HOMO (27%) LUMO+3 → HOMO (50%)
289	0.064	LUMO+1→ HOMO–1 (35%)			

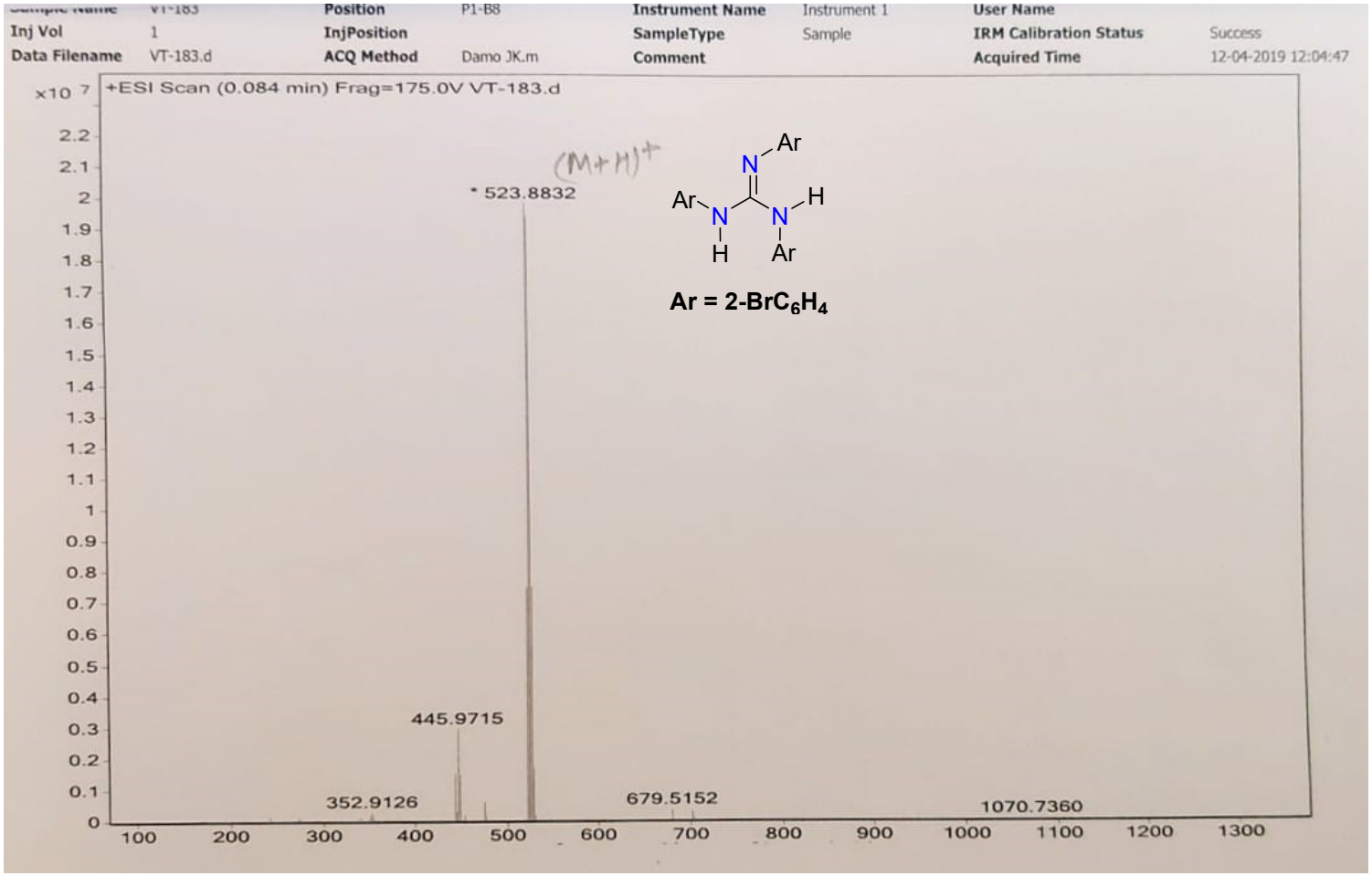
Position P1-B8
Instrument Name Instrument 1
User Name
Inj Vol 1
InjPosition
SampleType Sample
IRM Calibration Status Success
Data Filename VT-183.d
ACQ Method Damo JK.m
Comment
Acquired Time 12-04-2019 12:04:47
+ESI Scan (0.084 min) Frag=175.0V VT-183.d
x10 7
(M+H)+
523.8832
445.9715
352.9126
679.5152
1070.7360
Ar = 2-BrC6H4

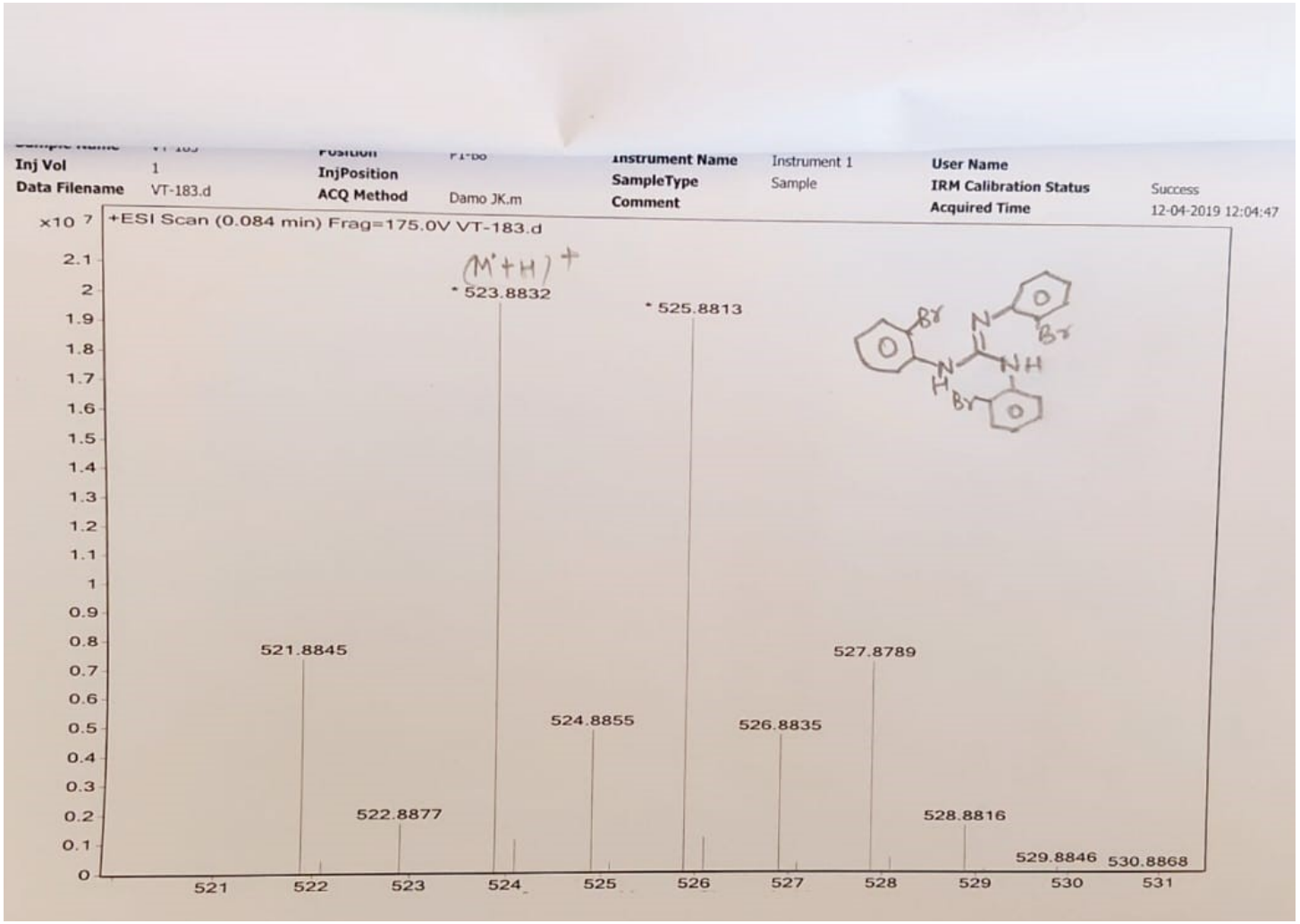
Inj Vol 1
Data Filename VT-183.d
InjPosition
ACQ Method Damo JK.m
Instrument Name Instrument 1
SampleType Sample
Comment
User Name
IRM Calibration Status Success
Acquired Time 12-04-2019 12:04:47
+ESI Scan (0.084 min) Frag=175.0V VT-183.d
x10 7
(M+H)+
523.8832
525.8813
521.8845
522.8877
524.8855
526.8835
527.8789
528.8816
529.8846
530.8868
Br
Br
Br
N
NH
O

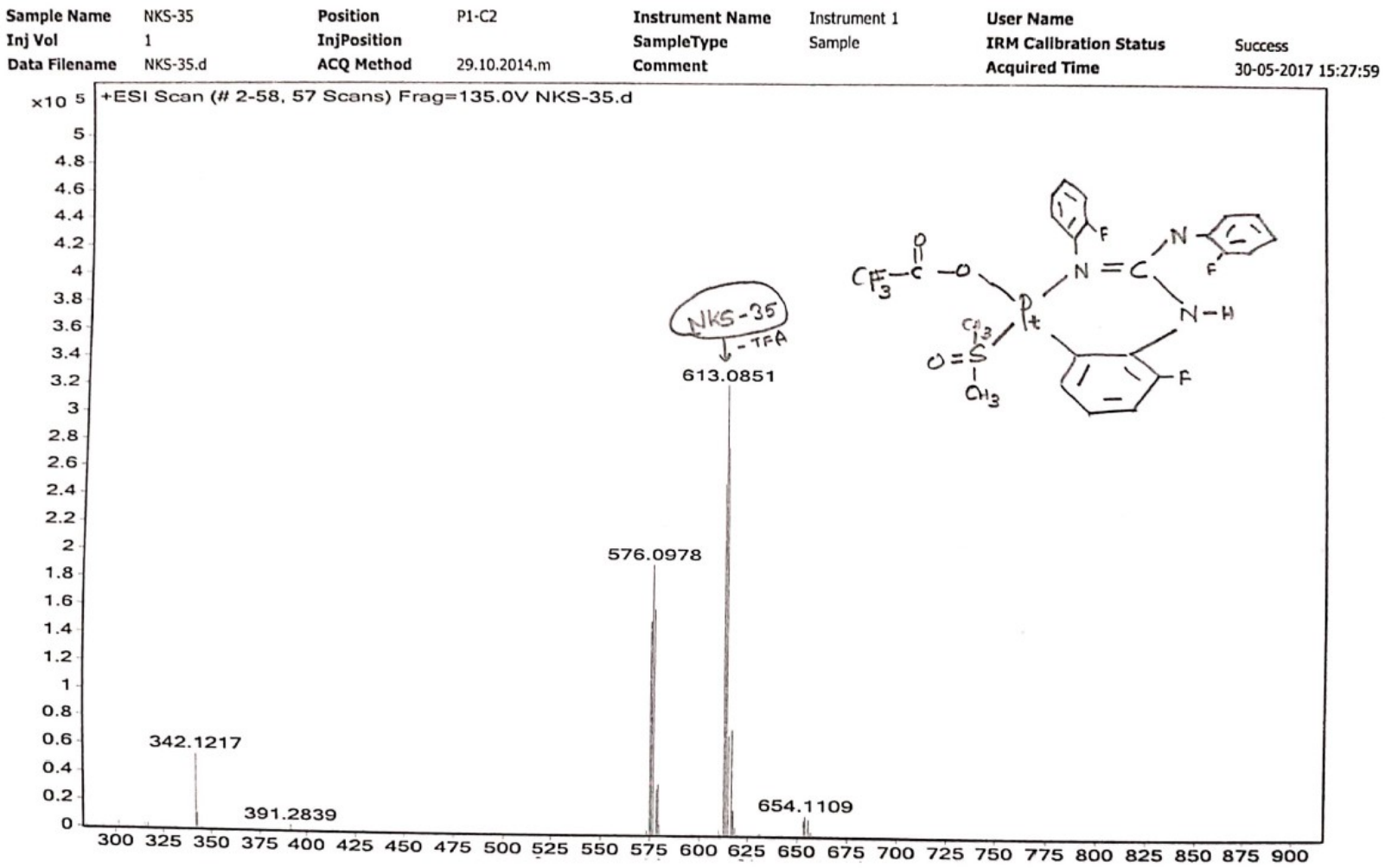
Sample Name NKS-35
Position P1-C2
Instrument Name Instrument 1
User Name
Inj Vol 1
InjPosition
SampleType Sample
IRM Calibration Status Success
Data Filename NKS-35.d
ACQ Method 29.10.2014.m
Comment
Acquired Time 30-05-2017 15:27:59
+ESI Scan (# 2-58, 57 Scans) Frag=135.0V NKS-35.d
x10 5
NKS-35
-TFA
613.0851
576.0978
342.1217
391.2839
654.1109

Complex 6

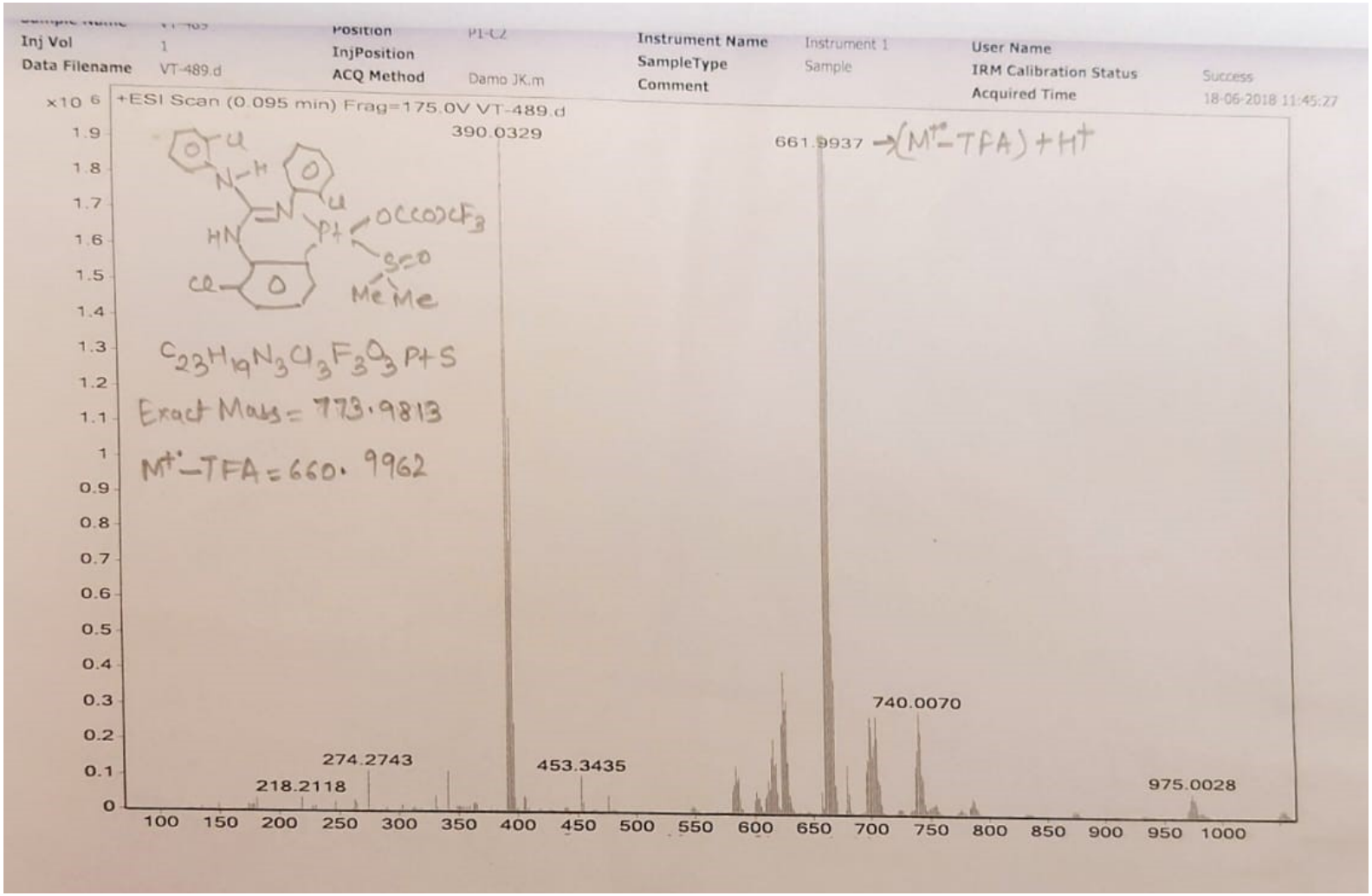
Inj Vol 1
Data Filename VT-489.d
Position P1-C2
InjPosition
ACQ Method Damo JK.m
Instrument Name Instrument 1
SampleType Sample
Comment
User Name
IRM Calibration Status Success
Acquired Time 18-06-2018 11:45:27
x10 6
+ESI Scan (0.095 min) Frag=175.0V VT-489.d
390.0329
661.9937
(M+ - TFA) + H+
740.0070
274.2743
453.3435
218.2118
975.0028
C23H19N3Cl3F3O3Pt S
Exact Mass = 773.9813
M+ - TFA = 660.9962

Complex 7

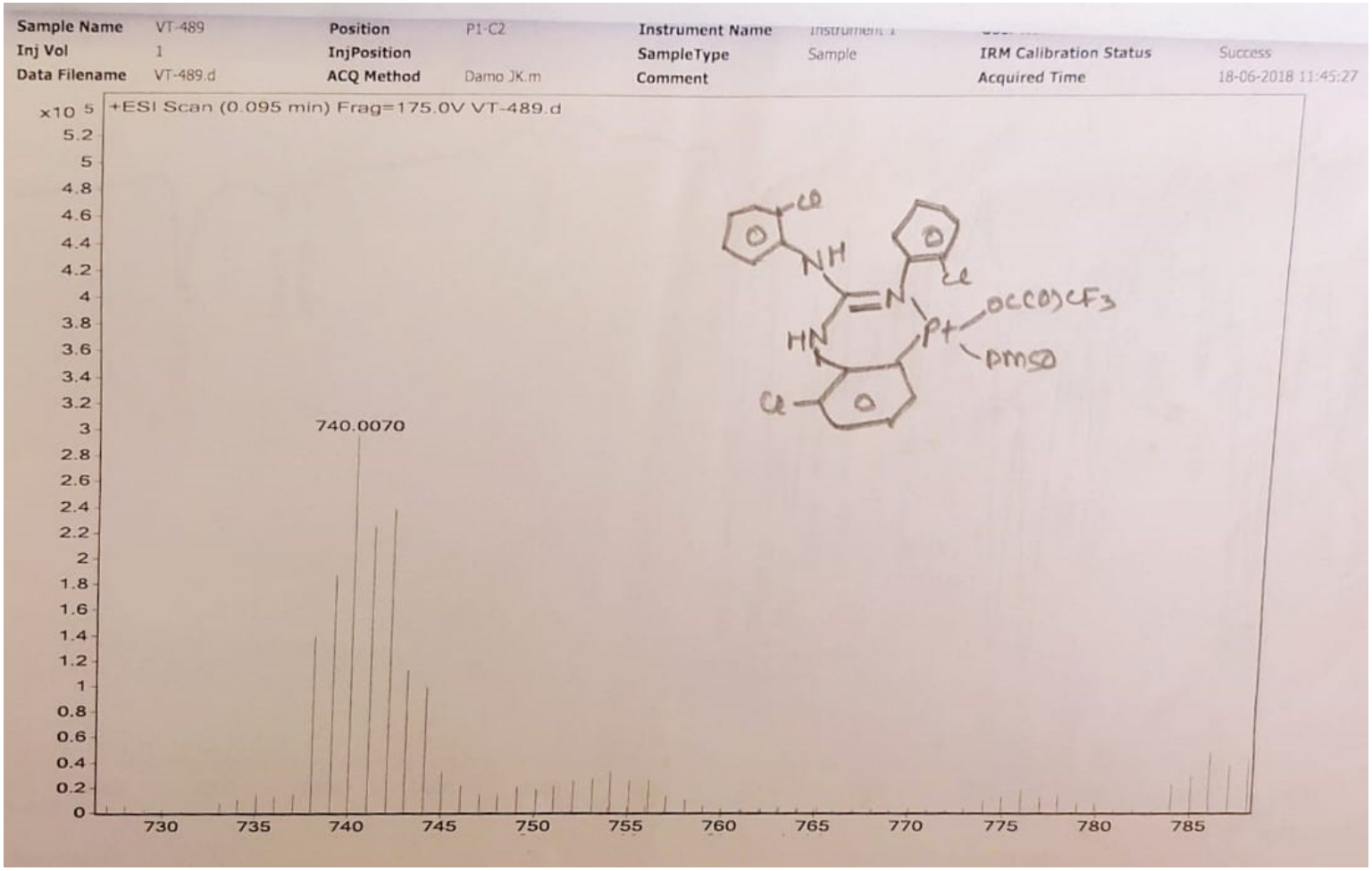
Sample Name VT-489
Position P1-C2
Instrument Name
Inj Vol 1
InjPosition
SampleType Sample
IRM Calibration Status Success
Data Filename VT-489.d
ACQ Method Damo JK.m
Comment
Acquired Time 18-06-2018 11:45:27
+ESI Scan (0.095 min) Frag=175.0V VT-489.d
x10 5
740.0070
OCCO)CF3
DMSO

Complex 7

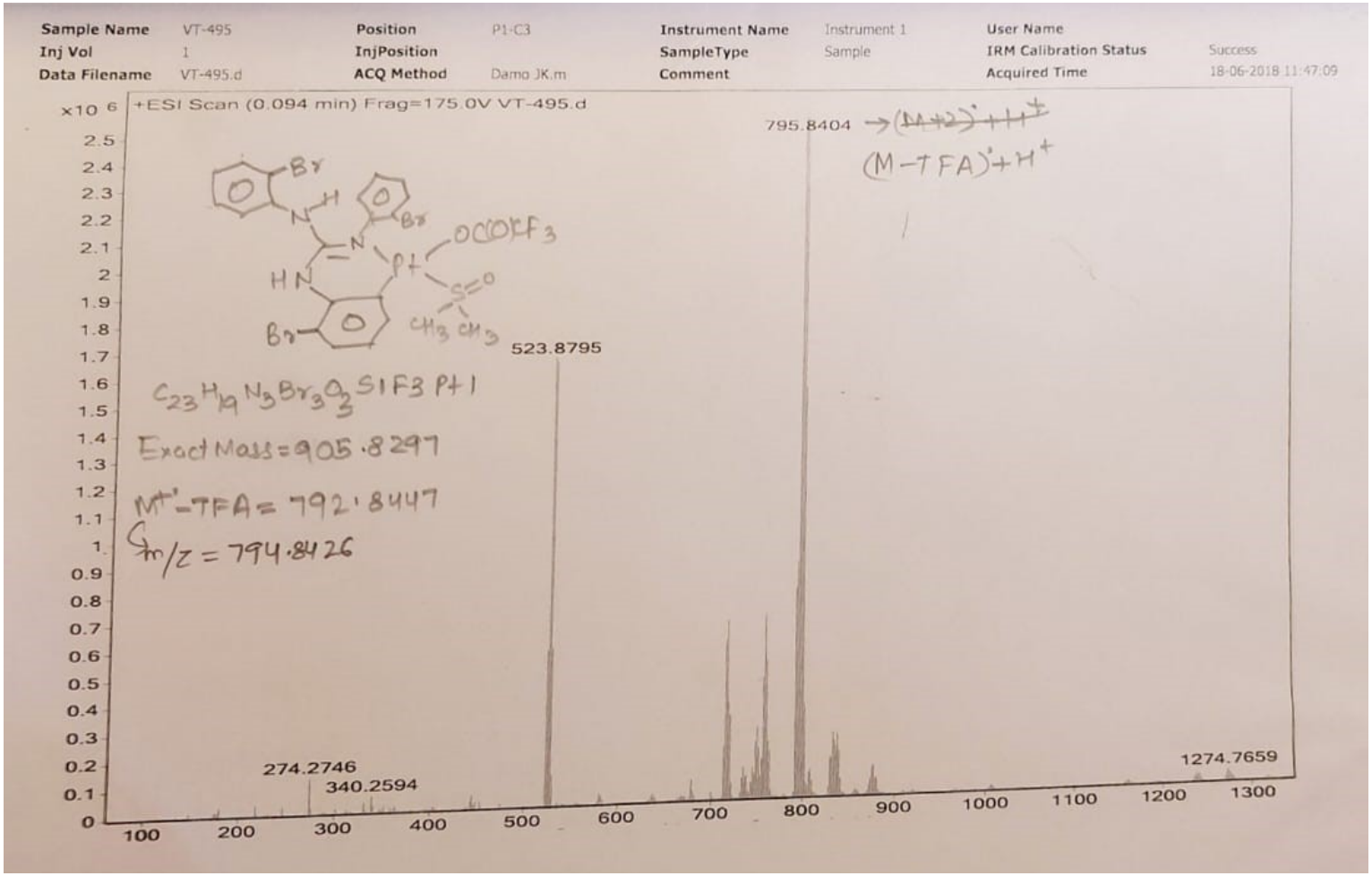
Sample Name VT-495
Position P1-C3
Instrument Name Instrument 1
User Name
Inj Vol 1
InjPosition
SampleType Sample
IRM Calibration Status Success
Data Filename VT-495.d
ACQ Method Damo JK.m
Comment
Acquired Time 18-06-2018 11:47:09
+ESI Scan (0.094 min) Frag=175.0V VT-495.d
x10 6
795.8404
(M-TFA)+H+
523.8795
C23H19N3Br3O3S1F3Pt1
Exact Mass=905.8297
M+-TFA=792.8447
m/z=794.8426
274.2746
340.2594
1274.7659

Complex 8

Complex 8

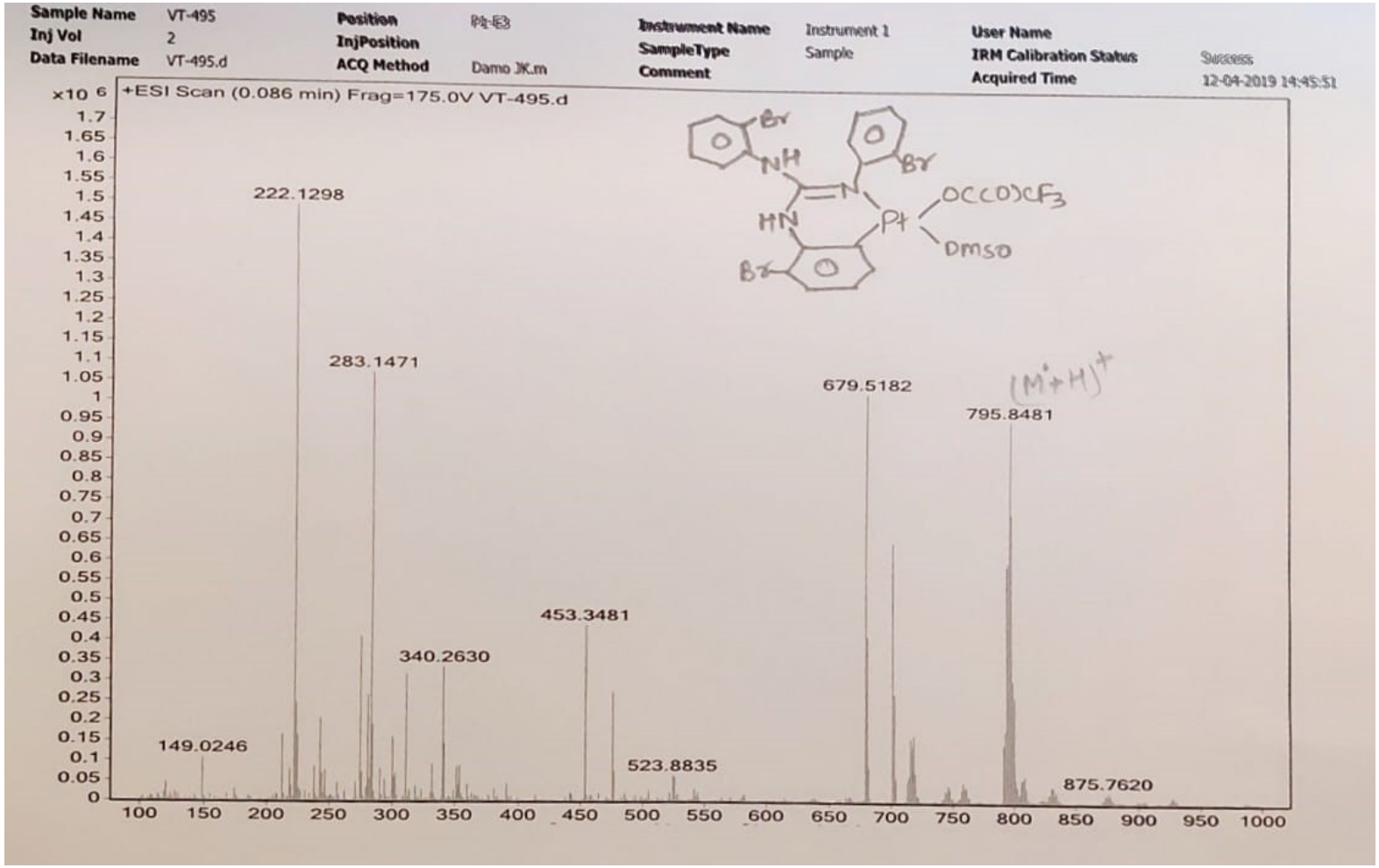
Sample Name VT-495
Inj Vol 2
Data Filename VT-495.d
Position P1-E3
InjPosition
ACQ Method Damo JK.m
Instrument Name Instrument 1
SampleType Sample
Comment
User Name
IRM Calibration Status Success
Acquired Time 12-04-2019 14:45:51
x10 6
+ESI Scan (0.086 min) Frag=175.0V VT-495.d
222.1298
283.1471
679.5182
795.8481
(M+H)+
453.3481
340.2630
149.0246
523.8835
875.7620
OCCO)CF3
DMSO
Pt
NH
HN
Br

Complex 8

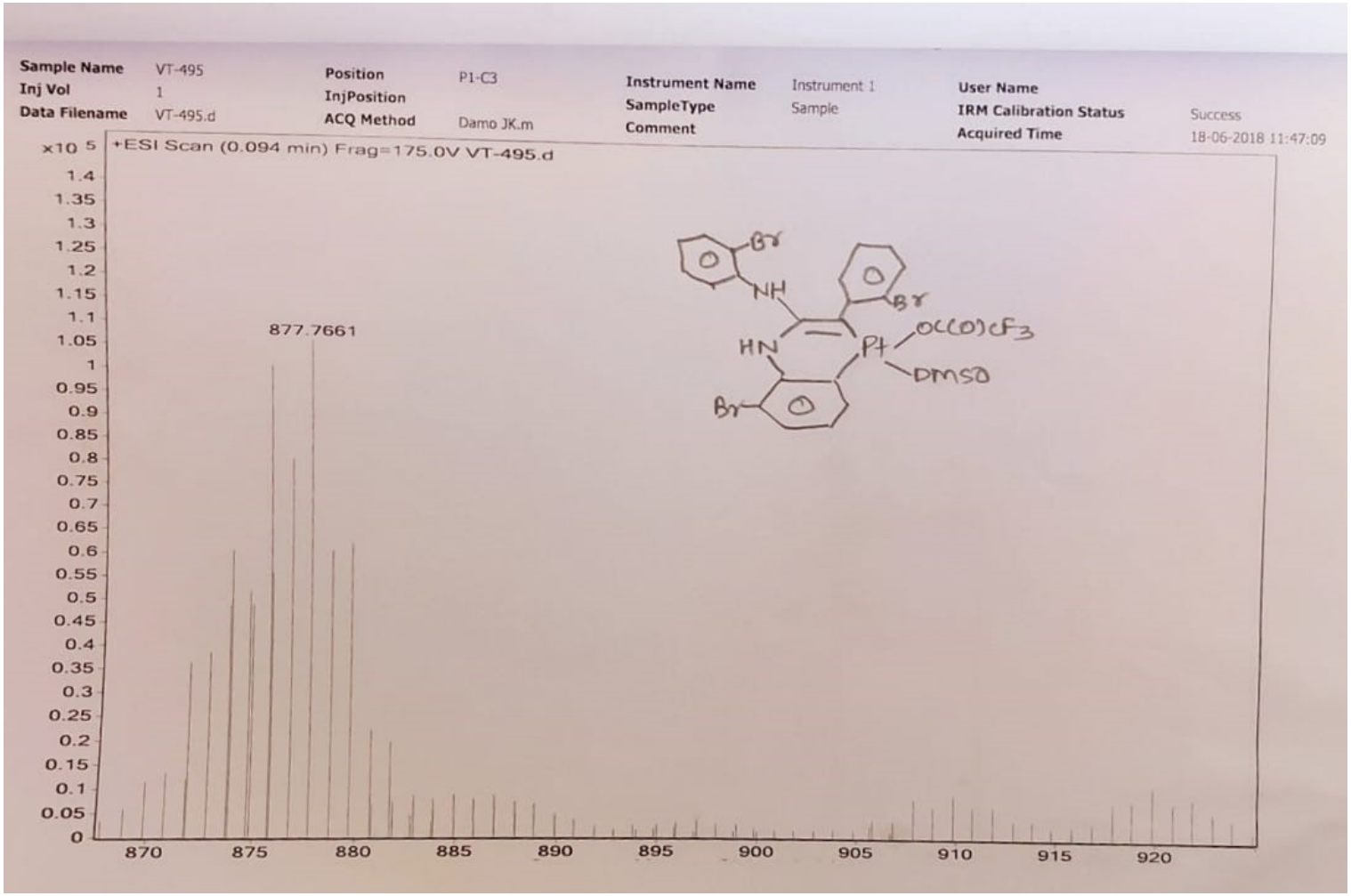
Sample Name VT-495
Inj Vol 1
Data Filename VT-495.d
Position P1-C3
InjPosition
ACQ Method Damo JK.m
Instrument Name Instrument 1
SampleType Sample
Comment
User Name
IRM Calibration Status Success
Acquired Time 18-06-2018 11:47:09
+ESI Scan (0.094 min) Frag=175.0V VT-495.d
x10 5
877.7661
OC(O)CF3
DMSO
NH
HN
Pt
Br

Complex 8

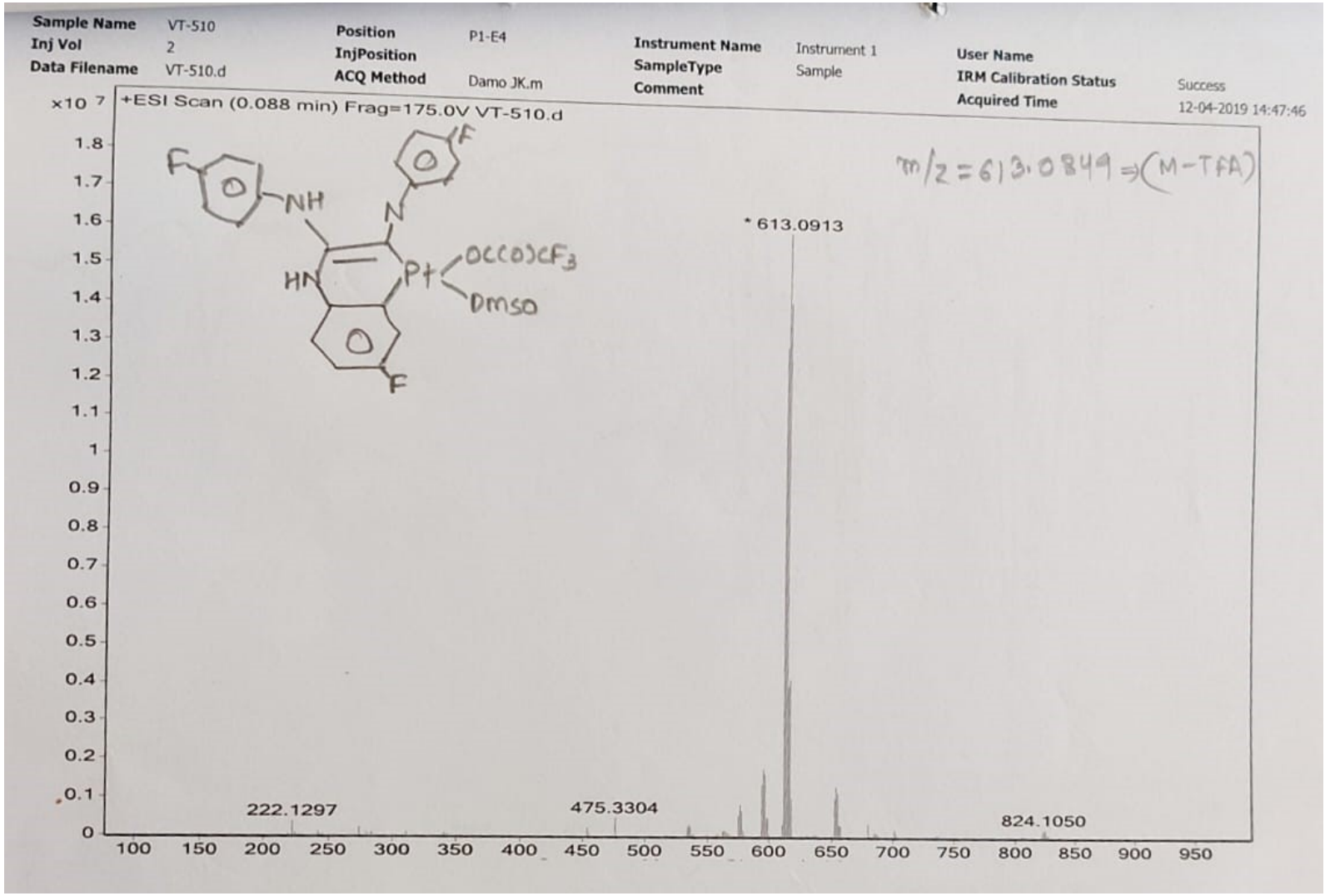
Sample Name VT-510
Inj Vol 2
Data Filename VT-510.d
Position P1-E4
InjPosition
ACQ Method Damo JK.m
Instrument Name Instrument 1
SampleType Sample
Comment
User Name
IRM Calibration Status Success
Acquired Time 12-04-2019 14:47:46
×10 7
+ESI Scan (0.088 min) Frag=175.0V VT-510.d
m/z = 613.0849 ⇒ (M-TFA)
* 613.0913
222.1297
475.3304
824.1050
OC(O)CF3
Dmso
NH
HN
N
Pt
F

Complex 9

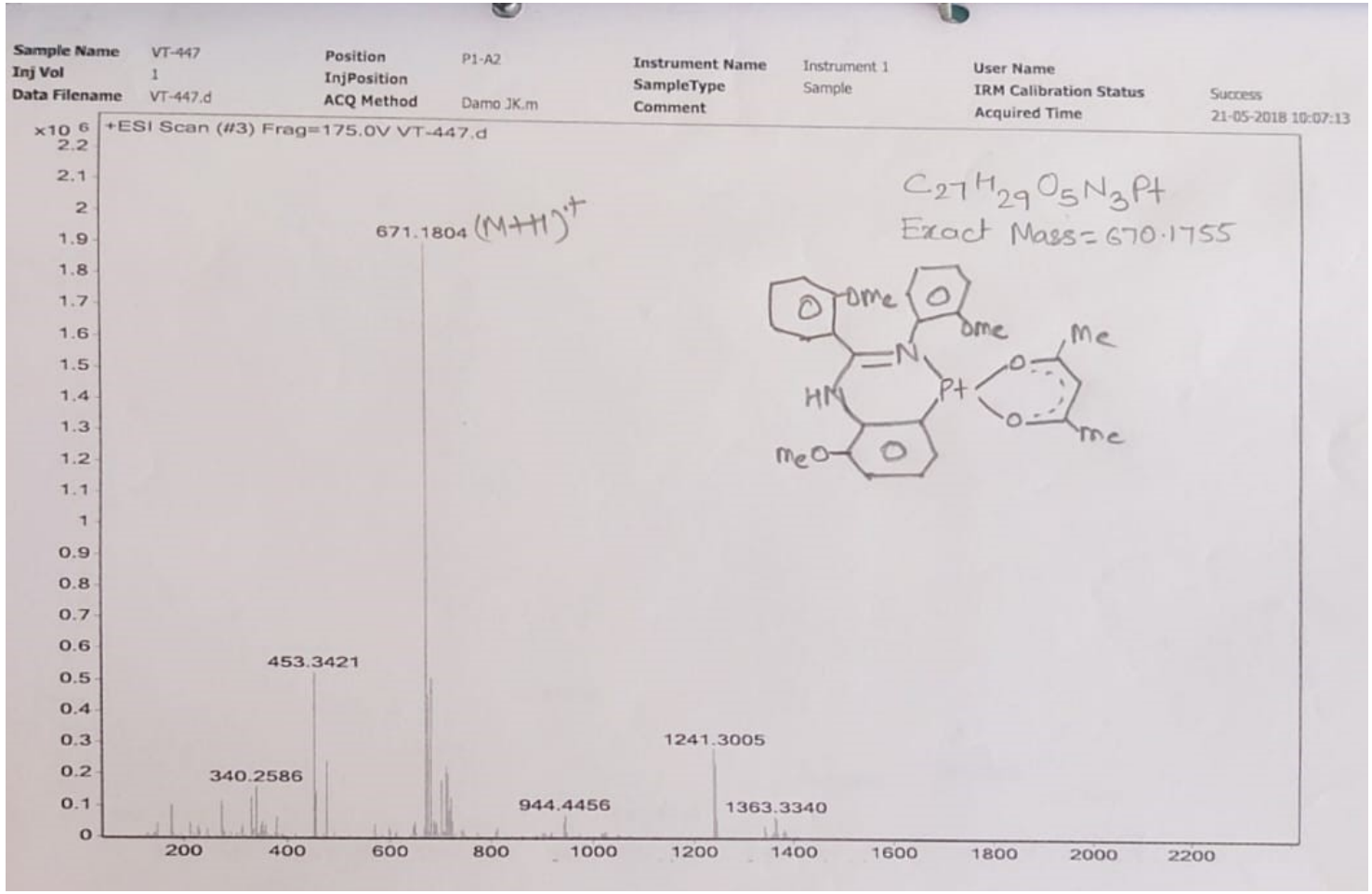
Sample Name VT-447
Inj Vol 1
Data Filename VT-447.d
Position P1-A2
InjPosition
ACQ Method Damo JK.m
Instrument Name Instrument 1
SampleType Sample
Comment
User Name
IRM Calibration Status Success
Acquired Time 21-05-2018 10:07:13
+ESI Scan (#3) Frag=175.0V VT-447.d
x10 6
671.1804 (M+H)+
453.3421
340.2586
944.4456
1241.3005
1363.3340
C27H29O5N3Pt
Exact Mass=670.1755
OMe
OMe
Me
Me
HN
Pt
MeO

Complex 10

Qualitative Compound Report

Data File	VT-449.d	**Sample Name**	VT-449
Sample Type	Sample	**Position**	P1-A1
Instrument Name	Instrument 1	**User Name**	
Acq Method	Damo JK.m	**Acquired Time**	21-05-2018 10:05:27
IRM Calibration Status	Success	**DA Method**	Default.m
Comment			

Sample Group	**Info.**
Acquisition SW Version	6200 series TOF/6500 series Q-TOF B.05.01 (B5125.1)

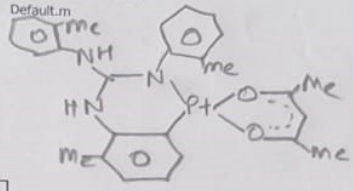

Compound Table

Compound Label	RT	Mass	MFG Formula
Cpd 2: 4	4	625.1741	<none>

Compound Label	*m/z*	RT	Algorithm	Mass
Cpd 2: 4	626.1814	4	Find by Molecular Feature	625.1741

MFE MS Spectrum

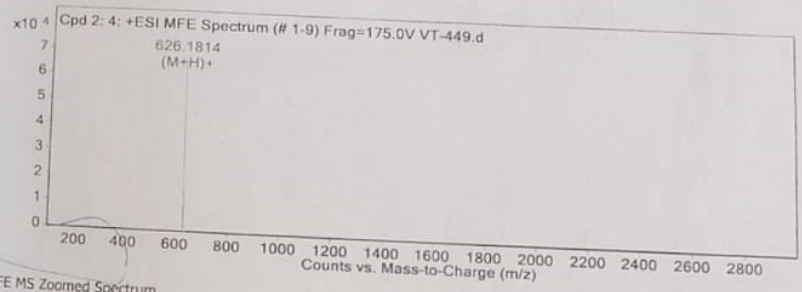

MFE MS Zoomed Spectrum

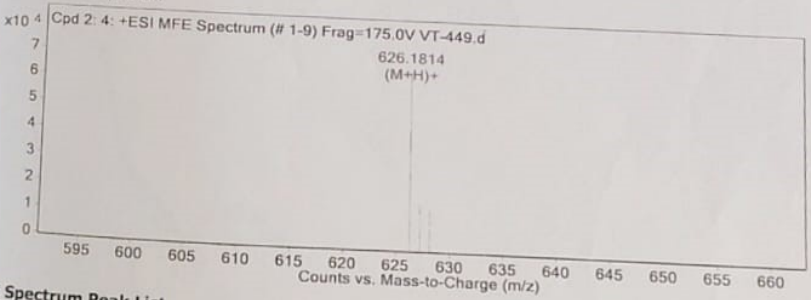

MS Spectrum Peak List

m/z	z	Abund	Ion
626.1814	1	66196.11	(M+H)+
627.1837	1	16867.11	(M+H)+
628.1796	1	15321.1	(M+H)+

--- End Of Report ---

Complex 11

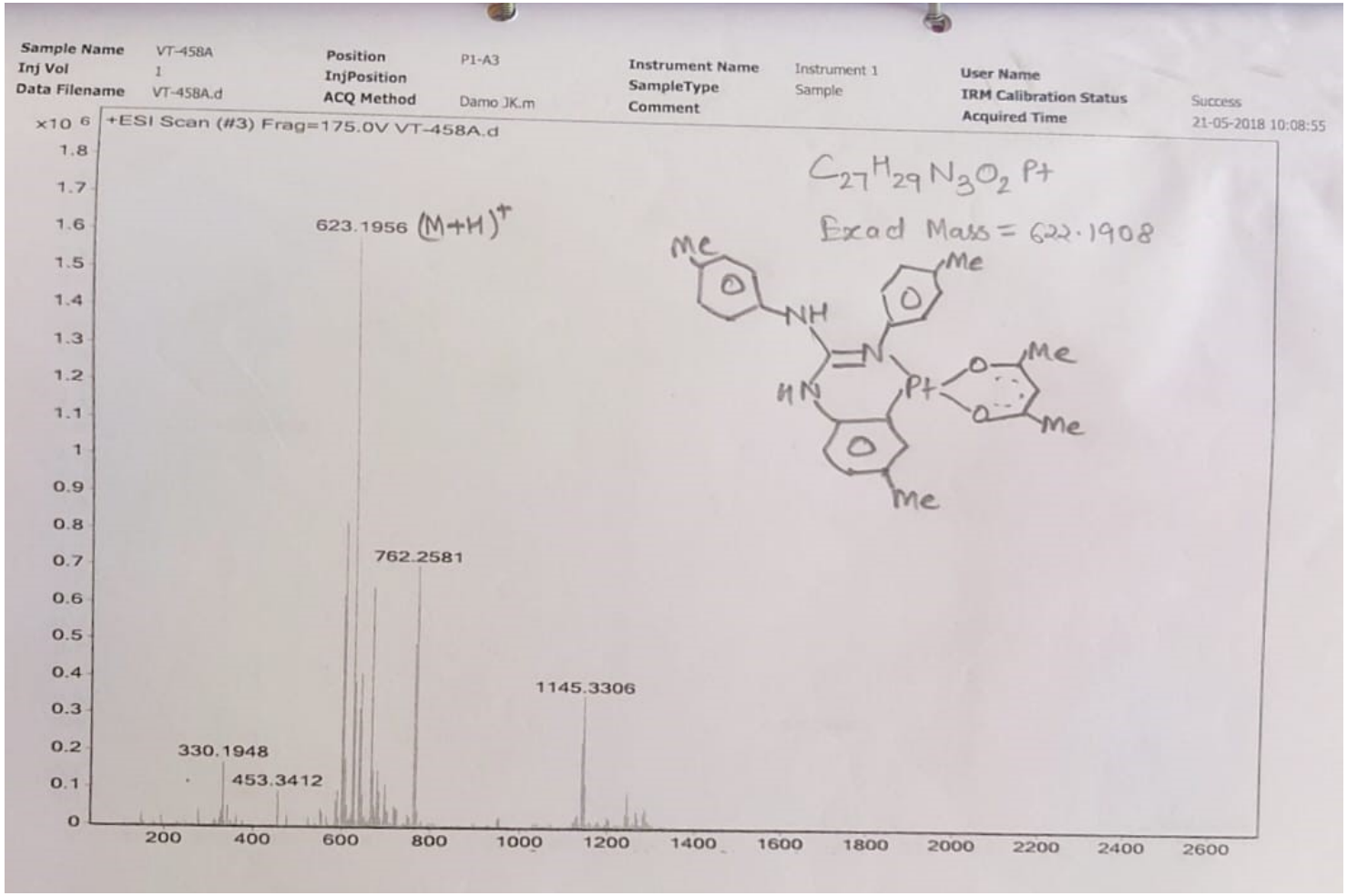
Sample Name VT-458A
Inj Vol 1
Data Filename VT-458A.d
Position P1-A3
InjPosition
ACQ Method Damo JK.m
Instrument Name Instrument 1
SampleType Sample
Comment
User Name
IRM Calibration Status Success
Acquired Time 21-05-2018 10:08:55
x10 6
+ESI Scan (#3) Frag=175.0V VT-458A.d
623.1956 (M+H)+
762.2581
1145.3306
330.1948
453.3412
C27H29N3O2Pt+
Exact Mass = 622.1908
Me
NH
N
HN
Pt
O
1.8
1.7
1.6
1.5
1.4
1.3
1.2
1.1
1
0.9
0.8
0.7
0.6
0.5
0.4
0.3
0.2
0.1
0
200
400
600
800
1000
1200
1400
1600
1800
2000
2200
2400
2600

Complex 12

Qualitative Compound Report

Data File	VT-466.d	Sample Name	VT-466
Sample Type	Sample	Position	P1-A1
Instrument Name	Instrument 1	User Name	
Acq Method	Damo JK.m	Acquired Time	05-07-2018 11:33:55
IRM Calibration Status	Success	DA Method	Default.m
Comment			

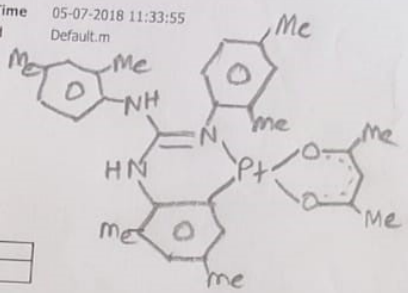

Sample Group		Info.
Acquisition SW Version	6200 series TOF/6500 series Q-TOF B.05.01 (B5125.1)	

Compound Table

Compound Label	RT	Mass	MFG Formula
Cpd 4: 0.090	0.09	664.2383	<none>

Compound Label	*m/z*	RT	Algorithm	Mass
Cpd 4: 0.090	665.2456	0.09	Find by Molecular Feature	664.2383

MFE MS Spectrum

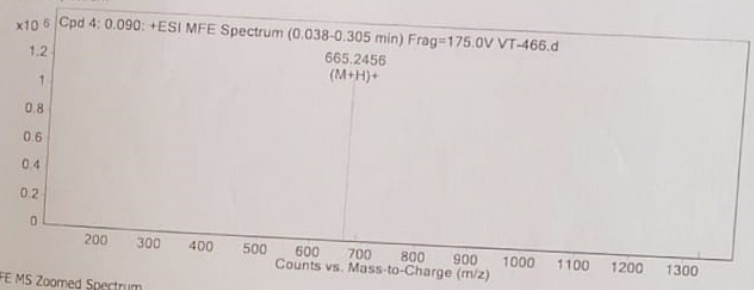

MFE MS Zoomed Spectrum

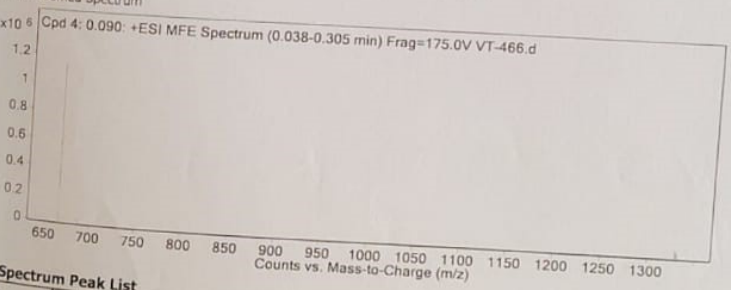

MS Spectrum Peak List

m/z	z	Abund	Ion
665.2456	1	1139623.38	(M+H)+
687.2261	1	43533.89	(M+Na)+
1329.4813	1	55080.16	(2M+H)+
1330.4829	1	50781.88	(2M+H)+
1331.4847	1	35908.16	(2M+H)+

Complex 13

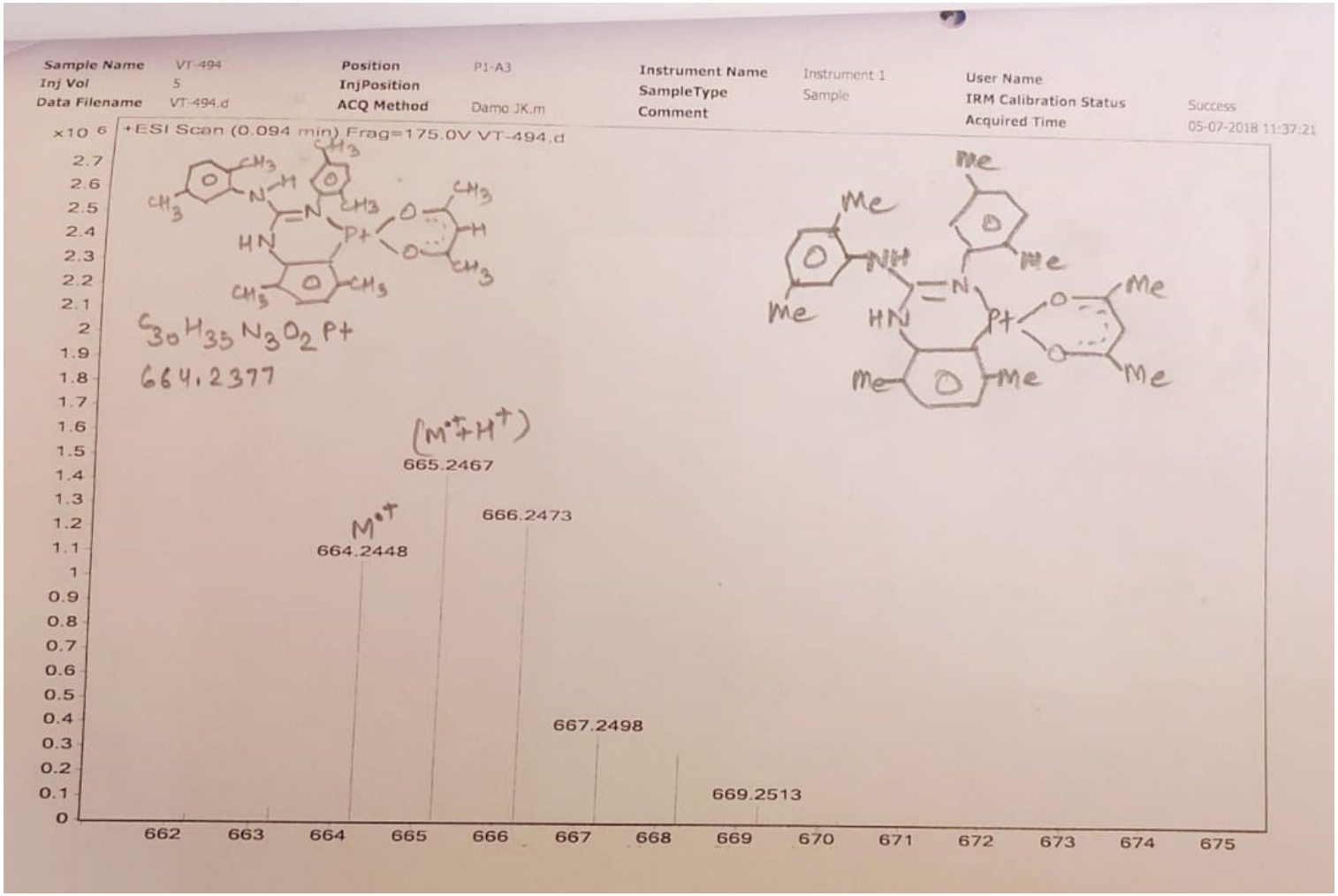
Sample Name VT-494
Inj Vol 5
Data Filename VT-494.d
Position P1-A3
InjPosition
ACQ Method Damo JK.m
Instrument Name Instrument 1
SampleType Sample
Comment
User Name
IRM Calibration Status Success
Acquired Time 05-07-2018 11:37:21
x10 6
+ESI Scan (0.094 min) Frag=175.0V VT-494.d
C30H35N3O2Pt+
664.2377
(M•++H+)
665.2467
M•+
664.2448
666.2473
667.2498
669.2513

Complex 14

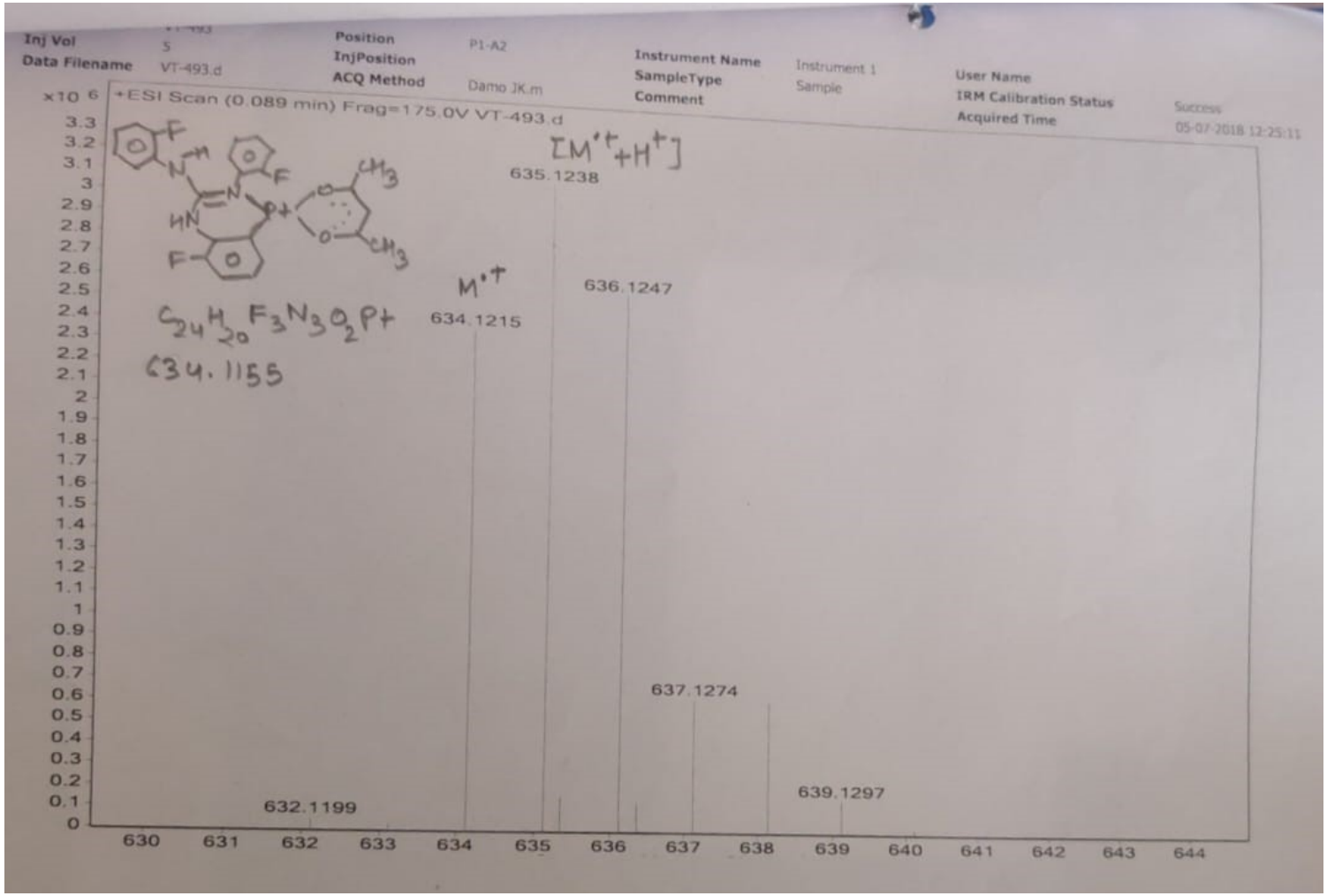
Inj Vol
Data Filename
VT-493.d
Position
P1-A2
InjPosition
ACQ Method
Damo JK.m
Instrument Name
Instrument 1
SampleType
Sample
Comment
User Name
IRM Calibration Status
Success
Acquired Time
05-07-2018 12:25:11
x10 6
+ESI Scan (0.089 min) Frag=175.0V VT-493.d
[M'+ +H+]
635.1238
M'+
634.1215
636.1247
637.1274
639.1297
632.1199
C24H20F3N3O2P+
634.1155

Complex 15

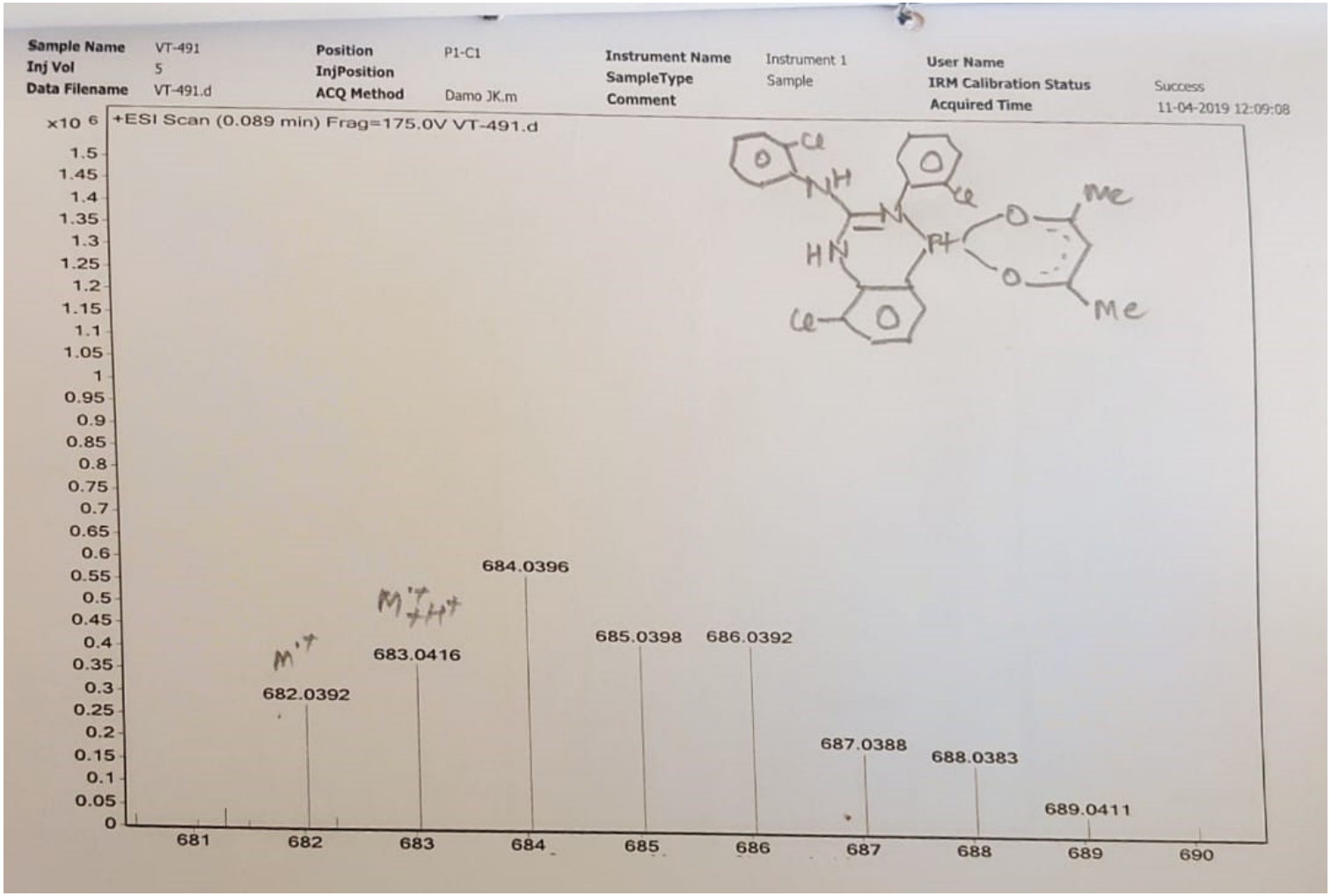
Sample Name VT-491
Inj Vol 5
Data Filename VT-491.d
Position P1-C1
InjPosition
ACQ Method Damo JK.m
Instrument Name Instrument 1
SampleType Sample
Comment
User Name
IRM Calibration Status Success
Acquired Time 11-04-2019 12:09:08
+ESI Scan (0.089 min) Frag=175.0V VT-491.d
x10 6
682.0392
683.0416
684.0396
685.0398
686.0392
687.0388
688.0383
689.0411

Complex 16

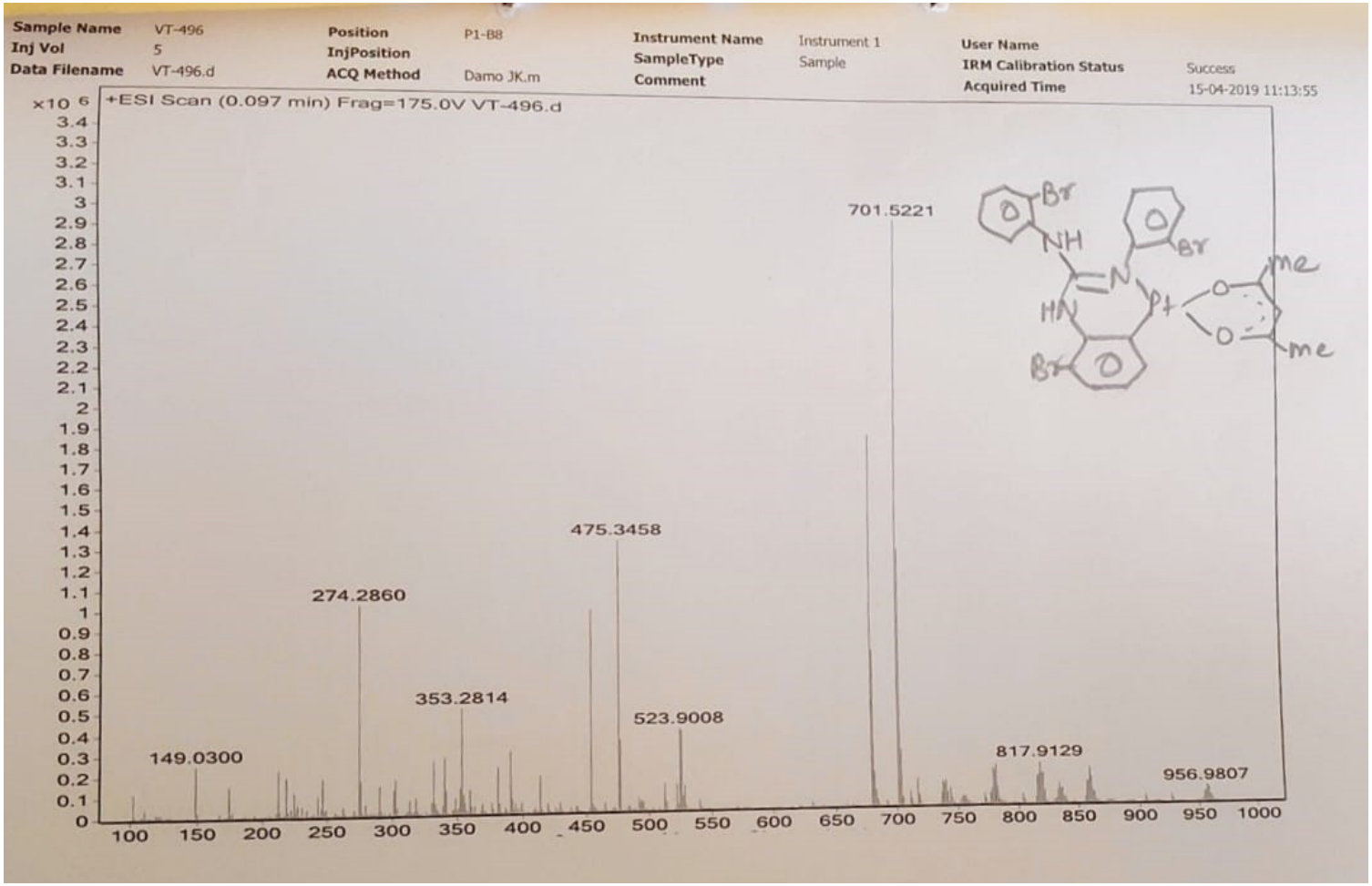
Sample Name VT-496
Inj Vol 5
Data Filename VT-496.d
Position P1-B8
InjPosition
ACQ Method Damo JK.m
Instrument Name Instrument 1
SampleType Sample
Comment
User Name
IRM Calibration Status Success
Acquired Time 15-04-2019 11:13:55
+ESI Scan (0.097 min) Frag=175.0V VT-496.d
x10 6
701.5221
475.3458
274.2860
353.2814
523.9008
149.0300
817.9129
956.9807
Br
NH
HN
N
Pt
O
me

Complex 17

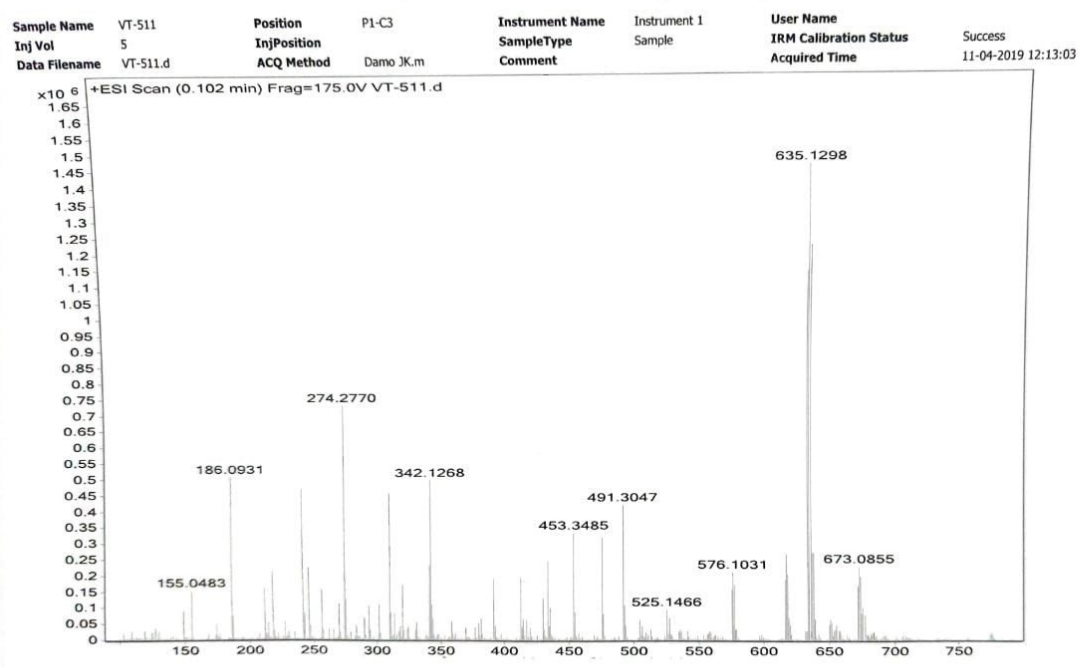
Sample Name VT-511
Inj Vol 5
Data Filename VT-511.d
Position P1-C3
InjPosition
ACQ Method Damo JK.m
Instrument Name Instrument 1
SampleType Sample
Comment
User Name
IRM Calibration Status Success
Acquired Time 11-04-2019 12:13:03
+ESI Scan (0.102 min) Frag=175.0V VT-511.d
x10 6
635.1298
274.2770
186.0931
342.1268
491.3047
453.3485
576.1031
673.0855
155.0483
525.1466

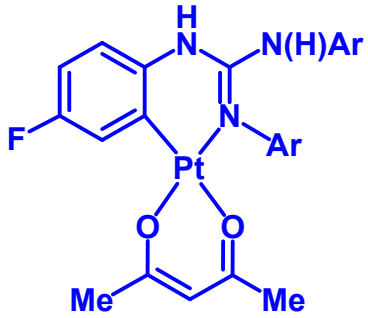
H
N
N(H)Ar
F
N
Ar
Pt
O
O
Me
Me

Ar = 4-FC_6H_4 (**18**)

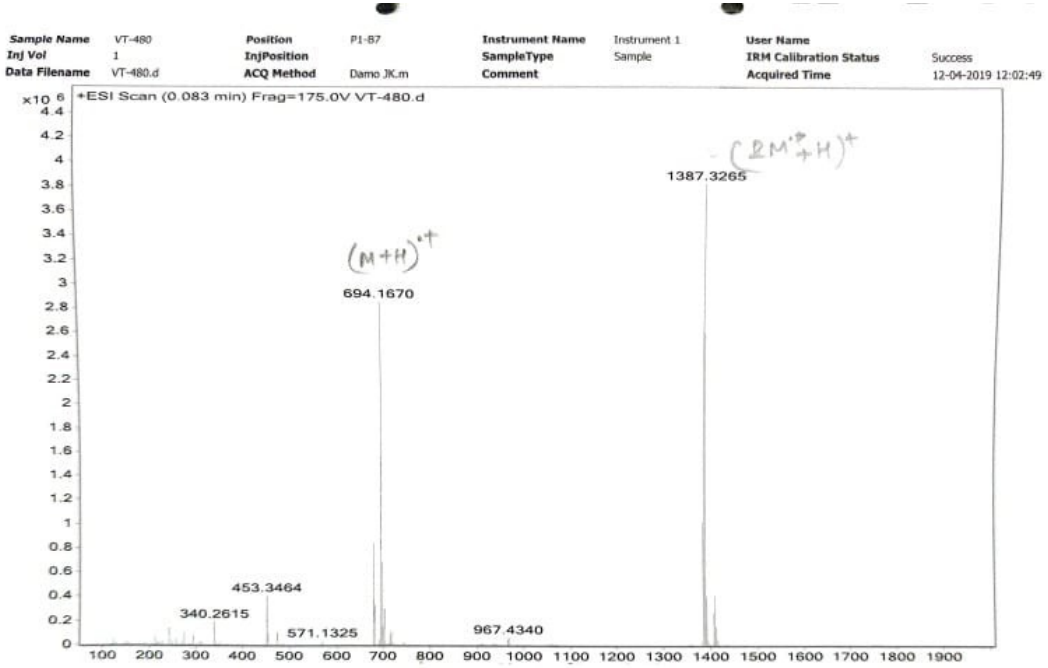
Sample Name VT-480
Inj Vol 1
Data Filename VT-480.d
Position P1-B7
InjPosition
ACQ Method Damo JK.m
Instrument Name Instrument 1
SampleType Sample
Comment
User Name
IRM Calibration Status Success
Acquired Time 12-04-2019 12:02:49
+ESI Scan (0.083 min) Frag=175.0V VT-480.d
x10 6
1387.3265
694.1670
453.3464
340.2615
571.1325
967.4340

Complex 19

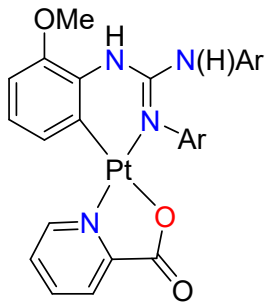
OMe
H
N
N(H)Ar
N
Ar
Pt
N
O
O

References

1. K. Pradeesh, J. J. Baumberg, and G. V. Prakash, *Optic Express*, 2009, **17**, 22171–22178.
2. K. Gopi, B. Rathi and N. Thirupathi, *J. Chem. Sci.* 2010, **122**, 157 –167.
3. P. Elumalai, N. Thirupathi and M. Nethaji, *Inorg. Chem*. 2013, **52**, 1883−1894.
4. R. Kumar and N. Thirupathi, *RSC Adv.* 2017, **7**, 33890–33904.
5. N. K. Sinha, V. Mishra and N. Thirupathi, *Inorg. Chem.* 2023, **62**, 7644–7661.
6. V. Mishra and N. Thirupathi, *ACS Omega* 2018, **3**, 6075−6090.
7. Bruker (**2004**). *APEX2*. Bruker AXS Inc., Madison, Wisconsin, USA.
8. Bruker (**2004**). *SAINT*/*XPREP*. Bruker AXS Inc., Madison, Wisconsin, USA.
9. Bruker (**1999**). *SADABS*. Bruker AXS Inc., Madison, Wisconsin, USA.
10. Rigaku Oxford Diffraction (**2015**). CrysAlis PRO and CrysAlis RED. Oxford Diffraction Ltd, Abingdon, England.
11. CrysAlisPro, version 1.171.34.49; Oxford Diffraction Ltd: Oxford, U.K., **2011**.
12. (a) G. M. Sheldrick, University of Gottingen, Gottingen, Germany, **2017**. (b) L. J. Farrugia, WinGX Suite for Small Molecule Single-Crystal Crystallography. *J. Appl. Crystallogr*. 1999, **32**, 837–838.
13. O. V. Dolomanov, L. J. Bourhis, R. J. Gildea and J. A. K. Howard, H. Puschmann, OLEX2: A complete structure solution, refinement and analysis program. *J. Appl. Crystallogr*. 2009, **42**, 339–341.
14. G. Cavallo, P. Metrangolo, R. Milani, T. Pilati, A. Priimagi, G. Resnati and G. Terraneo, *Chem. Rev.*, 2016, **116**, 2478–2601.

15. V. V. Sivchik, A. I. Solomatina, Y. Chen, A. J. Karttunen, S. P. Tunik, P. Chou and I. O. Koshevoy, *Angew. Chem.*, 2015, **127**, 14263–14266.